WATER QUALITY AND SEDIMENT BIOGEOCHEMISTRY IN THE URBAN JORDAN RIVER, UT

by

Mitchell Clay Hogsett

A dissertation submitted to the faculty of
The University of Utah
in partial fulfillment of the requirements for the degree of

Doctor of Philosophy

Department of Civil and Environmental Engineering

The University of Utah

May 2015

Copyright © Mitchell Clay Hogsett 2015

All Rights Reserved

The University of Utah Graduate School

STATEMENT OF DISSERTATION APPROVAL

The dissertation of **Mitchell Clay Hogsett**

has been approved by the following supervisory committee members:

Ramesh Goel	, Chair	**7-30-2014** Date Approved
Otakuye Conroy–Ben	, Member	**7-30-2014** Date Approved
Michelle Baker	, Member	**7-31-2014** Date Approved
Theron Miller	, Member	**7-30-2014** Date Approved
Carl Adams	, Member	**7-30-2014** Date Approved
Steven Burian	, Member	**8-2-2014**

and by **Michael Barber** , Chair/Dean of

the Department/College/School of **Civil and Environmental Engineering**

and by David B. Kieda, Dean of The Graduate School.

ABSTRACT

Urban rivers are plagued with a variety of ailments ranging from hydraulic modifications, organic matter enrichment, loss of biodiversity, toxic pollutant loads, and chronically low dissolved oxygen (DO) concentrations. Utah's Jordan River is no exception, and the purpose of this research was to better understand the chronic DO deficits found in the lower river flowing through Salt Lake City. The primary goals were focused on identifying and quantifying DO dynamics in the water column and at the sediment-water interface, macronutrient dynamics, sediment methane production, sediment organic matter (OM) standing stocks, size speciation of sediment OM, and the estimation of OM loads associated with primary production in the Upper Jordan River. Solids, liquids, and gases were investigated to identify linkages and to conduct mass balances on both DO and OM to better understand the urban Jordan River.

TABLE OF CONTENTS

LIST OF ACRONYMS

AOB	ammonia oxidizing bacteria
BOD	biochemical oxygen demand
BOD_5	5-day biochemical oxygen demand
cfs	cubic feet per second
C	carbon
Chl-a	chlorophyll-a
C:N:P	carbon to nitrogen to phosphorus molar ratio
COD	chemical oxygen demand
CPOM	course particulate organic matter
CR_{24}	24-hour community respiration
DO	dissolved oxygen
DOC	dissolved organic carbon
DOM	dissolved organic matter
DP	dissolved phosphorus, orthophosphate
FPOM	fine particulate organic matter
GBD	gas bubble deterioration
GBT	gas bubble trauma
GPP	24-hour gross primary production
GW	groundwater
LJR	Lower Jordan River
LNP	Legacy Nature Preserve
LWD	large woody debris
NPP	net primary production
NDM	net daily metabolism
NBOD	nitrogenous biochemical oxygen demand
NOB	nitrite oxidizing bacteria
OM	organic matter
ORP	oxidation-reduction potential
POM	particulate organic matter
POTW	publicly owned treatment works
ppmV	volumetric parts per million
rbCOD	readily biodegradable chemical oxygen demand
SCUBA	self contained underwater breathing apparatus
SD	standard deviation
SOD	sediment oxygen demand
STORET	Storage and Retrieval identification number
STP	standard temperature and pressure
TDS	total dissolved solids

TSS	total suspended solids
TMDL	total maximum daily load
TIN	total inorganic nitrogen (sum of nitrite, nitrate, and ammonia nitrogen)
TN	total nitrogen
TP	total phosphorus
UBOD	ultimate biochemical oxygen demand
UJR	Upper Jordan River
USEPA	United Stated Environmental Protection Agency
USGS	United States Geological Survey
Utah DWQ	Utah Division of Water Quality
WC	water column
WRF	water reclamation facility
WQ	water quality
WWTP	wastewater treatment plant
%TS	percent total solids
%VS	percent volatile solids

LIST OF COMMOMLY USED PARAMETERS

$CH_{4,OD}$	oxygen demand required to oxidize sediment methane flux (g DO/m^2/day)
$CPOM_{aer,stretch}$	standing stock of sediment CPOM (kg OM)
CR_{24}	24-hour community respiration (g DO/m^2/day)
CR_{GW}	low DO groundwater intrusion flux (g DO/m^2/day)
$CR_{GW,24}$	24-hour community respiration adjusted for GW intrusion (g DO/m^2/day)
GPP	gross primary production (g DO/m^2/day)
NDM	net daily metabolism (g DO/m^2/day)
NDM_{adj}	Single-station NDM adjusted for low DO GW intrusion (g DO/m^2/day)
OM_{aerial}	standing stock of sediment organic matter (g OM/m^2)
$OM_{aer,stretch}$	standing stock of sediment OM matter (kg OM)
SOD	sediment oxygen demand flux (g DO/m^2/day)
SOD_{20}	sediment oxygen demand flux normalized to 20°C (g DO/m^2/day)
TDS	total dissolved solids, salt content (mg salt/L)
TOD	tray oxygen demand flux (g DO/m^2/day)
TPP	tray gross primary production (g DO/m^2/day)
TSS	total suspended solids (mg solids/L)
VSS	volatile suspended solids (mg burnable/L)
WC_{dark}	water column dark respiration rate (g DO/m^3/day)
WC_{light}	water column gross primary production rate (g DO/m^3/day)
$\%_{SOD}$	percent of nighttime DO deficit associated with the sediments
%TOC	percent total organic carbon (mass organic carbon/mass dry sediment) • also referred to as TOC
%TS	percent total solids (mass dry sediment/mass wet sediment) • also referred to as $\%TS_{bulk}$ and TS
%VS	percent volatile solids (mass burnable/mass dry sediment) • also referred to as $\%VS_{bulk}$ and VS
$\%VS_{bulk\ avg}$	three sample average %VS across width of river
$\%VS_{wet}$	percent volatile solids of wet sediment (mass burnable/mass wet sediment)
$\%VS_{CPOM}$	percent of VS as CPOM (mass burnable CPOM/mass burnable dry sed.)
Q_{10}	change in rate of metabolism for 10°C temperature change

ACKNOWLEDGEMENTS

I would like to thank my advisor Dr. Ramesh Goel for the opportunities, guidance, and support during both my masters and doctorate research. I would also like to thank my lab mates for their input, help, and friendship. A special thanks to the Utah Division of Water Quality and the Jordan River/Farmington Bay Water Quality Council for funding this research while providing equipment, training, and insight. I would like to show my appreciation to Dr. Theron Miller for introducing me to a variety of field sampling methods and sharing his knowledge regarding water quality in the Wasatch Front. Finally, I would like to thank my committee members for their valuable suggestions, criticisms, and perspectives.

CHAPTER 1

INTRODUCTION

The Jordan River flows from Utah Lake along the urbanizing Wasatch Front before entering a complex of constructed wetlands and finally draining into the terminal Great Salt Lake. Utah's Jordan River is a highly managed urban river that has been the recipient of both anthropogenic and natural pollutants. In recent years, there has been a growing awareness concerning the issues influencing the health and function of the Jordan River. These issues include channelization, urban stormwater runoff, industrial/municipal wastewater discharges, eutrophication, loss of riparian habitat, excessive incision/sedimentation, flow diversions, agricultural diffuse runoff, and water management. It is important to recognize that the continued growth and urbanization in the Salt Lake Valley will add to the load of waste and pollutants that will eventually find their way into the Jordan River.

The Jordan River has been classified as impaired in the lower three hydraulic reaches in terms of dissolved oxygen (DO) and *E. Coli*. (Utah DWQ 2013, Table 1.1). DO impairments can result in a variety of both acute and chronic water quality (WQ) problems. These problems include bad smells, degradation of the native aquatic community, problematic nutrient/toxicant transformations, and fish kills that can result from individual events, such as a large algal bloom die off (Tenore 1972; Heaney and Huber 1984; Dauer et al. 1992). This applied research will focus on identifying and

quantifying DO dynamics occurring in the water column and at the sediment–water interface.

There are many different water quality (WQ) models available to visualize the function and health of a lotic system (Cox 2003). The QUAL2kw model was adopted by the Utah Division of Water Quality (Utah DWQ) as a platform to store, share, and model WQ data collected from the Jordan River. During the Utah DWQ modeling efforts, the sediments were identified as a potential source of the river's chronic DO deficits. Models are extremely useful, but they require large amounts of planning, stakeholder involvement, and field-collected data for meaningful calibration (Beck 1987; Refsgaard et al. 2007; Cox 2003).

As part of this research, the field measured parameters sediment oxygen demand (SOD), methane, ammonium, and orthophosphate sediment fluxes can be directly incorporated into the QUAL2kw model framework (Pelletier et al. 2006). The measured water column (WC) nitrification rates, water column dark respiration (WC_{dark}), sediment denitrification fluxes, and net daily metabolism (NDM) can be directly compared to model outputs. The sediment standing stock of organic matter (OM) can be used to describe the existing OM present in the system that is not included in the QUAL2kw algorithm (Cox 2003).

A variety of factors can directly or indirectly contribute to DO deficits in a lotic system; the most important is the presence of organic matter in the water column and sediments (Edwards and Rolley 1965; Streeter and Phelps 1958). Bacteria utilize DO during OM degradation, and an additional DO demand is required for the oxidation of ammonia associated with organic nitrogen degradation (Fair et al. 1941). The ambient

DO concentrations in streams can be heavily influenced by sediment–water interactions, including periphyton respiration/primary production, OM decay, and the oxidation of reduced chemicals such as ammonia, sulfide, and methane.

The Jordan River experiences both "chronic" and "acute" DO deficits (Utah DWQ 2013). The chronic ailment is hypothesized to be a result of "steady state" OM decomposition in the sediments and WC. This requires a year-round source of OM to maintain a "steady state" DO deficit. Acute DO deficits in surface and marine waters are typically associated with a large algal bloom die-off (Diaz and Rosenberg 2008; Paerl et al. 1998). Acute DO deficits have been observed in the Lower Jordan River (LJR), and the most recent event occurred in July of 2013 following a large storm event (Theron Miller 2013, personal communication). This may have been a result of the impervious surface "first flush" phenomena, the disturbance of organically enriched instream sediments, or from reduced dissolved chemical species originating from rotting OM in the conduits being introduced into the Jordan River (Gromaire-Mertz et al. 1999; Deletic 1998; Bertrand-Krajewski et al. 1998). Terrestrial particulate OM transported into the LJR during storm events will eventually contribute to the steady state chronic DO deficits.

Similar to DO, the dynamics and availability of the macronutrients nitrogen and phosphorus are very important in understanding the pollution status of surface waters (Vollenweider 1971; Fisher et al. 1982). Excessive nutrient loads from point and nonpoint sources can lead to the eutrophication and subsequent degradation of water quality. The instream sources and sinks of nutrients are important to quantify for the successful management of surface waters. Ammonium, nitrate, and orthophosphate

dynamics occurring in the WC and at the sediment–water interface can be decoupled using chambers to isolate the potentially very different metabolisms (Forja and Gomex-Parra 1998). For example, the sediments may be a source of ammonium and phosphate due to OM decomposition while removing publicly owned treatment works (POTW) nitrate loads through sediment denitrification (Fisher et al. 2005; DeSimone and Howes 1996; Pauer and Auer 2000). Comparing external nutrient loads and internal cycling rates will allow insight to how the Jordan River may respond to future POTW nutrient discharge concentrations.

As surface waters become excessively productive due to anthropogenic activities, or eutrophication, WQ will deteriorate (Hilton et al. 2006). Benthic and WC primary production result in supersaturated ambient DO concentrations (>125%) in the Upper Jordan River (UJR), suggesting that instream produced OM from the UJR is a source of organic matter to the DO impaired Lower Jordan River (LJR). Net daily metabolism (NDM) in the Upper and Lower Jordan River were compared using two different methods due to the challenges associated with characterizing a 52-mile 4^{th} order stream. Light-dark chamber techniques were used to decouple the effects of reaeration while using DO as a surrogate for OM production and respiration (Bott et al. 1978; Odum 1956). Since chambers can only be placed near the riverbanks in water less than 1 meter deep, single-station diurnal DO techniques were also utilized to provide a better understanding of NDM at a reach based scale to include macrophytes and thalweg metabolisms (Chapra and Di Torro 1991; Chapra 1991).

Having an understanding of the standing stock of sediment OM is important for multiple reasons. Sediment OM will decay at varying rates while consuming DO, cycling

nutrients, and producing reduced chemical byproducts that may negatively influence stream health (Fair et al. 1941). The standing stock of sediment OM across the width of the river at seven locations was measured using the parameters total solids (%TS), volatile solids (%VS), total organic carbon (%TOC), and sediment density. A %TOC:%VS ratio for the LJR was developed to better understand the amount of carbon present in sediment OM. A relationship between SOD and %VS specific to the Lower Jordan River was also developed to allow easy estimation of SOD based on surface sediment OM.

OM loads to lotic environments are both autochthonous (instream production) and allochthonous (external) (Minshall 1978). Sources of allochthonous OM in an urban environment include litterfall transported over impervious surfaces and through stormwater conduits to downstream surface waters (Goonetilleke et al. 2005). Fresh litterfall, macrophytes debris, seeds, and sticks that are larger than 1 mm in size are classified as course particulate organic matter (CPOM) (Cummins 1974). Through the speciation of sediment OM in terms of CPOM and fine particulate organic matter (FPOM) while removing sticks, the CPOM portion was assumed to be terrestrial leaf litter and aquatic vegetation. The sources of FPOM were inconclusive since FPOM includes algae, bacteria, diatoms, fungus, small worms, and partially decomposed CPOM.

Swamp gas, a combination of methane and carbon dioxide, is produced during the anaerobic decay of OM in sediments (Segers 1998). In oxic surface waters, the vast majority of sediment diffused methane is oxidized at the oxic-anoxic-anaerobic interfaces within the sediments (Fenzel et al. 1990). If occurring, sediment methane production will contribute an oxygen demand leading to an increase in SOD (Di Toro et al. 1990).

Laboratory methods were utilized to maintain complete anaerobiosis to measure sediment methane production rates, which were then used to estimate sediment methane fluxes in the Jordan River.

Through the investigation and quantification of the previously mentioned WQ parameters, multiple mass balances on DO, OM, and nutrients were conducted. The data collected during this research can be used directly by the Utah DWQ to aid in populating the Jordan River QUAL2kw model, provides additional information about the Jordan River not predicted using the QUAL2kw model, and includes information relevant to future researchers investigating the Jordan River.

CHAPTER 2

PROBLEM STATEMENT AND RESEARCH OBJECTIVES

2.1 Problem Statement

The basis for this PhD research was to investigate dissolved oxygen (DO) dynamics and ambient water quality (WQ) with respect to sediment biogeochemistry in Utah's Jordan River. The goals of this research are two fold. The first was to increase the working knowledge concerning sediment oxygen demand (SOD), nutrient fluxes, sediment organic matter, methane fluxes, and net daily metabolism (NDM) in an urban river system. The second goal was to provide in situ WQ data to help regulatory agencies and stakeholders in understanding instream processes while contributing to the Jordan River TMDL development process.

SOD measurements conducted during my Master's research suggested that sediment processes drive ambient DO deficits in the Lower Jordan River (LJR). Further investigation was required to isolate and quantify these DO consuming processes. In addition to characterizing the sediments in the LJR, the upstream DO unimpaired lotic environment was investigated to better understand the entire Jordan River system. It is hypothesized that sediment OM enrichment is the driving factor in ambient DO deficits in the LJR, and this research characterized and quantified various reservoirs of OM and instream degradation processes.

2.2 Research Objectives

The basis of my doctoral research and the specific hypotheses are listed below.

Hypothesis 1: SOD is driven by sediment organic matter type and concentration in the Lower Jordan River: sediments containing more fine particulate organic matter will exert more SOD than those containing more coarse particulate organic matter at similar organic carbon concentrations, and sediment organic content is more important in estimating seasonal SOD rates compared to ambient water column temperature.

Hypothesis 2: In situ factors such as ambient pH, DO, and benthic community structure can significantly influence nutrient fluxes from sediments.

Hypothesis 3: %TOC and %VS are positively correlated with SOD, and both %TOC and %VS can be used as a surrogate for SOD in the Lower Jordan River (not the Upper Jordan River).

Hypothesis 4: Biogas (methane and carbon dioxide) production in the sediments of the Lower Jordan River is a significant DO consumer at the sediment–water interface.

To test these hypotheses, the following objectives were formulated and accomplished:

Objective 1: Measure seasonal SOD at locations representative of hydraulic reach based sediment characteristics, downstream and upstream of wastewater and stormwater discharge points and in other local surface waters.

Objective 2: Evaluate the flux and fate of nutrients as they interact with the sediments and WC using SOD chambers during in situ conditions and after manipulating chamber DO and pH.

Objective 3: Evaluate the contribution of primary production to DO dynamics and

organic carbon fixation using transparent SOD chambers and diurnal ambient water quality data.

Objective 4: Obtain sediment core samples at locations selected for SOD studies and quantify the bulk sediments and fine/coarse particulate organic matter in terms of %TOC, %TS, %VS, and $\%VS_{wet}$ to establish correlations between SOD and these parameters.

Objective 5: Evaluate methane fluxes from the sediments in the Lower Jordan River.

2.3 Research Contributions

Fig. 1 provides the WQ parameters investigated during this research and expected linkages. These parameters can be included into existing WQ models and mass balances. The sediment and WQ relationships investigated during this research are briefly described in terms of application.

The SOD:%VS relationship provides an alternative method to estimate Sediment Oxygen Demand (SOD) in silty sediments using standardized volatile solids (%VS) measurements. This relationship can be utilized by POTW, educational, and governmental laboratories that do not have the materials and expertise needed to directly measure SOD. The decomposition of organic matter has long been recognized as the driving factor contributing to SOD. Previous relationships required estimating aerial concentrations of OM, which requires knowledge of the depth of the biologically active sediment layer or benthal deposit. The proposed relationship is based solely on the organic portion of the top 2 cm of the surficial sediments and allows the rapid processing of large amounts of samples.

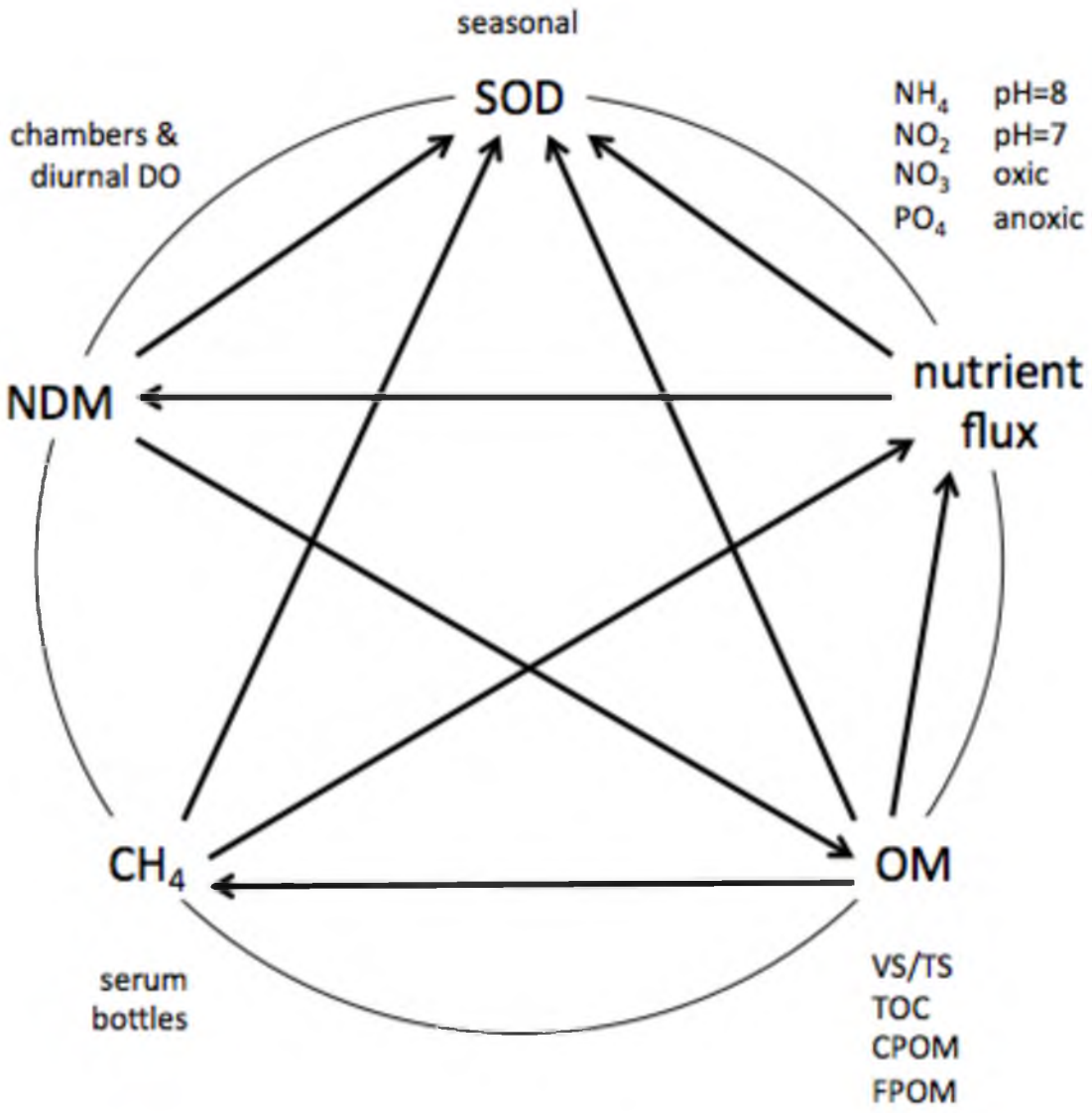

Fig. 1. Research parameters and expected linkages

Quantifying nitrogen and phosphorus sediment fluxes and water column rates allows the estimation of nutrient cycling and internal loadings. These fluxes can be compared to POTW nutrient loads to determine the relative contributions of internal versus external nutrient loadings.

The quantification of net daily metabolism (NDM) allows instream OM production and decomposition estimates. This information can be used to predict UJR OM loads resulting from eutrophication to the DO impaired LJR.

Percent total solids (%TS) is the percent solids matter in a wet sediment, and percent volatile solids (%VS) is the percent OM of the dry solids. The %VS:%TS relationship will aid in describing the surface sediments in the Jordan River, allow the calculation of sediment wet density, and provide a specific range to utilize the SOD:%VS relationship proposed in this study.

%VS measurements can be complicated by a variety of factors including lab protocols, sampling techniques, and the presence of inorganic carbon and clays (Heiri et al. 2001; Dean 1974). Carbonates and clay minerals are abundant in the alkaline Great Salt Lake Valley, and total organic carbon (%TOC) was measured to validate %VS as a surrogate for OM in the Jordan River.

By removing sticks from sediment samples, the course particulate organic matter (CPOM) represents terrestrial leaf and macrophyte debris before being degraded to less than 1 mm in size. Measuring both CPOM and the bulk OM found in the sediments may provide insight regarding the sources of OM to different stretches of the LJR. The fine particulate organic matter (FPOM) fraction represents degraded CPOM, periphyton, and subsurface microbes.

By measuring SOD and the flux of methane from the sediments, the relative contribution of methane oxidation in the benthos in relation to SOD can be calculated. Methane fluxes result in an ambient oxygen demand and are indicative of sediment OM enrichment.

CHAPTER 3

LITERATURE REVIEW

3.1 Water Quality in Lotic Systems

3.1.1 Earth's water resources

The majority of Earth's surface is covered with water (Fig. 2), but only 2.5% of the Earth's water resources are considered fresh, or having low total dissolved solids (TDS <500 mg/L). Only 0.3% of Earth's fresh water is surface water, and 0.007% is considered easily collectable surface water. Rivers account for an estimated 0.00015% of the Earth's total water (Gleick 1993). These rivers and streams are responsible for channeling hydraulic energy from the uplands to the oceans as an important part of the world's ongoing water cycle (Gleick 1993, Shiklomanov chapter).

Rivers play a vital role in both terrestrial and aquatic biology by providing diverse ecosystems, habitat, clean water, energy, and a constant supply of minerals and organic matter (Allan 1995; Naiman and Bilby 1998). Within a lotic system, or moving surface water, the water column and sediments dynamically interact in response to upstream influences while providing an environment responsible for maintaining a functioning aquatic ecosystem.

Surface waters provide potable water and many recreational benefits to society, yet more than 50% of America's surface waters are designated as impaired for various reasons (USEPA 2010b; USEPA 2006). 42% of the nation's sampled wadeable streams

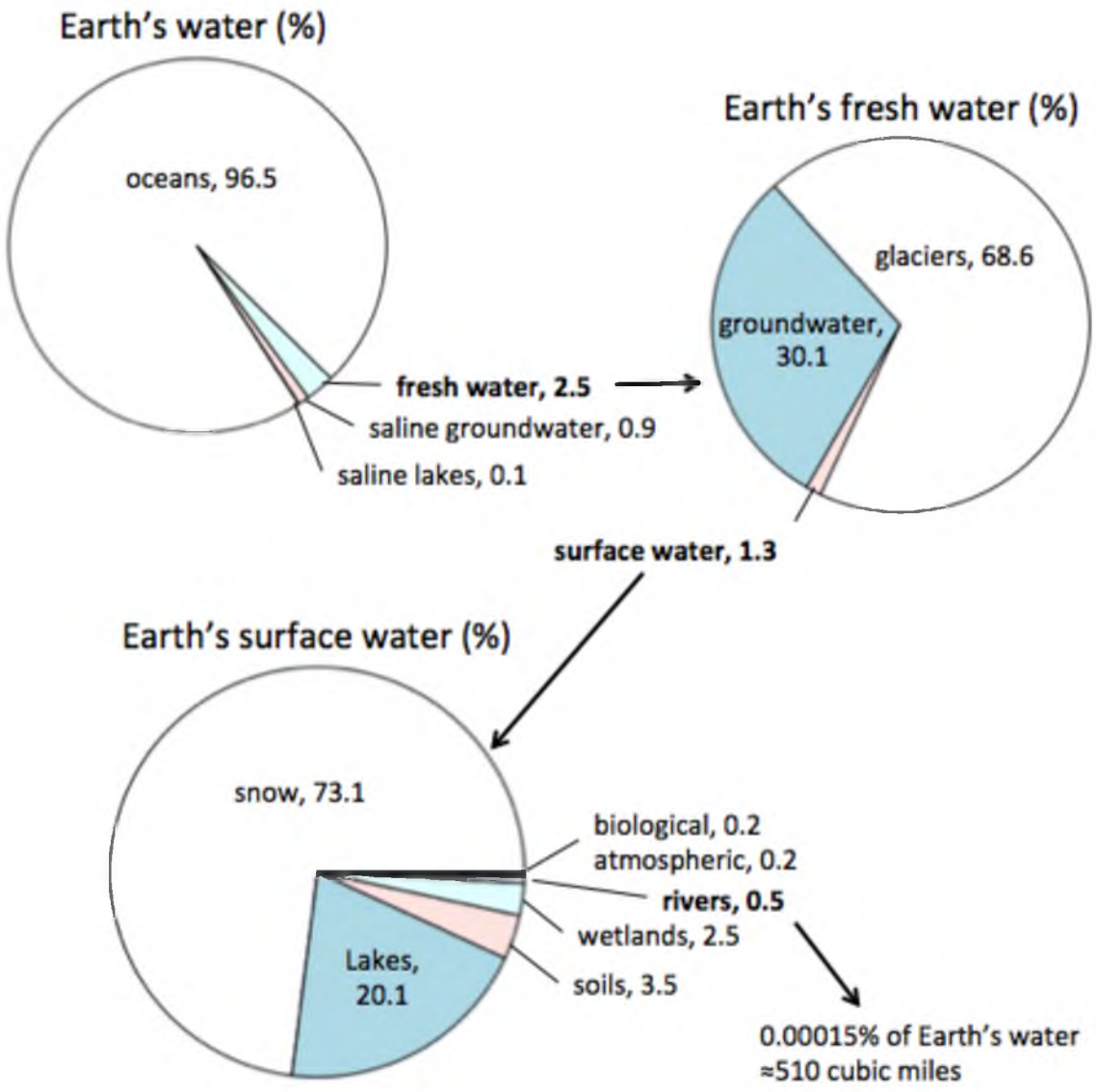

Fig. 2. General breakdown of the Earth's water resources
Note: adapted from Gleick 1993, Chapter 2

are classified as "poor" in terms of biological condition with only 28% characterized as "good" (USEPA 2006). The Western United States has the best biological condition with 45% of wadeable stream miles considered good and 27% considered as poor (USEPA 2006). Organic enrichment and contaminant inputs from urban and industrial discharges, aquaculture, stormwater, and agricultural runoff are stressors to surface water health. Water quality deterioration due to nutrients, organic carbon, and other pollutants is a widespread problem threatening the sustainability of global water resources while increasing the cost of potable water treatment (Makepeace et al. 1995).

The degradation of Earth's rivers is not an isolated problem in the United States, but a global challenge since all rivers flow downstream to lakes, estuaries, bays, fjords, seas, and oceans. The obvious, yet socially complex, consequences are portrayed in the dead zones present in the Gulf of Mexico and rapidly declining water quality in Washington's Puget Sound, where these habitats have historically been recognized as highly productive, important, and diverse ecosystems (Dodds 2006; Diaz and Rosenberg 2008).

3.1.2 Urban rivers

An important factor contributing to the degradation of surface water quality is urbanization (Bernhardt and Palmer 2007; Paul and Meyer 2001). Urbanization directly affects the water quality (WQ) of surface waters due to a variety of anthropogenic activities (Walsh et al. 2005). Common hydrological, biological, and chemical problems contributing to decreased WQ in urban rivers has been coined "urban stream syndrome" (Walsh et al. 2005). Urban rivers suffer from many ailments, including increased stormwater runoff resulting in flashy hydrographs, increased water temperature, loss of

riparian habitat, channelization, hydraulic manipulations, excessive sedimentation/incision, nutrient induced eutrophication, organic pollution, toxins, nonnative species invasion, and the general degradation of the upstream watershed (Booth 1990; Hilton et al. 2006; Sweeney et al. 2004, Pimentel et al. 2005; Paul and Meyer 2001; Meyer et al. 2005; Groffman et al. 2003).

Historically, water engineering and management practices focused on water quantity for agricultural, culinary, and flood control purposes. Management of the quality of surface waters have focused on "end of pipe" approaches that work great for flow quantity engineering, but have proved mostly ineffective for surface water quality management (Goonetilleke et al. 2005).

The sediment spatial heterogeneities characteristic of flowing waters include runs, rapids, riffles, pools, and depositional zones associated with river meanders. The diversity of flow regimes in a natural river results in patchiness of OM and the benthic community, leading to increased biodiversity (Casas 1996). Urban rivers tend to have a homogeneous bedform compared to the predevelopment conditions of the watershed due to the loss of riffles and meanders associated with channelization, stream incision, and sediment deposition (Miller and Boulton 2005).

The ability for a river ecosystem to assimilate nutrients, sediment, organics, and toxins is an important factor contributing to surface water quality and is compromised downstream of poorly planned urbanization (Bernhardt and Palmer 2007; Paul and Meyer 2001).

3.1.3 Total Maximum Daily Load (TMDL) studies

Section 303(d) of the Clean Water Act requires states, territories, and tribes to develop lists of impaired waters that are polluted based on the standards set by state and federal regulatory agencies. A Total Maximum Daily Load (TMDL) calculation for specific pollutants is performed to determine the pollutant load a specific surface water can receive without impairing the designated beneficial uses of that waterbody. In this context, the Clean Water Act requires a TMDL study to be undertaken for each pollutant responsible for the impairment of a surface waterbody. After the pollutant of concern is identified, a TMDL study determines the pollutant load allocations that can be discharged from both point and nonpoint sources. A complete TMDL study requires extensive monitoring, modeling, and laboratory and field scale experiments. Once appropriate loads are determined, management strategies can be developed and implemented to reduce the daily load of pollutants until the waterbody is brought back into compliance with water quality standards. The final stage of a TMDL includes load allocations and decision-making associated with revised pollutant discharge permits (Stackelberg and Neilson 2012; Boyd 2000).

3.2 Introduction to the Jordan River, Utah

3.2.1 The Great Basin, Lake Bonneville, and Great Salt Lake

The Great Basin is the largest endorheic, or landlocked, watershed in North America, extending North-South from Oregon to Southern California and East-West from central Utah to Eastern California. Within the Great Basin, lies the Great Salt Lake, which claims the title of the world's fourth largest terminal lake. The Great Salt Lake is a remnant of the historic freshwater Lake Bonneville that once filled the Wasatch Front

with water up to 1,000 feet deep (Spencer et al. 1984). Fig. 3 provides a map of Utah's current rivers with the historic Lake Bonneville shaded pink. The Great Salt Lake, Jordan River, and Utah Lake are located within the boundaries of the historic Lake Bonneville.

Since the watershed is terminal, the Great Salt Lake behaves like an evaporation pond and can have salinities ranging from 5–27% depending on location and lake level. For comparison, the world's oceans have an average salinity of roughly 3.5%. The three main sources of freshwater to the Great Salt Lake are the Bear (avg. flow 25 m^3/s), Weber (avg. flow 10 m^3/s), and Jordan Rivers (avg. flow 15 m^3/s), which contribute over 1 million tons of new salt to the Great Salt Lake annually. The Bear, Weber, and Jordan Rivers contribute roughly 50%, 20%, and 30% of the annual freshwater to the Great Salt Lake.

The Great Salt Lake proper is too saline for fish to live, and the primary aquatic life are brine shrimp (*Artemia*), shore flies (Ephydridae), and algae. Although the water column is very inhospitable for higher life forms, the wetlands surrounding the Great Salt Lake provide invaluable habitat for migratory waterfowl and shorebirds for feeding, mating, and resting on the Pacific Flyway extending from Alaska to Patagonia. The Great Salt Lake wetlands account for roughly 75% of Utah's wetlands and are concentrated along the northern and eastern shores receiving water from the Wasatch Mountains.

Utah Lake, the origin of the Jordan River, has a surface area of roughly 390 km^2 (145 square mile) and a storage capacity just shy of a million acre-feet (902,400 ac-ft). It is a shallow lake with an average depth of approximately 9–10 feet during normal reservoir operating conditions (Utah DWQ 2007). Utah Lake is the largest natural freshwater lake in the western United States in terms of surface area and has a maximum

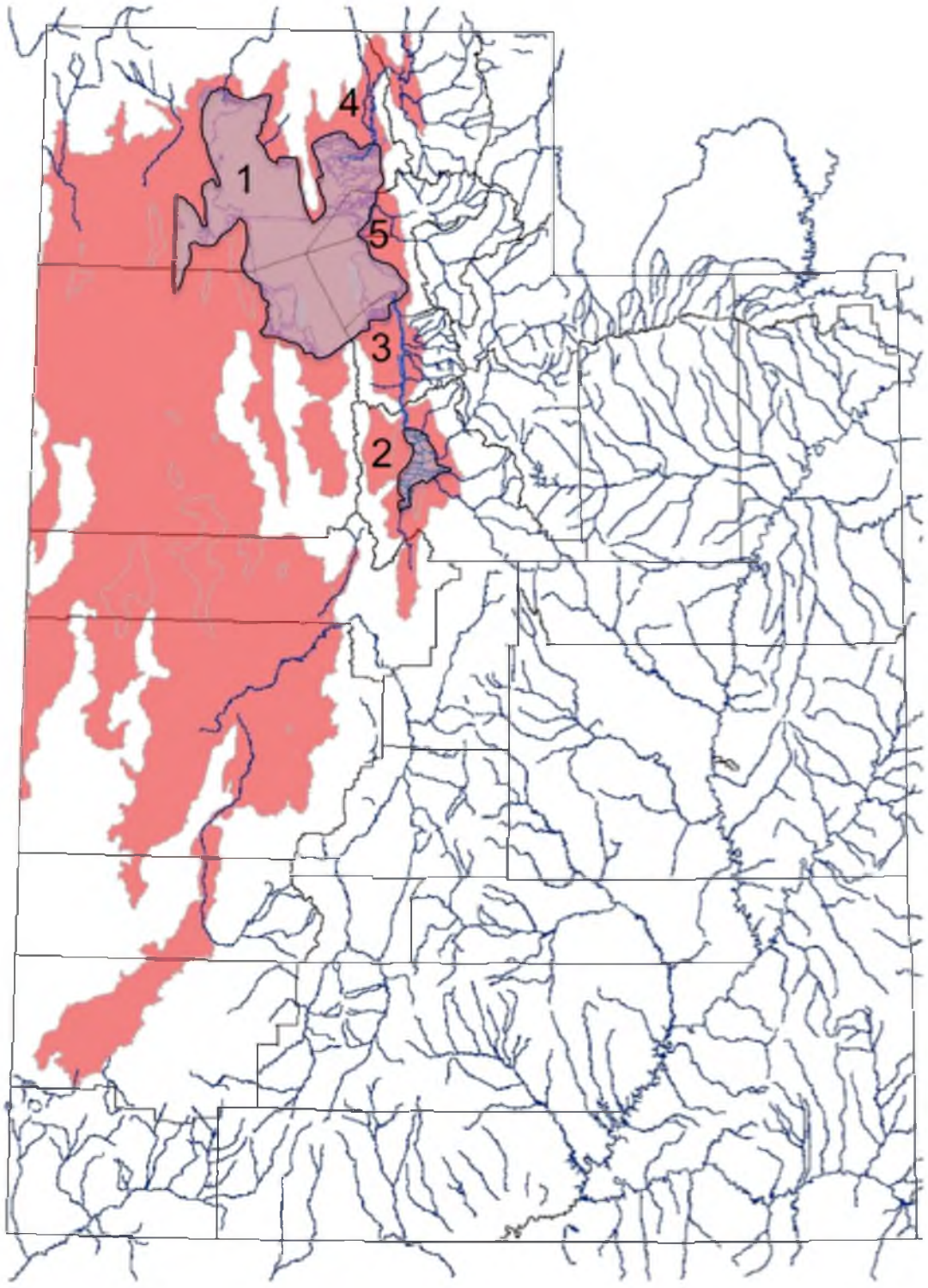

Fig. 3. Historic Lake Bonneville (shaded) and current lotic waters in Utah State
Note: 1 = Great Salt Lake, 2 = Utah Lake, 3 = Jordan River,
4 = Bear River, and 5 = Weber River

length and width of 24 and 13 miles, respectively.

Utah Lake is managed at a lake elevation of 4,489 feet above sea level, resulting in tributaries and groundwater inputs being the source of water to the Upper Jordan River (UJR) during the winter months. This results in much lower flows and decreased turbidity in the UJR during the winter months.

3.2.2 Utah's Jordan River

Utah's 4th order Jordan River flows 52 miles south to north from Utah Lake through the urbanized Salt Lake Valley before entering a series of managed wetlands before finally discharging into the terminal Great Salt Lake. Fig. 4 provides a general overview of the Jordan River with counties, municipalities, and a parcel map to visualize areas of urban development and population density.

The Jordan River passes through three counties, 15 municipalities, and 10 diversion dams/weirs and receives the direct discharge of three municipal wastewater treatment plants (WWTP). In addition, the Jordan River receives sediment and pollutant inputs from an 800 square mile watershed with the lowlands rapidly being urbanized while contributing additional untreated diffuse runoff.

The four mountain water tributaries to the Lower Jordan River include City Creek, Red Butte Creek, Emigration Creek, and Parleys Creek. All four of these tributaries have been incorporated into stormwater conveyance systems and piped below Salt Lake City as shown by the red circle in Fig. 5. The complete loss of habitat and stream function occurs when a river is enclosed in pipes by removing the stream from daylight, floodplains, hyporheic exchanges, and the riparian zone (Miller and Boulton 2005; Boughton and Neller 1981). Potable water is collected in the mountains from

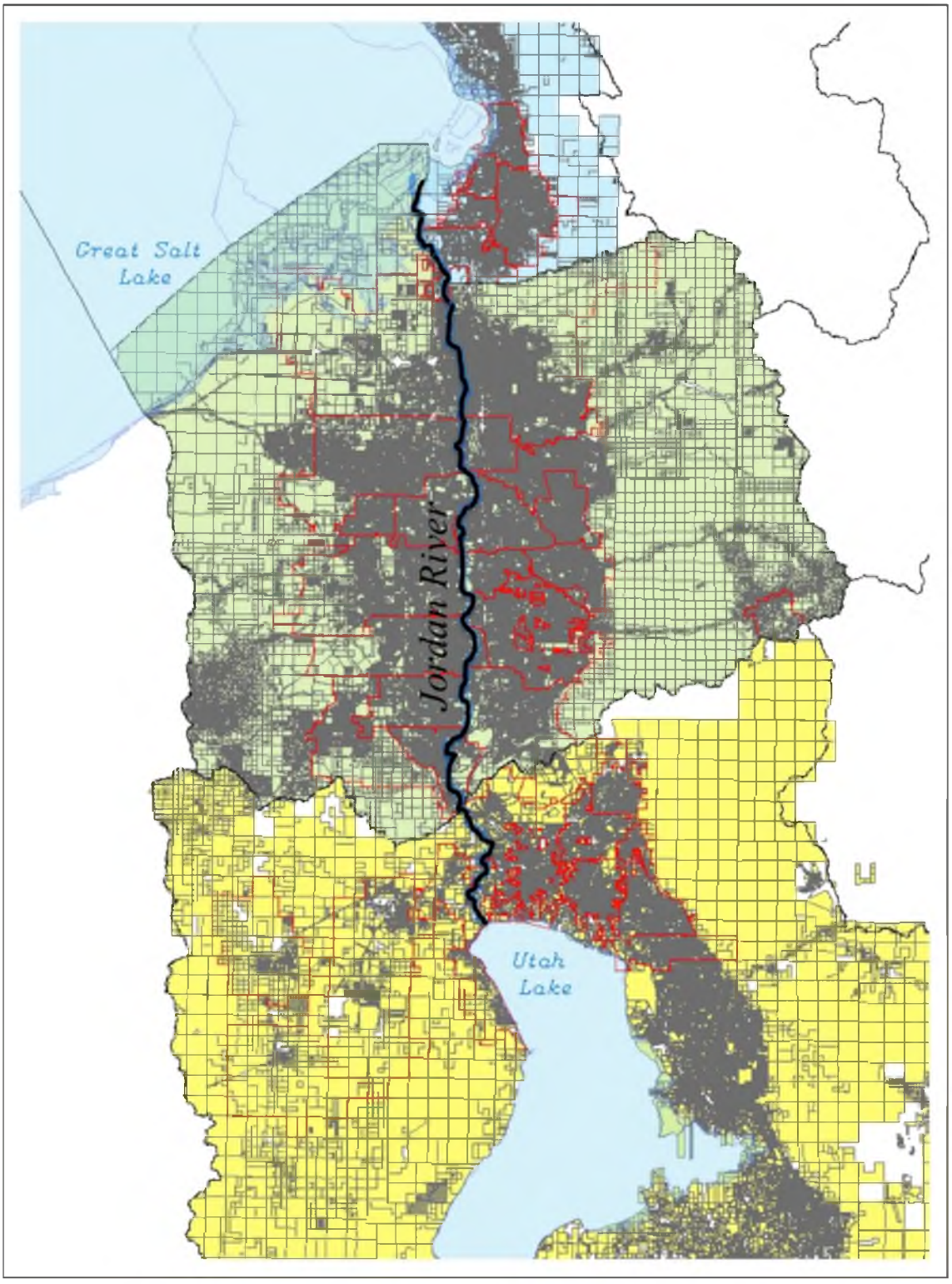

Fig. 4. Parcel map (property lines) for Davis, Salt Lake, and Utah Counties

Fig. 5. Primary tributaries to the Jordan River
Note: the red circle indicates streams piped underneath Salt Lake City and incorporated into stormwater conveyance system; orange diamonds identify bridge crossings

these streams, but these tributaries have historically been modified and managed as a conduit for stormwater conveyance, thereby losing all function as a stream before discharging into the Lower Jordan River (LJR).

Fig. 6 provides municipal WWTP locations along the Jordan River and upstream Utah Lake. The three POTWs directly discharging into the Jordan River at the time of this research include South Davis-South WWTP, Central Valley Water Reclamation Facility (WRF), and South Valley WRF. WWTPs discharging into Utah Lake indirectly add nutrients to the downstream Jordan River as suspended OM present as living phytoplankton and dead sestonic matter.

3.2.3 The Upper and Lower Jordan River

The urban Jordan River has been highly modified due to channelization, loss of riparian habitat, an extensive low head dam water diversion network, and upstream impoundments associated with Utah Lake, Deer Creek reservoir, and Jordanelle reservoir. Upstream diversions mitigate spring flooding and divert water for agriculture and potable uses. Fig. 7 provides a map showing dams and weirs located on the Jordan River and the complex canal network utilizing Jordan River and Utah Lake water.

The Surplus Canal diversion located at 2100 S was built to mitigate flooding in Salt Lake City during spring runoff and during large storm events. Roughly 72% (standard deviation (SD) = 16%) of the Jordan River's annual flow is diverted to the west towards the Great Salt Lake via the Surplus Canal. Due to the large removal of water from the Lower Jordan River at the Surplus Canal diversion, the Jordan River has been subdivided into two distinct sections in this dissertation. The Upper Jordan River (UJR) extends from Utah Lake to the Surplus Canal diversion and the Lower Jordan River

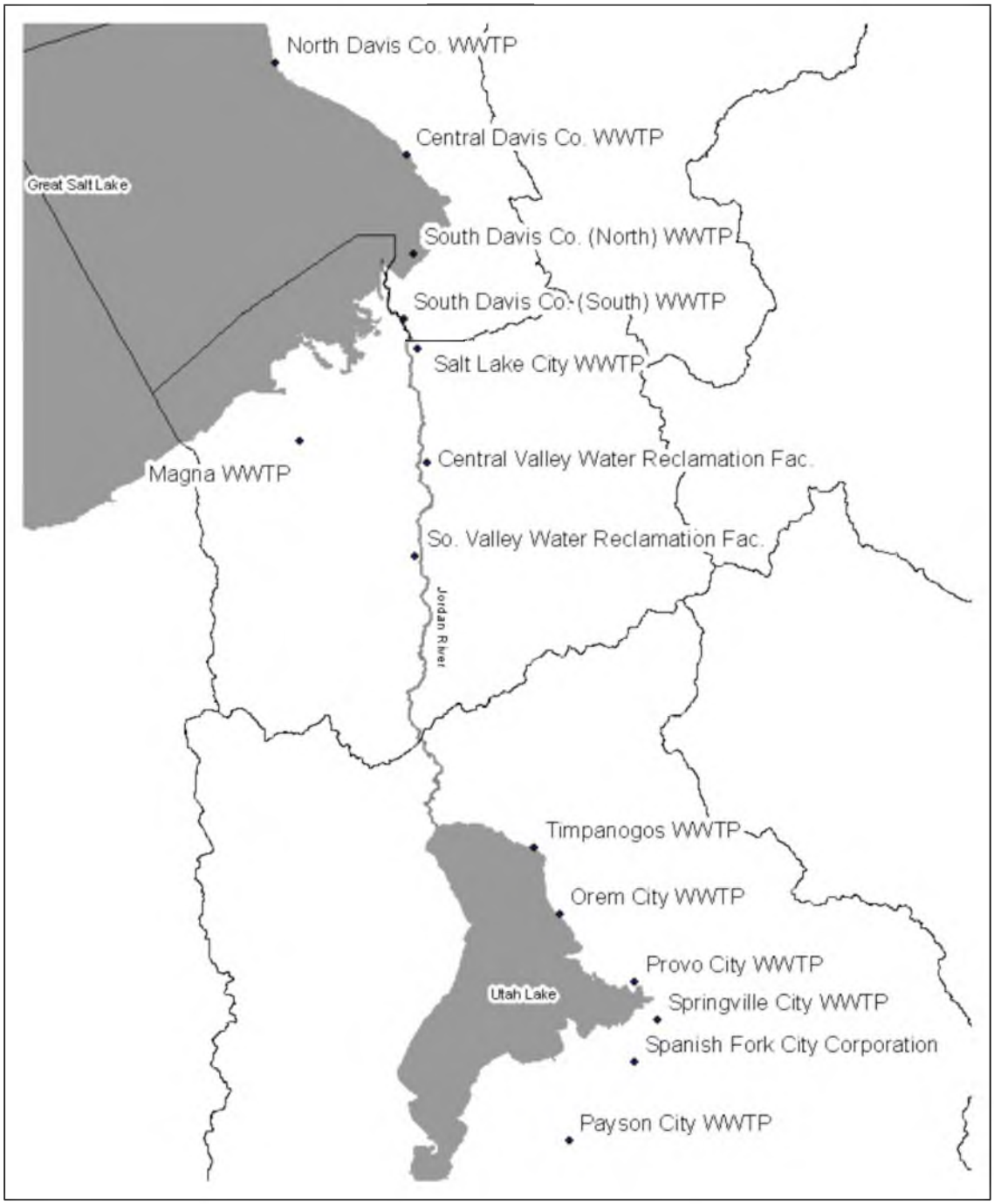

Fig. 6. WWTPs discharging to Utah Lake, Jordan River, and Great Salt Lake

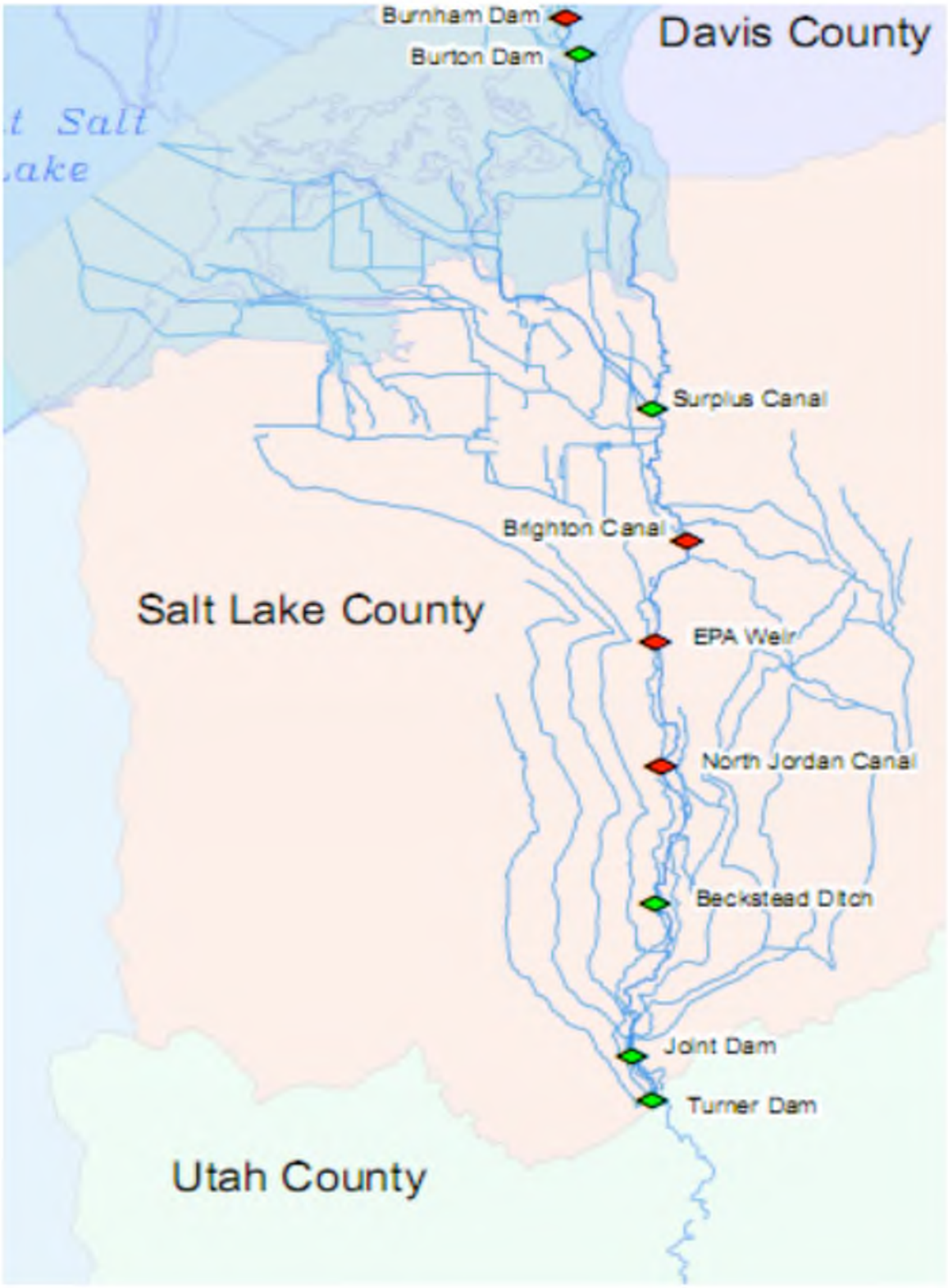

Fig. 7. Major diversions, canals, and flow control structures

(LJR) is located downstream of the diversion. This distinction in important since the Lower Jordan River does not experience the annual flow variations typical of a lotic system due to the decoupling of flows from the Upper Jordan River at the Surplus Canal diversion.

Fig. 8 provides mean daily stream flow rates for the Surplus Canal, UJR, and LJR over the time period of 2007–2012. Flow data were measured at the Surplus Canal overflow weir (purple line, United States Geologic Survey (USGS) station 10170500) and near the start of the Lower Jordan River at 1700 S (red line, USGS station 10171000). The Upper River data (blue line) were calculated by summing the mean daily flow for the previously mentioned sites.

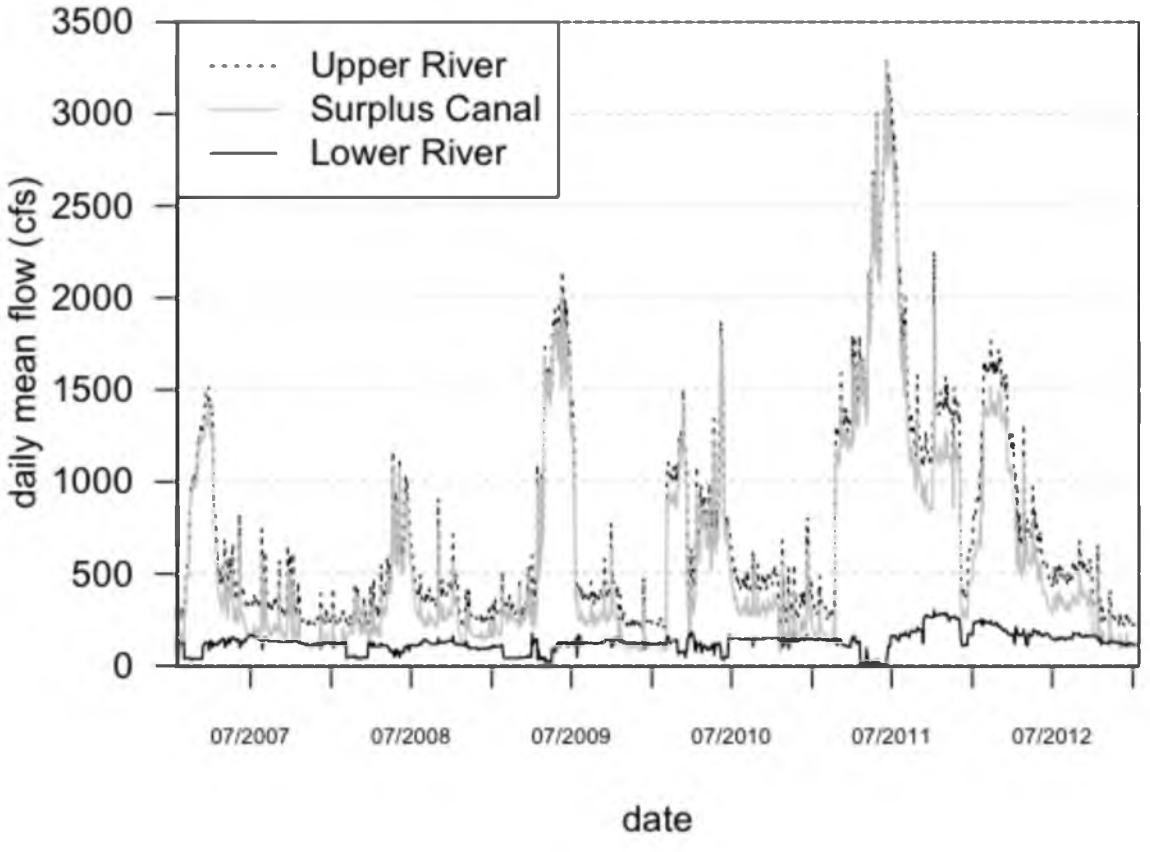

Fig. 8. Upper Jordan River, Lower Jordan River, and Surplus Canal annual flows

The annual mean daily flow rates observed during this time period for the Upper Jordan River, Surplus Canal, and Lower Jordan River were 704 (SD = 571), 576 (SD = 569), and 128 cfs (SD = 52), respectively. The relatively low flow rates and low standard deviation characteristic of the Lower Jordan River highlights its "tamed" nature. The maximum mean daily flow rate observed in the LJR over this time period was 303 cfs.

During large storm events the underflow weir allowing water into the LJR may be closed by Salt Lake City engineers to accommodate the flashy hydrographs associated with the impervious urban areas draining into the LJR. This can result in periods of little or no flow entering the LJR at 2100 S.

The six flow rate spikes in the UJR coincide with spring runoff, and the maximum mean daily flow rate of 3300 cubic feet per second (cfs) measured in 2011 was a result of the large mountain snowpack in the region (Fig. 8). The annual variations in the Jordan River are highlighted during this event where flows in the Upper Jordan River exceeded 850 cfs for 9 straight months from the managed release of water from Utah Lake into the Jordan River (Feb. 24, 2011, through Dec. 3, 2011).

The Jordan River has been partitioned into eight hydraulic reaches for assessment purposes. Multiple of these reaches have been classified as impaired for the designated uses of secondary recreational contact (2B), cold and warm water fisheries (3A, 3B), and agriculture (4). WQ indicators including E. coli, temperature, DO, and total dissolved solids (TDS) did not fulfill the standards associated with the designated uses (Utah DWQ 2013, Table 1.1). Impaired reaches of the Jordan River are provided in Table 1 and a map of the designated reaches is provided in Fig. 9.

Table 1. Jordan River hydraulic reach descriptions and impairments

Reach #	Description	Impairment
1	Burton dam to Davis County line (Cudahy Ln.)	3B
2	Cudahy Ln. to North Temple St. (City Creek tributary)	2B, 3B
3	North Temple St. to 2100 S (Surplus Canal)	2B, 3B
4	2100 S to 6400 S (Mill, Big and Little Cottonwood Cr.)	4
5	6400 S to 7800 S (Midvale Slag Superfund site)	2B, 3A, 4
6	7800 S to Bluffdale Rd. (14600 S)	3A
7	Bluffdale Rd. to Salt Lake County line (Traverse Mtns.)	3A, 4
8	Salt Lake County line to Utah Lake	3A, 4

Note: adapted from Utah DWQ 2013, Table 1.1

3.3 Dissolved Oxygen Dynamics

3.3.1 Dissolved Oxygen (DO)

Dissolved oxygen (DO) impairments can be chronic as well as acute with extreme cases typically associated with individual events, such as a large algal bloom. This rapid increase in aquatic biomass eventually dies and settles to the sediments where it depletes ambient DO as organic matter undergoes bacterial decomposition in the benthic zone. The effects of highly organic sediments on ambient stream DO can be significant (Baity 1938; Rudolfs 1932). The presence of low DO itself does not mean that DO is a pollutant (Utley et al. 2008; Todd et al. 2009). Instead, low DO provides an indication of other activities, which may have triggered the low DO (Parr and Mason 2004; Stringfellow et al. 2009). Dissolved oxygen impairments can result in a variety of nuisance and problematic water quality (WQ) issues, including bad smells, degradation of the aquatic community, problematic toxicant chemical transformations, and fish kills.

Managing WQ using DO as an indicator parameter is common practice, and the pollution status of surface waters can be assessed through DO dynamics. DO is important since all aquatic fauna require oxygen for respiration, and low concentrations will stress,

Fig. 9. Jordan River hydraulic reaches

inhibit, and kill the native aquatic community. As a general rule of thumb, DO concentrations less than 50% saturation are stressful to most aquatic communities.

The use of new technologies such as luminescent dissolved oxygen probes allows diurnal monitoring of the ambient water column for identifying water quality impairments and collecting baseline data. These WQ monitoring probes allow large amounts of data to be confidently and efficiently collected over multiday time periods to better understand the daily fluctuations in DO and stream metabolism.

The actual DO saturation concentration is influenced by temperature, atmospheric pressure, and salinity. Fig. 10 provides the relationship between fresh water at sea level

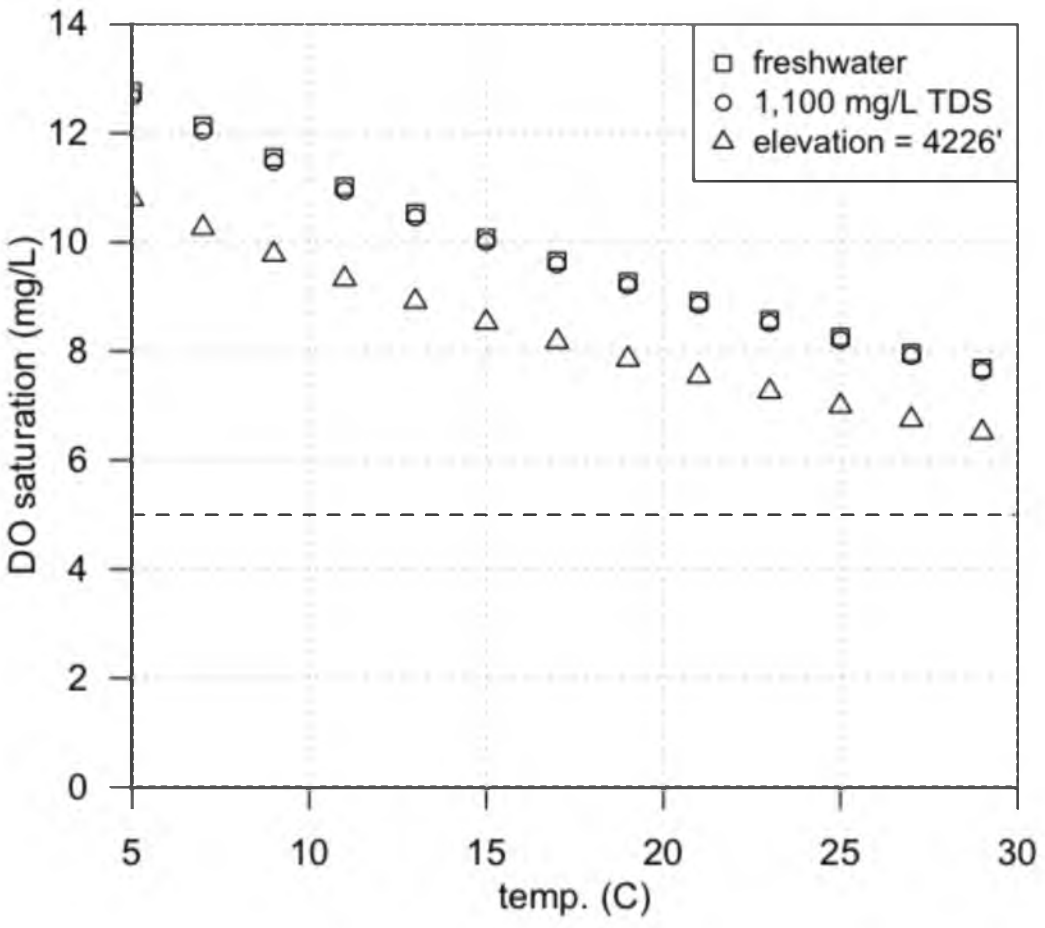

Fig. 10. DO in relation to temperature, salinity, and elevation above sea level

(squares), water having a salinity similar to the Jordan River of 1,100 mg TDS/L at sea level (circles), and Jordan River water at an elevation of 4226 feet (triangles). The dotted line represents 5 mg-DO/L, a common ambient DO level expected to be maintained in flowing waters to provide a healthy aquatic environment. DO saturation decreases with temperature, resulting in the majority of low DO events occurring in late summer in warm waters. In addition to decreasing ambient DO saturation, warmer temperatures increase stream metabolic rates.

Fig. 11 provides a general schematic of the biotic and abiotic DO consuming activities occurring in a river ecosystem during nighttime hours. These include

1) phytoplankton respiration
2) decay of instream flora/fauna
3) hyporheic exchanges
4) benthic respiration
5) flux of reduced chemical species
6) biochemical oxygen demand (BOD)
7) decay of course particulate organic matter (CPOM)
8) decay of fine particulate organic matter (FPOM)
9) respiration of fauna
10) macrophyte respiration

It should be noted that 1 and 10 will produce more DO than is utilized for respiration during daytime hours as a result of photosynthesis. Number 4 may produce a net positive flux of DO during daylight if periphyton are present on the surface of the benthic zone.

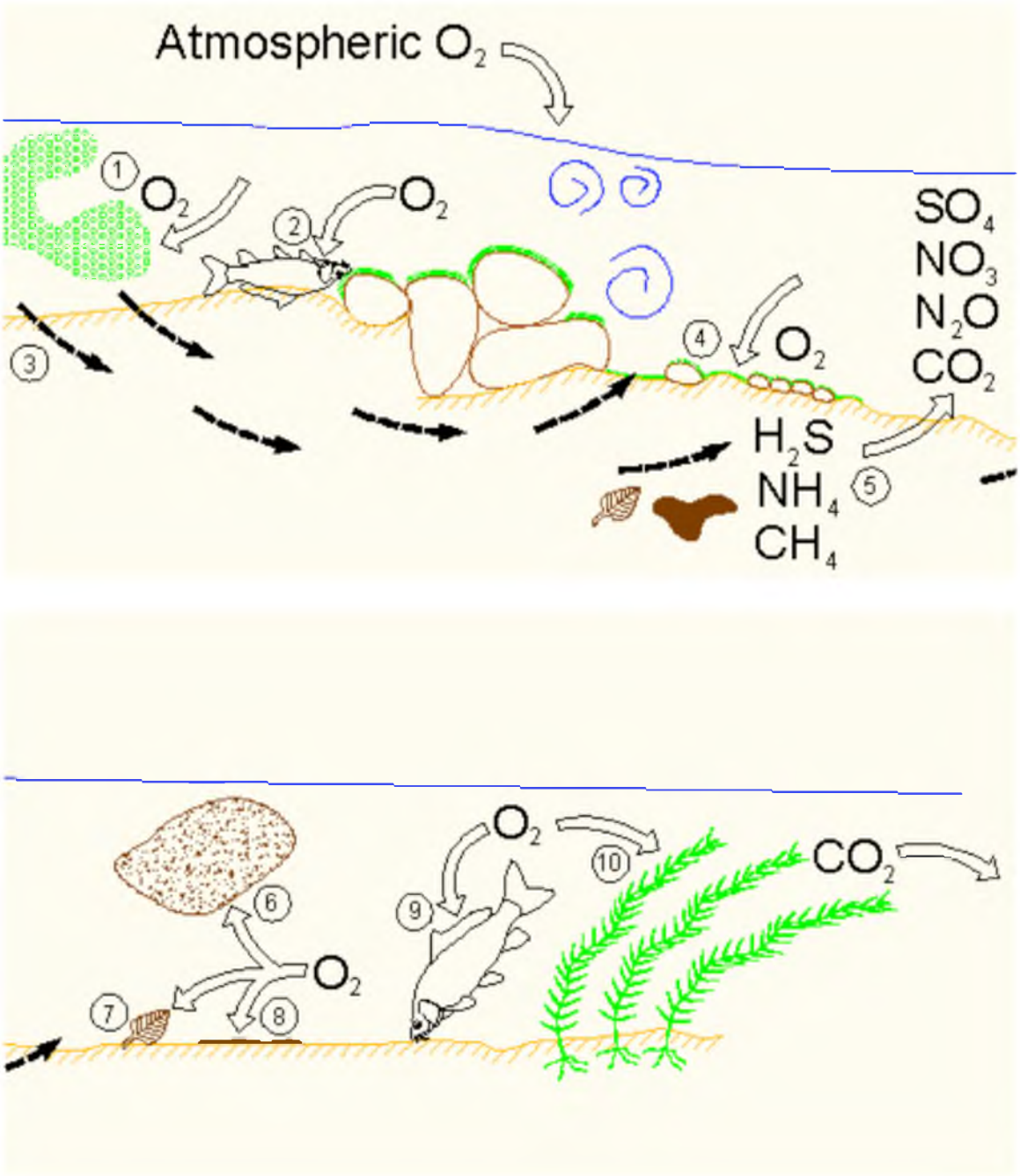

Fig. 11. Typical DO consuming activities occurring in the water column and at the sediment–water interface in a river system during nighttime

3.3.2 Reaeration

The replenishment of DO into the water column from atmospheric reaeration and daytime biological photosynthesis are constantly occurring at varying rates to achieve equilibrium between the ambient river DO deficit, or surplus, and atmospheric oxygen. The reaeration potential in a well-mixed surface water is generally expressed as a 1st order reaeration coefficient. As a result, the rate of physical reaeration increases in response to increased ambient DO deficits (Deatrick et al. 2007; Copeland and Duffer 1964). Since oxygen is considered to be poorly soluble in water due to a relatively high Henry's constant, approximately 0.8 atm*m^3/mole, ambient river DO levels may remain chronically low in slow moving and organically enriched sections (Chapra 2008, pg. 376).

Physical reaeration rates increase with any type of disturbance at the air-water interface. Disturbances increase the surface area of this interface allowing more atmospheric oxygen to diffuse across the air-water interface. Any form of turbulence to the water column, including wind, waves, rainfall, rapids, riffles, snags, and weirs, all increase reaeration locally.

Common techniques used to determine reaeration coefficients include conservative gas and dye injection into the stream (Tsivoglou et al. 1968), floating of a nitrogen gas filled diffusion dome (Cavinder 2002), diurnal models utilizing ambient DO profiles (Chapra and Di Toro 1991), and predictive equations based on stream depth, velocity, and slope (Bowie et al. 1985). All these techniques have advantages and challenges. For example, gas injection studies require substantial infrastructure including gas and dye sources, injection and sampling methods, and laboratory equipment to

quantify gas and dye concentrations. The gas injection method can become very expensive and labor intensive when investigating rivers with substantial flows. Diffusion dome studies are less expensive and can be utilized in large rivers, but cannot be employed in extremely turbulent or shallow conditions. Diurnal DO models are inexpensive and can estimate net daily metabolism, but can be heavily influenced by groundwater inputs and hyporheic exchanges (Hall and Tank 2005). Predictive equations are free, simple, and require only a small amount of initial data, but can be grossly misleading if incorrect assumptions are made in equation selection and parameter inputs.

A great deal of effort has been directed towards the generation of predictive equations used to estimate reaeration coefficients, and many of these equations have been produced using data acquired from rivers and streams with very distinct characteristics. As a result, the efficient use of predictive equations for the estimation of reaeration coefficients requires additional information regarding their history and appropriate use (Bowie et al. 1985). The O'Connor and Dobbins equation was developed using empirical observations in slow deep channels, 0.31–9 meters deep and 0.16–0.5 m/sec flow velocities, to estimate reaeration using a ratio based on steam velocity and depth (O'Connor and Dobbins 1958). The Churchill equation was generated from a dissolved oxygen mass balance following the release of low DO water from several dams and back calculating reaeration rates based on the ambient river waters' ability to achieve saturation downstream. Average depths and stream velocities used in the Churchill study were 0.6–3.4 meters and 0.6–1.6 m/sec, respectively (Churchill et al. 1962). The Owens and Gibbs equation was produced by deoxygenating several streams using sodium sulfite and measuring the increase in DO as water flowed downstream. Average depths and

stream velocities utilized in the Owens and Gibbs equation were 0.1–3.4 meters and 0.03–0.6 m/sec, respectively. This information was combined with Churchill's observations to develop Owens and Gibbs final equation (Owens et al. 1964).

It is common practice to use the O'Connor and Dobbins equation to predict reaeration coefficients in rivers that are relatively deep and slow moving, although other studies have shown that this equation overestimates reaeration in very slow moving sections (Leu et al. 1997). The Churchill equation applies best to relatively deep rivers characterized by elevated stream velocities, and the Owens and Gibbs equation is best suited for fast flowing shallow streams (Covar 1976; Zison et al. 1978).

Table 2 presents reaeration coefficients normalized to 20 centigrade for the various stretches of the Jordan River measured with a diffusion dome while floating down the thalweg (Hogsett and Goel 2013).

Fig. 12 provides the relationship between the diffusion dome measured reaeration coefficients and commonly used predictive equations (Covar 1976). The Float # in Table 2 is in relation to the float sections presented in Fig. 13. The parameters river depth and

Table 2. Reaeration coefficients for the Jordan River

River section	Reach #	$K_{2,20}$ (1/day)	Float #
1700 N to LNP NE	1 & 2	0.6	1 & 1b
1700 S to 900 S	3	4.2	2
3300 S to 2100 S	3 & 4	7.0	3
5400 S to 4170 S	4	5.1	4
9000 S to 7800 S	5 & 6	17.7	5
12600 S to 10600 S	6	11.0	6
Lehi	8	3.4	7

Note: $K_{2,20}$ = Reaeration coefficient normalized to 20 °C
1b = reaeration coefficient measured twice

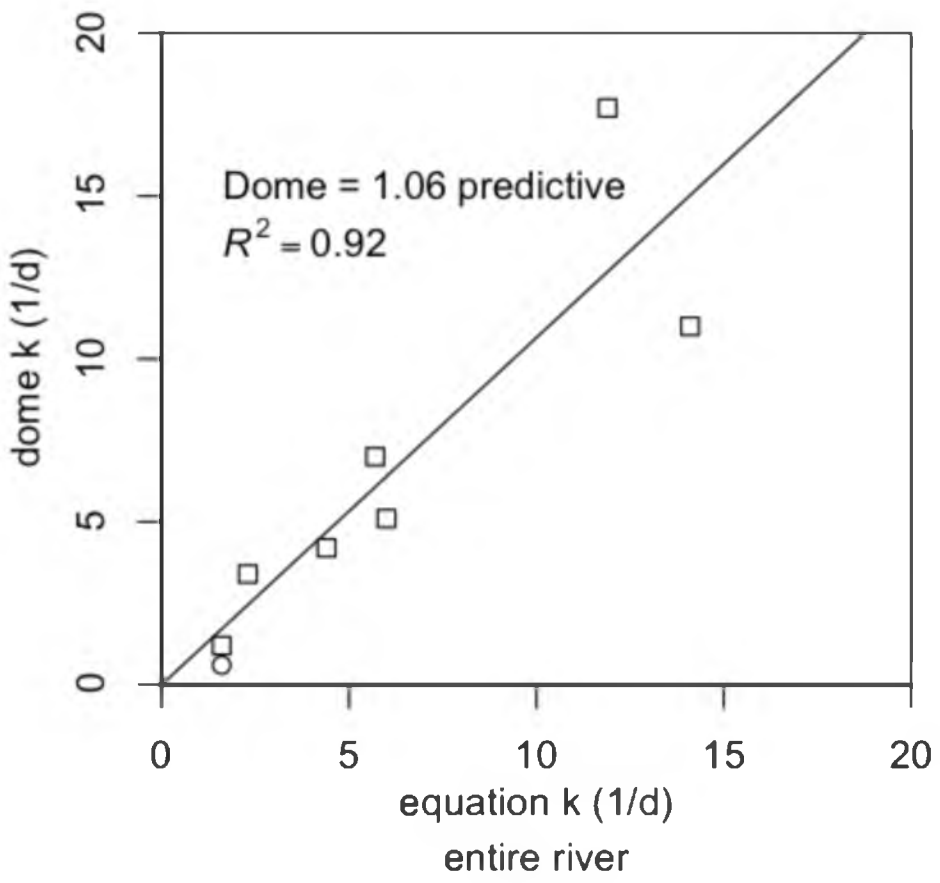

Fig. 12. Measured reaeration coefficients vs. suggested predictive equations

flow velocity were measured during the diffusion dome experiments. The diffusion dome reaeration coefficients were very similar to predictive equations within the range of k between 2 to 6 day^{-1}.

The low k value measured in Reach 1 is most likely a result of wind-induced reaeration becoming more important in this relatively slow moving hydraulic reach (Banks 1977; Cerco 1989). Reach 1 is located in the flood plains of the Great Salt Lake and receives minimal riparian buffering from wind and weather moving across the lake. The k estimate for wind induced reaeration in a shallow estuary 1 meter deep is 0.6 d^{-1} with an average wind speed of 8 mile/hour (Ro and Hunt 2006). The combination of

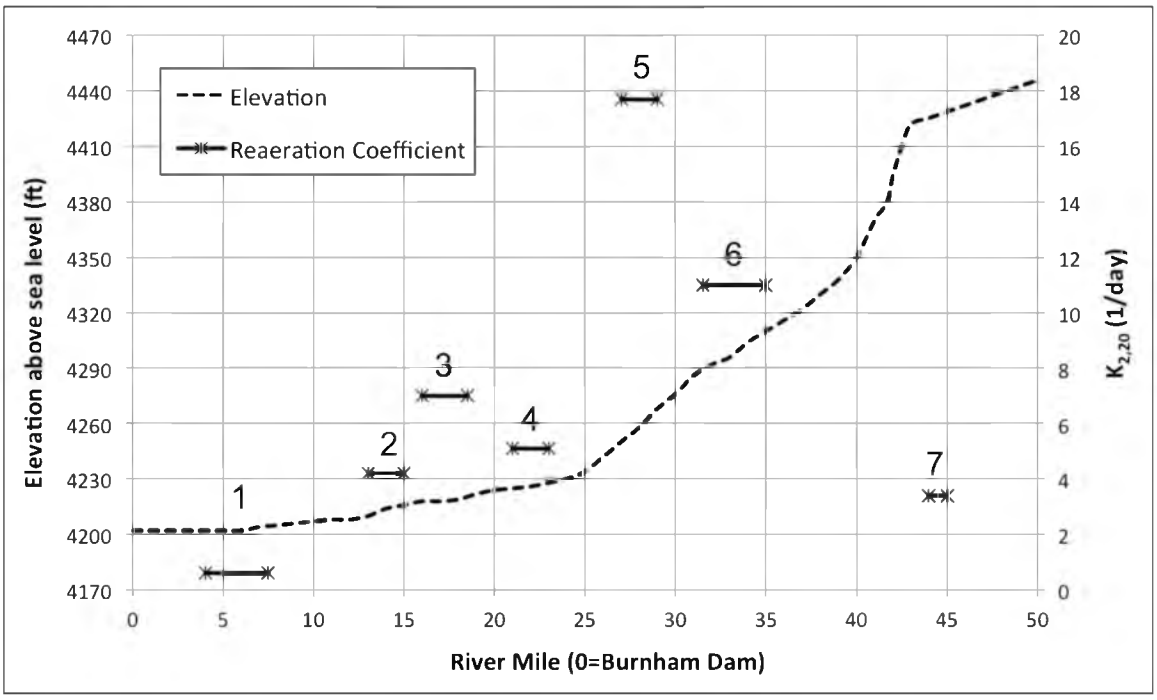

Fig. 13. Measured reaeration coefficients and elevation gradient for the Jordan River
Note: elevation profile adapted from Jensen 1986, Fig. 7

water and wind turbulence results in a k = 1.2 d^{-1} in Reach 1. This wind adjusted reaeration coefficient in Reach 1 was used for all calculations in the followings sections of this thesis.

Fig. 13 provides the elevation profile for the Jordan River and associated reaeration coefficients. It is obvious from Fig. 13 that the potential for reaeration is greater in the steeper midsection of the UJR and much lower in first 20 miles where the topography is relatively flat. Other reaeration studies conducted on the Jordan River estimated coefficients of 1.8 and 9.5 1/d for the sections between 1800 N–4800 S (river mile 5–21) and 4800 S–12300 S (river mile 21–34), respectively (Stephensen 1984). The low reaeration coefficient associated with Hydraulic Reach 8 is a result of its location in the slow moving backwaters above Turner Dam and downstream of Utah Lake.

3.3.3 Biochemical Oxygen Demand (BOD)

Surface and wastewater are routinely tested for biochemical oxygen demand (BOD) and chemical oxygen demand (COD) to characterize the waters' organic pollution status. COD tests entail oxidizing all organic carbon in a water sample using a strong acid and heat during a short time period (hours), while BOD tests utilize bacteria and DO to biologically oxidize organic carbon over much longer time scales (days).

BOD tests are typically carried out over a 5-day period under dark conditions to curtail photosynthesis. A 5-day testing period, BOD_5, is the standard due to 1st order reaction kinetics resulting in long time periods required to measure the ultimate BOD (UBOD). Since organic carbon comes in many qualities (glucose vs. cellulose), the UBOD will always be less than the COD measurements due the recalcitrant nature of biologically structural OM.

During this research the zero order parameter water column dark respiration (WC_{dark}) was used to describe the oxygen demand of the Jordan River. The units are per day as opposed to BOD_5. This is a beneficial timescale since river water is constantly moving downstream while interacting with changing environments.

3.3.4 Sediment Oxygen Demand (SOD)

Sediment oxygen demand (SOD) accounts for the depletion of dissolved oxygen due to the decomposition of settled organic matter (OM), the respiration of benthic flora and fauna, and the biotic and abiotic oxidation of reduced inorganic chemical species diffusing from the sediments (Utley et al. 2008; Todd et al. 2009; Walker and Snodgrass 1986). The degradation of OM is the ultimate source of SOD either directly, such as decay at the sediment–water interface, or indirectly, such as a sediment flux of reduced

chemicals. To complicate the parameter, SOD is also a function of the quality of OM present, the microbial community responsible for OM degradation, ecosystem metabolism, and the hospitality of the general environment to support the microbial and macroinvertebrate community (Young et al. 2008; Webster and Benfield 1986). The vast majority of the aquatic microbial population lives in the sediments with only a small fraction present in the water column (Ellis et al. 1998). The sediment–water interface, or benthic zone, and hyporheic zone are responsible for the majority of heterotrophic activity in stream ecosystems (Pusch et al. 1998). As a result, the SOD associated with organically enriched river sediments can be responsible for over 90% of the ambient oxygen deficit (Matlock et al. 2003; Hogsett and Goel 2013).

SOD can be measured in the laboratory using sediment cores as well as in situ using chamber methods. In situ measurements are preferred over laboratory scale experiments to avoid uncertainties associated with disturbing the sediments during collection, transportation, and testing. Mathematical modeling, using tools such as QUAL2Kw, are commonly used to simulate natural systems and predict DO dynamics based on field measurements of SOD and other parameters (Pelletier at al. 2006; Utley et al. 2008). Models that underestimate SOD or a lack of field sampling can greatly misrepresent diurnal DO profiles in streams.

Sources of organic matter contributing to SOD include the sedimentation of suspended solids originating from point dischargers; settled suspended solids associated with diffuse runoff, sloughed periphyton, and phytoplankton biomass that has settled to the river bottom; organic rich sediments that have eroded from upstream; organics traveling along the bottom of the river as bedload; and cryptic microbial growth.

Sources of phototrophic biomass (algae, macrophytes, diatoms, and cyanobacteria) to the Jordan River include Utah Lake, tributaries, and growth occurring within the mainstem of the Jordan River. Potential contributions to SOD resulting from the decomposition of phototrophic biomass within a river system can be large since tributaries and lake headwaters can be a consistent source of algal inoculum and sestonic particulate organic matter (Stringfellow et al. 2009). Other sources of organic material include nonpoint urban runoff and stormwater that can contribute additional organic matter during storm events and snowmelts (Goonetilleke et al. 2005; Paul and Meyer 2001).

In addition to the oxidation of organic compounds within the benthic zone and underlying sediments, the oxidation of inorganic compounds can contribute to SOD (Di Tora et al. 1990; Gelda et al. 1995; Wang 1981). Reduced compounds such as methane, ammonia, hydrogen sulfide, iron (II), and manganese (II) can be oxidized during transition from the anaerobic/anoxic zone within the sediments to the aerobic environment at the sediment–water interface.

Table 3 presents common electron acceptors utilized by sediment microbes as environmental conditions become more reductive. The last column provides an estimate of the redox potential (E_O) required for these reactions to become biologically favorable.

The significance is that after DO is depleted from sediment pore water, both abiotic reactions and biological respiration continue to occur, resulting in different chemical byproducts and nutrient cycling pathways that will eventually lead to an oxygen demand upon diffusion into the surface water.

The anaerobic sediment metabolism contributing to SOD is controlled, or limited,

Table 3. Preferred/available electron acceptors at decreasing redox potential

Substrate	Product	E_0 (mV)
$O_2 + H_2$	$2H_2O$	+330
$2NO_3^- + 5H_2 + 2H^+$	$N_2 + 6H_20$	+220
$NO_3 + 4H_2 + 2H^+$	$NH_4^+ + 3H_2O$	+220
$MnO_2 + H^2 + 2H^+$	$Mn^{2+} + 2H_2O$	+200
$2Fe(OH)^3 + H_2 + 4H^+$	$2Fe^{2+} + 6H_2O$	+120
$SO_4^2- + 4H_2$	$S^{2-} + 4H_2O$	-150
$CO_2 + 4H_2$	$CH_4 + 2H_2O$	-250

Note: adapted from Wetzel 2001, pg. 639

by the biogeochemical reactions and mass transport of dissolved ions and gasses through the sediments and across the sediment–water interface, assuming no hyporheic exchanges (Higashino et al. 2004). In sediments not conducive to hyporheic exchanges (silts and clays), the sediment boundary layer depths can be very thin, millimeters to centimeters.

The three most influential physical parameters influencing SOD in rivers are water temperature, water velocity, and the depth of the water column (Truax et al. 1995; Ziadat and Berdanier 2004). Lower temperatures result in a decrease in the metabolic rate of most microbes, and it is assumed that SOD rates will decrease accordingly. The water column depth is important since deeper depths are associated with slow moving waters, which have less mixing and decreased fluxes of DO to the benthic zone. At low flow velocities, DO transfer across the water–sediment interface is assumed to be the limiting factor driving SOD. It has been shown that SOD increases linearly within the flow velocity range between 0–10 cm/sec (Mackenthun and Stefan 1998). As velocities increase, SOD increases to a point where the dissolved oxygen consuming activities occurring within the sediments become the limiting factor and SOD rates reach a maximum (Nakamura and Stefan 1994). For perspective, the thalweg of the Lower Jordan River in Reach 1 has a mean velocity around 30 cm/sec, or three times greater

than required to overcome DO transfer limitations across the sediment–water interface. Further increases in water velocity can resuspend fine sediments within the water column. The resuspension of fine sediments due to elevated flow velocities temporarily increases BOD and SOD while exposing interstitial and sediment bound nutrients to the surface water (Malecki et al. 2004).

In addition to the various parameters contributing to DO consumption, many heterogeneities occurring within the sediment substrate can dramatically affect SOD locally. Variations in SOD are also expected to vary seasonally as flows, temperature, aquatic community structure, and sedimentation patterns change over the annual cycle.

3.3.5 SOD models

Previous researchers have developed relationships between SOD and various surrogates for OM. Prior to the Clean Water Act it was shown that the surficial 1 cm of sewage sludge may be aerobic, but the subsurface sludge is undergoing an anaerobic metabolism (Baity 1938). Baity's SOD predictive equation was based on the depth of the sewage sludge deposit. Fair, Moore, and Thomas (1941) developed a relationship based on aerial estimates of OM present in sewage sludge deposits found in a New England stream. Both of these relationships were developed before the Clean Water Act and an important variable was the depth of sludge layer. There are many challenges in accurately estimating the SOD contributing depth of the sludge layer including the "quality" of the OM matter (Fair et al. 1941; Di Toro et al. 1990; Gardiner et al. 1984; Barcelona 1983).

Gardiner et al. (1984) developed a relationship between sediment chemical oxygen demand (COD) and SOD in Green Bay sediments. Once again, the depth of the active sludge layer was required, and application of this relationship quickly becomes

complicated. Butts (1974) produced a relationship between chamber measured SOD in the Upper Illinois Waterway using data collected at 22 sites based on percent total solids (%TS) and percent volatile solids (%VS) of surface mud. Other methods to estimate SOD include the flux of reduced chemicals methane, sulphide, ammonia, and ferrous iron with these parameters accounting for 42%, 50%, 7%, and <1% of the SOD in anaerobic sediments, respectively (Gelda et al. 1995).

3.3.6 Primary Production (PP)

Terrestrial and aquatic primary production provide the organic matter required to support a healthy functioning food web in lotic ecosystems. Primary production results in the generation of OM and DO using the ambient solar flux as an energy source and bicarbonate as the carbon source according to the following general equation (Hauer and Lamberti 2007, pg. 664).

$$6CO_2 + 12H_2O + \text{sunlight} \rightarrow 6O_2 + C_6H_{12}O_6 + 6H_2O$$

This results in diurnal fluctuations in ambient DO concentrations and can lead to supersaturated conditions during the day. In addition, dissolved organic carbon (DOC) can be added to the stream during algal photosynthesis. Up to a 1/3 of the ambient water column DOC can be from algae during periods of peak photosynthesis creating diurnal biological DOC loadings (Kaplan and Bott 1982). As the sun falls below the horizon and photosynthesis ceases, algae, cyanobacteria, macrophytes, diatoms, and other primary producers utilize a portion of the organic carbon produced during daylight hours to support their nighttime metabolism (Hauer and Lamberti 2007, pg. 663). As a result, a net consumption of DO by the primary producers occurs in the absence of sunlight. This

results in lower DO concentrations in the nighttime and early morning hours compared to daytime values.

During photosynthesis, a portion of the reduced organic material is utilized for organism maintenance and survival, or autotrophic respiration (R_a). Organic carbon stored as biomass for growth and reproduction is referred to as net primary productivity (NPP). The gross primary productivity (GPP) is estimated by the following equation (Hauer and Lamberti 2007, pg. 663):

$$GPP = NPP + R_a$$

The net daily metabolism (NDM) can be defined as the change in dissolved oxygen per day as a result of both gross primary production and community respiration (CR_{24}) (Hauer and Lamberti 2007, pg. 665).

$$NDM = GPP - CR_{24}$$

3.3.7 DO supersaturation

Although DO is required for the aquatic respiration of eukaryotic fauna, too much DO can be deadly. This can occur in highly DO supersaturated waters as a direct result from excessive primary production leading to gas bubble trauma (GBT) or gas bubble deterioration (GBD). This potentially fatal phenomenon is typically associated with dinitrogen gas and large hydrostatic pressure changes. GBD is synonymous with the "bends" experienced by SCUBA (self contained underwater breathing apparatus) divers who have spent too much time deep underwater. If the diver swims to the surface too quickly, nitrogen gas bubbles may form within the bloodstream, potentially leading to

injury or death. Fig. 14 provides the saturation concentrations of nitrogen and oxygen in relation to temperature at sea level. Notice that the atmosphere is roughly 80% nitrogen, yet DO concentrations are not 5 times smaller in magnitude.

The United States Environmental Protection Agency (USEPA) has suggested a "total gas" supersaturation limit of 110% in shallow surface waters due to the acute mortality of sensitive fish species during reproduction and the year-round chronic stress to other species (Bouk et al. 1976; USEPA 1986). At a water temperature of 20 °C with nitrogen in equilibrium with the atmosphere, a DO concentration of 130% saturation

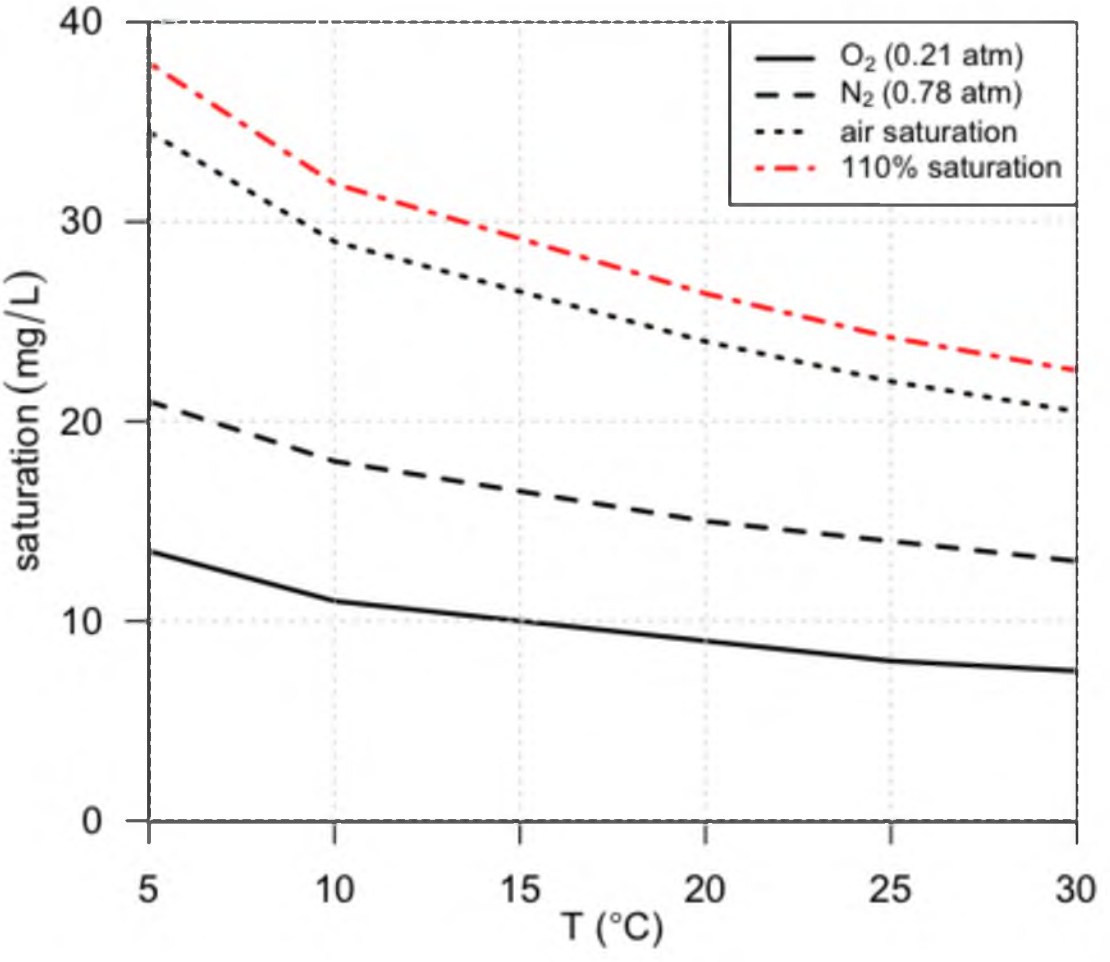

Fig. 14. Nitrogen and DO saturation concentrations

results in a "total gas" supersaturation value greater than 110%. DO saturation concentrations in the UJR have been routinely observed to peak at >130% and have been recorded as high as 150%. These high DO concentrations suggest eutrophication and may be stressful to the aquatic community (Renfro 1963). Fig. 15 shows oxygen bubbles forming in clear chambers when exposed to sunlight. These oxygen bubbles were produced in the benthos during photosynthesis in the UJR at a chamber DO concentration of 150% saturation.

3.3.8 Diurnal DO profiles

Odum (1956) originally introduced the in situ oxygen and gas monitoring techniques that are commonly used to estimate organic carbon fixation due to primary production. During the daytime, photosynthesis ensues and ambient DO concentrations increase. As the sun falls below the horizon, photosynthesis ceases and DO drops due to dark respiration until ambient DO concentrations reach equilibrium with the atmosphere, which is a function of the reaeration coefficient.

The characterization of the water column has long been standardized. BOD bottles measuring the nighttime respiration of the water column can be coupled with chlorophyll-A measurements and "light" bottles measuring DO production due to photosynthesis to estimate the water column's contribution to both CR_{24} and GPP (Wetzel and Likens 1979, Ch. 14). Measuring the metabolism of the benthos requires additional sampling protocols and parameters to separate the water column from the sediments.

Fig. 16 and 17 show two typical, and nearly identical, diurnal dissolved oxygen profiles measured in Reach 1 and 6 of the Jordan River. Reach 1 is where the river is

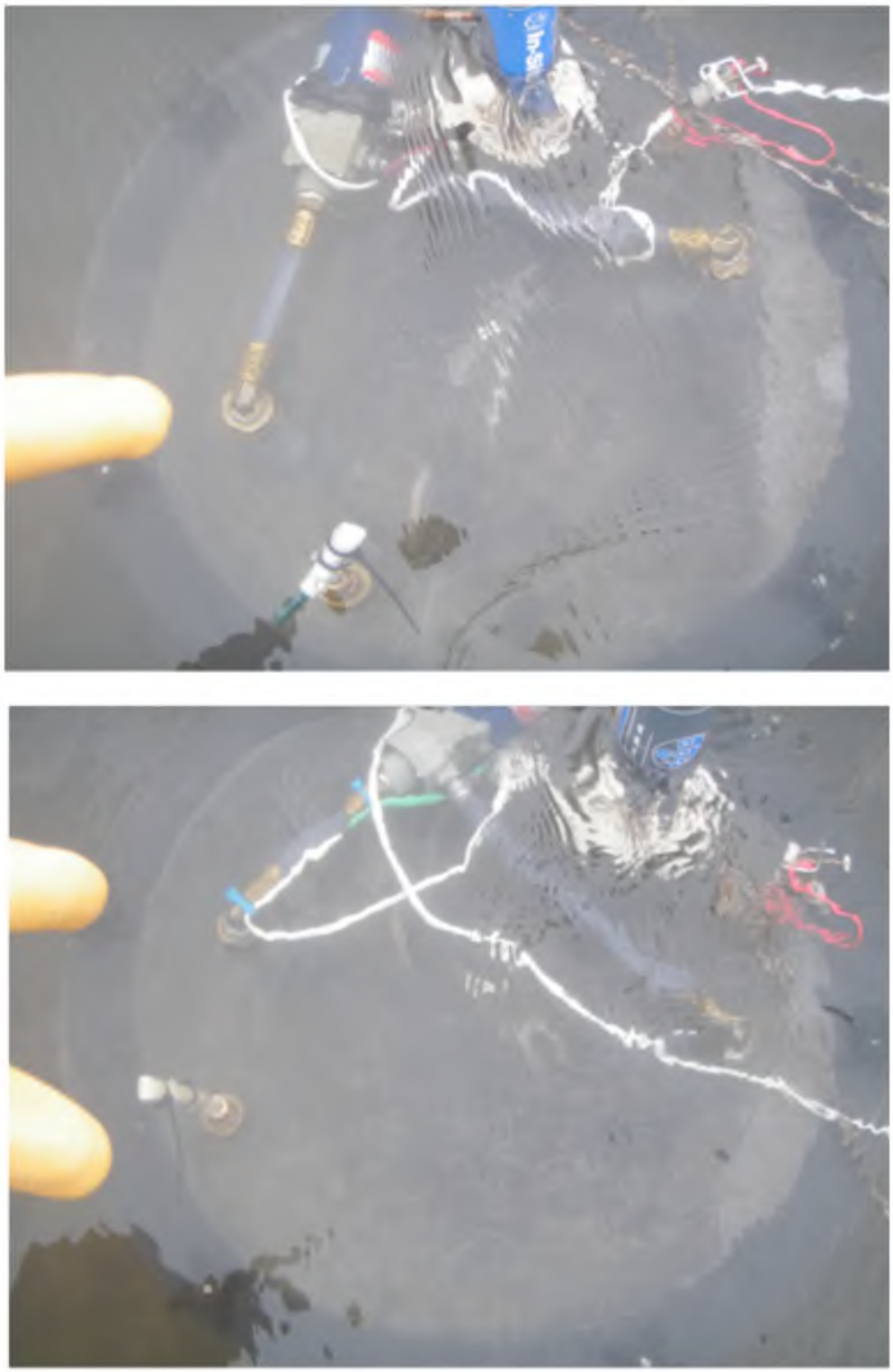

Fig. 15. Gas bubbles forming in closed chambers from supersaturated DO due to benthic photosynthesis (oxygen gas build up on right side of chambers)

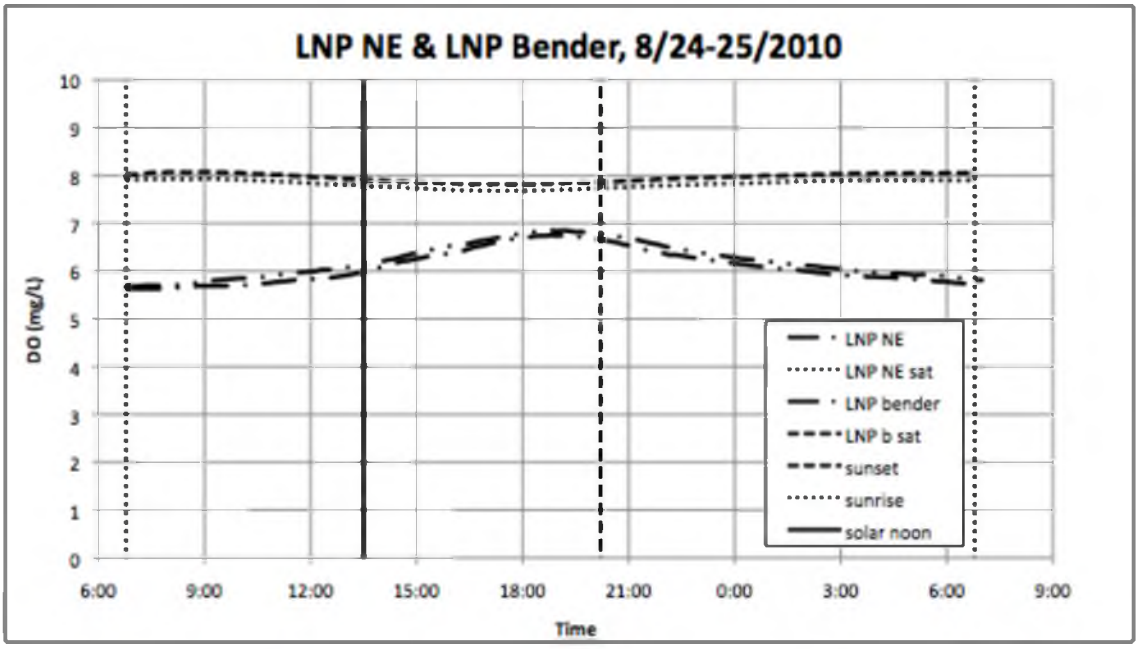

Fig. 16. Diurnal DO fluctuations in the Lower Jordan River

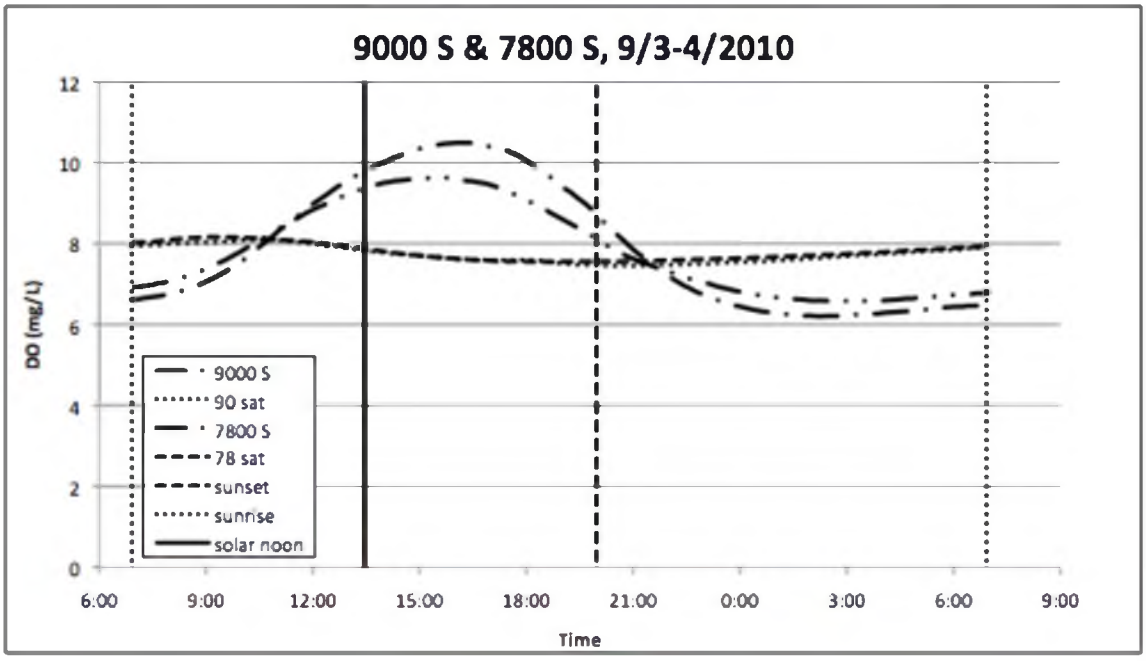

Fig. 17. Diurnal DO fluctuations in the Upper Jordan River

impaired in terms of DO. The chronic DO impairment assigned to Reach 1 by the Utah DWQ is a result of this diurnal DO deficit.

Dissolved oxygen is a byproduct of photosynthesis, and Fig. 17 shows no shortage of dissolved oxygen in the Upper Jordan River during the daylight hours. The 9000 S site reached 135% DO saturation in early September, which was greater than the 110% total gas supersaturation that will cause stress to the aquatic community (Bouk et al. 1976; USEPA 1986).

3.3.9 Eutrophication

> In its course from the source to the sea, the progressive eutrophication of a river water by drainage from cultivated and inhabited districts is an almost inevitable natural process. There are some rivers, however, which, by drainage from densely populated areas, receive excessive amounts of organic matter so that the river is said to be polluted. (Butcher 1947, pg. 186)

The word eutrophication originates from the Latin language meaning "good nourishment." The concept of eutrophication describes the general, yet predictable, degradation of a surface water due to excessive plant, algae, cyanobacteria, and biofilm growth resulting from anthropogenic loadings of nitrogen and phosphorus. Although primary production creates the OM necessary to support the aquatic food chain, if too much OM is produced, the aquatic system may not be able to "function" under the burden of the sequential OM decay.

The general ecological state of surface waters can be described using a trophic state index. In general, oligotrophic systems have very little nutrients and minimal aquatic biomass and tend to have very clear cold water. Oligotrophic systems are typically found in mountain lakes, and the headwaters of lotic systems and are socially "prized" for their perceived beauty and excellent cold-water fisheries. Mesotrophic

systems have more nutrients and aquatic biomass compared to an oligotrophic state. Eutrophic systems are characterized by high nutrient concentrations, poor visibility, high primary production, and variable DO concentrations (Wetzel 2001). Eutrophic ecosystems tend to by plagued by chronic nighttime DO deficits and may experience fish kills during acute events, such as an algal bloom die off or the turnover of a stratified lake where the hypolimnion has become anoxic. Hypereutrophic systems have very high primary production, low aquatic biomass diversity, and very low DO at night. Hypereutrophic systems tend to be very inhospitable due to temporary anoxia and become dominated by cyanobacteria (Chapman and Schelske 1997).

The idea of nutrient based eutrophication due to external anthropogenic loadings was originally identified, quantified, and confirmed in lake systems (Vollenweider 1971; Vollenweider 1976). During the 1990s, water quality managers agreed on the following list (Table 4) of observed changes in a lotic system indicating eutrophication (Hilton et al. 2006; Hilton and Irons 1998).

Water quality parameters commonly used to identify the degree of eutrophication, or trophic state, in lakes include total nitrogen (TN), total phosphorus (TP), Chlorophyll-a (Chl-a), and water clarity (turbidity or secchi depth) (Carlson 1977). Excessive

Table 4. Apparent cues eutrophication is occurring

1	Excessive growth of phytoplankton
2	Excessive growth of periphyton
3	Excessive growth of macrophytes (noted by flood defense engineers)
4	Reduced diversity of macrophytes
5	Shift from macrophyte dominance to benthic, filamentous or planktonic algae
6	Acute low DO events (typically at night)
7	Large pH fluctuations
8	Reoccurring cyanobacteria blooms
9	Water appears green or brown colored

phytoplankton and degraded water clarity are typically feedback from external nutrient loads. Rivers require a different perspective and deviations in sampling protocols to describe the trophic state compared to lakes (Dodds 2007). Table 5 provides a proposed trophic state index for streams that includes benthic characteristics (Dodds 1998). Instead of water clarity, benthic chlorophyll-a is used since rivers are much shallower than lakes, leading to the benthos playing a much larger role in GPP. This is evident by the max benthic Chl-a boundaries being 6–7 times larger than the sestonic, or suspended, fraction in a stream 1 meter deep (Table 5). In addition, water clarity becomes less important in rivers due to ample light reaching the benthos and the large amounts of inert total suspended solids (TSS) transported in lotic systems.

Applying Table 5 to the Jordan River, sestonic Chlorophyll-a (Chl-a) concentrations in the UJR were considered eutrophic in the August of 2006 while the LJR WC was mesotrophic (Utah DWQ 2013, pg. 31). Chl-a accounts for 1–2% of phytoplankton OM, and water column concentrations greater than 25 µg Chl-a/L are considered eutrophic in lakes (Dodds et al. 1998). Jordan River ambient dissolved nitrogen and phosphorus concentrations are typically higher than the eutrophic boundary downstream of WWTP discharges during base flows. In addition, the majority of the

Table 5. Stream Trophic State

	Stream trophic state boundaries	
parameter	oligotrophic-mesotrophic	mesotrophic-eutrophic
mean benthic Chl-a (mg/m^2)	20	70
max benthic Chl-a (mg/m^2)	60	200
sestonic Chl-a (µg/L)	10	30
TN (mg/L)	0.7	1.5
TP (mg/L)	0.025	0.075

Note: adapted from Dodds et al. 1998

phototrophic biomass identified in the Jordan River by Dr. Rushforth during the summer months was cyanophyta, a cyanobacteria also found in the upstream Utah Lake, which is another "apparent cue" of eutrophication suggested in Table 4 (Utah DWQ 2013, pg. 47).

Total phosphorus (TP) present primarily as dissolved phosphorus (DP) in lakes immediately following spring turnover has been shown to be directly related to summertime WC chlorophyll-a concentrations (mg-P:mg Chl-a = 1:1) (Dillon and Rigler 1974). The voluntary reduction in phosphate detergents by soap manufacturers in the 1970s from 12% to 5% decreased POTW effluent discharges by several mg-P/L, improving downstream WQ by reducing eutrophication (Lee et al. 1978; Litke 1999). Lake Erie, once known as the "dead lake" due to eutrophication has been reborn into a functioning waterbody in terms of its trophic state and fish communities following phosphorus abatement over a timescale of 3 decades (Ludsin et al. 2001). The diversion of POTW nutrient loads into Puget Sound led to the rehabilitation of the eutrophic Lake Washington while improving habitat for the freshwater lifecycle of native pacific salmon (Edmondson and Lehman 1981), although it should be noted that dilution is NOT the solution to macronutrient pollution, and the Puget Sound will now need to assimilate this additional nutrient loading. The United States Environmental Protection Agency (USEPA) has established a recommended limit for ambient total phosphorus (TP) concentrations of 0.1 mg-P/L for flowing waters, 0.05 mg-P/L for streams that enter lakes, and 0.025 mg-P/L in lakes and reservoirs (Mueller and Helsel 1996).

A recent report produced by the United States Geological Survey (USGS) reviewing nationwide surface and ground water quality data from 1992–2004 concluded

that ambient stream nutrient concentrations did not change appreciably even with a growing emphasis on nutrient removal from point sources. This was attributed to the large nonpoint source nutrient loadings that have yet to be adequately addressed, let alone identified (Dubroysky et al. 2010). Over 90% of the 190 urban and agricultural streams studied significantly exceeded nutrient background concentrations. Agricultural streams received the largest nutrient loads and had median total nitrogen (TN) concentrations of 4 mg-N/L, while urban streams had 1.5 mg-N/L. Total phosphorus concentrations were on average 0.25 mg-P/L in anthropogenically influenced surface waters. Natural background concentrations were 0.58 mg-N/L and 0.04 mg-P/L, roughly 6 times less, highlighting the amount of macronutrients humans add to our surface waters in both rural and urban settings under our current social practices (Dubroysky et al. 2010).

As of 2008, five states have adopted nutrient standards for all rivers and streams, and nine additional states regulate selected streams. The remaining 36 states, including Utah, have not adopted numeric criteria in the ongoing effort to improve and protect water quality (USEPA 2008).

3.4 Organic Matter (OM)

3.4.1 OM in the aquatic environment

Eutrophication results in the excessive production of organic matter (OM), but additional sources include the natural "background" instream production, terrestrial watershed loads, riparian vegetation loads, and urban stormwater loads. Organic matter can enter a stream through multiple pathways (Pusch et al. 1998):

- allochthonous point and nonpoint surface loads derived from terrestrial primary production

- dissolved organic carbon (DOC) from subsurface or hyporheic inputs
- downstream sediment migration during high flow events
- autochthonous primary production
- instream cycling of existing organic matter

The accumulation of excessive amounts of OM as a sediment sludge layer due to eutrophication and external OM loads is a long known problem and has been coined "benthal deposits" (Fillos and Swanson 1975). The "life cycle" of benthal deposits can be compared to the sludge production and stabilization occurring in a modern day biological wastewater treatment plant (WWTP) process where an external organic load (facility influent) initially undergoes a settling step similar to a depositional zone in a river. Microorganisms mineralize and recycle the settled OM into new viable organisms to perpetuate the process under aerobic, anoxic, and anaerobic conditions. Over time, the OM becomes more recalcitrant and the rate of carbon turnover slows. These processes are occurring within river sediments, and OM will become stabilized similar to WWTP biosolids following anaerobic digestion. Similar to anaerobic digesters, methane, ammonia, hydrogen sulfide, and other reduced chemicals are produced during anaerobic sediment decomposition, thereby transforming a portion of the OM into soluble and mobile oxygen consuming chemical species. As a result, SOD is ultimately a result of the "quality and quantity" of OM present in the surficial sediments.

3.4.2 OM size fractionation

In the most basic form of OM characterization, organic matter can be differentiated as dissolved organic matter (DOM) or particulate organic matter (POM). Organic matter classified as POM can be further characterized as fine particulate OM

(FPOM) and course particulate OM (CPOM) depending on the size of the particle. CPOM is defined as those particles larger than a 1 mm diameter, and FPOM includes all organic particles with diameters between 0.45 μm and 1 mm in size.

3.4.3 Dissolved Organic Matter (DOM)

Dissolved organic matter (DOM) is ever present in the aquatic environment and provides the carbon and electron source for heterotrophic microbes (Spencer et al. 2007; Baines and Pace 1991). DOM plays a crucial role in carbon and nutrient cycling as high molecular weight DOM is utilized for cell growth and maintenance while being further broken down to low molecular weight DOM (Amon and Benner 1996). The concentration of DOM in riverine systems varies on diurnal, seasonal, and annual cycles. Seasonal and annual variations are typically associated with hydrologic inputs, while daily fluctuations have been linked to primary production. It has been estimated that 13% of the inorganic carbon fixed to organic carbon during planktonic photosynthesis is lost to the ambient water through extracellular release (Baines and Pace 1991).

It is accepted that the DOM is responsible for the majority of the SOD associated with the decomposition of organic material, but over time CPOM is converted to FPOM and eventually DOM, resulting in a constant flux of DOM from organically enriched sediments (Hauer and Lamberti 2007, pg. 273).

3.4.4 Particulate organic matter (FPOM, CPOM, and LWD)

CPOM can be present in pockets or layers within the sediments due to seasonal loadings and erosion patterns. Autumn leaf loadings to a stream can become buried beneath inorganic sediments to be mineralized throughout the following year (Pusch et al.

1998). Highly recalcitrant large woody debris (LWD) does not directly contribute to DO dynamics in running waters. Wood requires years to decades to decompose due to its high lignin content and low surface area to volume ratio (Melillo et al. 1983; Webster and Benfield 1986). LWD is a valuable aquatic habitat in terms of substrate for biofilm growth and habitat for higher aquatic life forms.

3.4.5 Terrestrial OM (litterfall)

Terrestrial forests deposit 200–800 g-OM/m^2/year as litterfall and production rates are dependent on the availability of sun and water, which are directly related to latitude and precipitation (Meentemeyer et al. 1982). Litterfall includes all annual loadings of OM derived from trees and shrubs including leafs, bark, seeds, and branches. The vast majority, over 70%, of terrestrial litterfall occurs during autumn as leaf litter (Meentemeyer et al. 1982). The role of seasonal organic matter loads associated with autumn leaf litter accounted for 44% of the annual organic load in a section of the forested Bear Brook, NH (Fisher and Likens 1973). Over 70% of the OM loads to three headwater steams were from leaf fall, but only 3% of OM exports were CPOM, indicating a high conversion of CPOM to FPOM to DOM (Wallace et al. 1995; Cushing et al. 1993). In the deciduous forest streams of Eastern U.S., 86% of the organic carbon load was CPOM, and 58% of the annual leaf litter load occurred in autumn (Webster et al. 1995).

Initial leaf decomposition of dry leafs can occur rapidly with 17% of the carbon being leached into the water column as DOM in the first 3 days (Mcdowell and Fisher 1976). Up to 25% of the mass of dry leafs can leach within 24 hours of being submerged in water, while fresh cut green leafs do not leach as rapidly (Gessner et al. 1999; Webster

and Benfield 1986). The leaf litter decomposition rate has been estimated to be 1 year in most lotic systems, resulting in a steady-state leaf litter deposition/decomposition process over an annual cycle (Fisher and Likens 1973).

Leaf litter will undergo structural decomposition and mineralization carried out by a consortium of macroinvertebrates, fungi, and bacteria with dominant populations dictated by the prevailing ambient environmental conditions (Gessner et al. 1999). In Portugal's urban Ave River, fungi were responsible for 34% of leaf carbon losses, while bacteria removed 7.5% in alder leaf packs over a 42-day instream incubation period (Pascoal and Cassio 2004). The majority of leaf decomposition in urban streams was found to be a result of the microbial community, not macroinvertebrate shredders (Imberger et al. 2008). Within a couple days, submerged leafs are initially colonized by fungus followed by bacteria, whereas macrophyte debris are initially colonized by bacteria (Webster and Benfield 1986).

3.4.6 Urban OM

The majority of nutrient spiraling and CPOM degradation studies have been conducted in small streams (1^{st} to 3^{rd} order) in relatively undisturbed aquatic environments (Ensign and Doyle 2006). The 4^{th} order Jordan River fits into neither of these categories, but it does receive urban stormwater conveyed via creeks. The macroinvertebrate shredders indicative of high water quality (WQ) are not present in the fine sediments of the LJR, but can be found among the gravel and cobbles present in the UJR. Urban streams are typically dominated by disturbance-tolerant macroinvertebrates composed primarily of oligochaetes and chironomids, or aquatic worms and midges (Walsh et al. 2005).

Urban environments are largely impervious resulting in dust, organic matter, and pollutants being transported to the downstream surface water through stormwater conduits (Heaney and Huber 1984). Secondary growth of fungus and biofilms will colonize and degrade terrestrial OM during dry periods in stormwater conveyance systems and can flush out during rain events (Ellis 1977).

Stormwater conveyance systems typically bypass the riparian zone where nutrient removal and sediment retention naturally occur, thereby increasing pollutant loads to the receiving stream (Hatt et al. 2004). Benthic leaf litter in an urbanized stream with an efficient stormwater conveyance system was composed primarily of nonnative tree species planted along streets in Australia (Miller and Boulton 2005). The specie of leaf influences the rate of OM turnover, and nonnative species can influence benthic metabolism since macroinvertebrate diversity is very low in many urban streams. This lack of aquatic macroinvertebrate diversity can result in an overloading of OM to the system due to the lack of higher life forms capable of preconditioning additional substrate (Ryder and Miller 2005). Through urbanization, the Salt Lake valley has been ordained with nonnative deciduous shade trees lining impervious streets. This seasonal urban stormwater load of leaf organic matter may add to the organic loading to the Lower Jordan River.

3.5 Nutrient Cycling and Transformations

3.5.1 Aquatic nutrient dynamics

Fig. 18 provides a general overview of organic matter (OM) and nutrient cycling occurring in a lotic system in the water column and at the sediment–water interface. The following list describes the nutrient dynamics shown in Fig. 18.

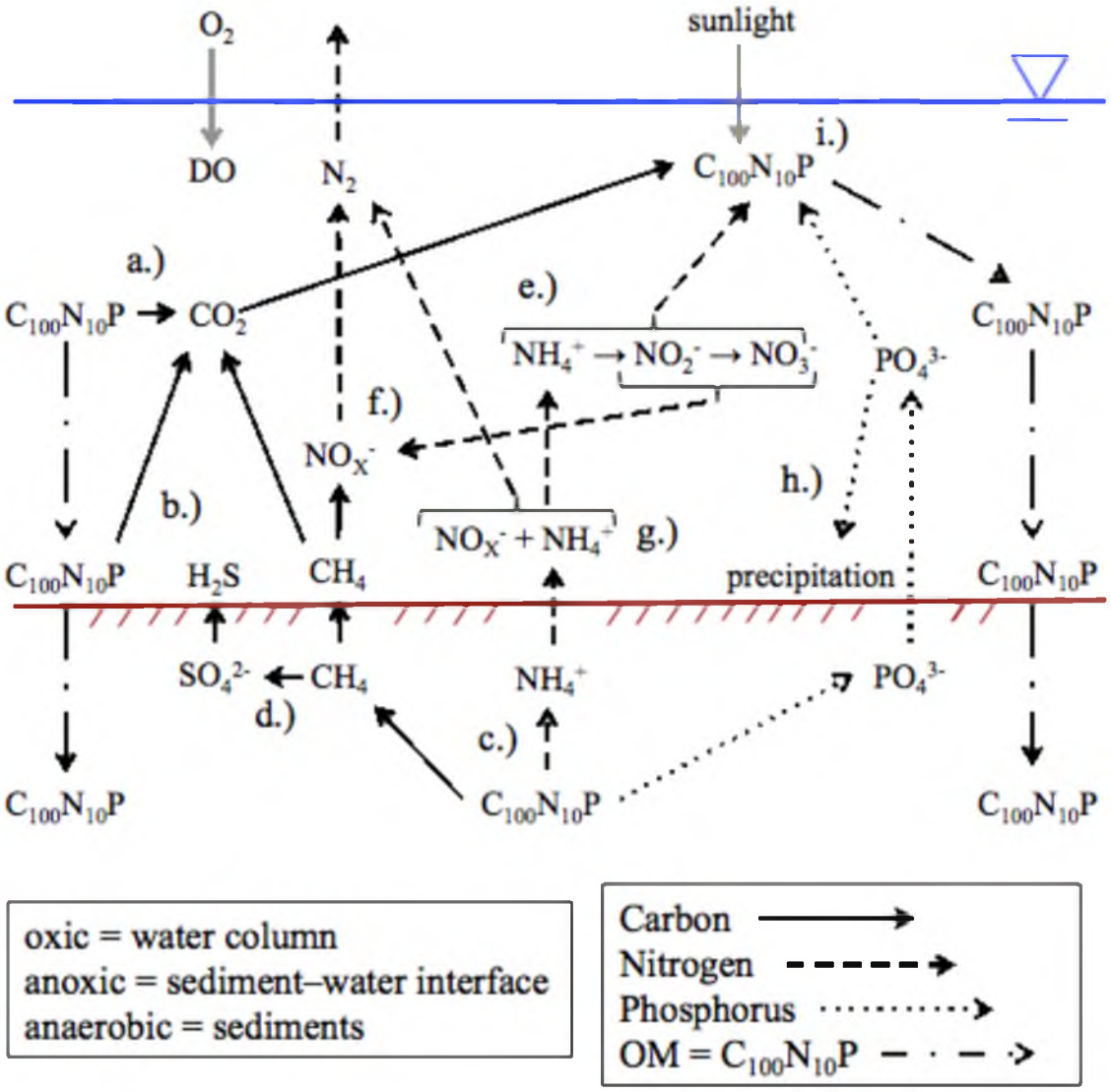

Fig. 18. Nutrient cycling dynamics

a.) biochemical oxygen demand (BOD), sestonic OM is oxidized in the water column and phytoplankton respire

b.) sediment oxygen demand (SOD), OM settles and is oxidized in the benthos and periphyton respire

c.) sediment anaerobic decay, OM becomes buried and a portion of the organic-C is reduced to methane and carbon dioxide while releasing

ammonium and phosphate to the water column as a sediment flux

d.) the low oxidation reduction potential (ORP) of the sediment pore water, fueled by OM decay, can lead to the reduction of other compounds (methane and other reduced chemicals diffuse out of the sediments contributing to SOD)

e.) nitrogenous biochemical oxygen demand (NBOD), Ammonium is oxidized to nitrate in the water column

f.) denitrification can occur at the sediment–water interface with methane being the readily biodegradable carbon and electron source (rbCOD)

g.) anaerobic ammonium oxidation (ANAMMOX) utilizes nitrite or nitrate and ammonium to produce N_2 gas

h.) orthophosphate may precipitate or sorb to the sediments in the alkaline Jordan River

i.) instream primary production cycles dissolved nitrogen and phosphorus into an organic form to start the process over, see step a.)

3.5.2 Particulate OM decay into dissolved nutrients

In a lotic aquatic environment, particulate OM (POM) is physically broken down with a portion of the POM and DOM being swept downstream and the remainder being consumed by heterotrophs producing additional OM and CO_2. The cycling of carbon (C), nitrogen (N), and phosphorus (P) associated with OM decay in the aquatic environment is referred to as nutrient spiraling (Newbold et al. 1981; Newbold et al. 1982; Ensign and Doyle 2006).

The majority of the carbon, nitrogen, and phosphorus cycling is a result of the

element entering an organic phase through direct assimilation or other biologically mediated processes. As a result, biologically active environments are conducive to nutrient cycling, and the preferred energy source for microbes living in the sediments are reduced carbon (Fischer et al. 2002). OM fuels the microbial community and acts as a stockpile of nutrients to become biologically available over time as the OM is degraded.

3.5.3 Methane (CH_4)

An estimated 37% of the current methane loads to the atmosphere are associated with natural systems, with wetlands being the largest source (USEPA 2010). Rivers and estuaries contribute 0.9% of the estimated natural loadings and 0.3% of total loadings to the atmosphere (USEPA 2010). The majority of natural sources of methane are biologically mediated resulting from methanogenesis occurring in wet environments with low redox potential and a source of biodegradable OM. These environments include surface water sediments, wetlands, WWTPs, landfills, rice paddies, and the guts of ruminants (four-stomached animals). Other major sources of methane to the atmosphere include the extraction of natural gas, fossil fuel combustion, and wildfires (USEPA 2010).

Once methane has entered the atmosphere, a single molecule is estimated to last 9–12 years until being oxidized to CO_2 in the troposphere (USEPA 2010). Methane is an important greenhouse gas influencing climate change and has a global warming potential 25 times greater than CO_2 over a 100-year period. The current atmospheric concentration of 1.7 ppmV methane is twice as high compared to preindustrial revolution concentrations. Carbon dioxide is currently at 400 ppmV, or 0.04%, and was 280 ppmV prior to the industrial revolution.

Methane is soluble in water at 1 atm (100%) at standard temperature and pressure (STP) to a concentration of 22 mg-CH_4/L. Methane is poorly soluble and has a Henry's equilibrium constant k_H = 1.3x10^{-3} (M/atm) (Stumm and Morgan 1996).

$$k_H = {[C_a]}/{p_a} \qquad (1)$$

k_H = Henry's equilibrium constant
$[C_a]$ = molar concentration dissolved in water
p_a = partial pressure in gas phase

For perspective, if 1 liter (L) of water saturated with dissolved methane was placed in a 2 L airtight container (i.e., 1 L water and 1 L headspace) and allowed to come into equilibrium at STP, 30 parts of methane would enter the gas phase for every 1 part remaining dissolved in the liquid. The k_H values for other common atmospheric gases are provided in Table 6 along with the relative percentage of the atmosphere and corresponding dissolved concentrations at STP in contact with atmospheric air. Atmospheric methane dissolving into surface waters results in negligible BOD since the atmospheric concentration is so low. Dissolved methane found in surface waters is typically associated with anaerobic decay occurring in the sediments. Hydrogen sulphide is the most soluble gas in Table 6 and when found in surface water suggests sediment

Table 6. Equilibrium constants of select compounds

	$K_{25°C}$ (M/atm)	% atmos	equalibrium (mg/L)
CH_4	1.29x10-3	0.00017	0.00004
O_2	1.26x10-3	21	8.5
N_2	6.61x10-4	78	14.4
H_2S	1.05x10-1		

Adapted from Stumm and Morgan 1996

OM decomposition and low redox potentials. Hydrogen sulphide can be smelled when silty sediments are physically disturbed in the LJR.

3.5.4 Diffusion and ebullition

Methane fluxes at the sediment–water interface can be very different than at the water–atmosphere interface due to water column oxidation, advection transport, and ebullition (Huttunen et al. 2006). Over 95% of the sediment derived methane flux across the air-water interface into the atmosphere in a hypereutrophic lake was due to ebullition, not sediment diffusion (Casper et al. 2000). In a study of eutrophic shallow lakes, 40–60% of atmospheric methane fluxes were due to ebullition (Bastviken et al. 2004). Increases in sediment methane ebullition have been observed in lakes during periods of quickly dropping barometric pressure (Casper et al. 2000; Bastviken et al. 2004). Deeper water column depths result in sediments that release less methane as ebullition, and shallow water column depths of 0–2 meters resulted in the highest swamp gas ebullition fluxes (Bastviken et al. 2004).

3.5.5 Nitrogen

As microbes utilize DO during the oxic degradation of organic matter, an additional DO demand is required for the subsequent oxidation of ammonium associated with organic nitrogen (Fair et al. 1941). The oxygen demand required for nitrification can add an additional 30% to the oxygen demand associated with only organic carbon. Ammonium produced during the decomposition of organic material within the sediments requires 4.57 g-O_2/g-N to complete the two-step biological nitrification process ($NH_4^+ \rightarrow NO_2^- \rightarrow NO_3^-$) according to the following stoichiometric equations (Tchobanoglous et al.

2003):

$$\text{(Nitritation)} \quad 2NH_4^+ + 3O_2 \rightarrow 2NO_2^- + 4H^+ + 2H_2O$$

$$\text{(Nitratation)} \quad 2NO_2^- + O_2 \rightarrow 2NO_3^-$$

$$\text{(combined Nitrification)} \quad NH_4^- + 2O_2 \rightarrow NO_3^- + 2H^+ + H_2O$$

The first metabolism, nitritation, is carried out by autotrophic nitrosobacteria, also known as ammonia oxidizing bacteria (AOB) utilizing 3.43 g-O_2/g-NH_4^+-N to produce nitrite. Nitrite is toxic in the aquatic environment and does not accumulate in healthy lotic systems due to the rapid oxidation to nitrate by autotrophic nitrobacteria, or nitrite oxidizing bacteria (NOB). The oxidation of nitrite, or nitratation, requires 1.14 g-O_2/g-NO_2^--N. Ambient nitrite concentrations in surface waters are typically less than 0.002 mg NO_2-N/L due to the close proximity in the environment of these two different bacteria (Lewis et al. 1986). Nitrate is the most common form of dissolved nitrogen found in aerobic surface waters. Nitrate will eventually be reduced or bioassimilated by phototrophs and bacteria during cell growth and can be utilized as an electron acceptor under low DO conditions during microbial denitrification.

Methane produced in organically enriched sediments can be utilized as a readily biodegradable substrate (rbCOD) for some heterotrophic denitrifying bacteria. This results in a much lower theoretical DO requirement of 1.71 g-O_2/g-N for the complete nitrification and denitrification process utilizing ammonia and methane produced during the anaerobic decomposition of OM (Chapra 2008). The following equations provide stoichiometric equations for methane driven denitrification, and the combined processes of nitrification and denitrification utilizing methane from decaying OM:

$$^{5}/_{8}CH_4 + HNO_3 \rightarrow {}^{5}/_{8}CO_2 + {}^{1}/_{2}N_2 + {}^{7}/_{4}H_2O$$

$$NH_3 + {}^{3}/_{4}O_2 \rightarrow {}^{1}/_{2}N_2 + {}^{6}/_{4}H_2O$$

This is important because methane can be oxidized using either nitrite or nitrate as an electron acceptor instead of DO, thereby decreasing the ambient DO demand required for the direct oxidation of both methane and ammonia independently (Chapra 2008, pg. 459). This results in an additional nitrogenous oxygen demand of roughly 11% of the carbon oxygen demand, compared to 30% when nitrate is not used as an electron acceptor during methane oxidation. This is important in degraded urban rivers since nitrate is typically in abundance due to POTW discharges and can be utilized to oxidize sediment produced methane.

3.5.6 Phosphorus

Most aquatic systems are capable of storing large amounts of phosphorus (P) within the sediments and act as a P sink as sedimentation ensues. The storage and/or release of sediment bound phosphorus is influenced by sediment mineralogy, sediment OM content, ambient water chemistry, and the benthic community (Wetzel 2001, pg. 245). In hard water rivers, the solubility of inorganic phosphorus decreases as pH exceeds 8.5, and precipitation can be driven by photosynthesis in highly productive environments (Olsen et al. 2009).

There are four principal methods that phosphorus may enter the sediments of a surface water:

- sedimentation of phosphorus rich minerals
- sorption/precipitation of inorganic P with iron, manganese, clays,

carbonates, and amorphous oxyhydroxides

- bioassimilation of dissolved P via aquatic biota
- sedimentation of organic P from both autochthonous and allochthonous sources

The sedimentation of phosphorus rich minerals is typically associated with watershed geology. The immobilization of dissolved P through sorption and precipitation is influenced by sediment geochemistry and ambient water quality. The bioassimilation of dissolved P is associated with cell growth. The death and subsequent sedimentation of phototrophs and autochthonous OM introduced into the surface water removes phosphorus from the water column, but contributes to SOD and positive sediment phosphate fluxes over the long term. All aquatic life relies on phosphorus, but excessive availability is linked to eutrophication (Marsden 1989).

3.5.7 C:N:P ratios

Oceanic planktonic biomass samples have very similar carbon, nitrogen, and phosphorus molar ratios and can be generalized according to the Redfield Ratio expressed in moles (Table 7) (Redfield 1934). The significance of this observation was that the ambient oceanic water column C:N:P molar ratio was 106:16:1, the same as the ratios found in many of the living phytoplankton. The C:N:P molar ratios found in Table 7 are organized in terms of nitrogen enrichment, with WWTP influent containing the highest concentration of organic nitrogen and wood having the least.

Organic matter found in organically enriched river sediments and sludge are composed of 3–5% organic nitrogen in terms of dry mass (Baity 1938; Fair et al. 1941; Rudolfs 1932; McDonnell and Hall 1969). Terrestrial soils have a C:N ratio of 14 while

Table 7. Organic C:N:P molar ratios found in the environment

	organic C:N:P molar ratios				
	C	N	P	C:N	reference
WWTP influent	53	13	1	4	Tchobanoglous et al. 2003, pg. 558
WWTP bacteria	65	13	1	5	Tchobanoglous et al. 2003, pg. 558
oceanic algae	106	16	1	7	Redfield 1934
soil bacteria	60	7	1	9	Cleveland and Liptzin 2007
river mud	117	10		12	Rolley and Owens 1967
grass clippings	>120	10		>12	Humanure Handbook 2005
terrestrial soil	186	13	1	14	Cleveland and Liptzin 2007
cow manure	190	10		19	Humanure Handbook 2005
foliage	1,212	28	1	43	Mcgroddy et al. 2004
leaf litter	3,007	45	1	67	Mcgroddy et al. 2004
cardboard	>4,000	10		>400	Humanure Handbook 2005
wood	>5,600	10		>560	Humanure Handbook 2005

river and estuarine muds tend to be more nitrogen enriched with a ratio of 11.7 (Rolley and Owens 1967). Soil bacteria have a slightly lower C:N ratio of 8.5, and wastewater bacteria typically have C:N ratios around 5:1, while POTW influent has an average ratio of 4:1 (Cleveland and Liptzin 2007; Tchobanoglous et al. 2003, Table 3–15, pg. 558). It is worth noting that the macronutrient N:P ratios for WWTP bacteria are the same as the influent wastewater used to grow the microbes during biological wastewater treatment, similar to Redfield's observation that plankton have similar stoichiometry to the "soup" they grew in.

CHAPTER 4

MATERIALS AND METHODS

4.1 Sediment Oxygen Demand (SOD)

4.1.1 SOD sampling locations

Sediment oxygen demand (SOD) sampling locations were preselected based on hydraulic reaches, tributaries, stormwater outfalls, and the proximity to WWTP point discharges. Recommendations from the Utah Division of Water Quality (Utah DWQ) and other stakeholders were incorporated into site selection. A list of sampled sites for SOD and a short description is provided in Table 8.

4.1.2 SOD chamber details

Three aluminum SOD chambers, one Control and two Testing, were utilized in the Jordan River SOD study. A fourth chamber was brought to each site as a spare in the case of pump failures or other unforeseen circumstances. The top section of each chamber consisted of a lid housing the pump, plumbing, water sampling tube, water quality probe connection, and attachments for ropes used to lift the SOD chamber out of the water. A submersible pump was mounted on each chamber to circulate water inside the chamber at a predetermined flow rate of 11 L/min at an average flow velocity of 8 cm/sec. The influent and effluent ends of the plumbing were located inside the chamber and were connected to a polyvinyl chloride (PVC) water distribution system. The

Table 8. SOD sampling locations and descriptions

2009, 2010, 2011, 2012, and 2013 SOD Study Sites			
Mile	Reach	Site Name	Description
0.1	1	Burnham	100 m upstream of Burnham Dam, end of Reach 1
2.8	1	LNP NE	0.3 miles downstream of South Davis WWTP
3	1	LNP SW	350' downstream of South Davis WWTP
3.2	1	Cudahy Ln	450' upstream of South Davis-S WWTP
8.9	2	300 N	downstream of City Cr./stormwater
10.7	3	700 S	downstream of 900 S stormwater/tributary discharge
11.2	3	900 S-N	175' downstream of the stormwater discharge
11.3	3	900 S-S	185' upstream of the stormwater discharge
13.1	3	1700 S	downstream of the Surplus Canal diversion dam
13.7	3	2100 S	350' downstream of the Surplus Canal diversion
14.3	4	2300 S	1000' upstream of the Surplus Canal diversion
14.8	4	2600 S	1,350' downstream of Mill Cr.
15	4	2780 S	downstream of Mill Cr. (E and W banks)
16.8	4	3650 S	above Mill Cr. and below Big Cottonwood Cr.
20.9	4	5400 S	200' upstream of the 5400 S bridge
24	5	7600 S	70' downstream of the flow control structure
24.1	5	7800 S	100' upstream of the 7800 S bridge
26	6	9000 S	100' upstream of the 9000 S bridge
34.1	6	SR 154	upstream of the SR 154 bridge
46.2	7	14600 S	0.65 miles upstream of the 14600 S bridge
52	8	US-73	0.4 miles upstream of the US-73 bridge

distribution pipe, or diffuser, contained 10 small holes to evenly distribute the re-circulated flow within the chamber

Both the Control and Testing SOD chamber configurations were identical in construction and operation except for the bottom sections. The lids were attached to the chambers via coupling flange, bolts, and a neoprene gasket. In the Control chamber configuration, the bottom of the chamber was sealed to measure oxygen consumption

associated with the water column only. In the Testing SOD chamber configuration, the bottom was open and the river water contained in the chamber was in constant contact with the river sediments during the experimental period. Thus, the Testing SOD chamber measured DO consumption associated with the sediments as well as in the water column. Before use in the field, each chamber was carefully tested in the lab for water tightness and the ability of the submersible pump to effectively circulate water within the chamber. Lab scale testing was accomplished using a large livestock-watering trough filled with tap water.

The original Control chamber (which measured WC_{dark}) had a working volume of 44 liters, and the Testing SOD chambers had working volumes of 38 liters. This discrepancy in volumes is a result of the additional space provided in the Control chamber that is not seated 1½" into the sediments. The SOD calculation accounts for these variations in volume when calculating SOD fluxes. A smaller Control chamber having a volume of 38 L replaced the larger original chamber in 2010. When deployed, the Testing SOD chambers encapsulated a sediment area of 0.16 m^2. Fig. 19 provides a general schematic of the SOD chambers deployed.

Water quality probes, or sondes (probe in French) were provided by the Utah Division of Water Quality. The probes utilized were In-Situ Inc. model Troll 9500, capable of measuring DO, temperature, conductivity, pH, and barometric pressure. All sensors were utilized during sampling, but only DO and temperature were used directly while calculating oxygen demands. Conductivity was used to determine when the probes were placed in the water and when they were taken out. The probes were quality control checked and calibrated, if necessary, in the lab before all sampling events.

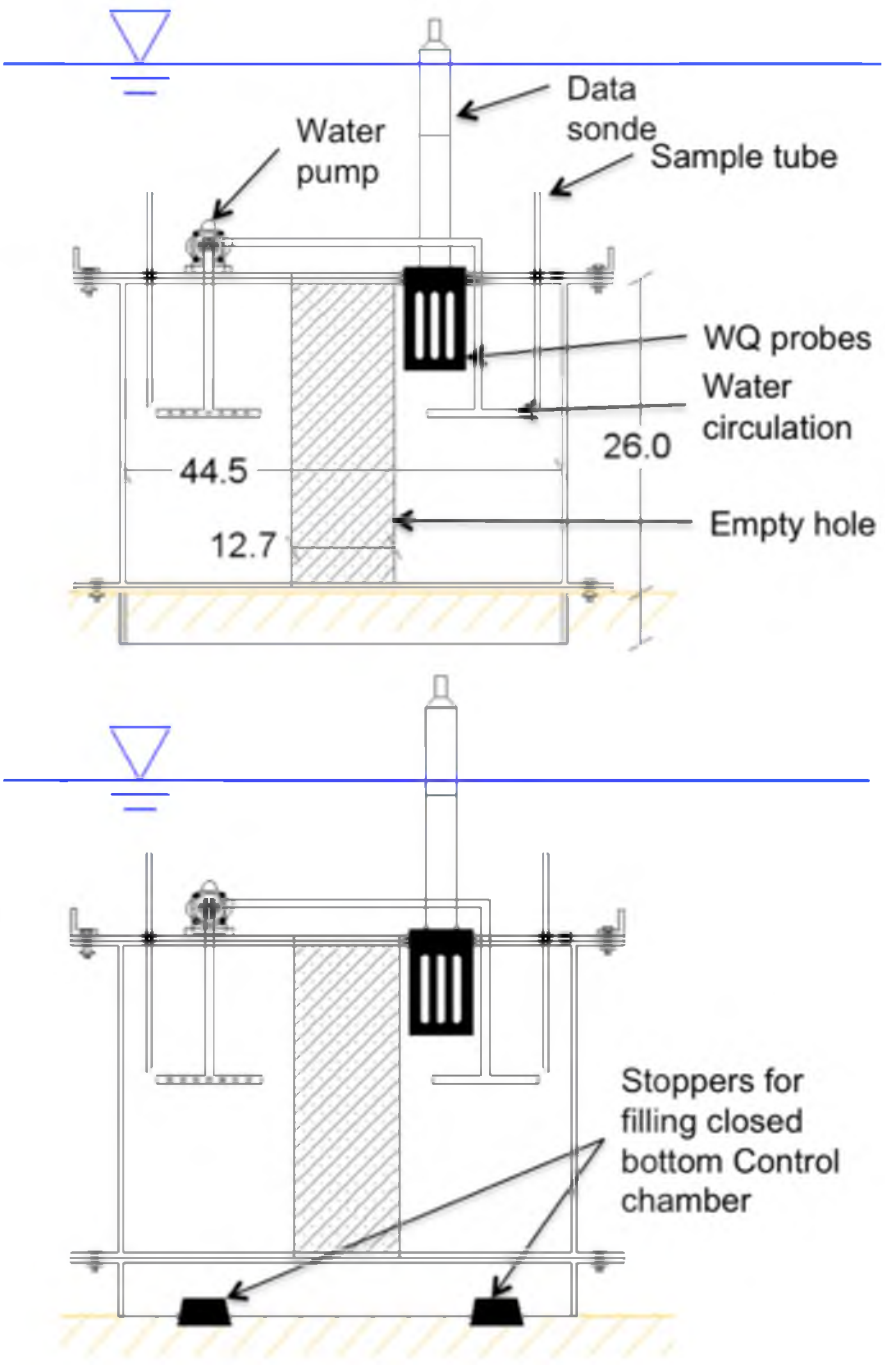

Fig. 19. Testing (top) and WC (bottom) SOD chamber schematics
Note: dimensions in cm

4.1.3 SOD chamber deployment

SOD sampling locations were positioned on the inside of river bends and along straight sections of the Jordan River. Safety issues were addressed by sampling on the inside of meanders since the fast flowing deep water (thalweg), steep riverbanks, and associated riverbank undercutting were avoided. Sampling locations were chosen to represent the sediment substrate characteristics corresponding to that particular stretch of the Jordan River. For example, if the typical sediments were silty muck, sand, or gravel, then the chambers were deployed in sediments having those characteristics.

A great deal of time was allotted to walking both the riverbanks and within the Jordan River proper to locate suitable SOD sampling locations that were reasonable representations of the particular section of river under consideration. The time spent walking the Jordan River allowed for a better understanding of the sediment characteristics and provided an opportunity to locate any obstructions that may cause potential safety issues or SOD chamber deployment problems such as rebar, barbed wire, construction debris, riprap, shopping carts, submerged logs, etc.

After the exact location of SOD chamber deployment was determined, the water quality probes were turned on for data collection. The author deployed all SOD chambers to minimize sediment disturbances and to provide consistency in the chamber deployment protocol.

The Control chamber was placed first due to the additional time required for the Control chamber to reach a stable DO reading. Two large stoppers were removed from the bottom of the Control chamber, and the chamber was immersed in the river sideways and allowed to fill with ambient river water. Deviations in the filling angle were required

at sites that were too shallow to completely submerge the Control chamber perpendicularly. If possible, the Control chamber was filled sideways in a deeper section of the river immediately downstream or off to the side to minimize sediment disturbances.

After filling the Control chamber with river water, the chamber was flipped upside down while keeping the chamber completely submerged. The pump was turned on to purge any trapped air out of the pump and associated plumbing. After 10–15 seconds of running the pump, the pump was turned off and any remaining air in the Control chamber was allowed to escape by removing a small stopper located on the bottom outer edge of the chamber in the tilted position. After all air had been removed from the Control chamber, all three stoppers were replaced while keeping the Control chamber completely submerged. It is necessary to remove all air from the chambers if accurate oxygen depletion rates are to be measured. Air left in the system contains oxygen that will slowly dissolve into the chamber water, leading to an underestimation of respiration.

The Control chamber was then carefully placed on top of the sediments while taking great care not to disturb the surrounding area. Depending on the slope of the river bottom and flow velocities, the Control chamber was attached to a wood stake hammered into the sediments to stop downstream chamber drift. After the Control chamber was situated, the water quality probe was submerged into the water, gently swirled to remove air bubbles attached to the probes, and screwed into the probe housing on the Control chamber lid. After placement of the water quality sonde, the water circulation pump was turned on for the remainder of the testing period.

Similar to the Control chamber, the two Testing chambers were filled with river

water and flipped upside down while running the pumps to remove any air trapped in the pump and plumbing. After 10–15 seconds, the pumps were turned off and the Testing chambers were then flipped right side up while keeping the chambers submerged. The Testing chambers were deployed upstream of the Control chamber to ensure undisturbed sediments. After placing the Testing chambers into the sediments by hand and body weight, proper placement was confirmed by carefully checking the coupling flange connecting the bottom sections of the Testing chambers. Seating the chambers to a depth of 1½" was achieved by setting the coupling flange of the chambers parallel to the surrounding sediments.

Obstructions such as rocks, riprap, logs, urban garbage, etc., were commonly encountered, and the Testing chamber was redeployed upstream to ensure a proper seal in the river sediments. After seating the two Testing chambers, the water quality probes were installed and the pumps were turned on. To ensure the pumps were working correctly during the testing period, the pumps were periodically touched by hand, foot, or stick to feel for vibrations indicating the pumps were on.

4.1.4 Calculation of SOD and WC_{dark}

The sediment oxygen demand (SOD) fluxes and dark water column respiration (WC_{dark}) rates were calculated using the following equations (Butts 1974; Butts 1978; Murphy and Hicks 1986; Chiaro et al. 1980):

$$SOD = 1.44\left({}^{V}/_{A}\right)(b_{SOD} - b_{WC}) \qquad (2)$$

$SOD = Sediment\ Oxygen\ Demand\ \left({}^{g}/_{m^2\ day}\right)$
$1.44 = unit\ conversion\ \left({}^{mg}/_{L\ min} \rightarrow {}^{g}/_{L\ day}\right)$
$V = volume\ of\ SOD\ and\ WC\ chambers\ (38\ L)$

$A = sediment\ area\ within\ the\ chamber\ (0.16\ m^2)$
$b_{SOD} = bulk\ DO\ depletion\ rate\ in\ SOD\ chamber\ \left({}^{mg}/_{L\ min}\right)$
$b_{WC} = DO\ depletion\ rate\ in\ WC\ chamber\ \left({}^{mg}/_{L\ min}\right)$

$$WC_{dark} = 1440(b_{wc}) \quad (3)$$

$WC_{dark} = DO\ depletion\ rate\ in\ WC\ chamber\ \left({}^{g}/_{m^3\ day}\right)$
$1440 = unit\ conversion\ \left({}^{mg}/_{L\ min} \rightarrow {}^{g}/_{m^3\ day}\right)$

WC_{dark} is the volumetric oxygen consumption rate measured in the Control chamber and represents the dark respiration associated with the water column. This parameter is comparable to a 1-day biochemical oxygen demand (BOD) test having no nitrification inhibitor. SOD is expressed as a two-dimensional flux associated with the sediments and benthos since the oxygen demand required by the water column has been subtracted. The working volumes and sediment areas were constant since the Testing chambers were placed to a uniform depth of 1½". The SOD fluxes were initially calculated for both of the Testing chambers and then averaged for further analysis and oxygen mass balances. A flow diagram for the procedures used to calculate SOD is provided in Fig. 20.

A prior warning concerning the presentation of the dark respiration parameters SOD and WC_{dark} needs to be addressed. SOD is the amount of oxygen utilized by the sediments, which is typically represented in the literature as a positive flux. Alternatively, from the perspective of the river water and when performing DO mass balances, this is a loss of DO and will be a negative flux. As a result, many of the graphs in this dissertation represent SOD and WC_{dark} as positive values since this was easier to visualize, but all tables and mass balances are from the perspective of the ambient water column and are

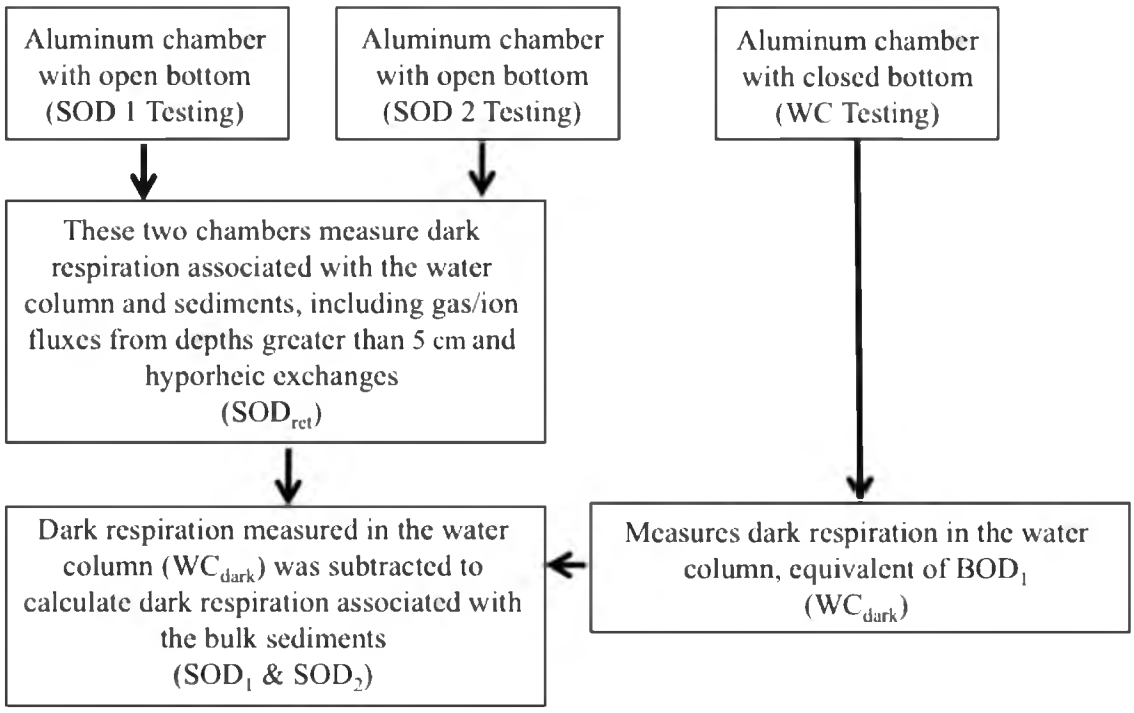

Fig. 20. Dark respiration (SOD and WC_{dark}) calculation flow diagram

presented as negative values.

SOD values found in literature are typically normalized to 20 °C (SOD_{20}) using the following modified van 't Hoff form of the Arrhenius equation based on ambient water temperature (Berthelson et al. 1996; Chapra 2008, Table 2.3):

$$SOD_{20} = \frac{SOD}{\theta^{t-20}} \qquad (4)$$

$SOD_{20} = SOD\ normalized\ to\ 20\ ℃$
$t = observed\ temperature\ (℃)$
$\theta = temperature\ normalization\ coefficient$
$1.065 = (Berthelson\ et\ al. 1996)$
$1.08 = (Chapra\ 2008)$
$1.047 = WC\ BOD\ decomposition\ (Chapra\ 2008)$

The ambient DO deficit is a result of various biogeochemical activities occurring in the water column and at the sediment–water interface. Through the use of chambers,

these parameters are decoupled, and the percent of the ambient oxygen demand associated with the sediments ($\%_{SOD}$) can be calculated accordingly:

$$\%_{SOD} = \left(\frac{SOD}{SOD + (WC_{dark}) * d}\right) 100 \quad (5)$$

$$d = mean\ river\ depth\ at\ the\ sampled\ site\ (m)$$

The mean river-wide depth at each site was calculated after mapping river cross sections in the Lower Jordan River and estimated in the Upper Jordan River by walking across the river while noting depth.

4.1.5 Utah Lake SOD

SOD and WC_{dark} measurements were performed in Utah Lake to characterize the sediments and water column in the large shallow waterbody draining to the Jordan River. Fig. 21 provides a general overview of Utah Lake, the surrounding topography, municipalities, and SOD sampling locations.

The site names, geographical coordinates, USEPA assigned STOrage and RETrieval (STORET) sampling identification numbers, and dates sampled are provided in Table 9. SOD measurements in the Jordan River did not require special arrangements due to the shallow water depths at most locations. However, the water depth in Utah Lake was 4 meters at some locations. Utah Lake SOD sampling required the use of SCUBA gear, a custom made sampling barge to deploy the chambers, and an anchored float tube to carry the deep cycle 12V battery. The barge was constructed in a fashion such that it was easy to transport from the University of Utah to Utah Lake, light enough to be carried by one person, convenient and straightforward for the nuances of sampling SOD,

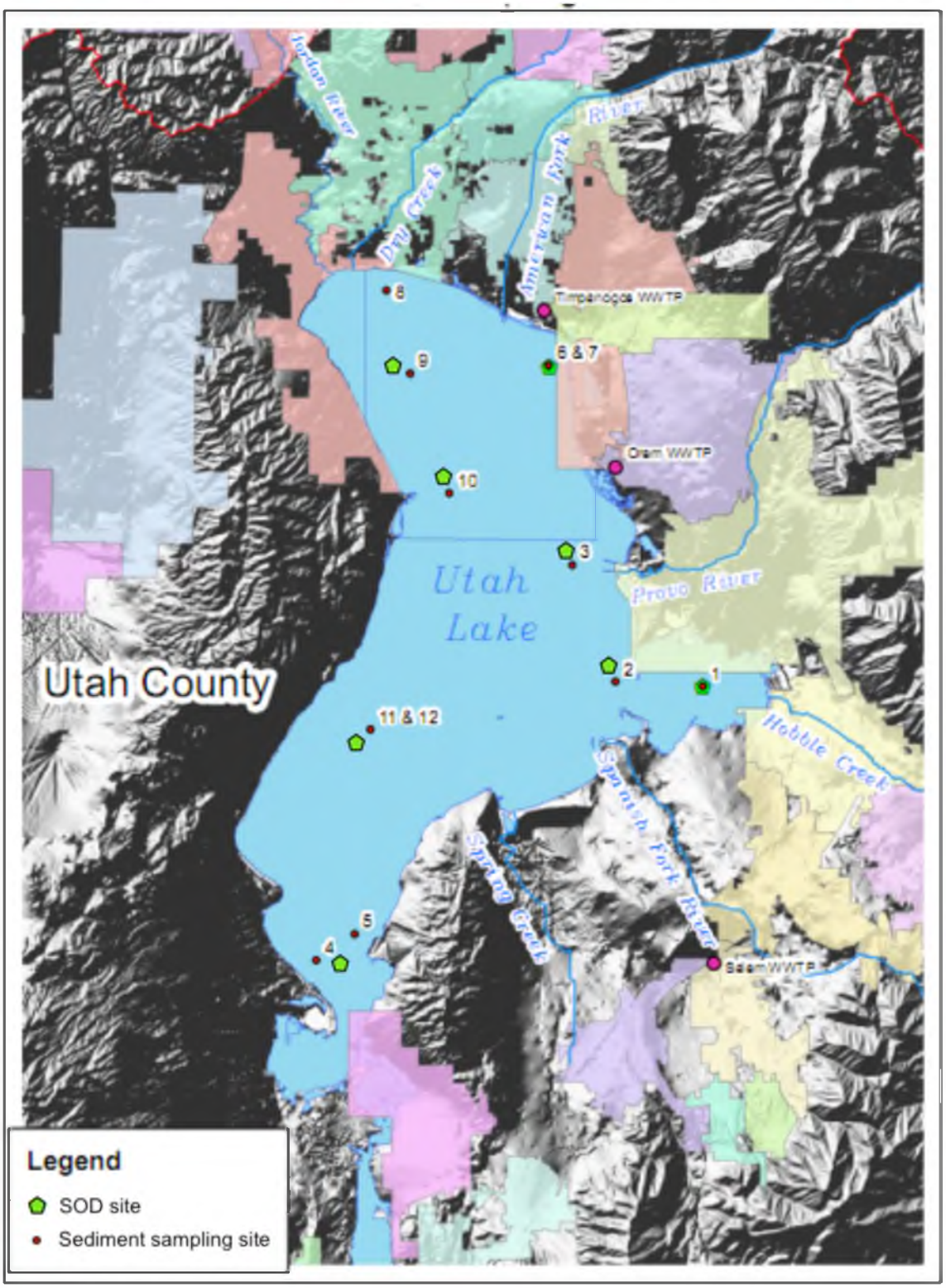

Fig. 21. Utah Lake SOD and sediment sampling sites

Table 9. Utah Lake SOD sampling sites and dates

site #	Location	Easting	Northing	STORET #	Date
1	Provo Bay	441119	4449033	4917450	9/14/10
2	Entrance to Provo Bay	437811	4448947	4917770	8/3/12
3	1.3 miles W of Provo River	435143	4454575	4917390	8/2/12
5	Goshen Bay	425157	4437673	4917620	8/3/12
6	0.5 miles W of Geneva Steel	434005	4463666	4917320	9/24/10
9	2 miles E of Saratoga Springs	426061	4466105	4917520	9/30/11
10	1 mile E of Pelican Point	429499	4457869	4917370	8/4/12
12	Goshen Bay entrance	425054	4445601	4917500	8/4/12

durable, and to minimize any disturbance to the sediments during chamber deployment by providing a stable lowering and lifting function (Fig. 22).

The motorboat used to access Utah Lake SOD sites was anchored further away from the chambers than the length of anchor line utilized to secure the vessel. As a general nautical rule, 10 feet of anchor line is required for every 1 foot of water depth. Changing wind directions causes the boat to arc around the anchor, posing a collision hazard to the SCUBA diver upon resurfacing in the turbid water. This was learned through experience. Fig. 23 shows the chambers being deployed outside the anchor radius

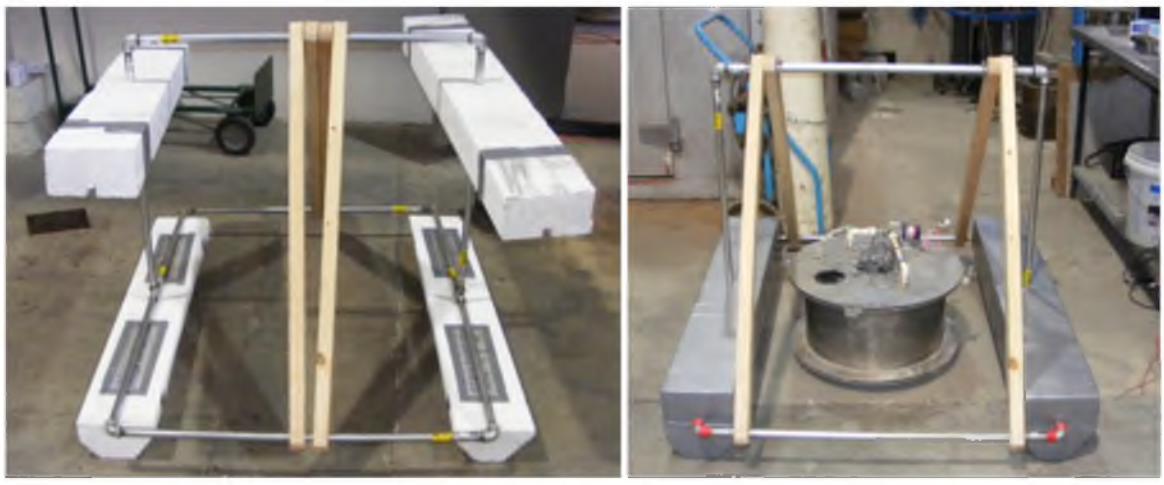

Fig. 22. SOD chamber deployment barge being built (left) and final product

Fig. 23. SOD chamber deployment barge (left) and float tube used to carry the battery to power SOD chamber pumps (right)

and the final setup with three chambers deployed while powered by the battery on the anchored float tube.

4.1.6 State Canal SOD

The purpose of conducting SOD in State Canal was to obtain SOD values for extremely organically enriched sediments and to evaluate SOD downstream of the Jordan River. The State Canal sampling site was located downstream of the South Davis County-North wastewater treatment plant (WWTP) discharge and upstream of the Bountiful Pond "tributary" (Fig. 24). SOD was measured off the west bank in water 1 meter deep. State Canal was roughly 2 meters deep center channel at this location. Sediment cores were taken at the SOD site and from the bridge west of the parking lot.

4.2 Chamber Net Daily Metabolism (NDM)

4.2.1 Chamber NDM sampling locations

Seven sites were selected to evaluate the dark and light metabolisms of both the water column and benthos. The LNP NE and 300 N sites where located within Reaches 1 and 2 where DO deficits are routinely observed during daylight hours. The 2100 S site was located just below the Surplus Canal diversion and signifies the beginning of the

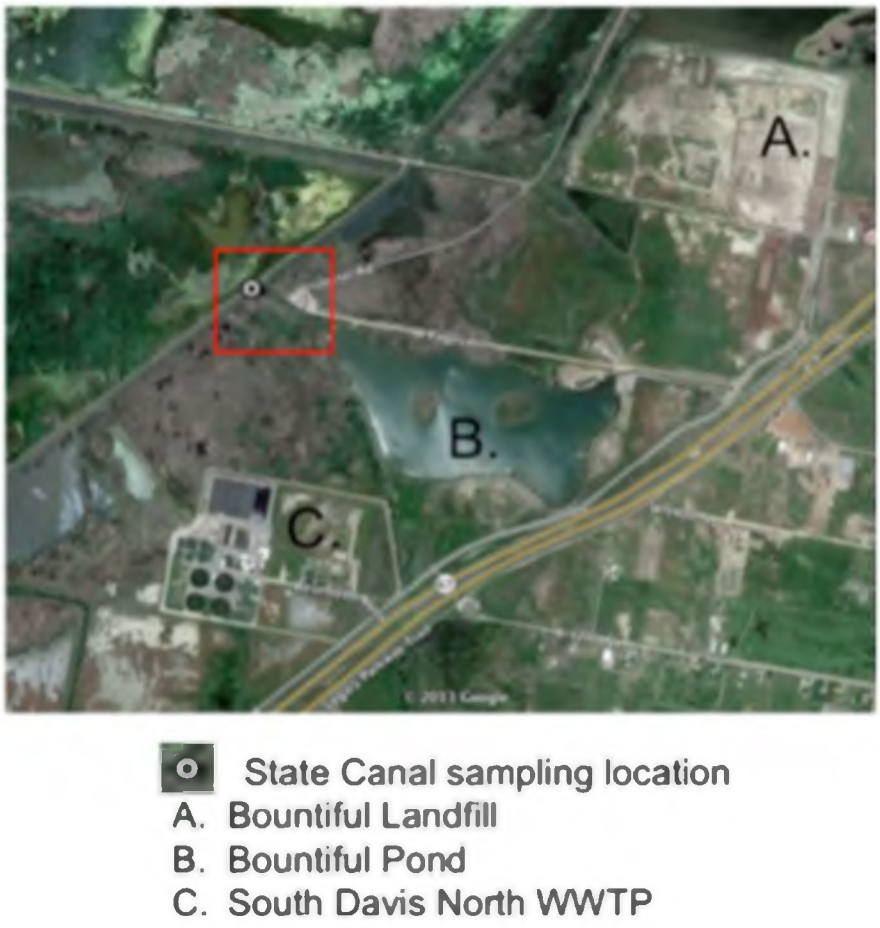

Fig. 24. State Canal sampling site

Lower Jordan River. The 1700 S site was located downstream of the 2100 S site and provided a comparison of sediment composition as the average size decreased from sandy gravel to sand. The 5400 S site was located in the Upper Jordan River downstream of the South Valley WRF discharge. The 7600 S site was located upstream of all online WWTP direct discharges to the Jordan River in a cobble dominated substrate conducive to periphyton growth. The 9000 S site was also located above all online WWTPs and had sediments composed of sands to investigate the potential for periphyton to colonize this mobile substrate. All sites except for the 7600 S and 2100 S sites have been used for previous SOD studies and allow direct comparisons.

4.2.2 NDM chamber details

To measure water column and benthic dark respiration and light metabolisms, custom chambers were constructed of transparent bulletproof plastic (Lexan) by the South Davis-S WWTP machine shop. The NDM chambers were built to be directly comparable to the existing SOD chambers, and all chambers had a working volume of 38 L and encapsulated a sediment area of 0.16 m^2 (Fig. 25).

Unlike the aluminum SOD chambers, which were open at the bottom, the NDM chambers were closed at the bottom. Hence, the Testing NDM chamber and the Control NDM chamber were the exact same in construction. At the time of testing, however, a preincubated sediment tray containing local sediment was placed in the Testing NDM

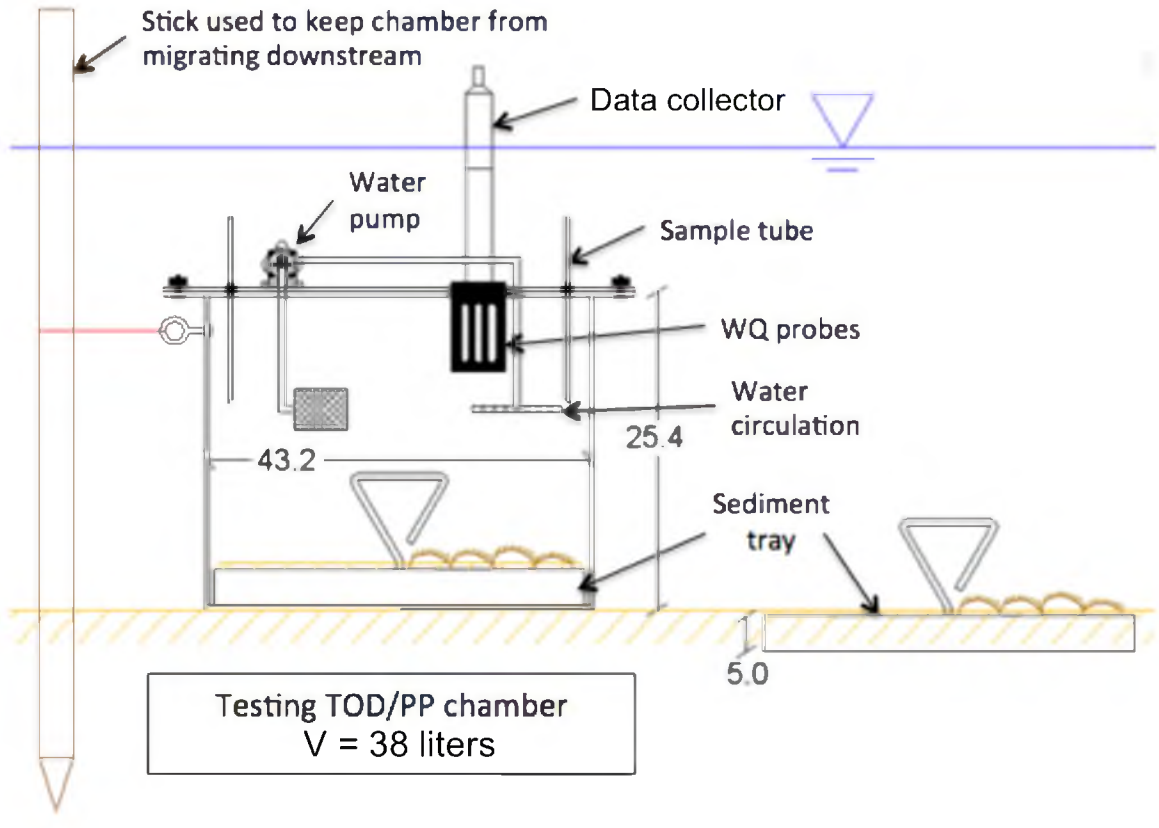

Fig. 25. NDM chamber in use and tray incubation

chambers.

The use of sediment trays allowed for the study of a wide range of undisturbed substrates ranging from silts, sands, gravel, cobbles, and detritus. The top 5 cm of local sediments were transferred to the sediment trays by shovel. The trays were then buried to allow roughly 1 cm of sediments above the lip of the tray to reduce localized flow variations (Hauer and Lamberti 2007, Ch. 28). The trays were then allowed to sit within the river for a minimum of 3 weeks to allow recolonization of the benthic community, including both heterotrophs and autotrophs (Bott et al. 1985). While the trays were left in the river bottom, bedload CPOM (leafs, phragmites stalks, detached macrophytes, sticks, etc.) and anthropogenic litter needed to be regularly removed from the tray handles protruding from the sediments.

In addition, the sites needed to be regularly visited to confirm that the trays did not erode out of the sediments due to fluctuating stream velocities. If the lids of the trays were observed above the sediments, the trays were carefully removed without disturbing the contents, holes redug, and the trays replaced. The tray handles where thoroughly cleaned with a steel wool pad before chamber testing to remove any benthic growth present on the exposed sediment tray handle. After the recolonization period, the sediment trays were carefully removed and placed in the closed bottom clear chambers for the primary production and dark respiration experiments.

The use of sealed chambers containing sediment trays allows the measurement of both heterotrophic and autotrophic respiration and abiotic processes occurring at the sediment–water interface while excluding hyporheic exchanges, groundwater intrusion, and deep sediment gas fluxes (Grace and Imberger 2006). In addition, the trays allowed

the measurement of sediment dark respiration in cobble sediments that SOD chambers cannot be deployed in due to erosive flow velocities and poor chamber sealing. Fig. 26 shows sediment trays containing silt in Reach 1 (left) and gravel at 7600 S located in the Upper Jordan River (right).

4.2.3 NDM chamber deployment

At each site a total of five chambers were installed, two aluminum open bottom SOD chambers and three transparent closed bottom NDM chambers. Two of the closed bottom transparent NDM chambers were used to measure tray oxygen demand (TOD) and tray gross primary production (TPP) and contained sediment trays. These chambers measured respiration rates under dark conditions and the net oxygen production rates under sunlit conditions. The transparent NDM chambers were initially covered with two black bags to measure dark respiration associated with the aquatic community present in the sediment trays and in the water column. The third clear chamber was filled with ambient river water and initially covered with two black plastic bags to measure water

Fig. 26. Silts and cobbles following incubation in the Jordan River

column dark respiration (WC_{dark}). Under dark conditions this chamber acted as the control for the two aluminum SOD chambers and the two black-bagged NDM chambers containing sediment trays. After initially measuring dark respiration, the black bags where removed from the three clear chambers by carefully cutting the bags with a knife. In this way, the NDM chambers measured oxygen depletion and net production in the absence and presence of sunlight throughout the day. The three NDM chambers were initially covered with black plastic bags for 120–180 minutes depending on the length of the photoperiod. The length of the photoperiod is important since sampling occurred both in the summer and winter months. The chambers were deployed for a total of 4~6 hours.

Sediment tray dark respiration, or tray oxygen demand (TOD), was initially measured in the NDM chambers during the morning hours. Dark respiration needs to be measured before light metabolism (primary production) within the productive Jordan River because chamber studies require a DO deficit, and supersaturated DO conditions are typically encountered in the UJR shortly after sunrise. Supersaturated DO at the beginning of testing will result in oxygen bubbles forming on the top and sides of the chamber, skewing results since these bubbles will redissolve as a DO deficit develops within the chambers under dark conditions. Therefore, the chambers were initially filled with ambient river water with a DO deficit during the morning hours for all experiments. Another advantage to measuring respiration before production is that the DO levels in the chambers are allowed to decrease further before measuring primary production, allowing longer testing times before the chamber reaches DO saturation.

The black bags were removed close to solar noon (approximately 1:00 PM in summer and 11:30 AM in the winter) to measure light metabolism with the assumption

that the maximum rate of primary production in the benthos and water column was occurring at this time. After the water contained in the chambers becomes DO saturated, the measured rate of DO production is underestimated since much of the oxygen occurs as gas bubbles, not dissolved oxygen.

4.2.4 Calculation of WC_{dark}, TOD, WC_{light}, and TPP

Similar to the SOD calculations, WC_{dark} is the dark respiration rate in the water column measured using the black-bagged transparent chamber containing only river water. TOD is the tray oxygen demand and is calculated using the black-bagged transparent chambers containing sediment trays under dark conditions. TOD is similar to SOD except that it does not account for methane fluxes from deeper than 1.5", hyporheic exchanges, or low DO groundwater intrusion. Both autotrophic and heterotrophic dark respiration in the sediments and water column are assumed to occur at a consistent rate throughout the diurnal period. Therefore, the dark respiration oxygen depletion rates TOD and WC_{dark} can be used directly in NDM estimates and are calculated using the SOD equations.

Photosynthesis only occurs during daytime at varying rates; therefore, the maximum rate of photosynthesis was measured midday. The maximum net rate of sediment tray primary production ($TP_{m,net}$) and the maximum net rate of water column primary production ($WCP_{m,net}$) were calculated using the following equations based on chamber DO depletion and production rates under light conditions. Notice that when TOD is subtracted, TPP_m increases since respiration is an oxygen sink. Also note that the $WC_{light,m}$ is the net rate measured in the chamber and does not have WC_{dark} subtracted at this stage.

$$TPP_m = \left[1.44\,{}^{V}/_{A}\left(TPP_{m,bulk} - WC_{light,m}\right)\right] - TOD \quad (6)$$

$TPP_m = maximum\ rate\ of\ sediment\ tray\ PP\ \left({}^{g}/_{m^2\ day}\right)$

$TPP_{m,bulk} = maximum\ rate\ of\ sediment\ tray\ bulk\ PP\ \left({}^{mg}/_{L\ min}\right)$

$WC_{light,m,} = maximum\ \ rate\ of\ water\ column\ net\ PP\ \left({}^{mg}/_{L\ min}\right)$

$TOD = sediment\ tray\ oxygen\ demand\ \left({}^{g}/_{m^2\ day}\right)$

Since TPP_m and $WC_{light,m}$ were measured midday and are assumed to be the maximum rate of photosynthesis, they cannot be directly compared to SOD, TOD, and WC_{dark} respiration rates. Therefore, both TPP_m and $WC_{light,m}$ were converted to gross average daily oxygen production rates by normalizing the maximum rate to a Gaussian curve over the length of the photoperiod to calculate the final parameters TPP and WC_{light} using the following equations (Chapra 2008, pg. 436):

$$TPP = TPP_m\left({}^{2f}/_{\pi}\right) \quad (7)$$

$TPP = avg.daily\ sediment\ tray\ PP\ \left({}^{g}/_{m^2\ day}\right)$

$TPP_m = maximum\ rate\ of\ sediment\ tray\ bulk\ PP\ \left({}^{g}/_{m^2\ day}\right)$

$f = photoperiod\ ,fraction\ of\ day\ recieving\ sunlight\ (d)$

$\pi = 3.14$

$$WC_{light} = (WC_{light,m} - WC_{dark})\left({}^{2f}/_{\pi}\right) \quad (8)$$

$WC_{light} = avg.daily\ water\ column\ PP\ \left({}^{g}/_{m^2\ day}\right)$

After normalizing the maximum oxygen production rates to a 24-hr average based on the length of the photoperiod, SOD, TOD, and TPP can be directly compared. By dividing TPP by TOD a general benthic indication of heterotrophic (<1) or autotrophic (>1) conditions can be obtained. This ratio can also be applied to the water column to determine the degree of autotrophy:heterotrophy associated with seston and phytoplankton (Vannote et al. 1980).

Although the parameters TPP and WC_{light} are represented as gross fluxes and rates, they do not account for increases in phototroph respiration during photosynthesis. This was not a consideration in the context of a river DO mass balance since the phototrophs may respire and photosynthesize at rates higher than measured, but they are utilizing DO that they produced, and the final NDM answer will be the same (Grace and Imberger 2006). The final chamber derived NDM flux was calculated accordingly:

$$NDM = TOD + TPP + \left(WC_{dark} + WC_{light}\right) * d \qquad (9)$$

$$NDM = chamber\ measured\ net\ daily\ metabolism\ \left({}^{g\ DO}/_{m^2 * day}\right)$$
$$d = mean\ riverwide\ depth\ (m)$$

If a volumetric NDM rate is desired instead of a flux, divide the sediment parameters by mean river depth and sum the water column parameters. The schematic in Fig. 27 shows the complete protocol for light and dark metabolism chamber measurements used during this research.

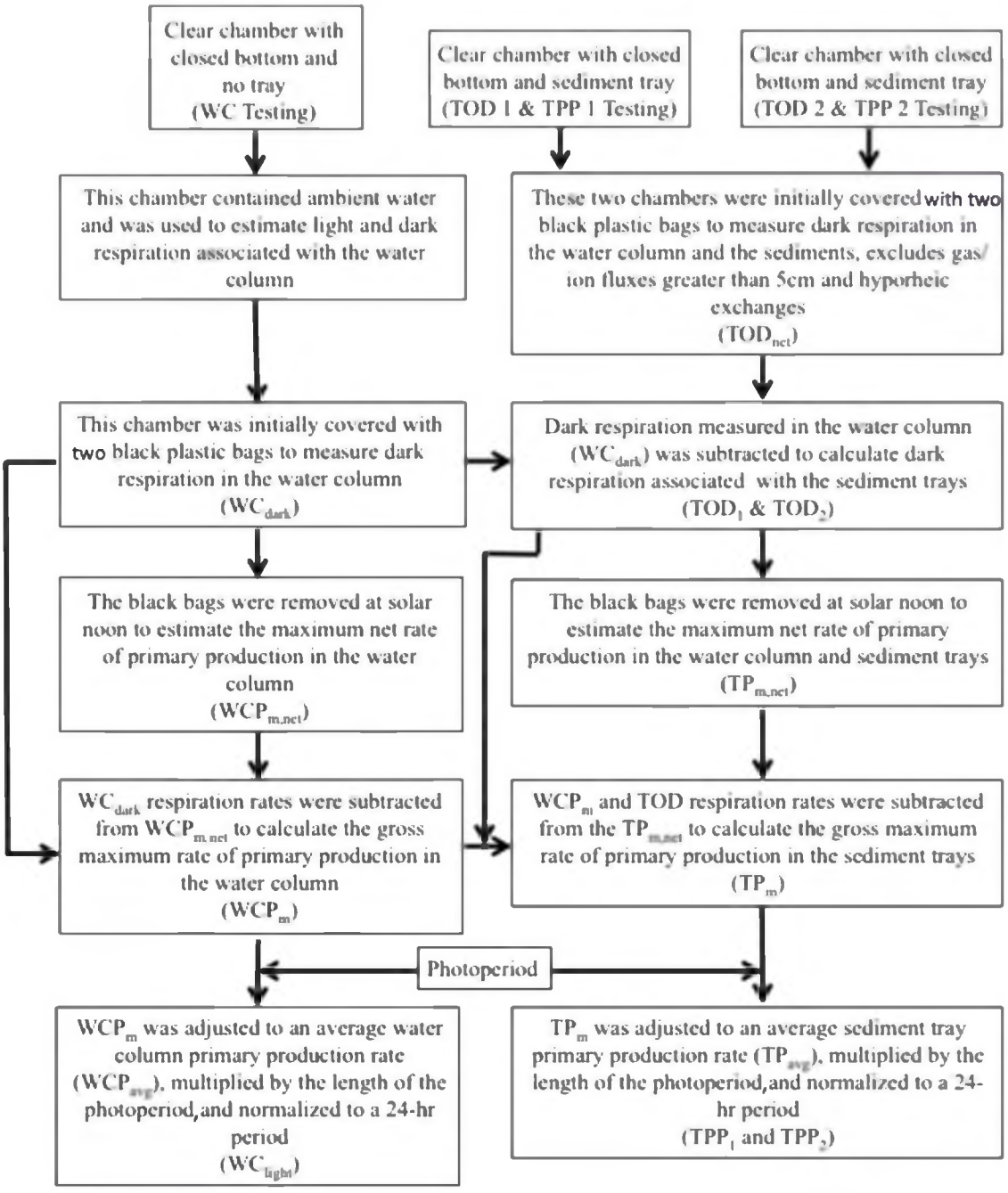

Fig. 27. General schematic of the experimental strategy used for chamber NDM

4.3 Estimating NDM Using Diurnal DO Curves

4.3.1 Calculation of single-station GPP, CR_{24}, and NDM

Diurnal DO curves can be used to estimate stream metabolism based on the nighttime DO deficit, daytime DO deficit or surplus, length of photoperiod, and reaeration coefficient (Chapra and Di Toro 1991; Chapra 2008; Odum 1956). Diurnal DO models initially calculate a nighttime respiration rate and normalize this rate over a 24-hour cycle with the assumption that respiration is occurring at a constant rate during the daytime (CR_{24}). Net primary production (NPP) is measured during daytime, and GPP is estimated by including the contribution of the "constant" respiration during the photoperiod to estimate GPP. Ambient DO measurements in the Jordan River were collected every 5 minutes using In-Situ Troll 9500 data sondes.

There are many diurnal DO NDM models available, and a variety were used including single-station excel, upstream-downstream excel, Bob Hall's single-station R model, and basic equations (Hauer and Lamberti 2007, ch. 28). The single-station basic equations, or "visual" analysis, was ultimately used since it provides the same answers without the need of a computer, as long as the reaeration coefficient is known.

Fig. 28 provides an example diurnal DO profile for a stream metabolism estimate in the UJR where the reaeration coefficient is 6, the length of photoperiod is 13 hours, and the average depth is 0.8 meters.

The nighttime steady state DO deficit was -1.5 mg-DO/L, and this respiration rate is assumed to be constant throughout the 24-hour cycle. After multiplying the reaeration coefficient by the ambient nighttime DO deficit and normalizing to the mean river depth, CR_{24} is estimated.

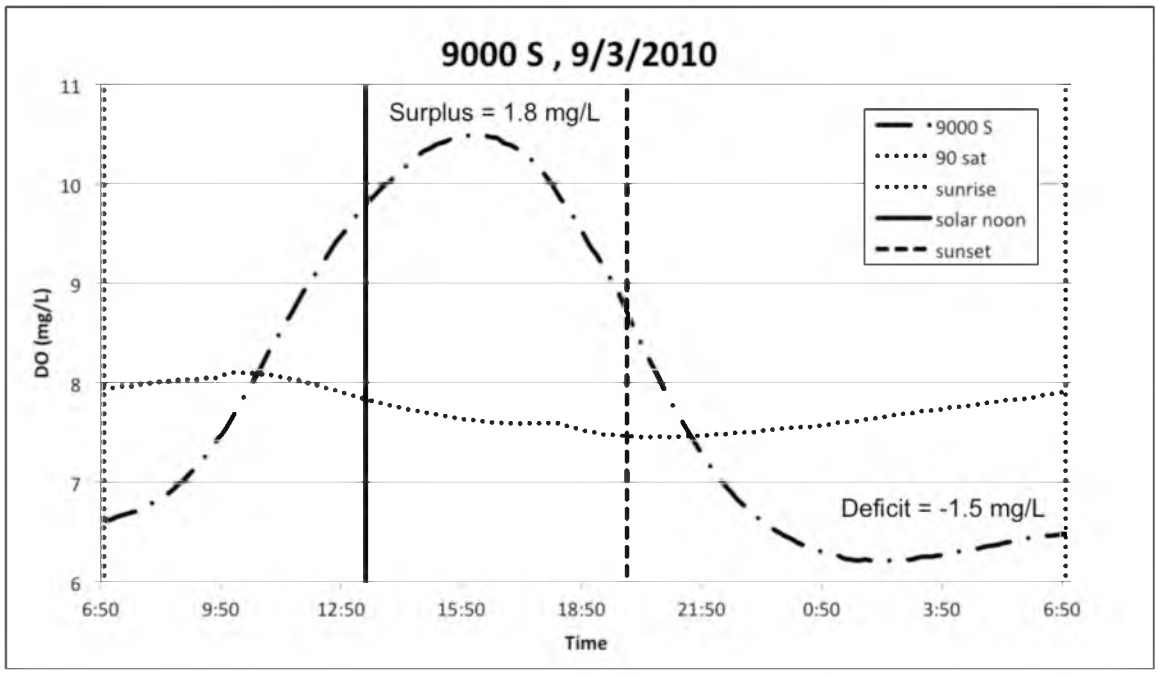

Fig. 28. Visual NDM estimate from diurnal DO curve in UJR

$$CR_{24} = K(C_{night} - C_{sat})d \qquad (10)$$

$CR_{24} = community\ respiration\ \left({}^{g\ DO}/_{m^2\ day}\right)$

$K = reaeration\ coefficient\ \left({}^{1}/_{day}\right)$

$C_{night} = steady\ state\ or\ lowest\ nighttime\ DO\ concentration\ \left({}^{mg\ DO}/_{L}\right)$

$C_{sat} = saturation\ at\ time\ of\ C_{night}\ \left({}^{mg\ DO}/_{L}\right)$

$C_{night} - C_{sat} = nighttime\ DO\ deficit\ \left({}^{mg\ DO}/_{L}\right)$

$d = mean\ stream\ depth\ (m)$

To estimate stream GPP, the maximum daytime DO deficit or surplus can be normalized to depth and photoperiod using a half-sinusoid model to account for the changing rates of photosynthesis in relation to the solar flux (Chapra 2008). Finally, the

dark respiration normalized to the photoperiod is subtracted to account for daytime respiration masked by DO production. NDM is expressed as the sum of DO fluxes from GPP and CR_{24}, similar to the NDM chamber equations.

$$P_m = K(C_{max} - C_{sat})d \quad (11)$$

$P_m = maximum\ net\ flux\ of\ DO\ from\ primary\ production\ \left({}^{g\ DO}/_{m^2\ day}\right)$

$C_{max} = maximum\ daytime\ DO\ concentration\ \left({}^{mg\ DO}/_{L}\right)$

$C_{max} - C_{sat} = maximum\ daytime\ DO\ surplus\ \left({}^{mg\ DO}/_{L}\right)$

$$GPP = \left(P_m * {}^{2f}/_{\pi}\right) - (f * CR_{24}) \quad (12)$$

$GPP = gross\ daily\ stream\ DO\ production\ \left({}^{g\ DO}/_{m^2\ day}\right)$

$f = photoperiod\ ,fraction\ of\ day\ recieving\ sunlight\ (d)$

$\pi = 3.14$

$$NDM = GPP + CR_{24} \quad (13)$$

$NDM = net\ daily\ metabolism\ \left({}^{g\ DO}/_{m^2\ day}\right)$

As shown in the example equations below, the CR_{24}, GPP, and NDM was -7.2, 8.5, and 1.3 $g/m^2/d$ for the 9000 S site, respectively (Fig. 28). A positive NDM indicates that OM is being produced in abundance and is a source of OM to downstream hydraulic reaches.

$$CR_{24} = (6\ day^{-1})\left(-1.5\ {}^{mg\ DO}/_{L}\right)(0.8\ m) = -7.2\ {}^{g\ DO}/_{m^2\ day}$$

$$P_m = (6\ day^{-1})\left(2.8\ {}^{mg\ DO}/_{L}\right)(0.8\ m) = 13.4\ {}^{g\ DO}/_{m^2\ day}$$

$$GPP = P_m\left(2 * {}^{13\ hr}/_{24\ hr}/_{\pi}\right) - CR_{24}\left({}^{13\ hr}/_{24\ hr}\right) = 8.5\ {}^{g\ DO}/_{m^2\ day}$$

$$NDM = (8.5 - 7.2)\ {}^{g\ DO}/_{m^2\ day} = 1.3\ {}^{g\ DO}/_{m^2\ day}$$

Fig. 29 shows a diurnal DO profile for the LJR in Reach 1 where a DO deficit is typical over the 24-hour cycle. The nighttime DO deficit was -2.3 mg-DO/L, and the daytime surplus, or deficit in this example, was -0.9 mg-DO/L. The reaeration coefficient was 1.2 d^{-1}, length of photoperiod was 13 hours, and the average depth was 1.2 meters.

The CR_{24}, GPP, and NDM were -3.3, 1.3, and -2.0 g-DO/m^2/d, respectively. Reach 1 in the LJR was heterotrophic in this example.

$$CR_{24} = (1.2\ day^{-1})\left(-2.3\ {}^{mg\ DO}/_{L}\right)(1.2\ m) = -3.3\ {}^{g\ DO}/_{m^2\ day}$$

$$P_m = (1.2\ day^{-1})\left(-0.9\ {}^{mg\ DO}/_{L}\right)(1.2\ m) = -1.3\ {}^{g\ DO}/_{m^2\ day}$$

$$GPP = P_m\left(2 * {}^{13\ hr}/_{24\ hr}/_{\pi}\right) - CR_{24}\left({}^{13\ hr}/_{24\ hr}\right) = 1.3\ {}^{g\ DO}/_{m^2\ day}$$

$$NDM = (1.3 - 3.3)\ {}^{g\ DO}/_{m^2\ day} = -2.0\ {}^{g\ DO}/_{m^2\ day}$$

The LJR had a net DO consumption, while the UJR had a net DO production in these examples. Using diurnal DO profiles, the NDM chamber experiments can be compared to alternative methods for estimating stream metabolism.

4.3.2 Adjusting single-station NDM for groundwater intrusion

Groundwater (GW) is known to enter the UJR, and if the groundwater is low in DO, then the dilution of ambient DO due to the influx of GW will overestimate CR_{24},

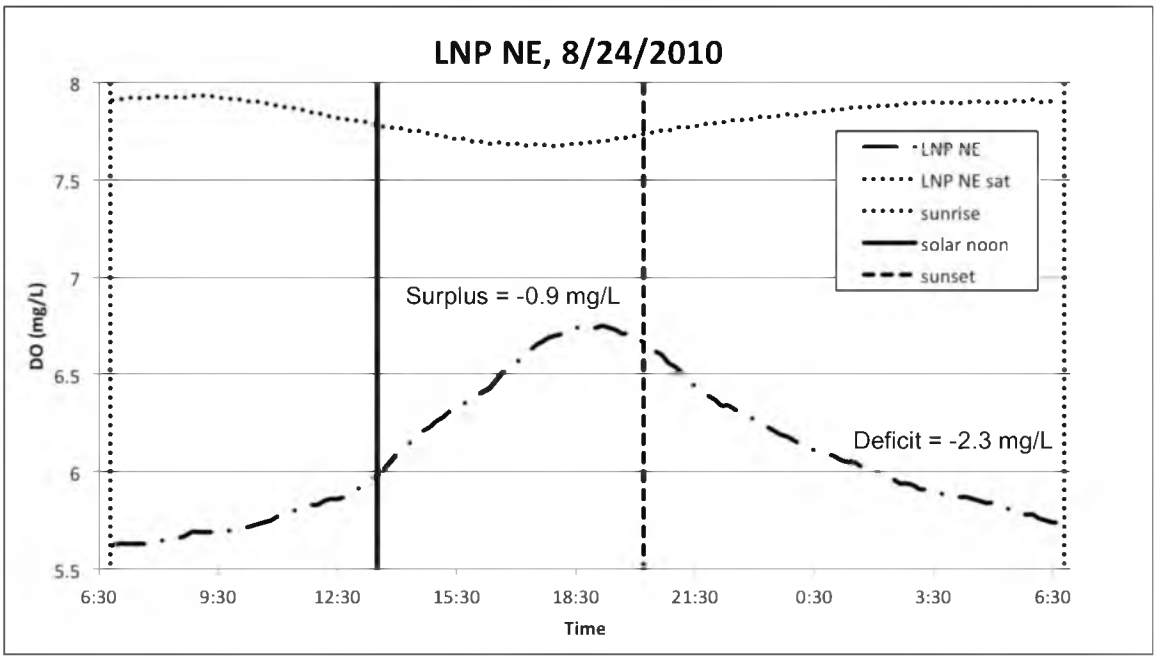

Fig. 29. Visual NDM estimate from diurnal DO curve in LJR

leading to an underestimation of NDM using the single-station diurnal DO method (Hall and Tank 2005). This hydraulic DO dilution process is shown in Fig. 30.

Estimates of groundwater intrusion in the UJR are provided in the Jordan River TMDL as a percentage of total flow (Utah DWQ 2013, Fig. 1.4). Groundwater DO concentrations were measured using minipiezometers at 30, 60, and 90 cm depths in the gravel and sand sediments of the UJR (Bridge 2005; Malcom et al. 2004). Using river flow rates, the percentage of flow from groundwater, groundwater DO concentrations, stream velocity, length of river under consideration, and average width, the DO deficit associated with anoxic GW can be expressed as a flux (CR_{GW}) using the following relationship.

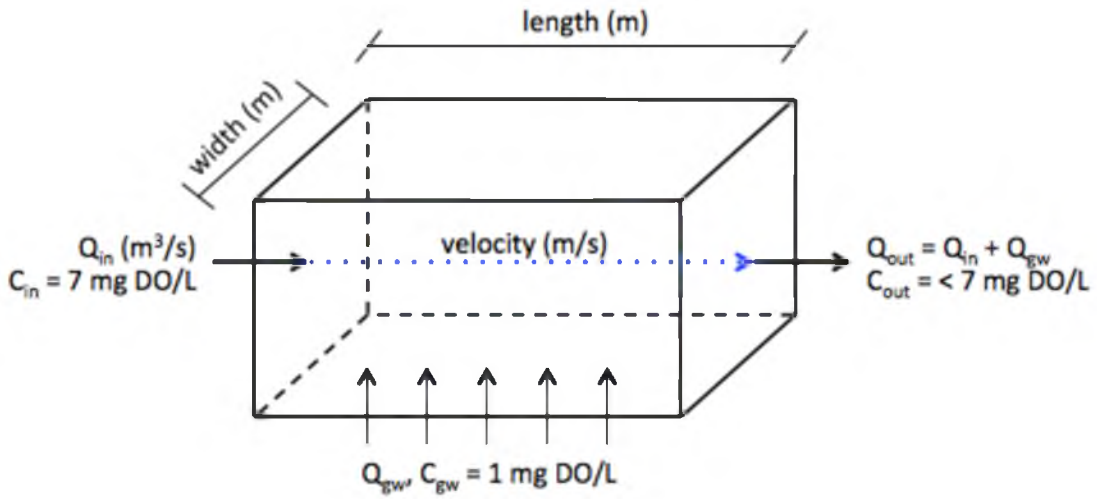

Fig. 30. Groundwater DO dilutions

$$CR_{GW} = \frac{(Q * x) * \%_{GW} * (C_{GW} - C_S)}{l * w} * \left(\frac{v * x}{l}\right) * 1\ day \qquad (14)$$

$CR_{GW} = negative\ sediment\ DO\ flux\ due\ to\ GW\ \left({}^{g\ DO}/_{m^2\ day}\right)$

$Q = river\ flow\ rate\ at\ end\ of\ hydraulic\ reach\ \left({}^{m^3}/_{sec}\right)$

$x = unit\ conversion, 86{,}400 = \frac{60\ sec}{min} * \frac{60\ min}{hr} * \frac{24\ hr}{day}, \left({}^{sec}/_{day}\right)$

$\%_{GW} = ratio\ of\ GW\ flow\ in\ relation\ to\ Q\ \left({}^{\%}/_{100}\right)$

$C_{GW} = DO\ concentration\ of\ GW\ \left({}^{mg\ DO}/_{L}\right)$

$C_S = DO\ saturation\ concentration\ in\ ambient\ river\ \left({}^{mg\ DO}/_{L}\right)$

$C_{GW} - C_S = GW\ DO\ deficit\ \left(-{}^{mg\ DO}/_{L}\right)$

$l = hydraulic\ reach\ length\ (m)$
$w = mean\ hydraulic\ reach\ width\ (m)$
$v = river\ velocity\ \left({}^{m}/_{sec}\right)$

$\left(\frac{v * x}{l}\right) * 1\ day = number\ of\ times\ flow\ passes\ over\ sediments$

The parameter CR_{gw} can then be subtracted from the CR_{24} estimate obtained from the single-station method to separate the biological DO consuming activities occurring at the sediment–water interface from groundwater DO dilutions. This is important since this research focuses on using DO as a surrogate for OM dynamics, and hydraulic dilutions may horribly underestimate NDM results. The final equation for estimating NDM using a single-station method adjusted for GW dilutions is provided below.

$$NDM_{adj} = GPP + (CR_{24} - CR_{GW}) \quad (15)$$

Table 10 provides information used to estimate CR_{GW} to account for hydraulic DO dilutions associated with GW intrusion in the Upper Jordan River. During baseflow conditions, roughly 15% of the Upper Jordan River's flow is comprised of groundwater above 9000 S, and 5% of the flow is GW downstream until the confluence of Little Cottonwood Creek (LCC) (Utah DWQ 2013, Fig. 1.4).

Table 10. GW intrusion parameters used to adjust single-station model

	parameters for UJR GW DO dilutions in single-station model				
	Q (m^3/sec)	length (m)	width (m)	v (m/s)	CR_{GW} (g DO/m^2/d)
above 9000 S	4	22,000	13	0.6	-2.6
9000 S-LCC	3	10,000	17	0.6	-2.4

LCC = Little Cottonwood Creek tributary
flow, length and velocity (v) data from Aug 2009 QUAL2kw (Utah DWQ)
tributaries were not included in flow
since rivers are moving, used v to calculate HRT for calculations
15% GW above 9000 S (TMDL, Fig. 1.4)
5% GW above 9000 S (TMDL, Fig. 1.4)
GW has a DO concentration of 1 mg-DO/L

4.4 Nutrient Fluxes

4.4.1 Nutrient flux sampling locations

Nutrient Fluxes were measured at the same time as SOD in the LJR during the 2010, 2012, and 2013 summer sampling seasons.

4.4.2 Nutrient flux protocols

Jordan River nutrient dynamics were measured by utilizing the contained volume of water provided by the SOD chambers to monitor changes in dissolved nitrogen and phosphorus concentrations (Callender and Hammond 1982). Three samples were taken at 90-minute intervals during the 3-hour SOD testing period. It should be noted that the environmental conditions investigated while measuring nutrient dynamics represent the dark metabolism and do not include the daytime dynamics associated with biological assimilation due to photosynthesis.

To measure sediment nutrient fluxes during anoxic conditions, the SOD chamber was injected with a slurry of sodium sulphite and trace amounts of cobalt chloride to scavenge DO in the chamber while producing sulphate according to the following chemical reaction.

$$2SO_3{}^{2-} + O_2 \rightarrow 2SO_4{}^{2-}$$

The sulphite slurry was made immediately before injection with 20 mL of ambient river water and preweighed vials of salt to drop the DO concentration by 1 mg-DO/L in the 38 L chamber. The amount of salt added to the slurry to achieve zero DO in the chamber was determined in the field using the ambient DO concentration measured at the beginning of testing. Removing 7 mg-DO/L increases the sulphate concentration in

the chamber by 44 mg-SO_4/L. Background sulphate concentrations in the Jordan River are greater than 150 mg-SO_4/L, and it was assumed that the relatively small increase in sulphate concentration would not negatively influence biological activity.

For pH manipulations, 2N hydrochloric acid was injected into the chamber. The exact amount of acid required to drop the chamber pH to 7 was determined in the field by titrating a sediment core with 26 cm of overlying water, which is the same as the height of the SOD chamber when installed. Background chloride concentrations in the Jordan River are higher than 150 mg-Cl^-/L, and it was assumed that the addition of chloride would not negatively influence biological activity.

Nutrient flux samples were taken via syringe from a closable sampling tube incorporated into the SOD chamber lid. Initially, 20 mL was extracted and discarded to account for the 10 mL of river water present in the sampling tube. An additional 50 mL was then extracted for dissolved nutrient analysis. After collecting the water sample, the sampling tube was then pinched off via hose clamp to ensure no interaction between the ambient river water and the encapsulated water within the SOD chamber. Water quality samples were immediately filtered using a 0.45-micron filter before storage on ice for lab analysis.

Water samples were analyzed for ammonia-N, nitrite-N, nitrate-N, and orthophosphate-P using ion-exchange chromatography and photometric methods. All samples were filtered, cooler stored, and analyzed within 48-hours following sample collection. Nitrite-N, nitrate-N, and phosphate-P concentrations were analyzed using ion exchange chromatography (IC) per USEPA standard method 300.0 A. Ammonia-N was analyzed using the colorimetric HACH method 10205.

4.4.3 Nutrient flux calculations

Similar to the SOD calculations, nutrient fluxes were calculated using the normalization equation for sediment area and chamber volume while subtracting the water column rates (Chiaro et al. 1980).

4.5 Sediment Organic Matter

This portion of research focused on sediment organic matter (OM) and organic carbon to evaluate whether the common measurement percent volatile solids (%VS) can be used as a surrogate for SOD. Particular focus was given to coarse and particulate organic matter in the sediments to better characterize the black muck found in the Lower Jordan River. In addition, the standing stock of organic matter in the sediments was estimated based on depth in the sediment column. Fig. 31 presents an overview of the methodology and relationships that were utilized.

4.5.1 %TS, %VS, and %TOC sampling locations

To account for the differences in OM found in depositional zones and the thalweg, samples were collected across the width of the river at each sampling location. The details of the sampled sites are provided in Table 11.

4.5.2 Sediment core collection and depth partitioning

Sediment samples were collected using a 3' long 2" inner diameter acrylic open-barrel core, or open-drive sampler (Glew et al. 2001, Ch. 5). To access sediments in the thalweg of the river, an additional 3' or 6' custom-made sediment core extension was used depending on the depth of the water column. The core sampler was pushed into the sediments and a #11 stopper inserted into the top of the coring unit to allow removal of

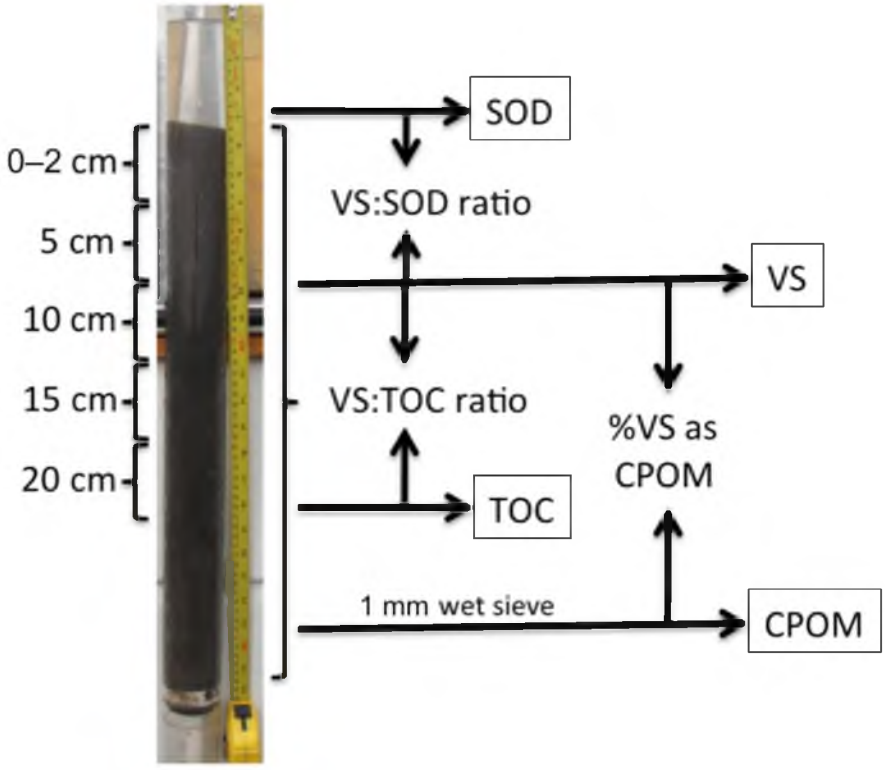

Fig. 31. Sediment core characterization relationships

Table 11. Site descriptions for 2012/2013 sampling

Reach	Site name	Description
1	Burnham Dam	end of the Lower Jordan River (before diversion to State Canal and managed wetlands)
1	LNP NE	below South Davis-S WWTP discharge
1	Cudahy Ln	above South Davis-S WWTP discharge (Reach 1–2 boundary)
2	300 N	below City Creek tributary/stormwater discharge
3	700 S	below Parleys, Emigration, and Red Butte Cr. tributaries/stormwater discharge
3	1700 S	near the beginning of the Lower Jordan River

an intact sediment core. Another stopper was inserted into the bottom of the core tube during transportation to the riverbank. Sediment core samples were extracted onsite using a 2" outer diameter plunger inserted into the bottom of the coring unit and pushed upwards (Glew 1988). This allowed sediment samples to be collected at specific depths within the sediment column.

Depth specific core samples were collected in 50 mL vials and stored on ice until analysis. Roughly 40 mL of sediment was collected at each depth while characterizing each 2 cm subsample.

$$V = \pi R^2 H = 40.5\ cm^3 \approx 40\ mL$$

$V = volume\ of\ wet\ sediment\ sample\ (mL)$
$R = inner\ radius\ of\ core\ sampler\ (2\ inches)$
$H = height\ of\ sample\ collected\ (2\ cm)$

Core samples were collected in deep water using a float tube and rope strung across the river. Fig. 32 provides a general schematic of the sediment core sampling protocol in the field.

The removable sediment core extension is critical for deep water (>1 meter deep) sampling for two reasons:

1. to remove the water column head from the core sampler since this extra weight will push out the sediment core when removed from the water
2. to minimize the distance the core needs to be extruded (i.e., 3' vs. 9'), to limit sediment disturbances, and to make the extrusion process easier and capable of being accomplished by one person.

Fig. 33 shows the sediment core extension being used in the Legacy Nature Preserve in Reach 1 where depths can exceed 1.5 meters in the thalweg. Intact sediment

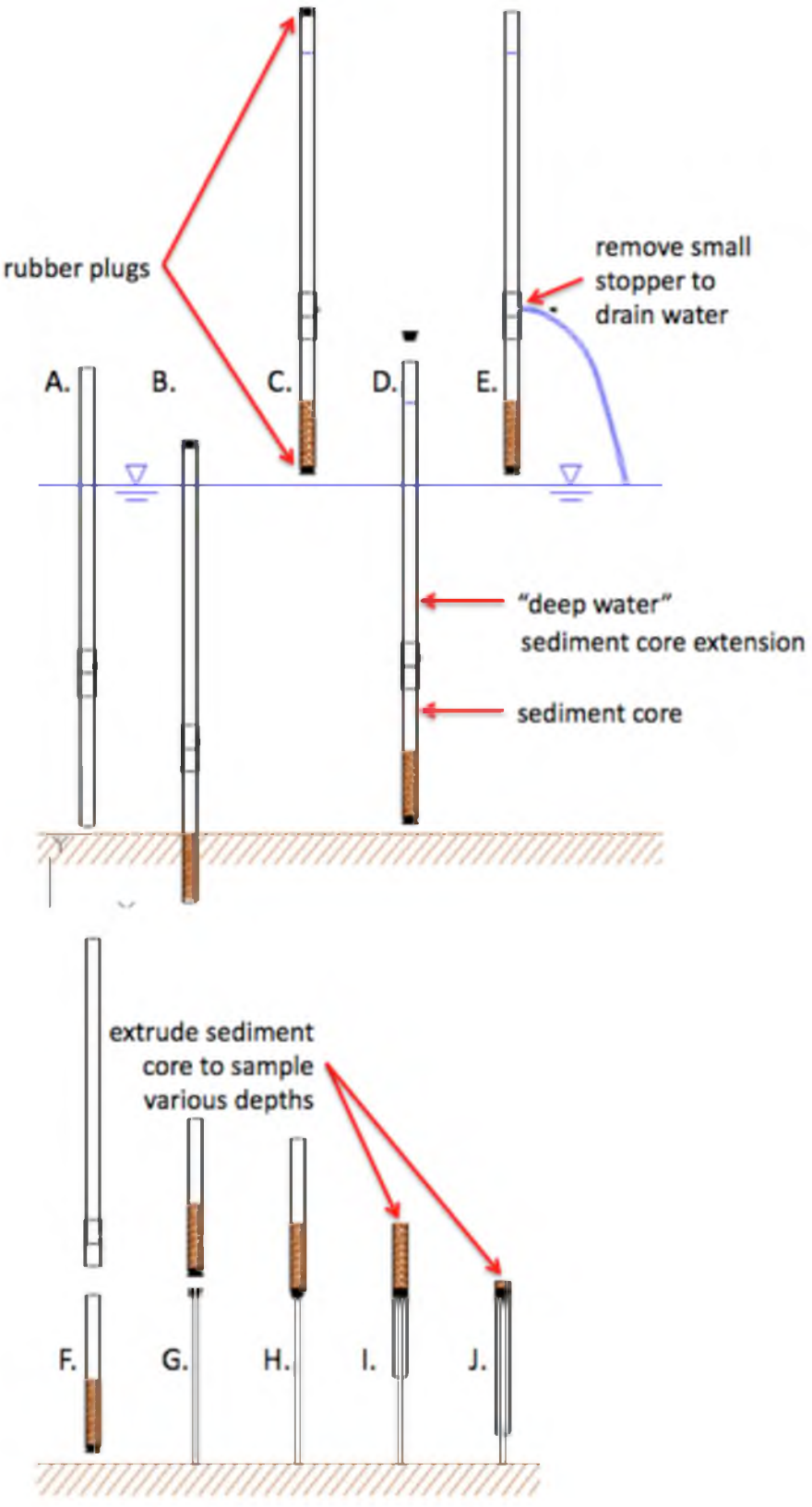

Fig. 32. Midriver multipiece sediment core sampler

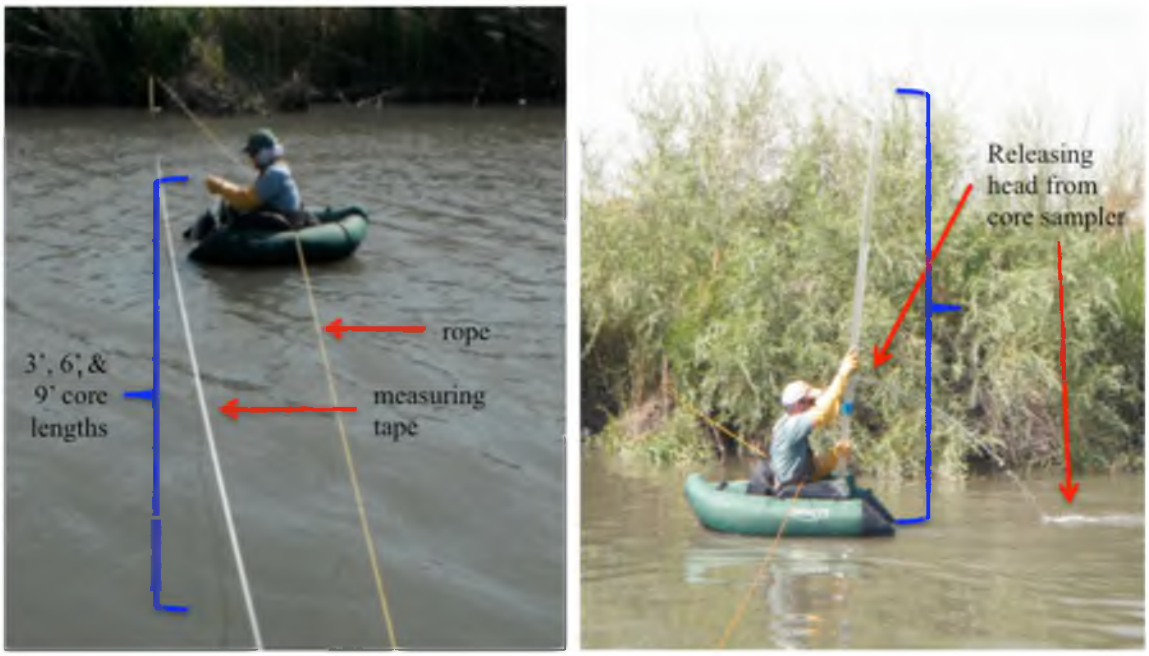

Fig. 33. Midriver sediment core sampling
Note: tape measure and rope strung across river (left) and removing water from the sediment core extension (right)

cores were subsampled in the field to include the top 0–2 cm of the surficial sediments and at 5 cm increments thereafter. Sticks and plastic were removed from the samples during collection since these objects will be measured as %VS, but they do not add to the ambient DO deficit. The rationale for collecting the top 0–2 cm as opposed to 1 cm while characterizing surficial sediments was to remove sampling bias associated with benthic growth covering the sediments that will inflate sediment OM estimates.

4.5.3 %TS and %VS calculations

Percent total solids (%TS) and percent volatile solids (%VS) were measured according to USEPA Method 1684 and Standard Methods (APHA 2005). The first 187 sediment samples were analyzed in duplicate for %TS and %VS. Due to the high reproducibility, duplicates were not performed on the following samples. Calculations

used to quantify sediment %TS, %VS, and the VS of the wet sediment ($\%VS_{wet}$) are provided below.

$$\%TS_{bulk} = \frac{(A-B)\times 100}{C-B} \quad (1)$$

$$\%VS_{bulk} = \frac{(A-D)\times 100}{A-B} \quad (2)$$

$$\%VS_{wet} = \%VS_{bulk} \times \left({}^{\%TS_{bulk}}/_{100}\right) \quad (3)$$

$\%TS_{bulk} = total\ solids\ of\ bulk\ wet\ sediments\ \left({}^{kg\ dry}/_{kg\ wet}\right)$

$\%VS_{bulk} = volatile\ solids\ of\ dried\ bulk\ sediments\ \left({}^{kg\ burnable}/_{kg\ dry}\right)$

$\%VS_{wet} = volatile\ solids\ of\ bulk\ wet\ sediments\ \left({}^{kg\ burnable}/_{kg\ wet}\right)$

$A = weight\ of\ dried\ residue + dish\ (mg)$
$B = weight\ of\ dish\ (mg)$
$C = weight\ of\ wet\ sample + dish\ (mg)$
$D = weight\ of\ residue\ and\ dish\ after\ combustion\ (mg)$
(APHA 2005)

4.5.4 CPOM and FPOM measurement and calculations

Sediment course and fine particulate matter (CPM and FPM) were separated from the bulk sediments by wet sieving (1 mm sieve) using a stream of tap water as not to destroy the structure of any course particulate organic matter (CPOM). CPM samples were then subjected to %TS, %VS, and %TOC analysis to determine the OM fraction. The final parameters of $\%VS_{CPOM}$ and $\%VS_{FPOM}$ represent the percentage of the bulk %VS present as either course or fine particulate OM. Equations used to quantify the amount of course and fine organic matter are provided on the following page.

$$\%TS_{CPM} = \frac{(A_{CPM} - B)\times 100}{C_{CPM} - B} \quad (4)$$

$$\%VS_{CPM} = \frac{(A_{CPM} - D_{CPM})\times 100}{A_{CPM} - B} \quad (5)$$

$$\%VS_{CPOM,wet} = \frac{(A_{CPM} - D_{CPM})\times 100}{C_{CPM} - B} \quad (6)$$

$$\%VS_{CPOM} = \frac{VS_{CPOM,wet}\times 100}{VS_{wet}} \quad (7)$$

$$C_{CPM} = B + F - G \quad (8)$$

$$\%VS_{FPOM} = 100\% - \%VS_{CPOM} \quad (9)$$

$\%TS_{CPM} = TS\ of\ CPM\ in\ bulk\ wet\ sediments\ \left({}^{kg\ dry}/_{kg\ wet}\right)$

$\%VS_{CPM} = VS\ of\ CPM\ in\ dried\ bulk\ sediments\ \left({}^{kg\ burnable}/_{kg\ dry}\right)$

$\%VS_{CPOM,wet} = VS\ of\ CPOM\ in\ bulk\ wet\ sediments\ \left({}^{kg\ burnable}/_{kg\ wet}\right)$

$\%VS_{CPOM} = VS\ of\ CPOM\ as\ a\ percentage\ of\ VS_{bulk}\ \left({}^{kg\ CPOM}/_{kg\ VS}\right)$

$\%VS_{FPOM} = VS\ of\ FPOM\ as\ a\ percentage\ of\ VS_{bulk}\ \left({}^{kg\ FPOM}/_{kg\ VS}\right)$

$A_{CPM} = weight\ of\ dried\ wet\ sieved\ CPM\ residue + dish\ (mg)$
$B = weight\ of\ dish\ (mg)$
$C_{CPM} = weight\ of\ bulk\ wet\ sample + dish\ (mg)$
$F = weight\ of\ bulk\ wet\ sample + plastic\ dish\ (mg)$
$G = weight\ of\ plastic\ dish\ (mg)$
$D_{CPM} = weight\ of\ CPM\ residue\ and\ dish\ after\ combustion\ (mg)$

4.5.5 %TOC measurement and calculations

Sediment percent total organic carbon (%TOC) of the bulk sediments was measured using a Shimadzu TOC-V with SSM-5000A solids sampling module. Percent total carbon (%TC) was measured by combusting a 200–400 mg dry sediment sample at 900 °C, volatilizing both inorganic and organic carbon, and measuring CO_2 evolution via infrared spectroscopy. Percent inorganic carbon (%IC) was measured at 200 °C using 85% phosphoric acid to evolve CO_2. %TOC was initially measured via the following relationship:

$$\%TOC = \%TC - \%IC \quad (10)$$

Due to challenges associated with inorganic carbon being present at higher concentrations than organic carbon in the alkaline sediments, the protocol was adjusted by using a 5% hydrochloric acid (HCl) pretreatment to remove inorganic carbon (Leipe et al. 2010). After confirming methods, all samples were acid pretreated to improve reliability in %TOC analysis in the alkaline sediments using the relationship.

$$\%TOC = \%TC_{HCl\ pretreated} \quad (11)$$

4.5.6 Sediment OM standing stock calculations

Aerial OM standing stocks can be estimated using the following equation to account for pore water and sediment wet density. A dry bulk density of 1.6 kg/L, representative of fine quartz sand, was used in all calculations. The following equations were used to estimate the amount of OM present in a square meter at a 2.5 cm depth at the surface and 5 cm sectional depths for subsurface sediment OM estimates.

$$OM_{aerial} = Y\left\{\left[\rho_w * \left(1 - \frac{\%TS}{100}\right)\right] + \left[\rho_s * \left(\frac{\%TS}{100}\right)\right]\right\}\left(\frac{L}{10^3\ cm^3}\right) d \left(\frac{10^4\ cm^2}{m^2}\right)$$

$$OM_{aerial} = Y\left\{\left[\rho_w * \left(1 - \frac{\%TS}{100}\right)\right] + \left[\rho_s * \left(\frac{\%TS}{100}\right)\right]\right\} d(10) \qquad (12)$$

$OM_{aerial} = standing\ stock\ of\ OM\ x\ cm\ deep\ \left({}^{g\ OM}/_{m^2}\right)$

$Y = \frac{10\ g * (\%VS_{wet})}{kg\ wet\ sediment} = \left(\frac{g\ OM}{kg\ wet\ sediment}\right)$

$\rho_w = density\ of\ water = 1\ {}^{kg}/_{L}$

$\rho_s = dry\ bulk\ density = 1.6\ {}^{kg}/_{L}\ \left(sand = 1.6\ {}^{g}/_{cm^3}\right)$

$d = depth\ of\ active\ sediment\ layer$
$surface = 2.5\ cm\ and\ subsurface = 5\ cm$

After calculating aerial sediment standing stocks of OM, these values can be applied to the Jordan River using the average length and width of each hydraulic reach.

$$OM_{aer,stretch} = (OM_{aerial} * L * w) * \left({}^{kg}/_{1000\ g}\right) \qquad (13)$$

$OM_{aer,stretch} = standing\ stock\ of\ OM\ along\ each\ stretch\ (kg\ OM)$
$L = length\ of\ river\ under\ consideration\ (m)$
$w = river\ width\ (m)$

Finally, the depth specific loads can be summed to estimate the cumulative OM present at different sediment column depths.

4.6 Sediment Methane Gas Fluxes

4.6.1 Sediment gas flux sampling locations

Sediment methane and carbon dioxide fluxes were measured at the CPOM sampling locations in the LJR during the Spring of 2012. An additional methane study was conducted in State Canal during the Spring of 2013.

4.6.2 Sediment gas flux sampling protocols

The poor solubility of methane was utilized by subjecting a sediment–water slurry to headspace gas extraction protocols commonly used for dissolved gas analysis. The dissolved methane fraction was considered insignificant due to the vortexing of the serum bottle sediment samples directly before analysis, and the low water volume to gas headspace ratio (V_{liquid}:$V_{headspace}$ = 0.2 for %TS = 50%, or 150 molecules CH_4 in the gas phase for every one dissolved methane molecule in the pore water).

Serum bottle sediment methane production batch tests were conducted by adding a known mass of wet sediments into a 75 mL serum bottle to a volume slightly less than 30 mL. Jordan River water was then added to the serum bottle so that the final volume of the sediment/water mixture was 30 mL, with 45 mL of headspace to allow standardized use of the ideal gas equation. The addition of LJR water was used only to provide the correct headspace volume, and the addition of water was kept to a minimum (<10 ml). In addition to simplifying Henry's Gas Law, the large relative headspace is required since multiple gas samples will be taken from each serum bottle during the experimental period, and negative relative pressures need to be avoided. Blank, or control, serum bottles containing only DI water where the only serum bottles that maintained a negative relative pressure during analysis, as expected. The serum bottles were capped with 20

mm aluminum crimp caps and 20 mm butyl rubber-teflon faced septa.

After sealing the bottles, the sediment slurry and headspace where purged for 15-minutes with nitrogen gas while gently mixing the slurry every 5-minutes to create anaerobic conditions. 26-gauge needles were used both for nitrogen purging and headspace gas analysis to minimize the size of puncture holes in the septa during multiple day testing to limit positive pressure induced headspace losses and potential atmospheric contamination. Since positive headspace pressures are produced during anaerobic decay, atmospheric contamination did not influence results. Figures 34 and 35 show prepared sediment serum bottles for the Burnham Dam site having silty muck sediments and the 700 S site having more sandy sediments.

The sediment serum bottles were left undisturbed to incubate at 20 °C in a dark cabinet for a time period of 5 days. 5 minutes before headspace gas chromatography analysis, the serum bottles were completely mixed by vortexing at a speed between 2–4 (per the speed dial) for 2 minutes while taking great care not to contaminate the septa bottom with sediment (Scientific Industries, Vortex Genie-2).

The samples were mixed prior to gas analysis to measure the maximum rate of

Fig. 34. Burnham Dam serum bottles (silt and muck)

Fig. 35. 700 S serum bottles (sand and silt)

sediment methane production while removing the gas-sediment diffusion complexities. Following vortexing, the headspace relative pressure was measured via manometer and 26-gauge hypodermic needle (Fisher Scientific, Traceable manometer). 200 microliter gas samples were collected with a gas tight syringe (Hamilton #81156) and injected into an Agilent Technology gas chromatograph 7890A with a thermal conductivity detector (TCD) at a detector temperature of 150 °C. Gas separation was carried out using a 30 meter capillary column (Agilent GS-Carbonplot) at an isothermal oven temperature (30 °C) over a 5-minute time interval. The carrier gas was helium at 27 cm/sec with an injector temperature of 185 °C and 1:30 split. The methane peak was at 2.6 minutes and carbon dioxide occurred at 4 minutes. The calibration curves for CH_4 and CO_2 were within the range of 0.02–25% in terms of partial pressure of the gas sample. The methane and carbon dioxide percentages were then used in the following gas equations. The percent of carbon dioxide can be substituted for methane in the following equations to estimate sediment production of the more soluble CO_2.

4.6.3 Sediment gas flux calculations

The ideal gas law is required to calculate the number of moles of methane (CH_4) present in the headspace of the serum bottle.

$$PV = nRT \quad (14)$$

$P = pressure\ (Pa)$
$V = volume\ (m^3)$
$n = moles\ of\ gas$
$R = gas\ constant = 8.314\ \left({}^{J}/_{K * mol}\right)$
$J = joule\ (Pa * m^3)$
$T = temperature\ (K)$

The following equations provide the parameters and units required to utilize the ideal gas law in this serum bottle study. Absolute pressure was calculated as the sum of atmospheric and relative headspace pressures.

$$\mu mol\ CH^4 = \frac{\left\{(P_{amb} + P_{HS})\left(10^3\ {}^{Pa}/_{kPa}\right)\right\}\left\{(V_{HS})\left({}^{L}/_{10^3\ mL}\right)\left(\frac{m^3}{10^3\ L}\right)\right\}\left\{\left(10^6\ {}^{\mu mol}/_{mole}\right)\left({}^{\%CH_4}/_{10^2}\right)\right\}}{\left(8.314\ {}^{J}/_{K * mol}\right)(T_{amb})}$$

$$\mu mol\ CH^4 = \frac{(P_{amb} + P_{HS})(V_{HS})(\%CH_4)(10)}{(8.314)(T_{amb})} \quad (15)$$

$\mu mol\ CH_4 = micromoles\ methane\ in\ headspace\ of\ bottle$
$P_{amb} = ambient\ atmospheric\ pressure\ (kPa) \cong 85.6$
$P_{HS} = serum\ bottle\ headspace\ pressure\ (kPa)$
$V_{HS} = serum\ bottle\ headspace\ volume\ (mL)$
$\%CH_4 = headspace\ methane\ as\ percent\ volume\ (GC\ output)$
$T_{amb} = ambient\ room\ temperature\ (K) \cong 293$

After determining the number of micromoles of methane produced in the sediment bottle, this value was normalized to wet sediment mass and days of incubation to calculate the wet sediment methane production rate (Y).

$$Y = \frac{(\mu mol\ CH_4)\left({}^{mol}/_{10^6\ \mu mol}\right)}{(m_{wet})\left({}^{kg}/_{10^3}\right)(t)} = \frac{mol\ CH_4}{(m_{wet})(t)(10^3)} \quad (16)$$

$$Y = \frac{mol\ CH_4}{(kg\ wet\ sediment)(day)}$$

$t = time\ (days)$
$m_{wet} = wet\ mass\ of\ sediments\ (g)$

Similar to sediment OM, the gravimetric methane production rate was converted to an aerial flux by incorporating the wet bulk density and depth of the sediment layer. For comparison reasons, this molar flux was converted into a SOD equivalent assuming that all methane is oxidized at the sediment water interface ($CH_{4,OD}$).

$$CH_{4,OD} = Y\left(\frac{16\ g\ CH_4}{mol}\right)\left(\frac{64\ g\ O_2}{16\ g\ CH_4}\right)\left\{\left[\rho_w * \left(1 - \frac{\%TS}{100}\right)\right] + \left[\rho_s * \left(\frac{\%TS}{100}\right)\right]\right\}\left(\frac{L}{10^3\ cm^3}\right) d\left(\frac{10^4\ cm^2}{m^2}\right)$$

$$CH_{4,OD} = Y(64\ g\ O_2)\left\{\left[\rho_w * \left(1 - \frac{\%TS}{100}\right)\right] + \left[\rho_s * \left(\frac{\%TS}{100}\right)\right]\right\} d(10) \quad (17)$$

$CH_{4,OD} = SOD\ associated\ with\ CH_4\ \left({}^{g\ DO}/_{m^2 * day}\right)$
$\rho_w = density\ of\ water = 1\ {}^{kg}/_{L}$
$\rho_s = dry\ bulk\ density = 1.6\ {}^{kg}/_{L}\ \left(sand = 1.6\ {}^{g}/_{cm^3}\right)$
$d = depth\ of\ active\ sediment\ layer$
$surface = 2.5\ cm\ and\ subsurface = 5\ cm$

To investigate temperature effects on methanogenesis, a Q_{10} study was conducted. The Q_{10} coefficient is an unitless ratio used to describe the change in a biological metabolism following a 10 °C temperature change. Sediment Q_{10} ratios can easily be measured while investigating methane production using serum bottle techniques.

$$Q_{10} = \left(\frac{R_2}{R_1}\right)^{10/(T_2 - T_1)} \quad (18)$$

$Q_{10} = unitless\ ratio$
$R = observed\ rate$
$T =$ temperature (°C)

The samples used in the Q_{10} study were collected during the winter and immediately monitored under "cold" conditions to minimize sampling artifacts associated with temperature changes to the original samples. Sediment serum bottles were initially stored for 2 days at 4 °C in a refrigerator to measure winter methane production, followed by 2 days at 20 °C in a dark cabinet to mimic summer conditions.

CHAPTER 5

RESULTS AND DISCUSSIONS

5.1 Sediment Oxygen Demand (SOD)

5.1.1 Jordan River SOD

SOD was measured at 27 locations along the length of the Jordan River and during different seasons. During SOD measurements, many types of sediments capable of exerting elevated oxygen demands were encountered including clays, silty mucks, sands, gravels, and cobbles. Duplicate SOD chambers were installed at each location to account for sediment heterogeneity. Fig. 36 provides the relationship between the duplicate SOD chambers for all chamber deployments. The blue dots represent sampling events in the Lower Jordan River (LJR). The sediments in the LJR were surprisingly homogeneous at individual sites and had a 1.05:1 relationship (circles) between the duplicate SOD chambers in the silty muck sediments characteristic of Reaches 1 and 2. The extremely homogeneous sediments found in Utah Lake (triangles) resulted in duplicate SOD chambers giving very reproducible DO fluxes. The small squares represent chamber installations in the Upper Jordan River (UJR). These sites had much more heterogeneous sediments composed of sand and gravel, and duplicate SOD fluxes were more variable.

Table 12 summarizes average SOD fluxes measured between 2009–2013 for all sites. Also included is the number of chamber placements (N) and the standard deviation (SD) of SOD measured over four years. In Table 12, the negative values indicate that

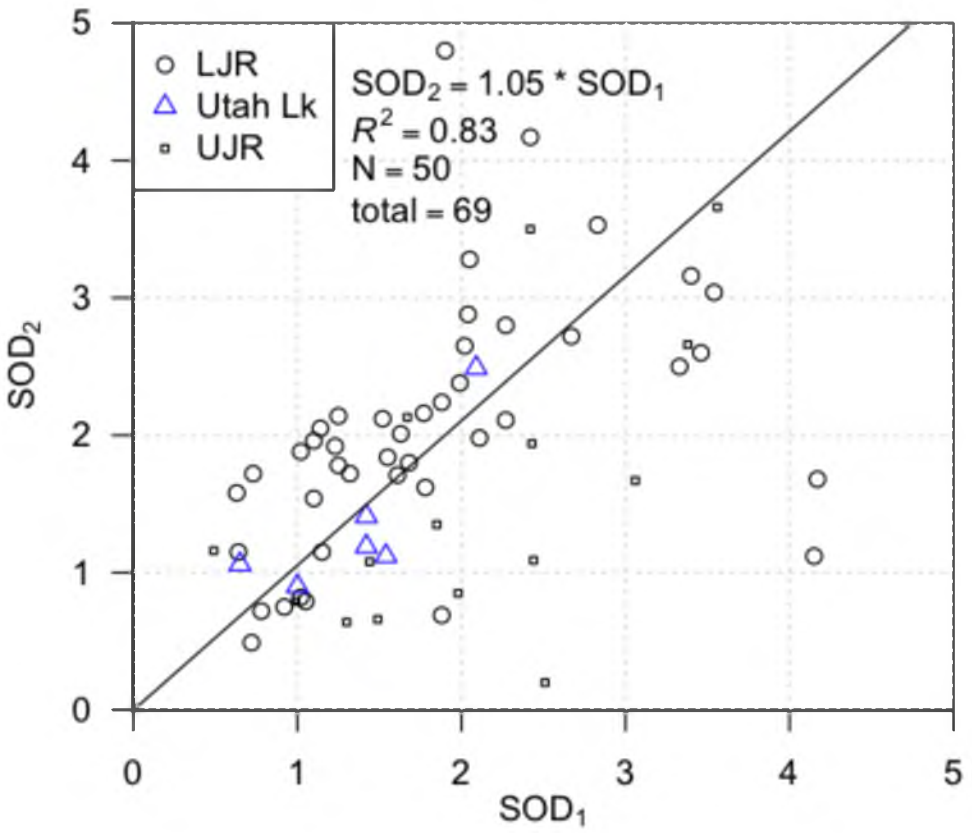

Fig. 36. Duplicate SOD chamber consistency

ambient DO was being consumed by the sediments. Appendix A provides additional SOD and WC_{dark} data. As a general rule, SOD values greater than -1 g-DO/m^2/d are associated with organically enriched sediments (Chapra 2008, pg. 452). The USEPA broadly classifies a SOD less than -1 g-DO/m^2/d as low and greater than -1 g-DO/m^2/d as high (USEPA 1985). Except for the 3600 S site, all sites in the Jordan River had an average SOD greater than -1 g-DO/m^2/d, signifying the presence of either organically enriched sediments or the presence of other biogeochemical activities consuming oxygen.

The 4-year standard deviation (SD) for in the LJR (Reaches 1–3) were equal to or less than 1.0 g-DO/m^2/d for all sites except Burnham Dam, where one chamber measured -4.8 g-DO/m^2/d. The high SD in the downstream State Canal was a result of one chamber

Table 12. Jordan River SOD

2009–2013 mean seasonal SOD (g-DO/m^2/d)					
site	mile	reach	mean SOD	SD	N
State Canal			-6.57	2.2	2
Burnham	0.5	1	-2.15	1.5	5
LNP NE	2.8	1	-2.13	0.8	21
LNP SW	3	1	-2.92	0.6	2
LNP Upper-N	3.1	1	-2.19	0.1	2
Cudahy Ln	3.2	1	-2.58	0.8	10
1700 N	5	2	-2.06	0.3	2
300 N	8.9	2	-1.82	1.0	17
700 S	10	3	-1.42	0.3	4
900 S-N	11.2	3	-1.66	0.6	5
900 S-S	11.3	3	-1.12	0.4	6
1300 S	12.5	3	-2.26		1
1700 S-N	13.1	3	-1.72	1.0	15
1700 S-S	13.15	3	-1.07	0.5	3
2100 S	13.7	3	-1.49	0.6	3
2300 S	13.7	4	-2.44	1.4	4
2600 S	14.7	4	-4.69		1
2780 S-E	15	4	-2.60	1.7	4
2780 S-W	15.1	4	-2.81	0.6	3
3600 S	16.8	4	-0.97	0.5	2
5400 S	20.9	4	-3.27	2.4	9
7600 S	23.9	5	-3.45	2.5	5
7800 S	24.1	5	-1.30	1.2	3
9000 S	26	5	-1.35	0.7	7
SR-154	34.1	6	-1.77	1.0	2
14600 S	37	7	-1.90	0.3	2
US-73	46.2	8	-1.51	0.9	4

Note: 142 SOD chamber installations in the Jordan River

measuring an extremely high SOD of -8.13 g-DO/m^2/d.

The most intriguing SOD results were obtained at sites located in the UJR where the sediments where dominated by gravel and sand substrates. The high SOD observed in Reaches 4 and 5 of the UJR are hypothesized to be a result of hyporheic upwelling or groundwater intrusion into the SOD chamber, not sediment OM decay (Hall and Tank 2005; Brunke and Gonser 1997).

Table 13 provides generalized benthic conditions based on 103 SOD measurements conducted in Illinois streams (Butts and Evans 1978). Table 13 refers to fine sediments, not coarse sands and gravels. These values provide an indication of the pollution status of the sediment in terms of organic matter enrichment based on measured SOD fluxes.

To obtain a snapshot of all SOD measurements with respect to the pollution status of the sediments, Fig. 37 provides all SOD fluxes measured in the Jordan River in relation to river mile. The three vertical lines represent the boundaries between Reaches 1–3. SOD measurements in the LJR were routinely classified as "moderately polluted" (65% of measurements) and Reach 1 was considered "polluted" in terms of organic

Table 13. Sediment condition for different SOD fluxes

SOD	Sediment condition
< -0.4	clean
-0.4 to -0.8	moderately clean
-0.8 to -1.6	slightly degraded
-1.6 to -2.4	moderately polluted
-2.4 to -4.0	polluted
-4.0 to -8.0	heavily polluted
> -8.0	sewage sludge like

adapted from Butts and Evans 1978, Table 13
20 °C fluxes

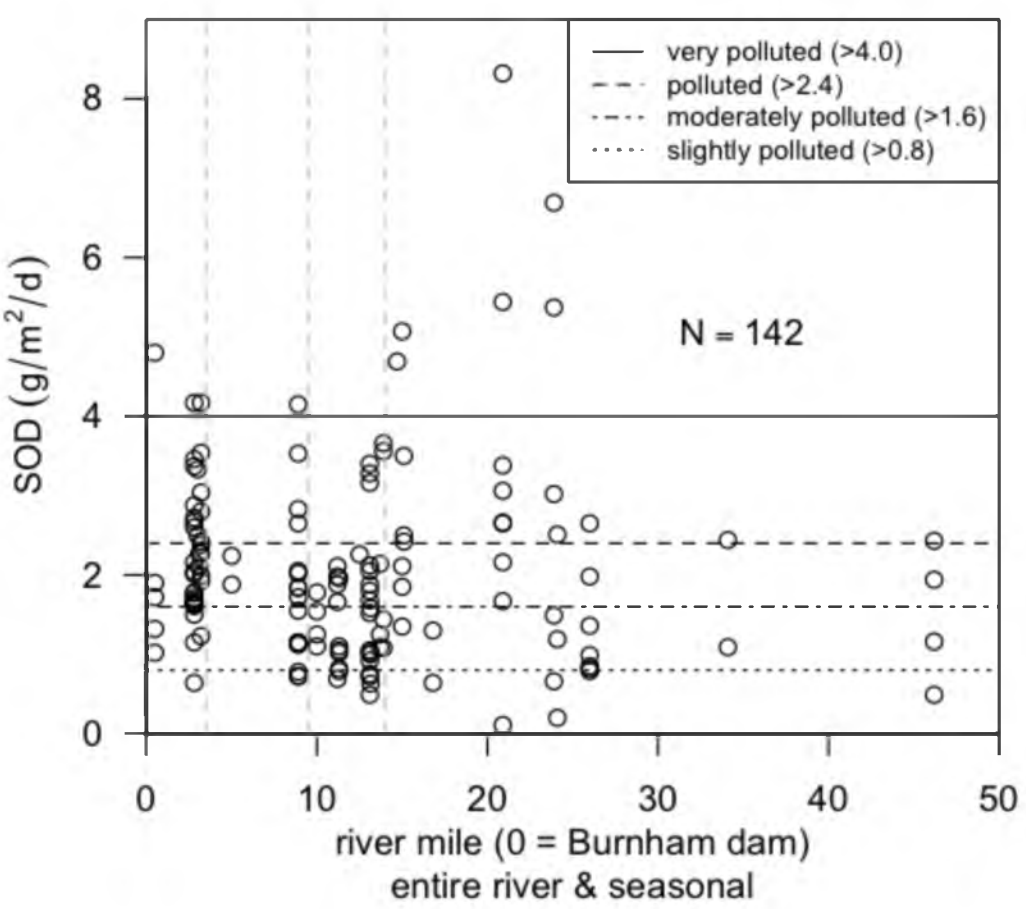

Fig. 37. All SOD data collected in the Jordan River
Note: presented from north to south along the Jordan River

matter (OM) enrichment (40% of measurements). The four SOD fluxes greater than -5 g-DO/m^2/d near mile 20 were measured in gravel sediments, and the sediment pollution status proposed by Table 13 does not apply. Hyporheic upwelling or groundwater intrusion was hypothesized to be the driving parameter in the reduction of DO in the open bottomed SOD chambers, not biological and abiotic processes occurring at the sediment–water interface.

Table 14 provides Reach based average SOD fluxes measured between 2009 and 2013. Hydraulic reach average SOD values were greater than -1.5 throughout the length of the Jordan River. Since the UJR and LJR are very different in terms of topography,

Table 14. Reach based average SOD values

Annual average SOD (g-DO/m^2/d)	
Reach 1	-2.29
Reach 2	-1.85
Reach 3	-1.53
Reach 4, backwater	-2.77
Reach 4, above BW	-2.85
Reach 5	-2.64
Reach 6	-1.77
Reach 8	-1.51

sediment type, and annual streamflow, these sections of the Jordan River will be addressed independently in the following sections.

Table 15 provides SOD fluxes measured in other degraded surface waters in the United States. Additional factors including BOD, flow velocity, reaeration potential, and river depth will dictate whether anoxia will occur in a slow moving river. From Table 15, it can be concluded that SOD fluxes measured in Reach 1 were similar to those found in aerated catfish ponds used for aquaculture, suggesting sediment organic enrichment (Berthelson et al. 1996). All hydraulic reaches in the Jordan River had average SOD fluxes higher than the Salem River, which is considered eutrophic, and had sediment oxygen demands similar to the Klamath and Lower Willamette Rivers that were characterized as having chronically low ambient DO. The extremely high SOD flux of -19.5 g-DO/m^2/d was measured prior to the Clean Water Act in river sediments capable of maintaining anoxic ambient conditions in the Lower Willamette River.

5.1.2 SOD Lower Jordan River

Fig. 38 provides a box plot for average SOD measured in the LJR. SOD increases with distance downstream in the LJR, consistent with the observed ambient DO

Table 15. Comparisons of SOD in other degraded surface waters

Surface Water	State	mean SOD_{20} ($g/m^2/d$)	N	STD DEV	Reference and notes
Saddle River	NJ	-1.3	5		1
Salem River	NJ	-1.5	6		2
Passaic River	NJ	-0.9	11	0.94	3
Arroyo Colorado River	TX	-0.6		0.38	4
7 blackwater streams	GA	-1.4	24		5
Klamath River	OR	-1.8	22		6
Lower Willamette River	OR	-2.1	45	0.57	7
Catfish ponds	MS	-2.5	86	0.93	8
Shrimp ponds		-6			9
Lower Willamette River	OR	-19.5			10
Reach 1, Jordan River	UT	-2.3	40	0.89	11

Reference and notes

1 (Heckathorn and Gibs 2010) eutrophic
2 (Heckathorn and Gibs 2010) eutrophic
3 (Urchin and Ahlert 1983) poor urban WQ
4 (Matlock et al. 2003) chronic low DO and fish kills
5 (Utley et al. 2008) chronic low DO
6 (Doyle and Lynch 2005) chronic low DO
7 (Caldwell and Doyle 1995) anoxic
8 (Berthelson et al. 1996) aquaculture
9 (Madenjian et al. 1990) aquaculture
10 (Thomas 1970) anoxic, before Clean Water Act
11 this study, chronic low DO

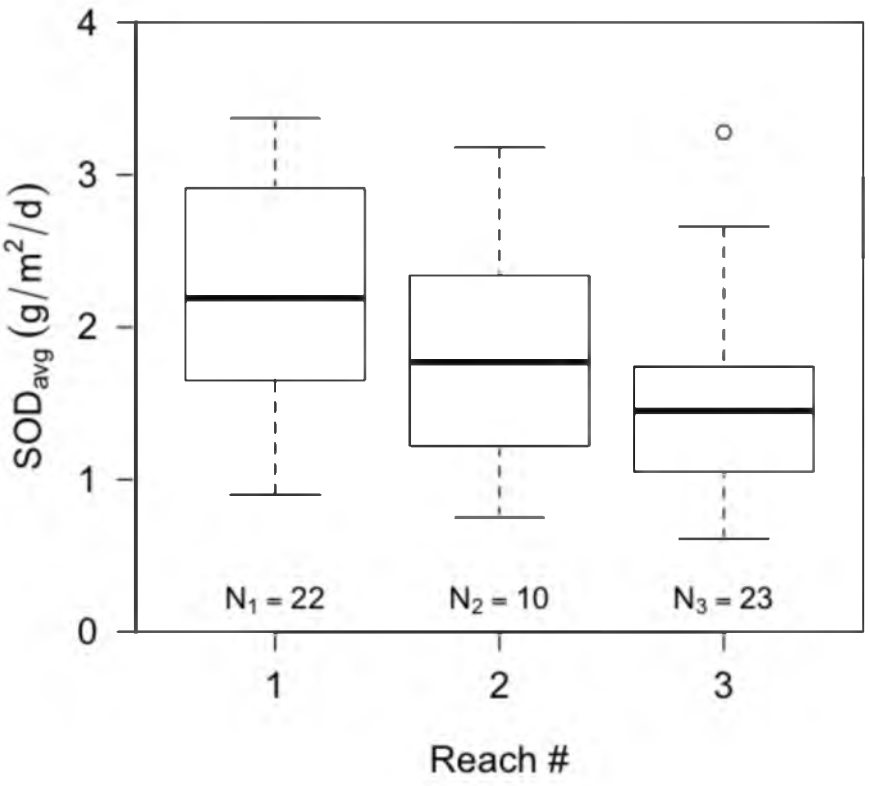

Fig. 38. LJR reach average SOD fluxes

deficit in the LJR (Utah DWQ 2013).

Hydraulic Reach 1 had sediments composed of fine silts and detritus that were easily penetrated with a sediment core sampler to depths greater than 60 cm in depositional zones and released considerable amounts of swamp gas when disturbed. Swamp gas, predominately methane and carbon dioxide, is commonly found in the sediments of stagnant and slow moving water bodies and is produced during the anaerobic decomposition of organic material. The diffusion of these reduced compounds, including methane, ammonia, and hydrogen sulfide increases SOD as these compounds are oxidized near the sediment–water interface (Di Toro et al. 1990).

Hydraulic Reach 1 is located within the historic Great Salt Lake flood plain and is a natural location for large amounts of sedimentation. Burnham Dam and the network of

canals, and weirs used to distribute freshwater to the downstream impounded wetlands creates a backwater effect in Hydraulic Reach 1. This backwater results in decreased flow velocities and increased settling of suspended matter. The accumulation of settled materials in natural systems typically occurs during the low flows associated with the summer and fall months (Whittemore 2004). Most rivers and streams in their natural state experience scouring of the benthos during the spring runnoff and during storm events (Lytle and Poff 2004; Biggs and Close 1989; Casey 1990; Naiman and Bibly 1998). These events do not regularly occur on the LJR due to the Surplus Canal diversion that routes the majority of the UJR's flow away from Salt Lake City. The managed flows resulting from the Surplus Canal diversion enhance sediment and particulate organic matter deposition due to decreased stream energy (Allan 1995). The depressed flow rates decrease reaeration potential and increase the hydraulic retention time in the LJR, resulting in additional time for the sediments to deplete DO from the water column (Parr and Mason 2003).

5.1.3 SOD Upper Jordan River

Correlations between SOD and sediment OM in gravel and sandy gravel sediments were not observed in this study, although SOD was almost always greater than -1 g-DO/m^2/d in the UJR. It has been suggested that clean sands have a SOD of -1 g-DO/m^2/d and dirty sands have a SOD of -2 g-DO/m^2/d based on visual observations (Butts 1974). SOD fluxes as high -5 and -8 g-DO/m^2/d were measured in clean gravel sediments in the UJR where there are swift flows and no DO impairment. SOD associated with gravel sediments may be attributed to the respiration of heterotrophic biofilms and autotrophs living on the surface of the gravel (Reid et al. 2006). These

biofilms attached to gravel and cobble substrate act very similar to the trickling filters used by many local municipal wastewater treatment facilities. Alternatively, the elevated SOD fluxes measured in Hydraulic Reaches 4 and 5 may be the result of localized upwelling of low DO water through the gravely substrate associated with the hyporheic activity or groundwater intrusion (Boulton et al. 1998; Wright et al. 2005).

5.1.4 Effect of land use and POTW discharges on SOD

Direct correlations between land use and SOD were not observed in the Jordan River, which has been noted in other SOD studies (Utley et al. 2008). Although SOD steadily increased in the LJR below the Surplus Canal diversion, sedimentation patterns driven by the natural topography of the LJR are most likely responsible for the consistent downstream increases in SOD. Flatter topography is associated with increased SOD due to enhanced settling of OM, but topography does not describe the sources of OM contributing to SOD.

No direct correlations between POTW discharges and SOD were noted, suggesting that nutrients and organic matter are quickly distributed downstream, making it difficult to link increases in SOD directly to point discharges (Utley et al. 2008). Increases in SOD were recorded following the South Valley Water Reclamation Facility and Central Valley Water Reclamation Facility (CVWRF) discharges, but these increases in SOD cannot be directly tied to the discharges of these facilities. Large amounts of deposition occur in the slow moving backwaters of the Surplus Canal diversion dam, and this was attributed to the elevated SOD measured downstream of the CVWRF discharge. Indirectly the POTWs are influencing SOD by discharging the macronutrients nitrogen and phosphorus. The abundance of these macronutrients may be contributing to the

eutrophication of the Jordan River, resulting in an indirect OM load via primary production in the water column and benthos (Stringfellow et al. 2009).

High SOD fluxes have been observed in rivers that receive minimal inputs of organic matter from point sources. These natural sources of potential SOD originate from particulate organics that are transported downstream from erosion and detritus entering the river system via runoff. Anthropogenic nonpoint discharges from construction, agriculture, and untreated urban stormwater runoff are undoubtedly contributing to the water quality issues in the Jordan River.

5.1.5 Water column oxygen demand (WC_{dark})

Fig. 39 provides the volumetric DO demand utilized by the water column (WC_{dark}) for each sampling event with the winter observations presented as "*" symbols. The vertical dashed lines indicated hydraulic reach boundaries in the LJR. The UJR had WC_{dark} demands higher than the LJR. This may be attributed to the biochemical oxygen demand (BOD) required to oxidize soluble and suspended OM in the water column or the respiration of phytoplankton and sloughed periphyton (metaphyton) in the swift flowing water conducive to suspended solids transport.

Oxygen demands associated with the water column were highest in the UJR and immediately downstream of the POTW discharge at the 1700 S, 2100 S, and 5400 S sites. This is most noticeable in the winter months when warm wastewater effluent increases the ambient river temperature and associated water column metabolism. The respiration rates measured in the water column decreased dramatically during the winter at sites less influenced by the warm WWTP effluent. Many of the winter sampling events resulted in the WC having zero oxygen demand.

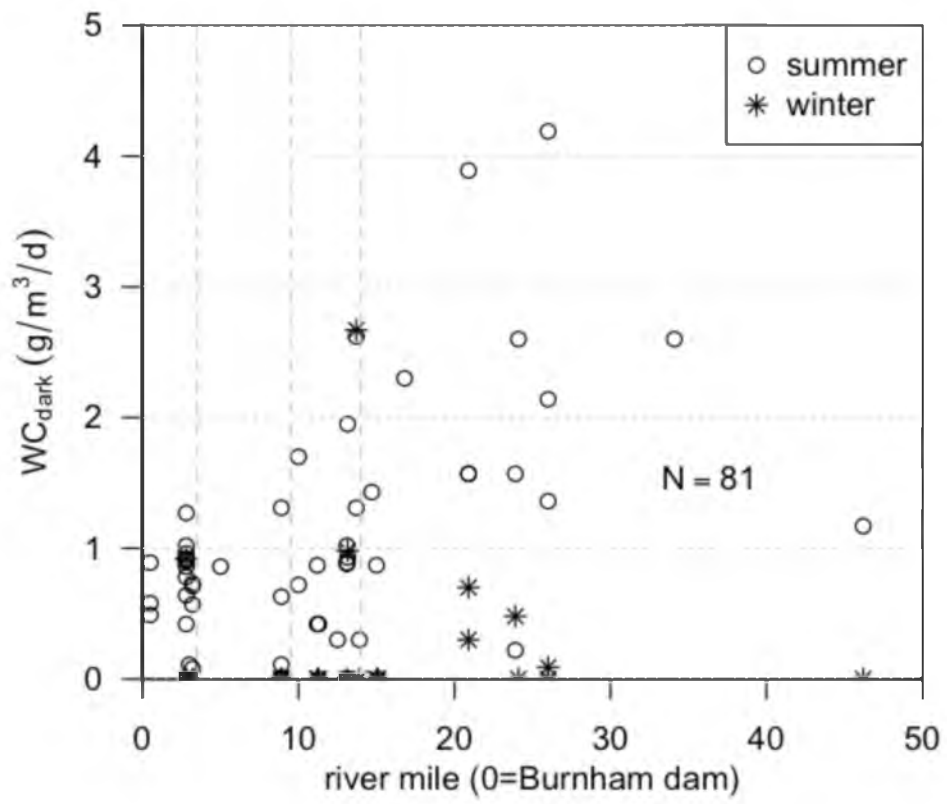

Fig. 39. WC_{dark} oxygen demand for the Jordan River

5.1.6 $\%_{SOD}$ of ambient DO deficit

SOD can account for the majority of ambient DO deficits in shallow water bodies (USEPA 1985). Ambient DO deficits in the Jordan River are heavily influenced by SOD throughout the 52-mile long river. Fig. 40 provides a graphical representation of $\%_{SOD}$ in relation to river mile in the LJR with the assumption that the flow managed LJR mean river depths are consistent throughout the year. The dotted red vertical line identifies the South Davis-South POTW discharge to the Lower Jordan River, and the various symbols identify seasons sampled with summer being the critical time period when ambient DO is the lowest.

SOD accounted for over 50% of the ambient DO deficit during 84% of the sampling events in the LJR (N = 46) and over 75% of the DO deficit during 58% of the

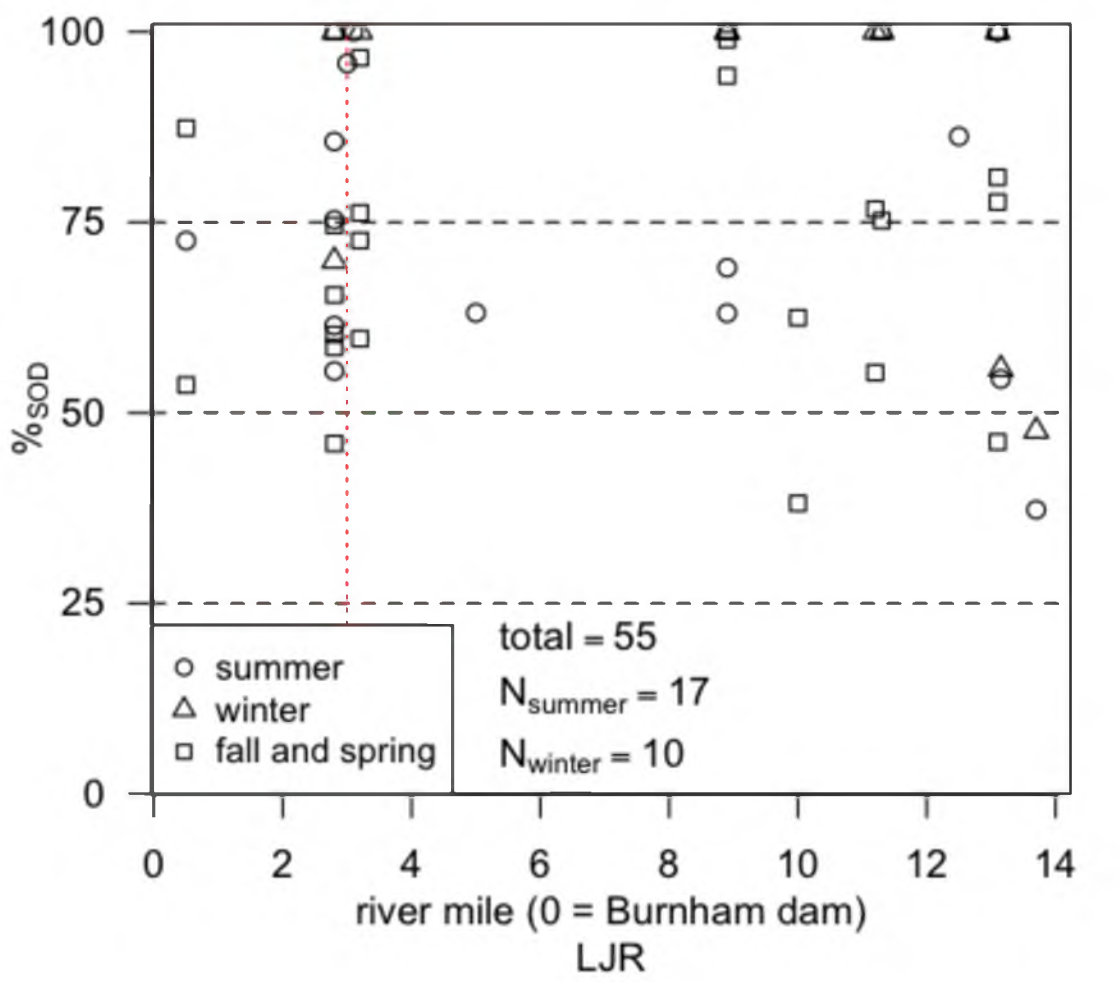

Fig. 40. Percent of ambient oxygen demand associated with sediments (LJR)

sampling events (N = 32). SOD in the DO impaired Arroyo Colorado River accounted for roughly 84% of ambient oxygen demand (N = 15) (Matlock et al. 2003). Many other rivers and shallow surface waters have shown that SOD is a driving parameter in ambient DO deficits (Rutherford et al. 1991; Todd et al. 2009). In general, the shallower the depth of the water column, the more important SOD becomes in relation to ambient DO deficits given similar sediment characteristics (Ziadat and Berdanier 2004). The LJR will most likely continue to experience chronic DO deficits until the sediments become less active in terms of SOD.

Fig. 41 provides $\%_{SOD}$ for all sampling events in the UJR under the assumption that the depths in the UJR decrease by 25% during the winter compared to summer baseflow conditions. The red vertical lines identify the Central Valley WRF and South Valley WRF discharges. The four star-shaped data points identify the sampling events where anoxic upwelling was suspected. These data points are considered "skewed" in this particular analysis since the introduction of low DO water originating from an external source should not be considered an instream biological process. This idea is revisited in Sections 5.2.1 and 5.3.2. Upstream of all online WWTP discharges, SOD accounted for less than 50% of ambient oxygen demand during summertime conditions during six of the seven sampling events

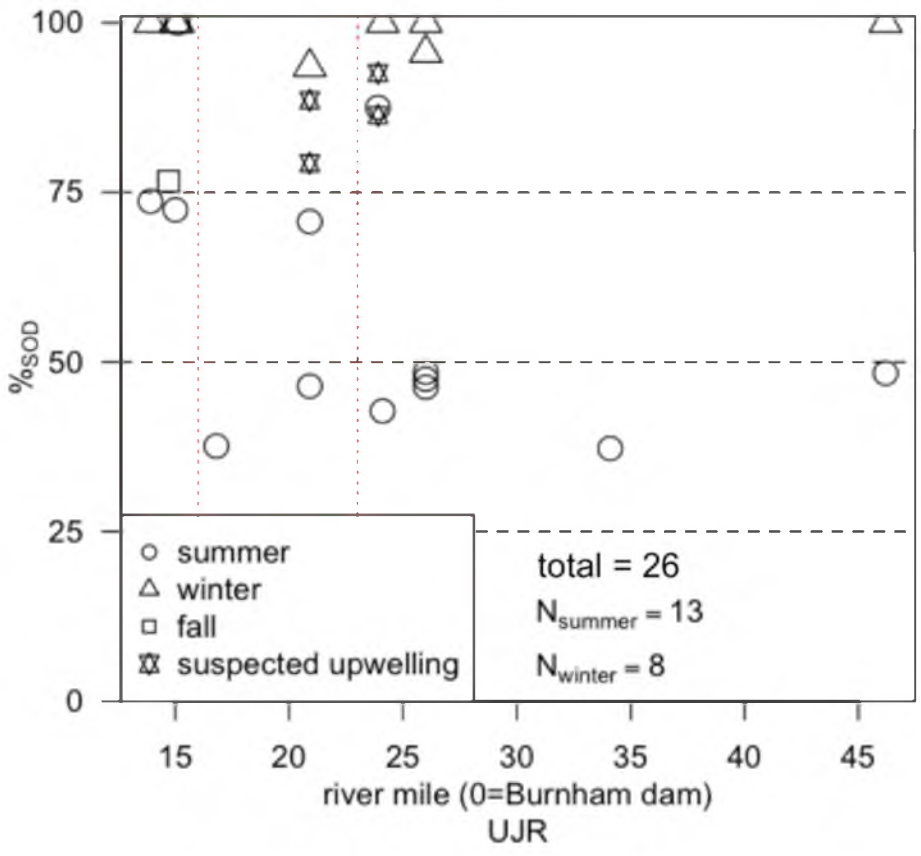

Fig. 41. Percent of ambient oxygen demand associated with sediments (UJR)

5.1.7 Temperature dependence of SOD and WC_{dark}

The dark metabolism of the water column decreased with temperature during the winter months (Fig. 39), but the sediments did not follow the anticipated Van der Hoff model reductions in metabolism due to decreased water temperature. The lack of a clear trend between SOD and ambient river temperature is highlighted in Fig. 42 where SOD did not decrease during the winter months as anticipated. The black squares represent summer measured SOD fluxes normalized to 20 °C (y-axis) using a temperature normalization coefficient (k) of 1.065. The reason the temperature normalized summer

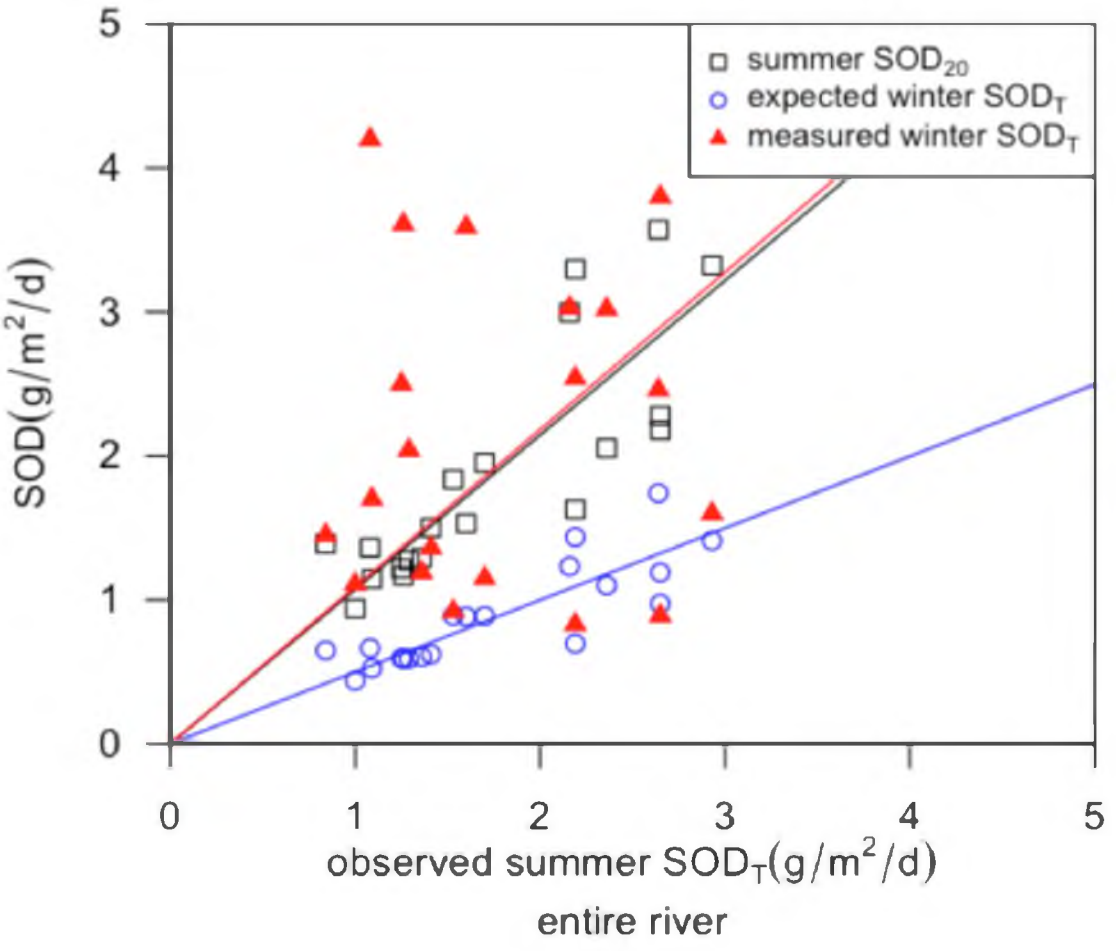

Fig. 42. SOD and temperature

observations (black squares) are at a near 1:1 ratio (SOD_{20}:SOD) is a result of ambient river temperatures being very close to 20 °C during summer sampling. The blue circles represent the expected wintertime SOD fluxes based on temperature normalization to the measured ambient winter temperatures. The red triangles identify the measured winter SOD fluxes. During the winters of 2009 and 2010, 46% and 71% of the sites had winter SOD fluxes higher than the observed summer values, respectively.

These deviations from accepted temperature normalization equations cannot be accounted for by adjusting the temperature normalization coefficient since no relationship was observed in regards to ambient water temperature, except that SOD remained elevated throughout the year.

The elevated winter SOD fluxes observed in both the Upper and Lower Jordan River are hypothesized to be a result of multiple contributing factors:

- groundwater upwelling may add low DO water to the UJR. This would be measured as SOD, but is not a biological process occurring at the sediment–water interface (see chamber NDM and single-station NDM estimates, Sections 5.2.1 and 5.3.2)
- decreased wintertime UJR flow rates coupled with decreased turbidity results in a more hospitable environment for periphyton growth due to less benthic scouring (see winter TPP, Section 5.2.3)
- the autumn deciduous leaf shedding throughout the watershed adds a seasonal OM load compromised of natural and urban OM (see CPOM, Section 5.4.3 and riparian OM load estimate 5.7.6)
- river-mud bacteria and other microbes live in a very inhospitable

environment and are most likely very tolerant to changing environmental conditions (see Seasonal NDM, Section 5.2.3)

- diffusion of reduced chemicals from the surface sediments is the rate limiting parameter for SOD during all seasons (see Q_{10} methanogens, Section 5.6.5)

5.1.8 Utah Lake SOD

The outlet of Utah Lake is the source of the Jordan River; therefore, lake water quality (WQ) directly affects WQ in the downstream Jordan River. SOD was measured at eight sites throughout the large shallow lake to characterize oxygen demands.

Ambient water quality conditions measured at each site are provided in Table 16. The elevated pH and supersaturated DO at the Provo Bay site are a result of primary production in the isolated bay receiving water from Hobble Creek, not the Provo River as the name would suggest. All sites visited during the afternoon hours had supersaturated ambient DO concentrations, even at sites located in the center of the lake. Ambient pH values were greater than 8.5 at all sites. Values greater than 9.0 were coupled with supersaturated ambient DO and were associated with water column primary production

Table 16. Ambient conditions at time of SOD sampling

site	%DO sat.	pH	temp. (°C)	depth (m)
Provo Bay	165	9.6	17.1	1
Provo Bay entrance	129	9	23.5	1
outside marina	81	8.6	22.5	3
Goshen Bay	73	9	22	1
Geneva Steel	110	8.6	18.3	2
Utah Lake Outlet	91	8.6	19.1	2.2
Pelican Point	114	8.9	23	3
Goshen Bay entrance	88	8.6	22.9	3

(phytoplankton). The highest pH values were observed in the shallow sites where water column depths were roughly 1 meter.

Table 17 shows the two-chamber average SOD, WC_{dark}, and chamber calculated nighttime ambient DO depletion rates. The SOD flux describes the amount of DO consumed at the two-dimensional sediment–water interface, and the WC_{dark} is presented as a volumetric rate to be comparable with BOD measurements. The ambient column is presented as a volumetric rate. The "ambient" values were calculated by normalizing SOD to a volumetric rate using lake water depth and summing the SOD and WC rates. Ambient volumetric rates represent the DO dynamics from the perspective of the water column, which is useful because most WQ scientists think in terms of volumetric rates and concentrations. When the WC is deeper than 1 meter, as is the case in most lakes, the sediments become less influential to ambient DO dynamics in unstratified lakes. It should be noted that lake stratification may result in an anoxic hypolimnion over the course of months, not days, but Utah Lake does not experience seasonal stratification.

The highly productive Provo Bay had the highest SOD flux measured in Utah Lake and the visually green water in the isolated hypereutrophic bay had the highest

Table 17. Observed SOD, WC, and estimated ambient DO depletion rates

site	SOD_{avg} g-DO/m^2/d	WC g-DO/m^3/d	ambient g-DO/m^3/d	$\%_{SOD}$
Provo Bay	-4.61	-6.66	-11.3	41
Provo Bay entrance	-1.42	-3.45	-4.9	29
outside marina	-1.49	-2.28	-2.8	18
Goshen Bay	-1.67	-3.4	-5.1	33
Geneva Steel	-2.04	-1.9	-2.9	35
Utah Lake Outlet	-1.03	-1.28	-1.7	27
Pelican Point	-1.06	-4.17	-4.5	8
Goshen Bay entrance	-0.9	-1.11	-1.4	21

WC_{dark} rate measured during this research. WC_{dark} rates measured in Utah Lake were two to 10 times higher than typically measured in the LJR. The senescence, settling, and decay of the phytoplankton respiring to create this extremely high WC_{dark} oxygen demand are the source of the high SOD of -4.6 g-DO/m^2/d measured in Provo Bay.

The sites located near the shores of Utah Lake (Provo Bay entrance, outside marina, Goshen Bay, and Geneva Steel) all had SOD fluxes ranging from -1.4 to -2 g-DO/m^2/d. The deep water sites located offshore (Utah Lake Outlet, Pelican Point, and Goshen Bay entrance) had decreased SOD fluxes ranging from -0.9 to -1.06 g-DO/m^2/d. The decreased SOD in the middle of Utah Lake compared to locations near townships suggests that sediment organic matter enrichment due to eutrophication is ongoing and more pronounced near civilization.

The $\%_{SOD}$ was less than 50% at all sites due to the increased WC depths associated with a lake compared to a river. In addition, the water column in Utah Lake was visually green from phytoplankton during sampling, which was not observed in the Jordan River. The decay of OM derived from phytoplankton is the source of SOD in Utah Lake and is most likely an OM load to the downstream Jordan River in the form of suspended seston and viable phytoplankton cells.

5.1.9 SOD:%VS relationship

Sediment volatile solids (%VS) was measured during 37 chamber installations in the Jordan River to investigate a surface sediment SOD:%VS relationship as an alternative method to estimate SOD using standard laboratory protocols. Correlations between SOD and %VS were observed in the fine silts and sands found in the LJR, Surplus Canal backwater, and in the downstream State Canal (Fig. 43). The backwaters

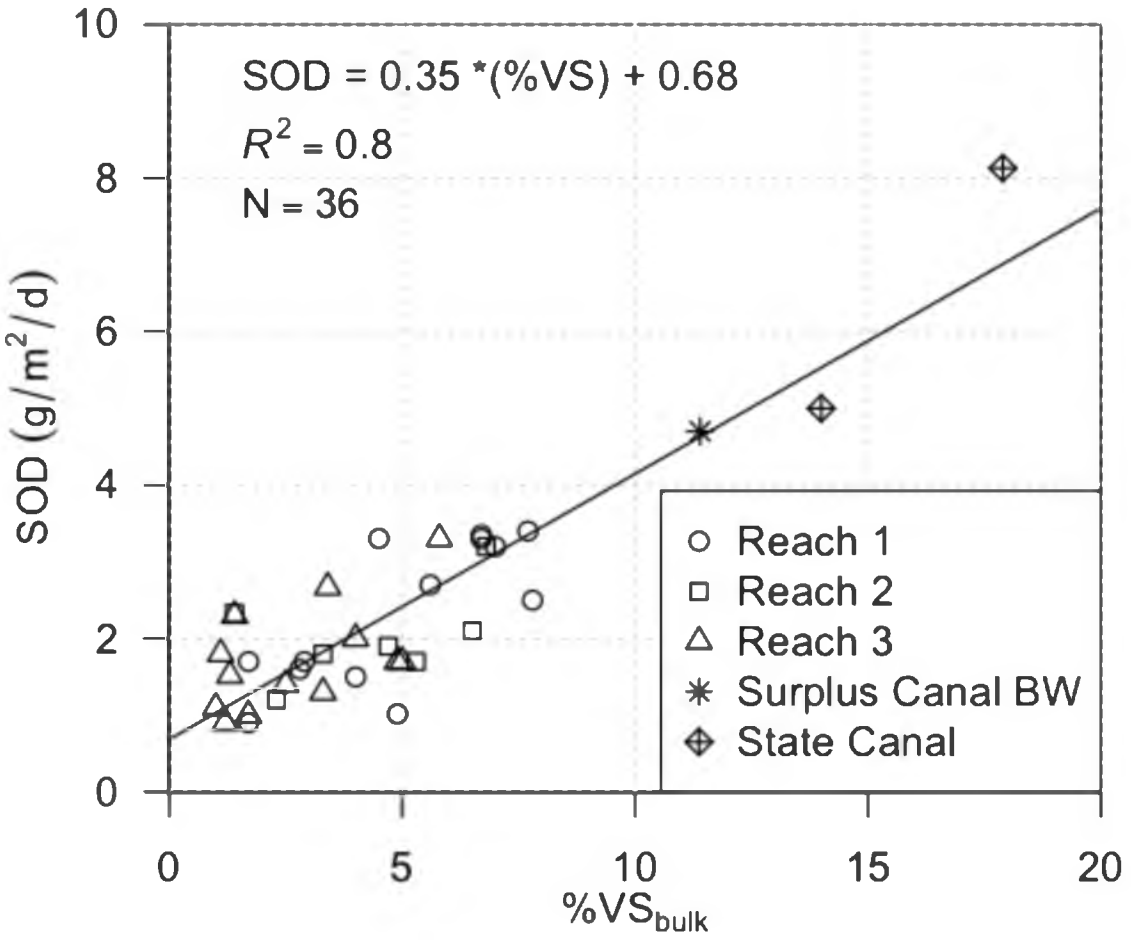

Fig. 43. SOD and %VS relationship in the Lower Jordan River
Note: 0–2 cm sediment depth

of the Surplus Canal diversion dam and State Canal are depositional zones and represent areas of enhanced deposition in the Jordan River. The top 0–2 cm of the surficial sediments were used in this regression since these are the sediments composed of the most recent deposition and contain the benthic community directly interacting with the ambient water. The standard error of the proposed SOD:VS relationship was +/-0.6 g-DO/m^2/d. The relationship between SOD and %VS of the top 0–2 cm of the surficial sediments was

$$SOD = 0.35(\%VS) + 0.68 \quad (19)$$

Other studies have developed general relationships between SOD and various surrogates for OM. These previous empirical equations had a square-root relationship between SOD and sediment OM parameters (Di Toro et al. 1990). The equation proposed in this research was not forced through zero through the use of a more complex regression with the goal to simplify the relationship and due to the fact that a SOD of zero has yet to be measured in the Jordan River.

Butts (1974) encountered silty sediments having %TS and %VS ranging from 30–80% and 1–25%, respectively and he produced the following relationship:

$$SOD = 6.5(\%TS^{-0.46})(\%VS^{0.38}) \quad (20)$$

Fig. 44 compares the Butts (1974) SOD model with LJR data. The pink linear equation represents Butts equation with %TS back calculated using the LJR 0–2 cm %VS:%TS relationship (see Section 5.4.2).

The Butts 1974 equation underestimated SOD in the LJR at fluxes greater than -2.5 g-DO/m^2/d. A SOD greater than -2.5 suggests polluted sediments and provides a strong indication that the sediments are negatively influencing WQ (Butts and Evans 1978).

In summary, the SOD:VS relationship for the Jordan River can be utilized to easily estimate SOD in silty sediments using standard methods for modeling purposes. This relationship could also be used to set goals for the reduction of SOD in the LJR in terms of surface sediment OM enrichment.

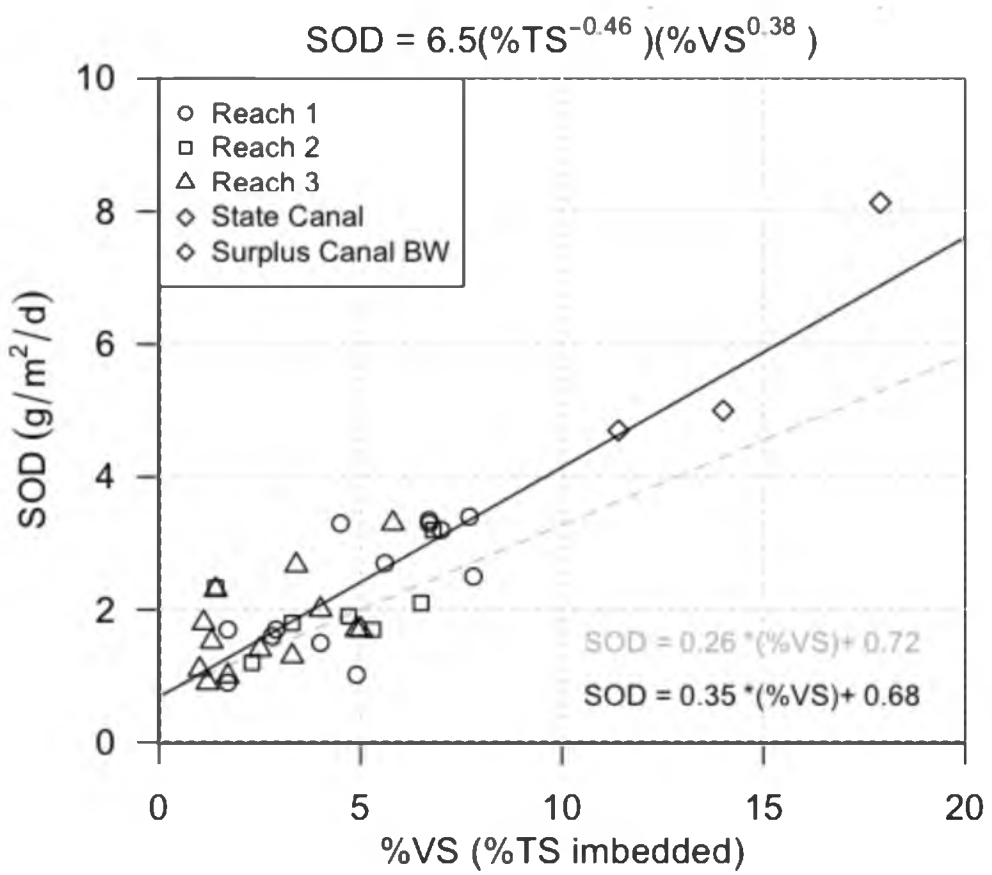

Fig. 44. SOD predictions using Butts (1974) equation

5.2 Chamber Net Daily Metabolism (NDM)

5.2.1 NDM and SOD chamber comparison

SOD measures the sediment oxygen demand utilizing open bottom aluminum chambers and tray oxygen demand (TOD) is the oxygen consumption associated with a sediment tray in a completely enclosed NDM chamber. SOD chambers measure oxygen consumption in the top 1.5" of the sediment column and include the oxidation of reduced gases diffusing from buried sediments and oxygen deficiencies associated with hyporheic exchanges and groundwater upwelling. TOD does not account for hyporheic exchanges, groundwater upwelling, or the diffusion of sediment gases deeper than 1.5".

Fig. 45 provides the relationship between TOD and SOD during 19 sampling

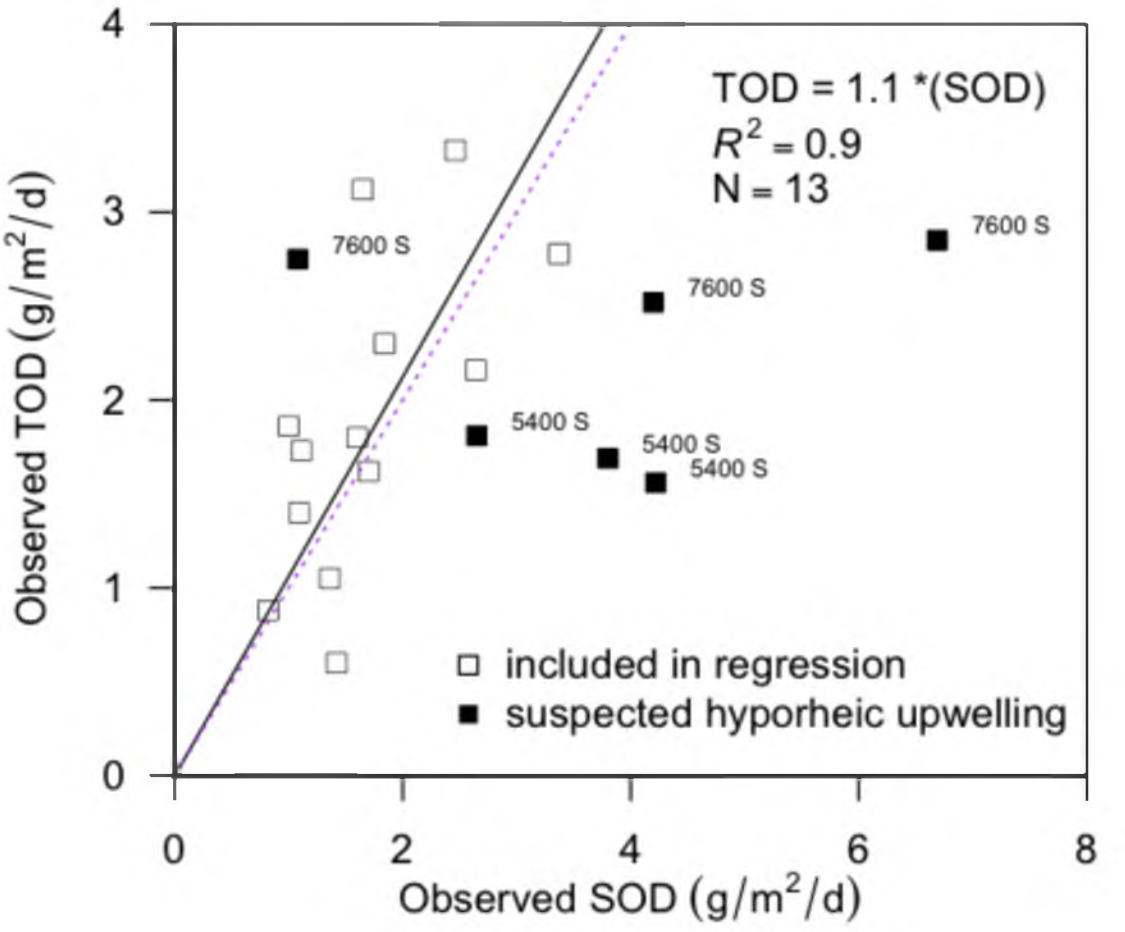

Fig. 45. TOD:SOD relationship

events where both styles of chambers were simultaneously deployed. Both chamber types produced very similar sediment oxygen demands in the silty muck sediments characteristic of the LJR and had a TOD:SOD relationship of 1.1:1 (hollow squares). Surprisingly, the SOD chambers measured much higher oxygen demands in the gravel sediments in the UJR (solid black squares). This was not expected, as any potential sampling error was originally anticipated to be associated with the SOD chambers measuring decreased oxygen demands due to the possibility of a poor seal in the gravel substrate. The sites suspected of low DO upwelling were not included in the regression presented in Fig. 45 (six sampling events).

Evidence of potential hyporheic upwelling or groundwater intrusion is shown as the black square data points in Fig. 45. The extremely high SOD flux greater than -6 $g/m^2/d$ measured during the July sampling event at the 7600 S site suggested upwelling of DO depleted water in the clean gravel sediments. Following this observation, the SOD chambers were placed near zones of suspected upwelling at the 5400 S and 7600 S sites.

The 1700 S site had TOD fluxes greater than the closed bottom SOD chambers. This trend was also observed at the 2100 S site during the August sampling event. This may be a result of heterogeneities in the benthic community and sediment substrate. It is also possible that ambient river water was able to enter the chamber via localized hyporheic flow under the lip of the SOD chamber in the sand and gravel sediments. Sediments were composed of clean gravels and sands at 2100 S, turning into sands at the 1700 S-S site.

5.2.2 NDM chamber dark and light metabolism

Table 18 provides average TOD, gross sediment tray primary production (TPP), WC_{dark}, gross water column primary production (WC_{light}), ambient water temperature, and length of the photoperiod for all NDM chamber sampling events. The sites were visited three times during midsummer, late summer, and winter to investigate seasonal effects on stream metabolism. Negative values indicate that DO is consumed and positive values indicate oxygen production. The sediment parameters are presented as fluxes and the water column is provided as volumetric rates.

The lowest TPP fluxes were measured at 300 N. The 300 N site was located along a straight channelized section of the LJR that is relatively deep (0.75 meters at the bank), experiencing bank undercutting, and is abutted by a veneer of riparian vegetation. The

Table 18. TOD, TPP, WC_{dark}, and WC_{light} measurements

		(g DO/m^2/d)		(g DO/m^3/d)		(°C)	(hrs)
Site	Date	TOD	TPP	WC_{dark}	WC_{light}	temp.	photoperiod
LNP NE	7/16/10	-2.8	4.7	-0.8	1.2	22.3	14.8
LNP NE	8/24/10	-1.8	2.7	-0.9	1.9	20.5	13.4
LNP NE	12/25/11	-3.3	1.2	-0.8	0.1	8.7	9.3
300 N	7/15/10	-2.3	1.8	-0.6	0.5	20.5	14.8
300 N	8/13/10	-2.2	0.2	-1.1	0.6	18.4	13.9
300 N	1/6/11	-1.8	0.7	0.0	0.0	6.6	9.4
1700 S	7/14/10	-1.9	1.0	-0.8	2.2	21.0	14.8
1700 S	8/26/10	-1.2	1.5	-1.6	1.7	20.4	13.3
1700 S	1/3/11	-1.7	1.5	-0.8	0.2	7.9	9.3
2100 S	7/13/10	-2.8	2.5	-1.1	2.7	21.3	14.9
2100 S	8/25/10	-1.4	3.2	-2.2	2.6	19.2	13.4
2100 S	1/7/11	-1.6	2.2	-2.3	0.5	7.7	9.4
5400 S	7/19/11	-1.8	3.5	-1.3	1.8	22.5	14.7
5400 S	9/2/10	-1.6	2.8	-1.3	2.6	18.6	13.0
5400 S	1/12/11	-1.7	4.1	-0.6	1.2	9.7	9.5
7600 S	7/20/10	-2.8	7.4	-1.3	1.1	21.0	14.7
7600 S	9/1/11	-2.8	5.8	-0.2	1.5	16.5	13.1
7600 S	1/15/11	-2.5	5.6	-0.4	1.1	8.5	9.6
9000 S	7/21/10	-0.9	2.0	-1.1	1.0	21.0	15.7
9000 S	9/3/10	-0.1	1.4	-1.8	5.8	18.6	13.0
9000 S	1/20/11	-1.0	3.2	-0.1	1.0	6.0	9.7

low benthic primary production measured at this site was attributed to the increased WC depth, presence of riparian vegetation intercepting the ambient solar flux, and a northwesterly flow direction increasing the amount of shading provided by the riparian vegetation.

The highest TPP rates were observed at the 7600 S site, which had cobble substrate conducive to periphyton colonization and was located upstream of all online WWTPs discharging to the Jordan River. Elevated TPP rates in the UJR (5400 S, 7600 S, and 9000 S) are a result of the relatively swift and shallow hydraulics and larger sediment

substrate capable of providing an anchor point for benthic organisms (Minshall et al. 1992). The benthic zone was visually covered with biofilms throughout the length of the Jordan River.

Algal biofilms in the benthos typically dominate primary production in most streams (Pusch et al. 1998). Net primary production of periphyton in other rivers ranged from <0.03–10 g-DO/m^2/day with most rivers sections producing less than 1.3 g-DO/m^2/day (Webster et al. 1995). The Jordan River benthic zone was more active in terms of primary production than the average river, and the UJR had benthic photosynthesis fluxes comparable to other eutrophic rivers (Webster et al. 1995).

Benthic gross primary production was higher than expected in Reach 1 at the LNP NE site and TPP fluxes were similar to those found in the UJR, and this will be discussed in more detail in the following sections.

Both WC_{dark} and WC_{light} were the highest following WWTP discharges at the 5400 S, 2100 S, and LNP NE sites, indicating that WWTP nutrient loads stimulate water column eutrophication in the Jordan River.

There were no trends in TPP decreasing with ambient water temperature in the UJR during the winter months, as was noted in the seasonal SOD study (Section 5.1.7). Turbidity of the ambient river water decreased dramatically during winter low flows.

This coupled with less bedload migrating downstream during the winter months most likely resulted in less scouring, creating an environment conducive to the elevated winter TPP fluxes observed in the UJR. Fig. 46 provides two pictures taken 4 days apart (Jan. 11 and 15, 2011) at the 9000 S site. These pictures provide a visual perspective regarding how fast the benthic community was growing during the winter months. The

Fig. 46. Periphyton regrowth during winter conditions at 9000 S (before and after)

surface benthic layer was scraped with a shovel to expose the clean gravel beneath (left), and the benthic community was recolonized within 4 days (right), highlighting the amount of biological activity occurring at the sediment–water interface in the Jordan River.

It should be noted that the turbidity of the Jordan River increased dramatically following a mild snowmelt while sampling at the 9000 S site. This observed increase in turbidity still resulted in winter TPP fluxes greater than measured in summer. Although many of the TPP fluxes measured during winter conditions were similar to the summer values, the maximum rate of photosynthesis was higher in the winter months before being (Table 18).

Fig. 47 provides a stacked bar chart for benthic and water column respiration and production during the July, September, and winter sampling events. The WC rates were normalized to the mean river depth for direct comparison with sediment fluxes. The water column is presented as the light grey and dark grey bars, and the sediments are colored white and black. The sum of WC_{light} and TPP is the chamber calculated gross primary production (GPP) flux in terms of DO. The sum of WC_{dark} and TOD is the chamber

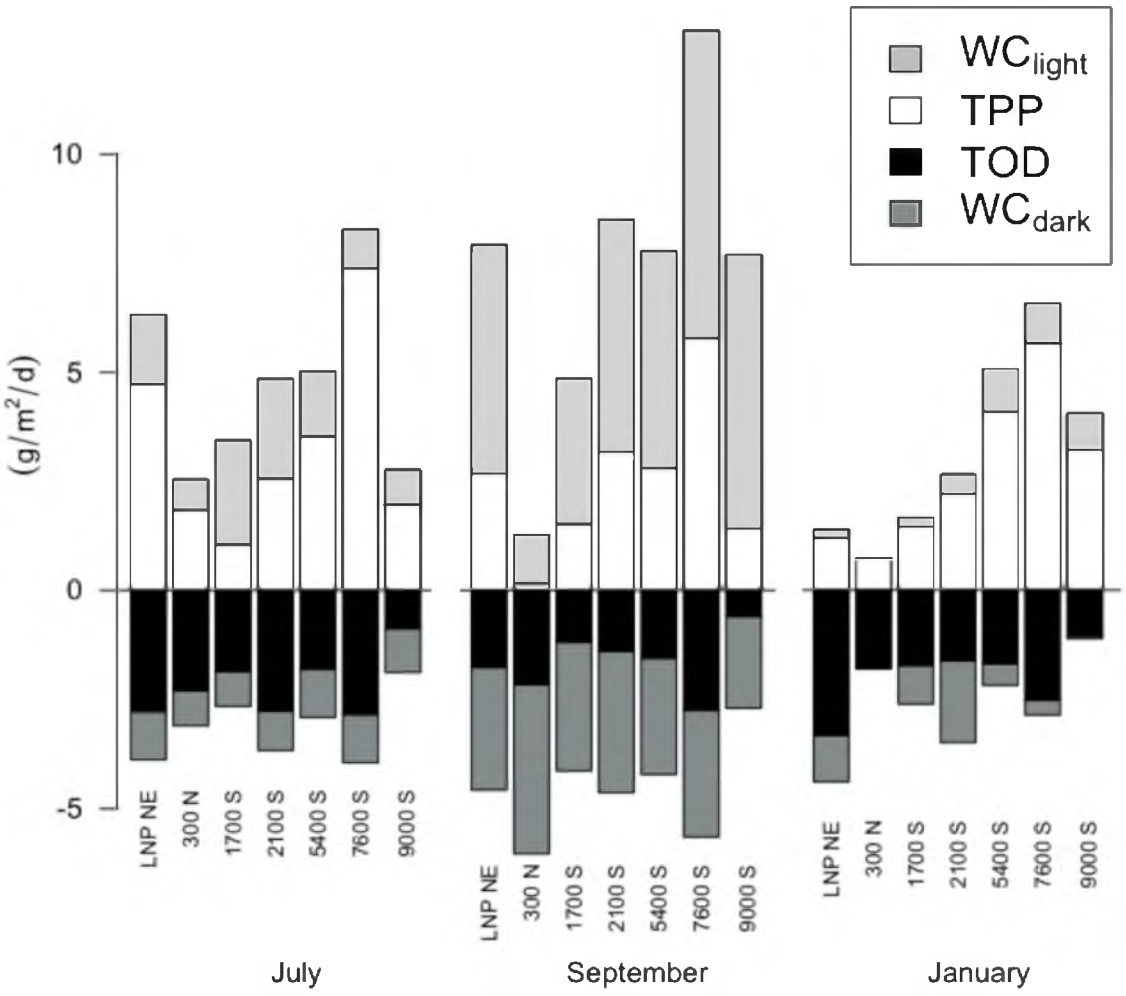

Fig. 47. GPP and CR_{24} during summer and winter
Note: GPP = TPP + WC_{light} and CR_{24} = TOD + WC_{dark}

calculated 24-hour community respiration (CR_{24}).

Phytoplankton and broken apart metaphyton present in the water column were responsible for the majority of the production and respiration during the critical time period during late summer (grey bars, September). This suggests that upstream eutrophication is a significant source of seasonal OM to the LJR. In addition, WC_{light} was elevated at the 9000 S and 7600 S sites located upstream of all WWTP discharges during late summer suggesting that Utah Lake may be a source of phytoplankton to the UJR (see

Utah Lake WC_{dark}, Section 5.1.8). Alternatively, the phytoplankton is sloughed periphyton, or metaphyton, growing upstream of 9000 S in the Upper Jordan River.

The benthic community was responsible for the vast majority of the primary production measured in the Jordan River during early summer and winter. Periphyton can be the largest and most active standing stock of algal biomass in a lotic system, requiring sediment–sampling protocols to properly quantify (Dodds 2006; Minshall et al. 1992).

The seasonal NDM chamber derived degree of autotrophy is provided in Fig. 48, where the UJR was autotrophic year round. The significance is that a ratio greater than 1 implies OM is being produced faster than it is being degraded, creating a source of OM to downstream reaches. The 1700 S and 2100 S sites in Reach 3 were autotrophic during the

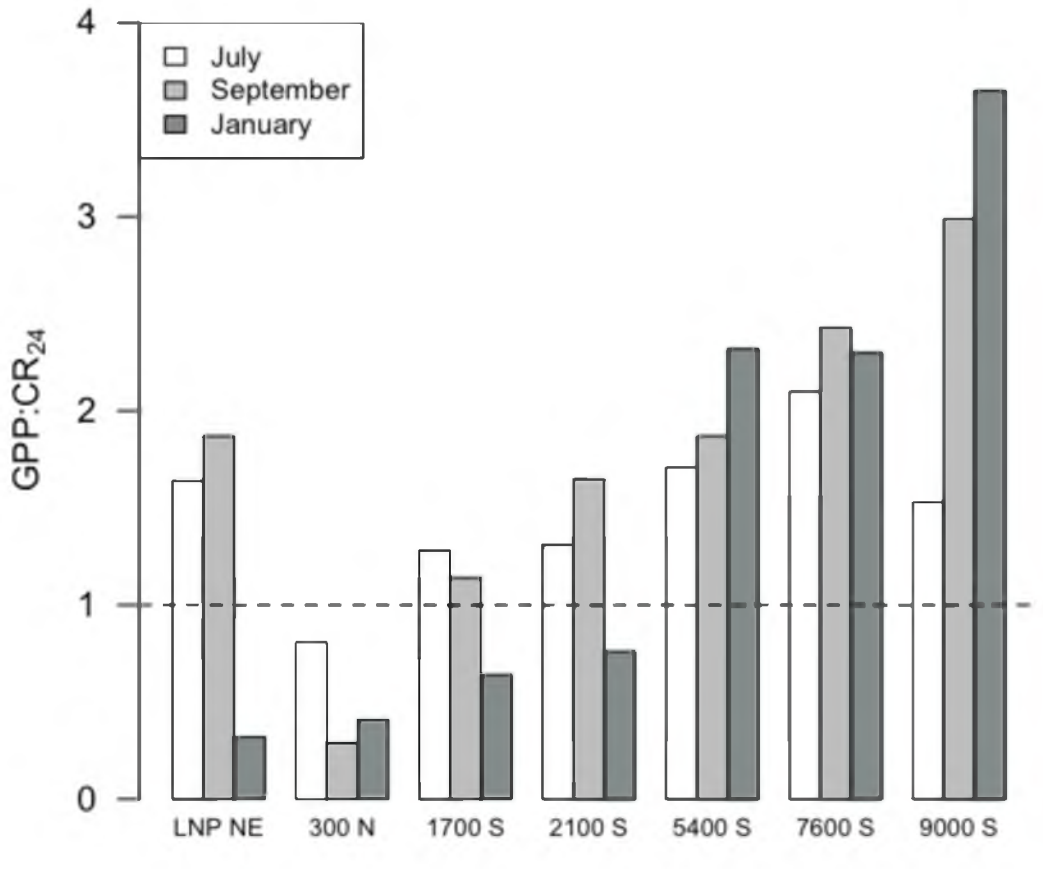

Fig. 48. Seasonal GPP:CR24 ratios

summer, and all sites in the LJR were heterotrophic during the winter.

The unexpected autotrophic conditions measured at the LNP NE site during the summer are a result of periphyton mats covering the sediments in the shallow sampling location. Unfortunately, NDM chamber sampling cannot be conducted in the 1.5 to 2 meter deep thalweg in Reach 1, which created a sampling bias towards "easy to access" productive sediments. Although the author does not believe that Reach 1 is autotrophic, the take home message is that the benthic zone was active in terms of primary production throughout the Jordan River.

5.2.3 Chamber Net Daily Metabolism (NDM)

Fig. 49 provides a bar chart for the chamber measured NDM. The UJR was a year-round source of instream-produced OM to the downstream LJR and Surplus Canal. The LJR became more heterotrophic with distance downstream, and all sites in the LJR were net DO consumers during the winter months. The positive NDM at the LNP NE site was a result of abundant periphyton growth on the silty sediments that became detached and floated to the surface in the afternoon due to oxygen gas production. This periphyton was assumed to be isolated to the shallow depositional zones in Reach 1, not in the thalweg. The overestimation of NDM using chambers is associated with the requirement of relatively shallow sampling locations in a medium sized river and is most likely a sampling artifact at all sites (Bott et al. 1978). As a result, the NDM estimates provided by chamber studies should be viewed as conservatively high.

The three season average chamber NDM metabolism parameters are provided in Table 19. The benthos were responsible for 50–87% of the CR_{24} and GPP in the Jordan River. The seasonal site average percent of CR_{24} and GPP associated with the benthos

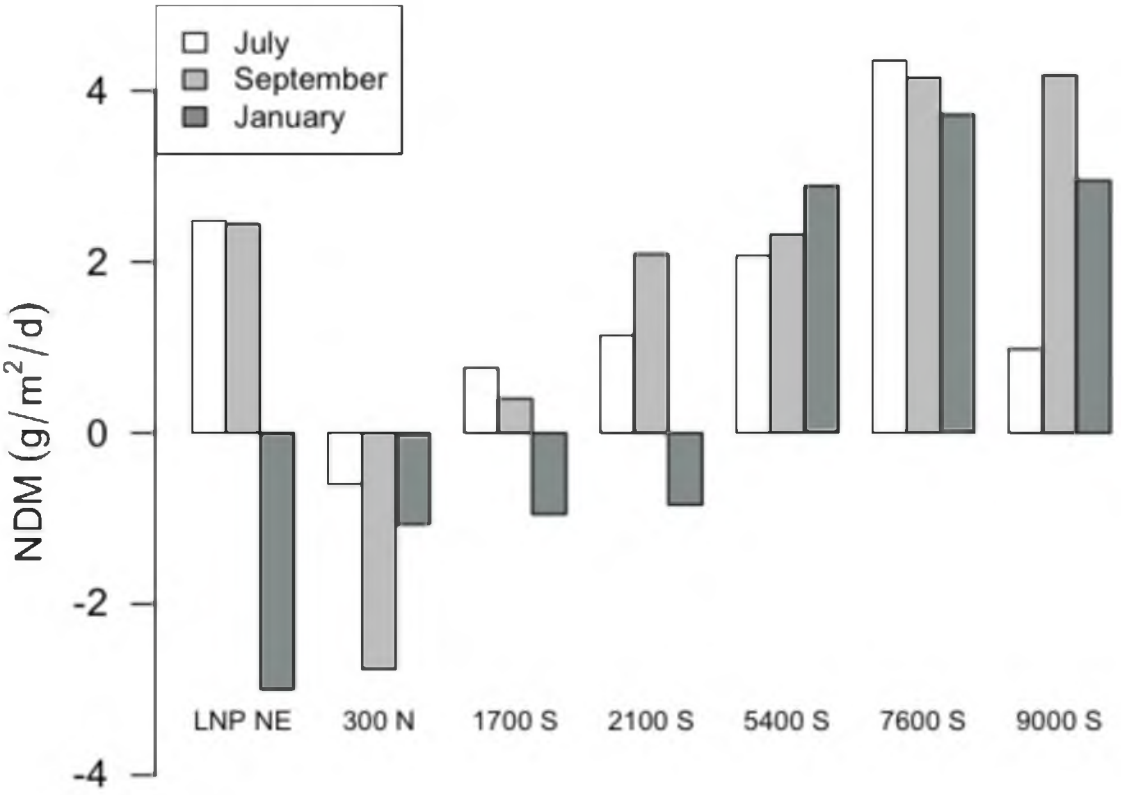

Fig. 49. Seasonal NDM

Table 19. Annual average chamber NDM

	average annual chamber NDM fluxes						
	(g DO/m^2/d)		(g DO/m^3/d)		(g DO/m^2/d)		
Site	TOD	TPP	WC_{dark}	WC_{light}	GPP	CR_{24}	NDM
LNP NE	-2.6	2.9	-0.8	1.1	4.2	-3.6	0.5
300 N	-2.1	0.9	-0.6	0.4	1.4	-2.8	-1.4
1700 S	-1.6	1.3	-1.1	1.4	2.6	-2.6	0.0
2100 S	-1.9	2.6	-1.9	1.9	4.0	-3.2	0.8
5400 S	-1.7	3.5	-1.1	1.9	4.9	-2.5	2.4
7600 S	-2.7	6.3	-0.6	1.3	7.2	-3.2	4.0
9000 S	-0.7	2.2	-1.0	2.6	4.2	-1.4	2.7

was 67% and 65%, respectively, for the entire length of the Jordan River. As was noted in the SOD study (Section 5.1.7), the benthos were responsible for the majority of the biological activity in the Jordan River.

5.3 Single-Station Diurnal DO Stream Metabolism

5.3.1 Diurnal DO profiles in the Jordan River

Fig. 50 shows the consistency in the UJR stream metabolism at the 9000 S and 7800 S sites over a 5-day period in late summer. The daytime ambient DO surplus peaks midday around 2 mg-DO/L (130% saturation), and during nighttime hours a deficit of roughly -2 mg-DO/L occurs (75% saturation). The increase in ambient DO following 0:00 does not influence the ambient DO deficit and is the result of the stream temperature decreasing during nighttime, resulting in an increase in ambient DO saturation in the well-mixed UJR. The sinusoidal nature in DO concentrations is very consistent,

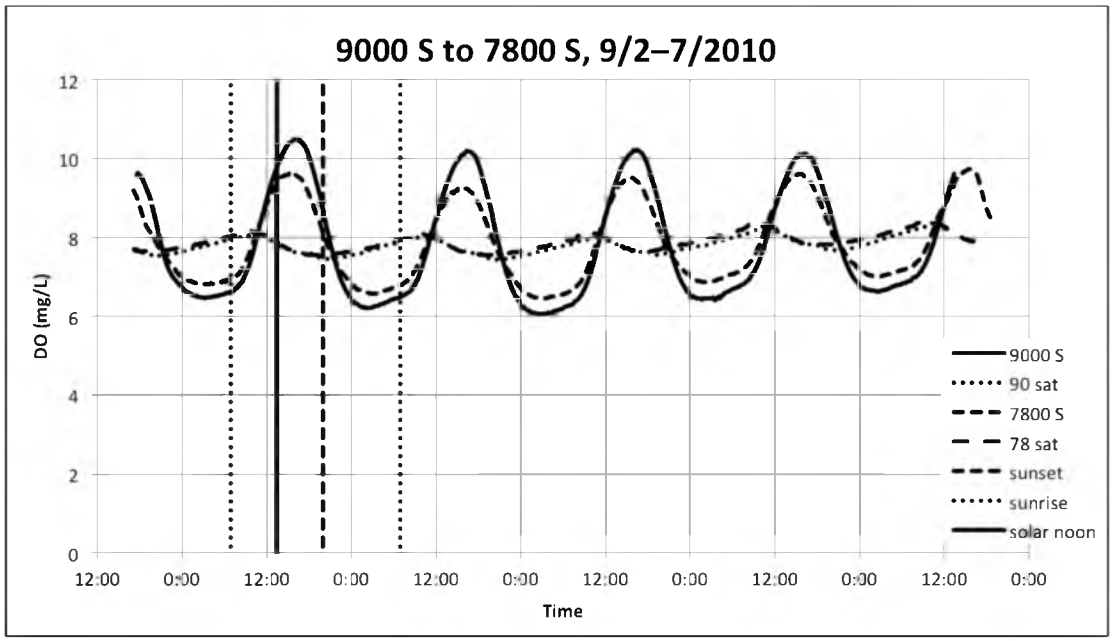

Fig. 50. 5-day diurnal DO profiles for the Upper Jordan River

indicating that both of these sites have a consistent diurnal metabolism.

Fig. 51 provides 24-hour DO profiles for additional sites in the UJR during the spring of 2012. All sites were supersaturated throughout the photoperiod with the 5400 S site reaching 156% saturation, indicating that the UJR may be a significant source of instream produced OM to the DO impaired LJR.

The Lehi site is located in Reach 8 near the outlet of Utah Lake and has the smallest diurnal DO swing and smallest reaeration coefficient in the UJR. The reason that the Lehi site remained supersaturated with DO throughout the night until 4:00 AM and did not begin to show signs of photosynthesis until 4 hours after sunrise is hypothesized to be result of Utah Lake phytoplankton. The diurnal DO profiles measured near the outlet of the lake were most likely the DO dynamics occurring in the eutrophic water column of Utah Lake before discharging into the Jordan River. This resulted in the diurnal DO data collected at the Lehi site being unsuitable for the stream metabolism analysis.

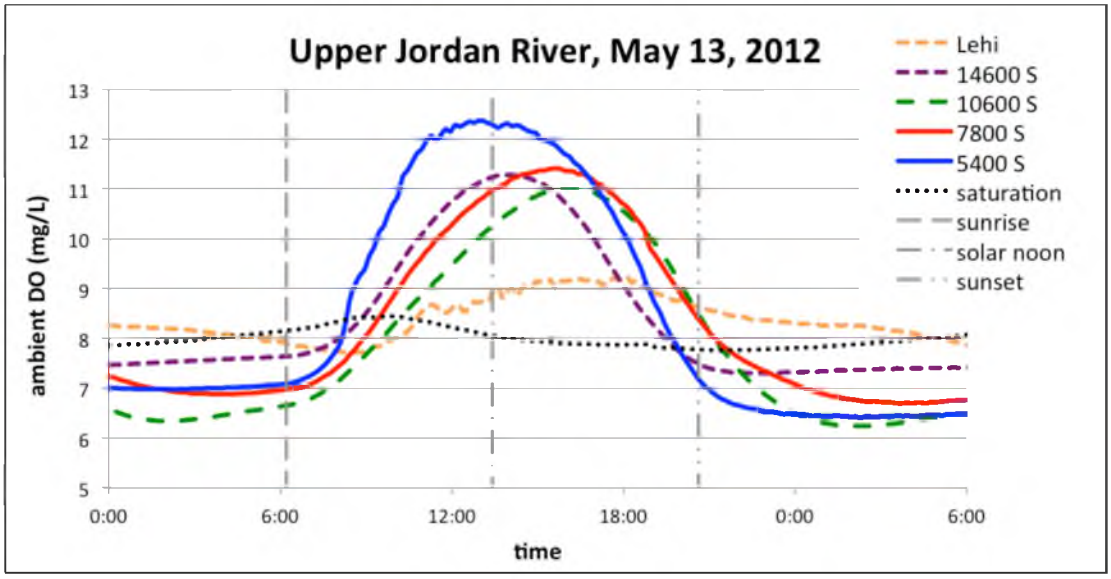

Fig. 51. May 2012 diurnal DO profiles for the Upper Jordan River

Fig. 52 shows diurnal DO curves collected in the LJR in early summer. The 700 S site was supersaturated for roughly 6 hours of the day and daytime DO deficits continued to increase with distance downstream of the Surplus Canal diversion. Interestingly, the nighttime DO deficit was -2 mg-DO/L at all four of these sites in the LJR independent of the different mean depths and reaeration coefficients. This constant DO deficit is the reason the LJR is considered chronically impaired for DO and is vulnerable to acute DO depletion events.

5.3.2 Single-station NDM model comparison

Diurnal DO models are excellent tools to characterize, document, and estimate autotrophic:heterotrophic ratios in lotic systems, and they can be used to estimate CR_{24}, GPP, and NDM if the reaeration coefficient is known. Limitations include that diurnal models will not differentiate between SOD or BOD, nor will they isolate the primary production associated with periphyton and phytoplankton. In addition, groundwater

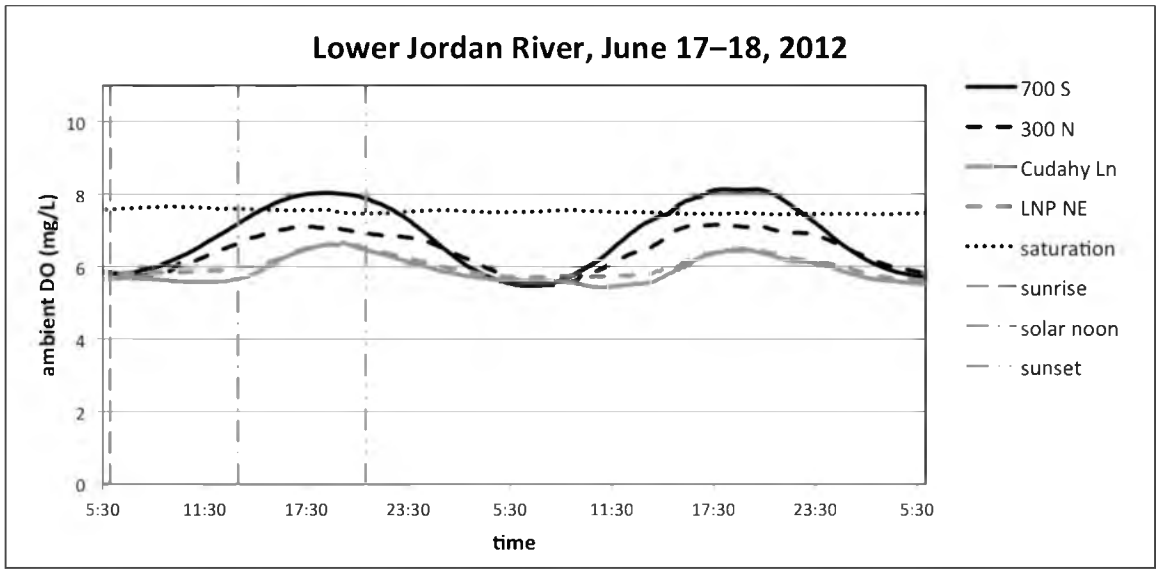

Fig. 52. Typical diurnal DO profiles for the Lower Jordan River

(GW) intrusion having a DO deficit will overestimate respiration while underestimating NDM if not accounted for when using the single-station method (Hall and Tank 2005). It has been suggested that rivers having more than 5% of their flow composed of GW should be sampled for NDM using chamber methods (Grace and Imberger 2006). The use of multiple methods, chambers and single-station calculations, to estimate NDM in the Jordan River provided both insight to the flaws of each method and added confidence to the general conclusions obtained using each method.

Provided in Table 20 are flux estimates of GPP, CR_{24}, and NDM based on diurnal DO profiles measured in the UJR utilizing the single-station method. The first set of parameters provides stream metabolic rates based on measured, or apparent, diurnal signatures, and the second list was adjusted for GW intrusion having a DO concentration of 1 mg-DO/L.

The river-wide mean depth (d) in meters and reaeration coefficient (k) are provided beneath the site name. The mean depth at each site was estimated by walking across the width of the river at each site in the UJR. The reaeration coefficients used in the UJR single-station NDM estimates are a combination of diffusion dome measured and predictive equations provided in the Literature Review (Section 3.3.2). NDM estimates neglecting the effects of GW intrusion and potential hyporheic exchanges estimated an average NDM of +0.1 g-DO/m^2/day in the UJR. This flux is slightly positive, but neutral enough to be overlooked as a large source of OM to the LJR.

An estimated 15% of the baseflow above 9000 S, and 5% between 9000 S and the Little Cottonwood Creek tributary are associated with GW intrusion (Utah DWQ 2013, Fig. 1.4). Under this scenario, -2.6 and -2.4 g-DO/m^2/d of the single-station estimated

Table 20. UJR Single-Station and GW adjusted model NDM outputs

		Single-Station model (g DO/m^2/d)			GW adjusted (g DO/m^2/d)		
	date	GPP	CR_{24}	NDM	GPP	$CR_{24,GW}$	NDM
14600 S	5/13/12	7.7	-5.9	1.8	7.7	-3.3	4.4
d = 0.3, k = 10	6/10/12	9.4	-8.7	0.7	9.4	-6.1	3.3
10600 S	5/13/12	12.1	-12	0.1	12.1	-9.4	2.7
d = 0.5, k = 6	6/10/12	6.2	-7.7	-1.5	6.2	-5.1	1.1
	7/24/12	8.7	-10.2	-1.5	8.7	-7.6	1.1
9000 S	7/20/10	7.8	-8.4	-0.6	7.8	-5.8	2.0
d = 0.8, k = 6	9/2/10	9.3	-8.8	0.5	9.3	-6.2	3.1
	1/16/11	9.5	-10.7	-1.2	9.5	-8.1	1.4
	1/15/12	1.1	-2	-0.9	1.1	0.6	1.7
7800 S	9/2/10	6.3	-6.55	-0.25	6.3	-4.2	2.1
d = 0.8, k = 6	1/16/11	8.3	-7.5	0.8	8.3	-5.1	3.2
	5/13/12	13.1	-11.45	1.65	13.1	-9.1	4.0
	6/10/12	6.6	-8.4	-1.8	6.6	-6.0	0.6
	7/24/12	13.3	-14	-0.7	13.3	-11.6	1.7
7600 S	9/2/10	2.65	-4.2	-1.55	2.7	-1.8	0.8
d = 0.8, k = 6	1/11/11	6.7	-4.7	2	6.7	-2.3	4.4
5400 S	6/5/10	5.9	-5	0.9	5.9	-2.6	3.3
d = 0.8, k = 5	9/2/10	2.7	-2.3	0.4	2.7	0.1	2.8
	1/21/11	5.1	-4.4	0.7	5.1	-2.0	3.1
	5/13/12	12.1	-9.6	2.5	12.1	-7.2	4.9
	6/10/12	8	-6.5	1.5	8.0	-4.1	3.9
	7/24/12	10.1	-9.4	0.7	10.1	-7.0	3.1
average		7.6	-7.4	0.1	7.6	-5.0	2.6

above 9000 S GW uses -2.6 g-DO/m^2/d
below 9000 S GW uses -2.4 g-DO/m^2/d

community respiration is a result of GW intrusion upstream and downstream of 9000 S, respectively. The positive GW adjusted CR_{24} fluxes measured at the 9000 S site in January and the 5400 S site in September do not reflect reality since photosynthesis cannot occur during the nighttime and are assumed to be a result of the generalized assumptions used to calculate GW contributions in this analysis. They were included in the average values in Table 20 since the same assumptions were used in all GW adjusted values. This resulted in a GW adjusted average autotrophic NDM of 2.6 g-DO/m^2/d in the

UJR. Appendix B provides diurnal DO profiles used in the single-station NDM analysis.

Fig. 53 provides a comparison between the chamber measured NDM and the single-station GW adjusted NDM estimate in the UJR. The elevated chamber NDM measured at the 7600 S and 9000 S sites are most likely a result of the sampling locations being closer to the banks where benthic communities are subjected to less scouring and shallow water depths (Bott et al. 1997; Bott et al. 1978; Grace and Imberger 2006).

The single-station NDM estimates for the LJR are provided in Table 21 and were not adjusted for GW intrusion. The average model estimates for NDM in Reaches 3, 2, and 1 were -1.5, -2.7, and -2.6 g-DO/m^2/d, respectively. The decrease in NDM with distance downstream in the LJR agrees with observations that SOD and ambient DO

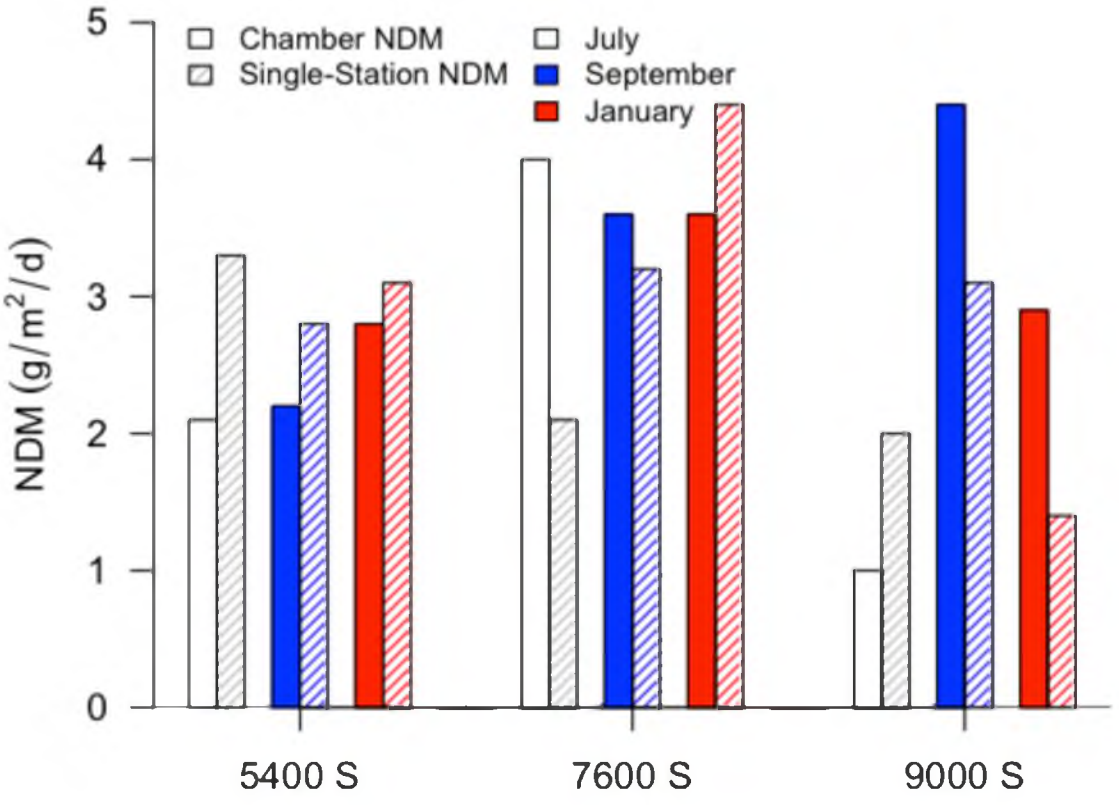

Fig. 53. UJR Chamber and single-station GW adjusted NDM estimates

Table 21. LJR Single-station model NDM outputs

		LJR Single-station (g DO/m^2/d)		
	date	GPP	CR_{24}	NDM
2100 S	7/6/10	3.1	-4	-0.9
d = 0.8, k = 6	8/25/10	4.3	-6.2	-1.9
	1/21/11	3.2	-5.7	-2.5
	8/23/12	11.6	-12.5	-0.9
1700 S	7/7/10	6.6	-6	0.6
d = 0.9, k = 4	8/25/10	4.3	-5.8	-1.5
	1/21/11	3.3	-4.7	-1.4
700 S, d = 1.3, k = 4	6/18/12	6.6	-10.3	-3.7
300 N	8/30/10	1.9	-5.2	-3.3
d = 1.3, k = 1.2	6/18/12	3.5	-5.5	-2
500 N	8/23/12	4.4	-7.6	-3.2
700 N	8/30/10	1.5	-4.9	-3.4
1700 N	7/16/10	3.8	-5.3	-1.5
Cudahy Ln	6/18/12	2.9	-6.1	-3.2
d = 1.5, k = 1.2	8/23/12	4.2	-8	-3.8
LNP NE	7/15/10	3.4	-6.4	-3
d = 1.2, k = 1.2	8/25/10	2.2	-4.4	-2.2
	6/18/12	2	-4.3	-2.3
Bender	8/25/10	2.2	-4.3	-2.1
Burnham	5/26/10	1.3	-3.4	-2.1
d = 1, k = 1.2	8/23/12	4.2	-6.2	-2

d = mean depth (m)
k = reaeration coeff. (1/day)

deficits increase with distance downstream.

Fig. 54 provides the relationship between chamber NDM and the single-station model NDM for the LJR. The lack of an equivalent ratio when comparing data in the LJR is a result of GPP being overestimated in the NDM chambers in the relatively deep slow moving LJR. This is shown by the regression line crossing the y-axis at +1 ($y = 1.1x + 1$). A 1:1 relationship is shown as the dotted line for reference. The overestimation of chamber GPP compared to single-station estimate in the LJR is pronounced due to the deeper river depths (>1m) resulting in greater biases towards sampling the benthos in

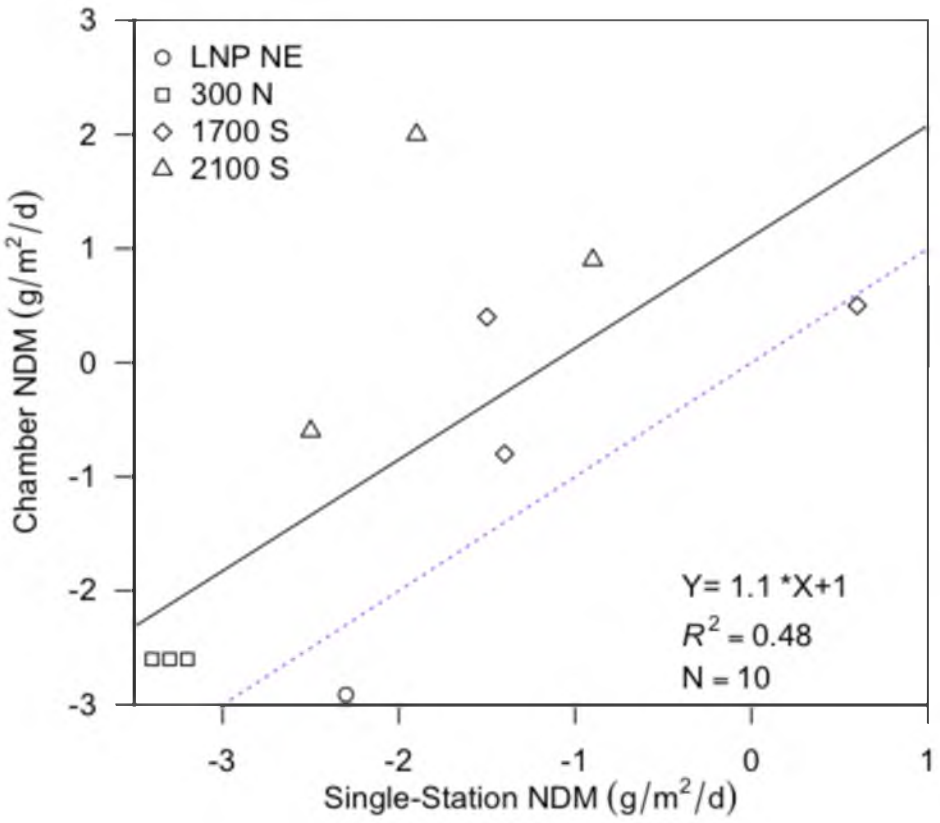

Fig. 54. Chamber vs. Single-station NDM relationship
Note: summer LNP NE data not included

shallow areas more conducive to benthic growth compared to the thalweg (Grace and Imberger 2006).

Overall, the NDM chambers tended to overestimate NDM in the LJR, but are very useful in isolating the sediments from the WC to determine the relative light and dark metabolic rates and fluxes. In addition, the use of chambers removes the requirement of knowing the reaeration coefficient, GW intrusion fluxes, and GW DO concentrations. By coupling multiple chamber NDM estimates with a large collection of diurnal DO NDM estimates, a great deal of information about the surface water in question can be obtained due to the strengths and weaknesses of both methods to estimate stream metabolism.

5.4 Sediment Organic Matter

5.4.1 Sediment %TOC

The commonly used sediment characterization measurement volatile solids (%VS) is a surrogate for organic matter (OM). Total organic carbon (%TOC) is another common sediment OM parameter, but is much more time consuming, challenging, and expensive compared to %VS. These challenges are compounded in sediments having a high inorganic carbon content, such as those found in the alkaline Great Salt Lake valley. Combustible OM is composed of carbon, hydrogen, and oxygen, and a relationship between sediment %TOC and %VS was produced to confirm that %VS measurements were a viable method to estimate OM in Jordan River sediments. In addition, this information was used to identify how much of the OM was present as organic carbon.

Fig. 55 provides the relationship compiled from 28 depth integrated sediment cores between sediment %TOC and %VS in the LJR. The LJR had a %TOC:%VS range between 0.4 to 0.6, similar to the range found in other sediments (Schumacher 2002; Dean 1974). The LJR had a mean %TOC:%VS ratio of 0.5, which is a common assumption used to correlate organic carbon and OM in sediments (Beaudoin 2003; Ball 1964). Site specific %TOC data can be found in Appendix D.

Easily biodegradable organic matter includes viable bacteria and phytoplankton containing 47–50% carbon (Tchobanoglous et al. 2003, Table 7-4). Cellulose, $C_6H_{12}O_5$, a major component of terrestrial leafs, macrophytes, and algal biofilms, is 44% carbon as dry mass. Pure bacteria cultures have %TOC:%VS ratios between 0.45–0.50 and wastewater bacteria found in activated sludge processes are generalized as 53% carbon in terms of dry OM (Bratbak and Dundras 1984; Tchobanoglous et al. 2003, pg. 558).

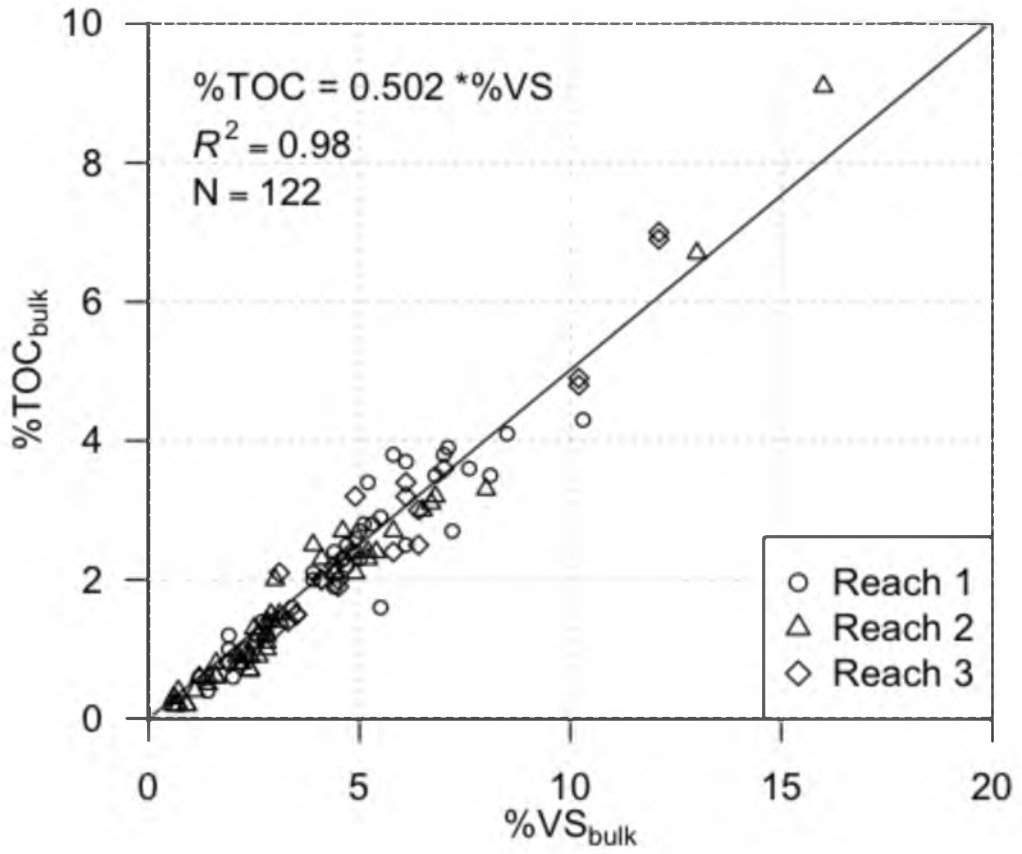

Fig. 55. LOI to %TOC conversion for the Lower Jordan River

Although the sources of sediment OM were not identified based on organic carbon content, the ratio agrees with other researchers across a wide range of %VS in the LJR.

The strong correlation between %TOC and %VS allows OM to be confidently measured using %VS protocols in the LJR. The primary advantage to using %VS as a surrogate for OM is the ease of processing large amounts of samples with minimal time, effort, and monetary overhead (Konen et al. 2002).

Previous researchers found the %TOC:%VS relationship to be nonlinear for %VS greater than 25%, but sediments this organically enriched were not encountered in the LJR (Leipe et al. 2010). Sediments exceeding 25% VS most likely do exist in the Jordan River, but will be found in areas of localized sedimentation, such as the backwaters of the

Surplus Canal and other diversion dams. Early researchers reported poor repeatability for samples less than 10% VS, but the relationship was very strong in the LJR (Mackereth 1966).

5.4.2 Sediment %TS and %VS

Fig. 56 provides photos of sediments found in the LJR. Note the dark color and sludge-like appearance of the sediments found in Reach 1. The surface sludge layer overlying dirty course sand at the 2300 S site is referred to as a benthal deposit.

The top 0–2 cm of the sediment column was less consolidated than depths 5 cm and deeper where the sediments had a higher bulk density (Fig. 57). The top 0–2 cm of the LJR sediment column consisted of a silty-muck benthal deposit overlaying more consolidated sediments. Similar to the principle of superposition used to describe sediments on a geologic scale, the surficial sediments are composed of the most recently deposited, or disturbed, material (Glew et al. 2001). Site specific %VS and %TS data are provided in Appendix B.

Studies relating SOD to OM prior to the Clean Water Act worked with benthal deposits having %TS as low as 10% and %VS ranging from 10–20%. Whereas Jordan River surface sediments where "cleaner" and range from 20–80% TS and 1–18% VS.

The relationships for surface (0–2 cm, R^2 = 0.89) and subsurface (5+ cm, R^2 = 0.79) sediment %VS and %TS in the Lower Jordan River where

$$\%VS_{surface} = -9.7 * (\ln \%TS) + 43 \quad (21)$$

$$\%VS_{subsurface} = -15.5 * (\ln \%TS) + 69 \quad (22)$$

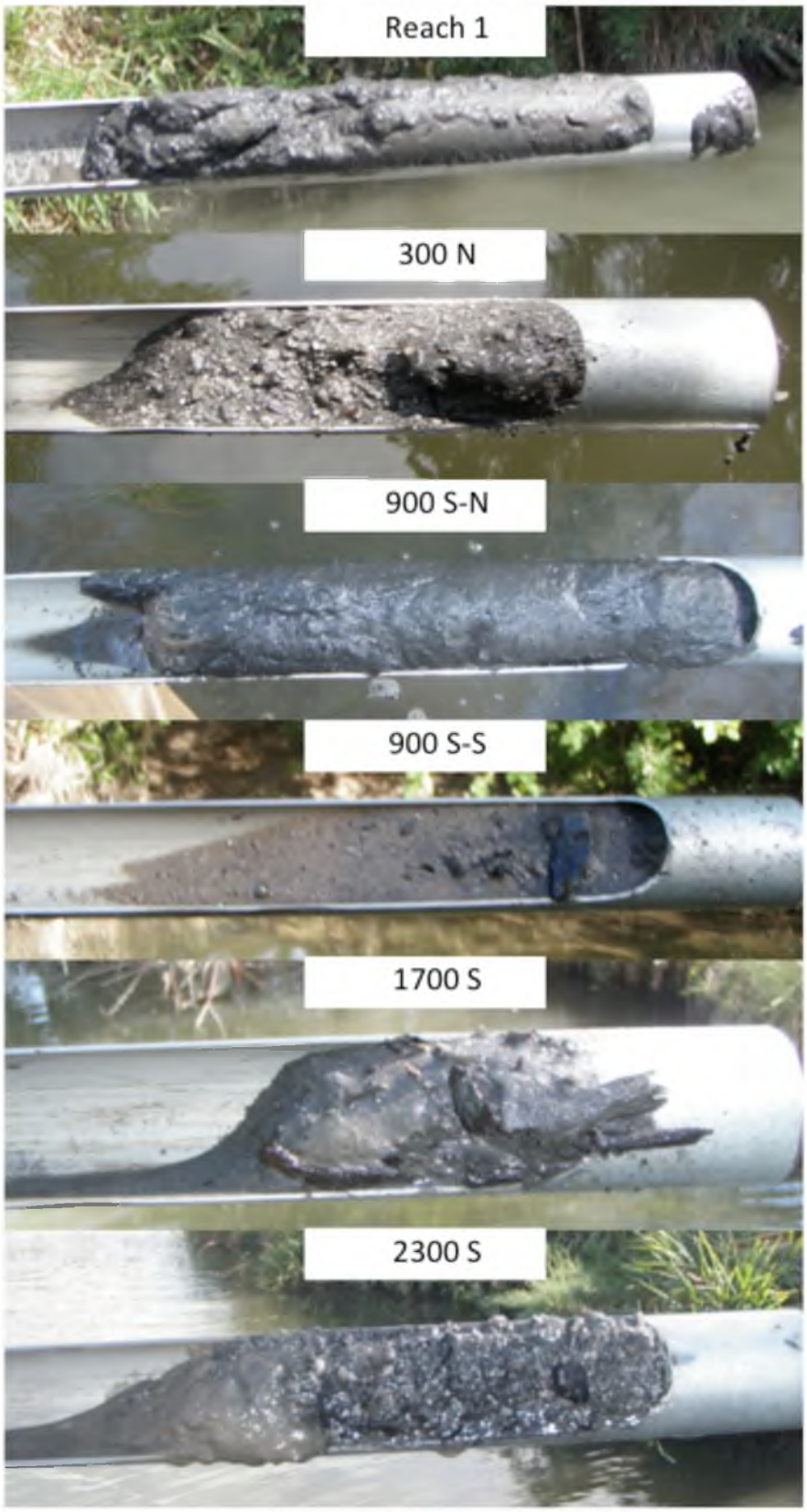

Fig. 56. Sediments found in the Lower Jordan River and Surplus Canal backwater

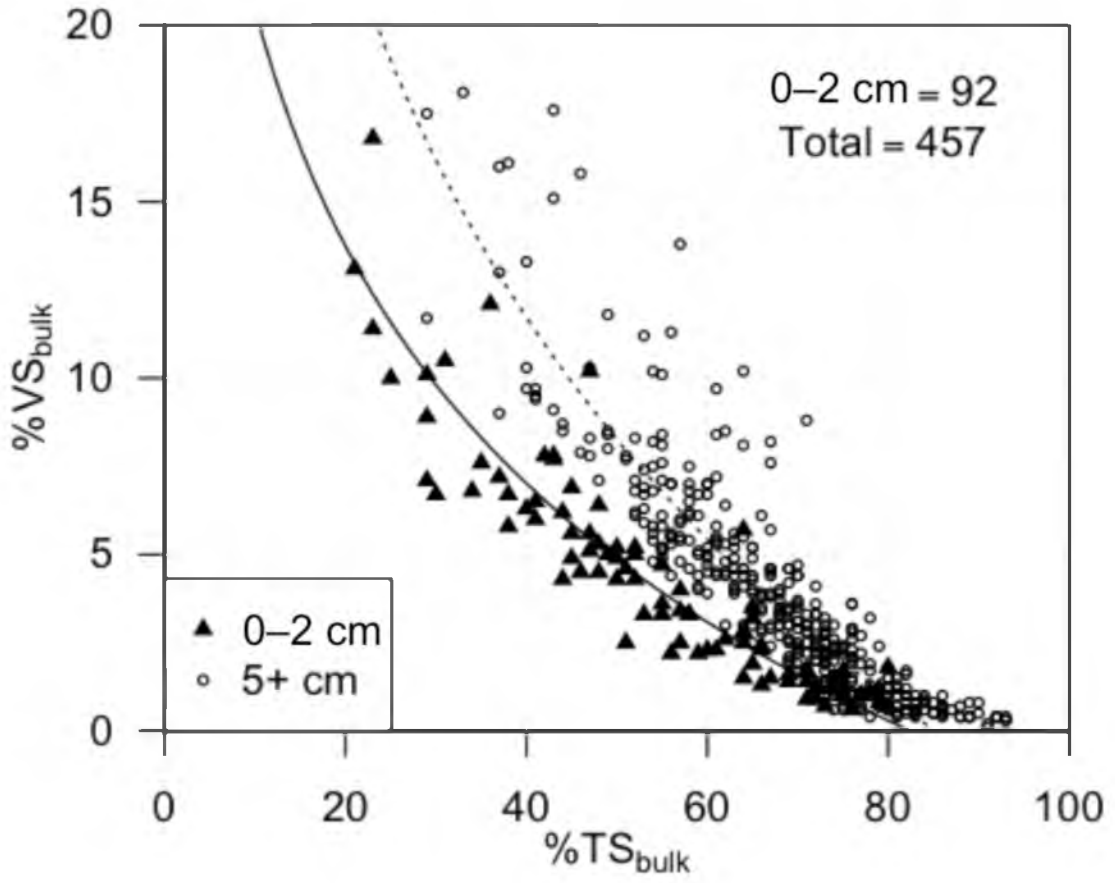

Fig. 57. Jordan River %VS and %TS relationship

The parameter %TS describes the water content, or how "muddy" the sediment is. This becomes a very important parameter when calculating the standing stock, or amount of OM present in the wet sediments, since the water content is required to calculate a bulk wet density. This parameter changes with both depth and %VS in the Jordan River.

Presented in Fig. 58 are hydraulic reach based average sediment %TS in terms of depth in the sediment column. The two important trends to note are that %TS increases with depth, and %TS increases significantly in the coarse sand and gravels found in Reaches 4–6. Increases in %TS with increasing sediment column depth are due to

- more consolidated sediments

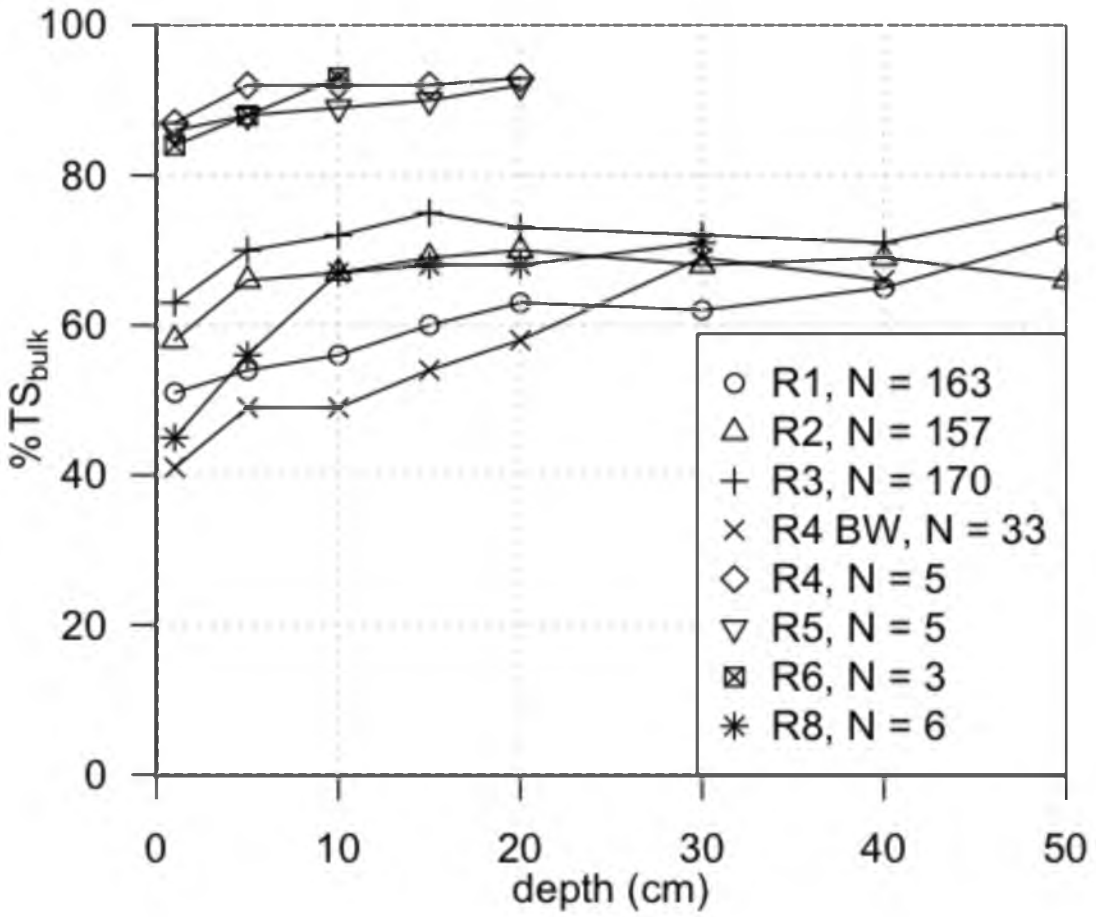

Fig. 58. Reach average sediment %TS

- gas production in the organically enriched sediments displaces pore water leading to dryer sediments (field observation)

%VS is defined as the percentage of the %TS that is combustible, or OM. The higher the %VS the more "mucky" the sediments become. Fig. 59 provides hydraulic reach average sediment %VS from over 500 samples collected in the Jordan River. The average %VS was consistently within the range of 3–6% in the top 10 cm of the sediment column in Reaches 1 and 2. Average bulk sediment %VS decreased more than an order of magnitude upstream of the Surplus Canal backwater. The most organically enriched sediments where found in the backwater of the Surplus Canal in Reach 4. %VS

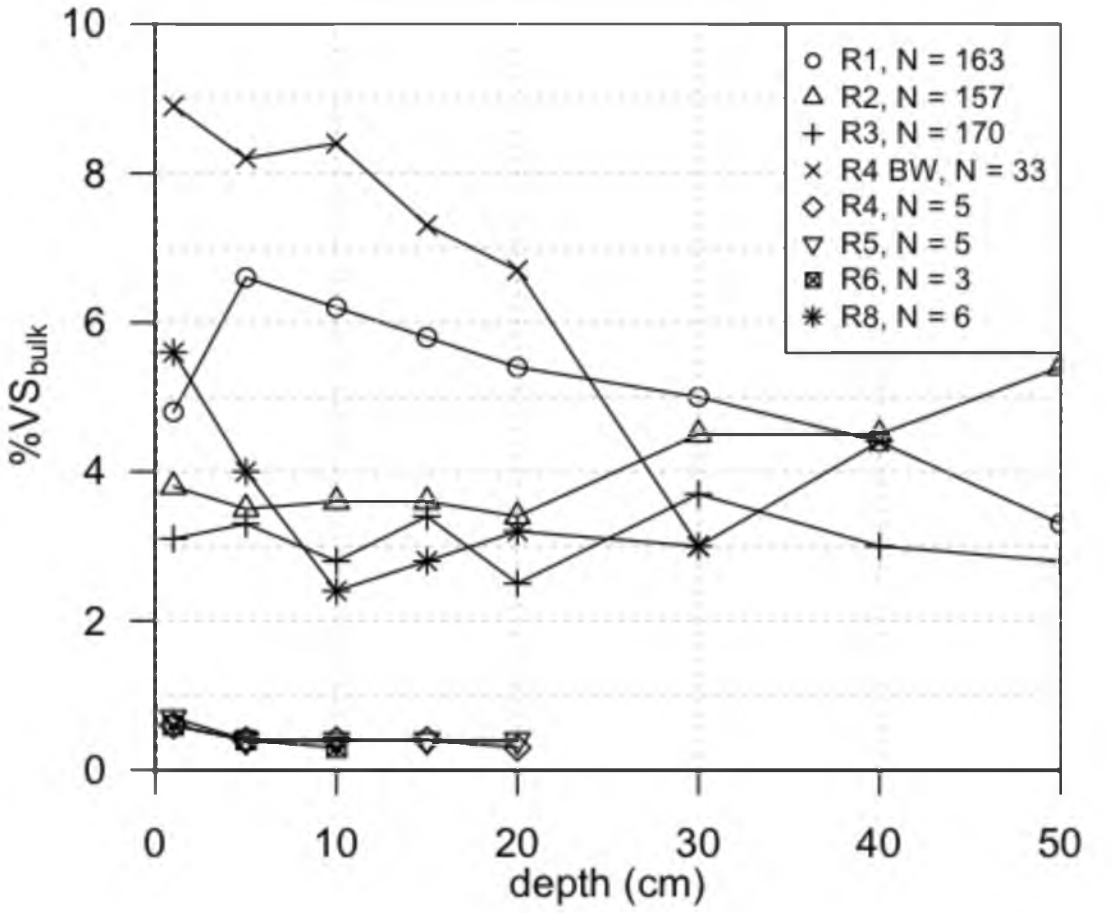

Fig. 59. Reach average sediment %VS

consistently increased in the fine sediments downstream of the Surplus Canal Diversion in the LJR. These increases are observed throughout the depth of the sediment column. In the limited number of observations made in Reach 8, near the outlet of Utah Lake, the benthal deposits had %VS similar to Reach 1 suggesting that Utah Lake is a source of OM to the downstream Jordan River.

In the LJR, sediments with %VS greater than 5% were visually observed to release swamp gas when disturbed, and %VS greater than 10% was accompanied by sporadic gas ebullition from undisturbed sediments. Ebullition was visually observed in

the Surplus Canal backwaters and at the 1300 S stormwater and tributary discharge. Sands and gravels collected in free flowing sections of the UJR had %VS less than 0.7% (5400 S, 7600 S, and 9000 S (N = 11)).

Fig. 60 provides a bar chart for the depth integrated cumulative $\%VS_{bulk}$ taken from three locations across the width of the river at 0–2, 5, and 10 cm depths. Sediment OM present at depths greater 0–2 cm provide information about the historical OM loading to the LJR. The 10 cm cumulative $\%VS_{bulk}$ consistently increased with distance downstream from the Surplus Canal diversion both in the thalweg and near the east bank. The exception was the LNP NE east bank site where large amounts of new sand were visually observed following the high water event of 2011. The thalweg in Reach 1 (sites 1–3) was not scoured to a sand layer, implying that the sediments across the entire width of the river are contributing to SOD and ambient DO deficits.

Fig. 61 provides the depth integrated average $\%VS_{bulk}$ of the sediments taken from the three locations across the width of the river. During the Spring 2012 sampling event the surface sediments (0–2 cm) had less $\%VS_{bulk}$ than the 5 and 10 cm depths in Reach 1. The unusually large snowpack in the winter of 2010–2011 resulted in a "managed" spring runoff lasting for 12 months in the UJR. It is hypothesized that the surface sediments encountered during the Spring 2012 sampling event were the deposition of inorganic sediments associated with upstream erosion and sediment displacement. As a general trend, the river-wide average sediment %VS increases as the LJR flows downstream from the Surplus Canal diversion. River-wide sediment characterization data are provided in Appendix D.

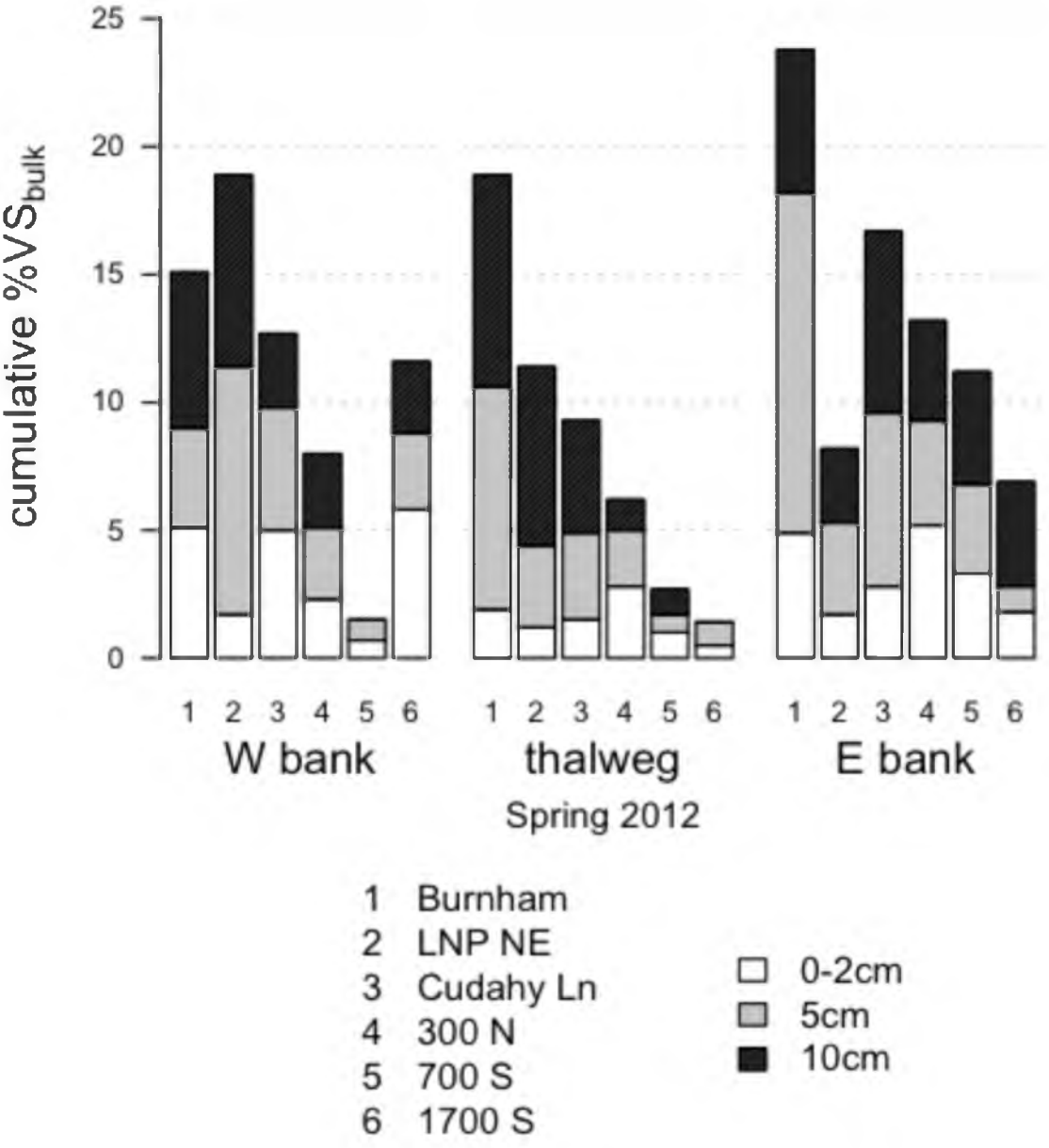

Fig. 60. River-wide sediment %VS
Note: highest surface sediment (0–2 cm) %VS at SOD site at 1700 S-W bank during Spring 2012

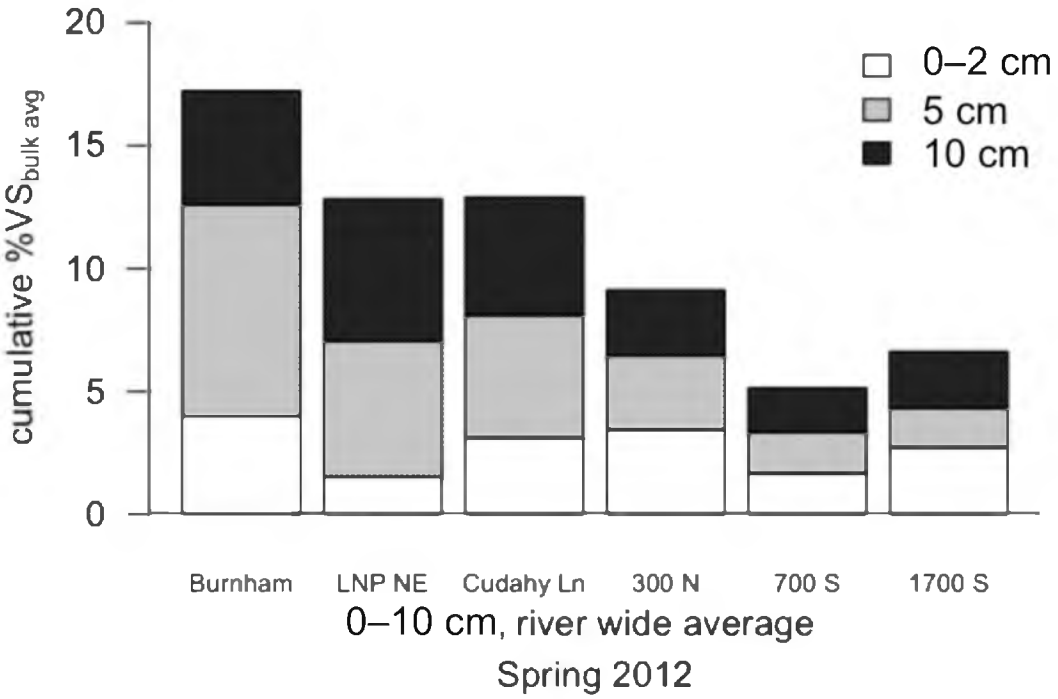

Fig. 61. Cumulative river-wide mean %VS in the top 10 cm of sediment column

5.4.3 CPOM and FPOM

221 sediment samples from the LJR were analyzed for course particulate organic matter (CPOM). CPOM includes all OM greater than 1 mm in size and represents terrestrial leaf litter and macrophyte debris since twigs, bark, and plastic were removed from the samples prior to analysis. To clarify, the parameter used to quantify the amount of CPOM is the percentage of the %VS found as CPOM ($\%VS_{CPOM}$). This parameter allows easy visualization of the relative amount of CPOM, but needs to be combined with $\%VS_{bulk}$ and $\%TS_{bulk}$ when calculating the standing stock of CPOM. River-wide $\%VS_{CPOM}$ data are provided in Appendix D.

Fig. 62 shows the cumulative sediment column $\%VS_{CPOM}$ for all sites across the width of the river. The highest concentrations of CPOM were found in the thalweg. Over 50% of sediment OM was present as CPOM from the Cudahy Ln site upstream in the

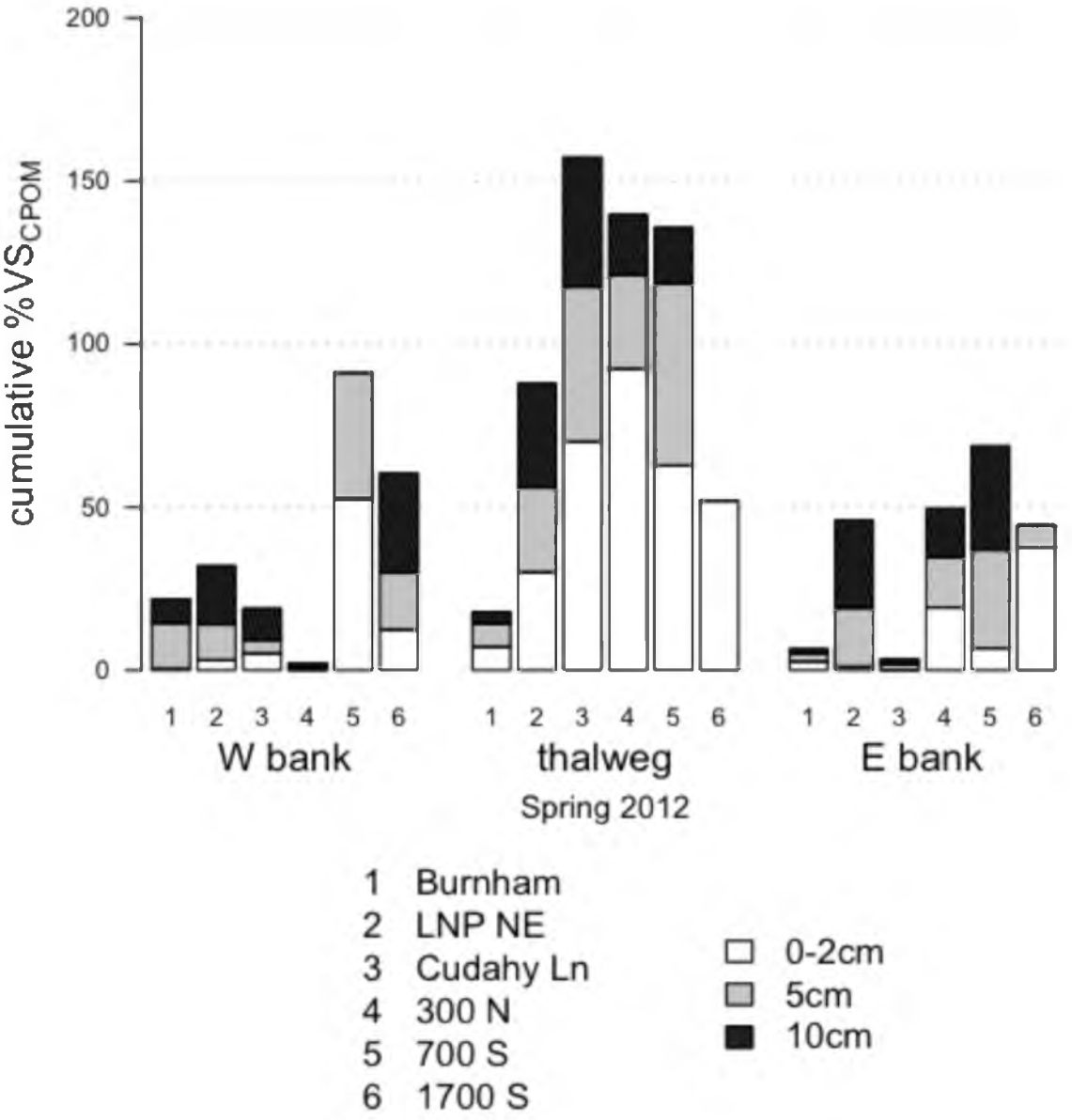

Fig. 62. River-wide cumulative sediment $\%VS_{CPOM}$

thalweg surface sediments (Reaches 2–3). Burnham Dam sediments had very little CPOM across the width of the river and sediment OM was composed of fine particulate organic matter (FPOM). The mean $\%VS_{CPOM}$ was 19% for the LJR.

The relative percentage of CPOM decreased with depth in the thalweg (Fig. 62, center). Fig. 60 above does not show a decrease in %VS with depth in the thalweg and it is hypothesized that the decreases in CPOM with depth are a result of biological CPOM processing to FPOM over time. Although the only macroinvertebrates observed in sediment cores in the LJR were worms, an estimated 60% of the CPOM ingested by shredders is excreted as FPOM in feces (Welch 1968). Bacteria and fungi are most likely responsible for the majority of CPOM conditioning and breakdown in the LJR.

Fig. 63 provides the river-wide average $\%VS_{bulk}$ (left) and $\%VS_{CPOM}$ (right). The river-wide average $\%VS_{CPOM}$ decreased with distance downstream in the LJR while the amount of $\%VS_{bulk}$ increased. The 700 S site is located downstream of the 1300 S and 900 S stormwater discharges, and these sediments had the highest concentration of CPOM, but it also had the least amount of sediment %VS.

All CPOM found in Reach 1 were assumed to be "leaf skeletons" or macrophyte remnants since twigs and sticks were removed from the sediment samples as part of sampling methodology. The identification of the source of FPOM is inconclusive since FPOM includes all algae, microbes, and degraded CPOM. The river-wide mean 10 cm depth integrated sediment column $\%VS_{CPOM}$ for the Burnham Dam, LNP NE, Cudahy Ln., 300 N, 700 S, and 1700 S sites were 4%, 18%, 18%, 25%, 30%, and 23%, respectively. The 300 N, 700 S, and 2100 S sites are located downstream of tributaries and stormwater outfalls and had elevated CPOM:FPOM ratios in the range of 0.5, similar

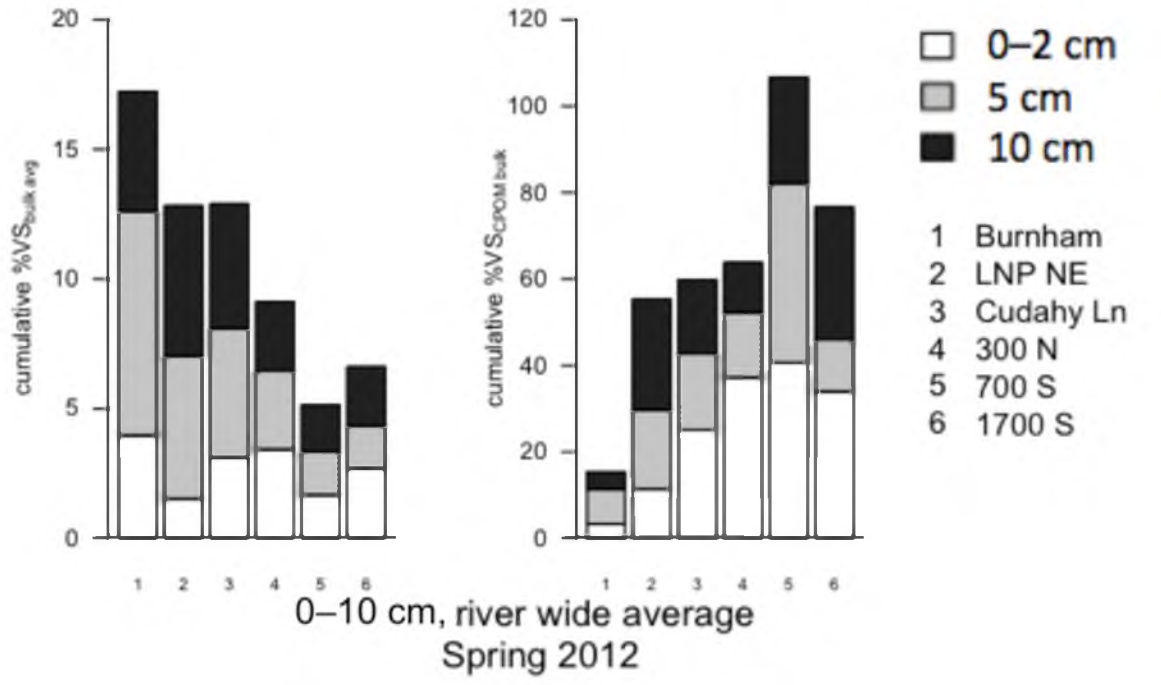

Fig. 63. River-wide average sediment $\%VS_{bulk}$ and $\%VS_{CPOM}$

to a much smaller 2nd order stream (Vannote et al. 1980). It is hypothesized that urban leaf matter is the source of this CPOM. The decrease in $\%VS_{CPOM}$ within Reach 1 resulted in CPOM:FPOM ratios dropping sharply to 0.05 at Burnham Dam and is most likely a result of two factors:

- CPOM originating from urban stormwater and entering Reach 1 as bedload has already undergone conditioning in Reaches 2 and 3 and is predominately FPOM.
- There is less riparian vegetation in Reach 1, resulting in less bank litterfall.

Riparian vegetation loads of OM are assumed to be insignificant given the scale of the urban watershed draining to the Jordan River (Imberger et al. 2011). Since algae are smaller than 1 mm in size, upstream eutrophication cannot be responsible for the CPOM aspect of the OM found in the Lower Jordan River.

The sediment surface area of Reaches 1, 2, and 3 account for 46%, 25%, and 29% of the total sediment surface area of the LJR (Section 5.7.1). Interestingly, the OM present in the top 0–2 cm of Reaches 1, 2, and 3 accounted for 47%, 27%, and 26% of the total OM in the surface sediments of the LJR after normalizing to an aerial OM standing stock. At depths of 5 and 10 cm, the OM present in Reach 1 accounted for over 60% of the OM in the LJR. This means that the surface sediments were very similar in terms of aerial OM content in all three reaches in the Spring of 2012, but the subsurface sediments in Reach 1 were more organically enriched compared to Reaches 2 and 3. This consistent surface sediment layer was attributed to upstream erosion associated with the large snowmelt in 2011 that decreased SOD and %VS throughout the LJR due to an influx of silt and sand prior to the 2012 sampling event.

5.4.4 Sediment column OM turnover estimates

Fig. 64 provides an estimate of the cumulative years required to oxidize the carbon and ammonia associated with the sediment OM based on measured SOD fluxes. It should be noted that readily biodegradable dissolved organic carbon (DOC) and methane will be utilized to denitrify water column nitrate at the sediment water interface, slightly decreasing the total amount of DO required to oxidize sediment derived OM (Chapra 2008). This results in a conservative estimation of the time required to oxidize OM under these assumptions. In addition, many of the organics are refractory and will take years to breakdown or will never contribute to an oxygen demand. One of the interesting aspects of Fig. 64 is the 1:1 relationship between cumulative years and depth. Reaches 1–3, the Surplus Canal backwater (R4 BW), and Reach 8 all follow the 1:1 relationship although they have very different wet sediment densities, OM contents, and SOD fluxes. These

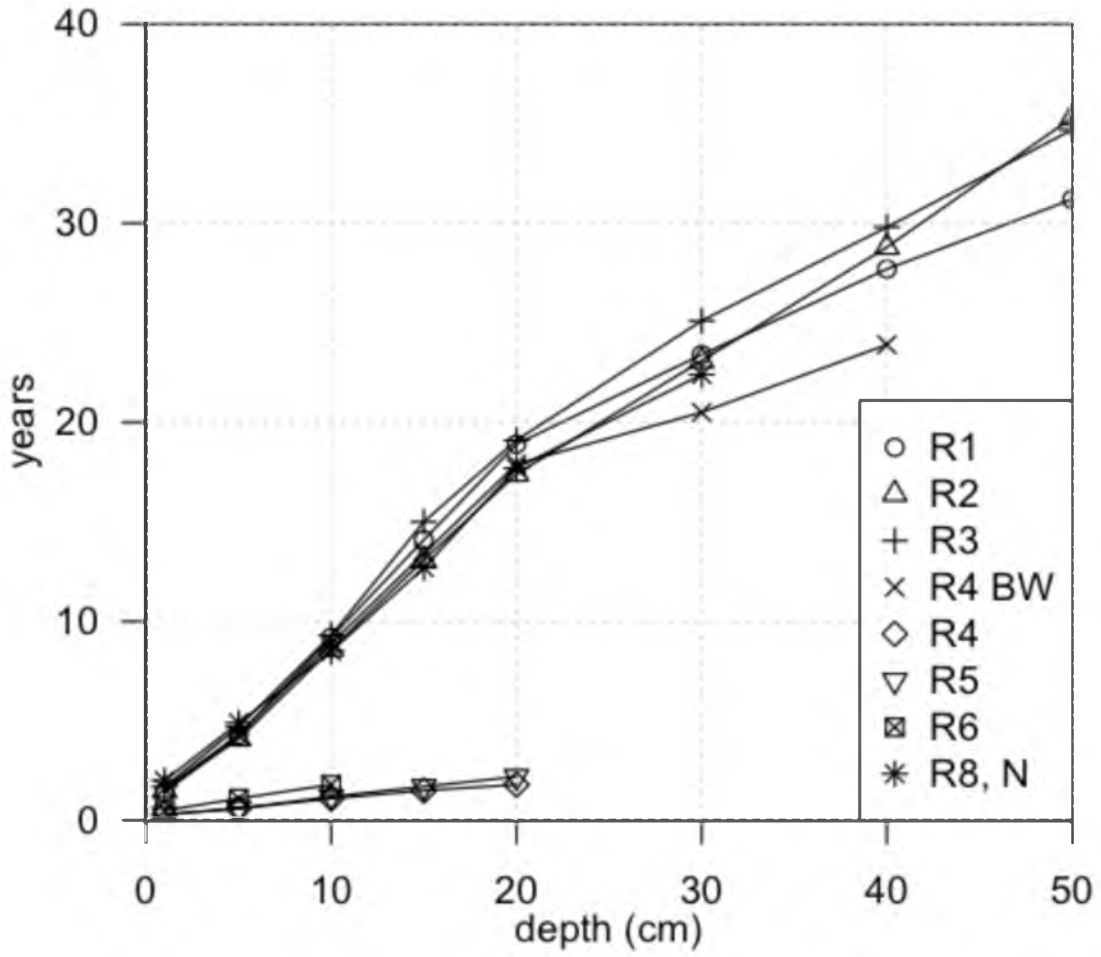

Fig. 64. Theoretical years to oxidize sediment column OM

rates coincide very closely with an annual cycle, suggesting that any reductions in OM loads to the LJR will improve WQ by reducing SOD. These OM load reductions could be achieved by reducing external loads from stormwater and tributaries, decreasing instream primary production, or both.

5.5 Dissolved Nutrient Fluxes

5.5.1 Ambient WQ

Provided in Table 22 are the ambient dissolved nutrient concentrations at the sites evaluated for nutrient fluxes. The LJR had a 3-year average ambient ammonium-N,

Table 22. Average nutrient concentrations measured during nutrient flux sampling

ambient dissolved nutrient concentration during nutrient flux sampling (mg/L)							
site	date	NH_4-N	NO_2-N	NO_3-N	TIN	PO_4-P	N:P
State Canal	2/6/13	3	0.3	6.3	9.6	0.95	22
Burnham	6/12/12	0.13	0.06	3.76	4	0.53	17
Burnham	6/14/13	0.33	0.13	2.95	3.4	0.55	14
LNP NE	6/3/10	1.49	0.23	0.06	1.8	0.12	33
LNP NE	4/3/12	0.4	0.08	1.83	2.3	0.29	18
LNP NE	6/15/12	0.39	0.16	3.95	4.5	0.65	15
LNP NE	6/15/13	0.33	0.11	3.1	3.5	0.53	15
Cudahy	6/3/10	1.33	0.24	0.06	1.6	0.1	36
Cudahy	6/13/12	0.21	0.15	3.53	3.9	0.61	14
Cudahy	6/13/13	0.27	0.16	2.96	3.4	0.56	13
300 N	6/7/10	0.06		0.59	0.7	0.07	21
300 N	4/14/12	0.17	0.08	2.31	2.6	0.43	13
300 N	6/12/13	0.1	0.06	2.42	2.6	0.43	13
700 S	6/14/12	0.1	0.07	3.32	3.5	0.58	13
700 S	6/10/13	0.11	0.05	2.17	2.3	0.36	14
900 S-N	6/8/10	0.05		0.57	0.6	0.11	12
900 S-S	6/8/10	0.08		0.64	0.7	0.1	16
1700 S-N	5/24/10	0.08	0.05	1.16	1.3	0.12	24
1700 S-N	4/16/12	0.13	0.07	2.1	2.3	0.49	10
1700 S-N	6/10/13	0.06		2.93	3	0.46	14
2600 S	6/2/10	5.64	1.13	0.22	7	0.29	53
5400 S	1/12/11	0.04		3.91	4	0.74	12
7600 S	1/15/11	0.03		1.85	1.9	0.1	42
9000 S	1/20/11	0.04		1.67	1.7	0.1	38
LJR avg.		0.31	0.11	2.13	2.5	0.37	15

Note: nitrite-N, nitrate-N, and phosphate-P DL = 0.05 mg/L
ammonium-N DL = 0.015 mg/L

nitrate-N, and orthophosphate-P concentrations of 0.3, 2.1, and 0.4 mg/L, respectively. These dissolved nutrient concentrations are higher than the total nitrogen (TN) and total phosphorus (TP) concentrations of 1.5 mg-N/L and 0.075 mg-P/L, indicating the potential for eutrophication in a lotic system (Dodd et al. 1998). The extremely high ammonium concentrations measured in State Canal and at the 2600 S site were coupled with high sediment OM content and extremely high SOD fluxes.

Generally, WQ scientists assume that nitrite concentrations are negligible in surface waters (Stanley and Hobbie 1981). The high nitrite concentrations found in Reach 1 and at the 2600 S site suggest incomplete nitrification in the water column or inhibited denitrification at the sediment–water interface. The organically enriched anaerobic sediments found in these river sections would be ideal for the microbial dissimilatory nitrate reduction metabolism carried out via fermentation that has been shown to result in nitrite accumulation in large rivers (Kelso et al. 1997). For perspective, aerobic surface waters tend to have nitrite concentrations less than 0.002 mg-N/L, or two orders of magnitude lower than measured in the LJR (Lewis and Morris 1986).

Both dissolved nitrogen and phosphorus were found in concentrations high enough for unrestricted phototrophic growth, but the elevated N:P ratios imply that phosphorus is the limiting nutrient. These ratios are even higher in the UJR upstream of all POTW discharges (7600 S and 9000 S), implying that P reductions from POTW loads to the Jordan River and the upstream Utah Lake will reduce eutrophication by limiting the availability of dissolved phosphorus. Additional external sources of nutrients to the Jordan River include groundwater, urban runoff, agriculture, and tributaries.

5.5.2 Sediment nutrient fluxes

Table 23 provides the 3-year average sediment nutrient fluxes for each site visited more than once in the LJR. Data from all nutrient flux sampling events can be found in Appendix G. The sediments were a source of ammonium at all sites in the LJR, suggesting sediment OM decay. Although the sediments were a source of ammonia-N, the sediments were a net sink for total dissolved inorganic nitrogen (TIN) due to the denitrification of nitrate loads originating from WWTP discharges. Nitrate removal was observed during all sampling events with the exception of two sites (LNP NE, 2012 and 300 N, 2010).

In Chesapeake Bay, silty sediments had increased ammonia and phosphorus fluxes compared to sandy substrate (Reay et al. 1995). Tidal flat sediments having less than 0.3% TOC (0.6% VS) had positive nitrate fluxes and exhibited positive ammonia fluxes at %TOC greater than 1.3% (2.6% VS) (Henriksen et al. 1983). The average %TOC in the surface sediments for Reaches 1–3 were all greater than 1.3% (Fig. 59 converted to %TOC), suggesting that the organically enriched sediments in the LJR are expected be a source of ammonia, not nitrate. Positive sediment phosphate fluxes were

Table 23. Average sediment nutrient fluxes in the Lower Jordan River

	average sediment flux ($g/m^2/d$)			
site	NH_4-N	NO_3-N	TIN	PO_4-P
Burnham	0.03	-0.69	-0.66	-0.08
LNP NE	0.04	-0.11	-0.09	0.06
Cudahy Ln	0.22	-0.28	-0.13	0.07
DWQ	0.04	-0.03	0.00	0.05
700 S	0.07	-0.27	-0.20	0.06
1700 S-N	0.14	-0.14	-0.04	0.11

Note: data from 16 sampling events over 3 years

characteristic of all sites in the LJR except the Burnham Dam site. This suggests that phosphorus loads from the sediments will most likely continue for some time following a decrease in anthropogenic phosphorus and OM loads (Larsen et al. 1981).

Table 24 provides average aerial sediment nutrient fluxes to Reaches 1–3 in the LJR, and Table 25 provides annual hydraulic reach sediment derived nutrient loads to the LJR. The sediments add over 5,000 kg of phosphate-P and 12,000 kg of ammonia-N to the LJR, but remove over 33,000 kg of nitrate-N from the water column. This results in the sediments removing roughly 21,000 kg of dissolved nitrogen from the water column annually. The LJR sediment derived ammonia and phosphate loads accounted for 5% and 1% of the total nutrient loadings discharged from the three online POTWs (Section 5.7.8).

Table 26 provides sediment fluxes measured in other freshwater and estuarine sediments under dark aerobic conditions. Fluxes of ammonia, nitrate, and phosphate can

Table 24. Sediment nutrient fluxes in the Lower Jordan River

	average sediment flux ($g/m^2/d$)			
site	NH_4-N	NO_3-N	TIN	PO_4-P
Reach 1	0.098	-0.361	-0.263	0.016
Reach 2	0.038	-0.028	0.010	0.052
Reach 3	0.106	-0.203	-0.098	0.087
Lower River	0.081	-0.197	-0.117	0.051

Table 25. Sediment nutrient loads to the Lower Jordan River

	Sediment Nutrient loading (kg/year)			
	Reach 1	Reach 2	Reach 3	LJR load
NH_4-N	6,455	1,352	4,332	12,139
NO_3-N	-23,738	-985	-8,343	-33,065
TIN	-17,283	368	-4,010	-20,925
PO_4-P	1,051	1,839	2,112	5,002

Note: data from 16 sampling events over 3 years

Table 26. Nutrient flux comparisons

Surface Water	Average sediment flux ($g/m^2/day$) NH_4-N	NO_3-N	PO_4-P	SOD	ref.
Anacostia River	0.205	-0.036	0.002	-2.2	1
Chester River	0.117	-0.006	0.011	-2.4	1
Potomac River	0.135	-0.007	0.009	-1.9	1
Chesapeake Bay	0.144	0.029	0.013		2
Chesapeake Bay	0.056	-0.011	0.011	-0.6	3
Yaquina Bay	-0.014	-0.135			4
Tagus Estuary		-0.018		-1.2	5
Firth of Thames Bay	0.342	0.026	0.012		6
Pacific cont. shelf	0.006	-0.01			7
WWTP biofilm nitri.		1 to 3			8
Lower Jordan River	0.081	-0.197	0.051	-1.9	9
Lower Jordan River	0.28	-0.551	0.216	-3.3	10

ref. and notes:
1 (Boynton et al. 2003) drains to Chesapeake Bay
2 (Boynton and Kemp 1985) one-year study
3 (Cowan and Boynton 1996) multi-year study
4 (Larned 2003) estuary wide flux
5 (Cabrita et al. 2000) largest wetland in Portugal
6 (Giles et al. 2006) mussel aquaculture sediments
7 (Christensen et al. 1987) offshore ocean sediments
8 (USEPA 1993) POTW design
9 This study, 2010 to 2013, 3-year average
10 This study, 2010 to 2013, 3-year maximum

vary considerably depending on historic water quality, sediment OM content, and sediment size. These parameters tend to be synergistic, such as large amounts of organic matter depositing with fine sediments while decomposing and influencing ambient WQ through nutrient cycling. Alternatively, sandy sediments may be downstream of a POTW discharging ammonia, which may lead to sediment and water column nitrification coupled with ambient DO deficits.

Sediment ammonia fluxes in the LJR were similar to degraded tributaries feeding Chesapeake Bay. Negative nitrate fluxes, or denitrification, in the LJR are the highest in

Table 26 This is hypothesized to be a result of elevated ambient nitrate concentrations originating from POTW discharges coupled with a source of sediment derived rbCOD diffusing from the anaerobic sediments in the LJR. Phosphorus fluxes were also higher in the LJR compared to the other waters presented in Table 26. The extremely high average P flux of 0.216 $g/m^2/d$ was measured at the 1700 S site in 2013 in a thick benthal deposit, highlighting the influence of benthal deposits on ambient WQ.

All surface waters are unique, and the nutrient dynamics occurring at the sediment–water interface coupled with ambient WQ, presence of toxins, sediment quality, current and historical nutrient and OM loadings, and trophic status all need to be taken into account to adequately describe the complex biochemical reactions influencing water quality.

5.5.3 Water column nutrient rates

The nutrient dynamics occurring in the WC during dark conditions are provided in Table 27. Ammonium and phosphorus were added to the WC during the degradation of water column BOD. Assuming the Redfield ratio, roughly 0.08 mg NH_4-N/L and 0.012 mg-P/L are added to the water column for every -1 g-DO/m^3/d as WC_{dark}.

Table 27. 3-year average dark WC rates in the LJR

	average WC dark metabolism rate ($g/m^3/d$)			
site	NH_4-N	NO_3-N	TIN	PO_4-P
Burnham	0.15	0.85	0.99	0.13
LNP NE	0.12	0.29	0.41	0.05
Cudahy Ln	-0.19	0.89	0.71	0.06
DWQ	-0.16	0.34	0.18	-0.09
700 S	0.09	1.59	1.68	0.27
1700 S-N	0.01	-0.42	-0.41	-0.05

Nitrate production rates associated with the two-step biological nitrification were high at all sites except the 1700 S-N site. The elevated nitrate production rates highlight the river's natural ability to transform ammonium-N into the less toxic nitrate-N (Malecki et al. 2004). The water column is oxygenated, contains abundant inorganic carbon, and has low rbCOD, allowing the slow growing autotrophic nitrifiers to establish a niche. Upstream of the South Valley WRF discharge (7600 S and 9000 S) the WC removed ammonia, nitrate, and phosphate (Table 28). Downstream of the discharge (5400 S), the WC behaved as a source of both ammonia and nitrate while removing less phosphate than upstream sites.

5.5.4 Fluxes in relation to other fluxes, SOD, WC_{dark}, and OM

Table 29 provides statistical relationships between sediment fluxes, WC rates, and other parameters measured during this research. The slope describes the sediment flux or WC rate for a particular dissolved nutrient in relation to ambient ammonia concentrations, surficial sediment %VS, and the simultaneously measured SOD and WC_{dark}. Positive slopes imply that the parameters are positively related and negative slopes indicate the opposite. Relationships between sediment fluxes and OM decay surrogates were all statistically significant ($p < 0.05$) with the exceptions of sediment P fluxes and sediment %VS and SOD. Correlations between water column rates, ambient

Table 28. Upper Jordan River dark WC nutrient dynamics

		Upper River WC dark metabolism rate ($g/m^3/d$)			
site	date	NH_4-N	NO_3-N	TIN	PO_4-P
5400 S	1/12/11	0.196	1.44	1.636	-0.039
7600 S	1/15/11	-0.025	-0.501	-0.526	-0.377
9000 S	1/20/11	-0.013	-0.125	-0.138	-0.365

Table 29. Relationships between fluxes and various OM decay surrogates

	Slope		p value		
Test	Sed.	WC	Sed.	WC	N
NO_3-N:NH_4-N	-	-	0.0006	0.75	27
PO_4-P:NH_4-N	-	+	0.002	0.35	26
PO_4-P:%VS	+		0.06		19
NH_4-N:%VS	+		0.01		19
NO_3-N:%VS	-		0.03		19
PO_4-P:SOD	+		0.05		25
PO_4-P:WC_{dark}		+		0.4	25
NH_4-N:SOD	+		0.01		25
NH_4-N:WC_{dark}		-		0.5	25
NO_3-N:SOD	-		0.03		25
NO_3-N:WC_{dark}		+		0.8	25

Notes: 0–2 cm %VS

ammonia concentrations, and WC_{dark} were all statistically insignificant ($p > 0.05$). The lack of correlations between water column rates and OM decay surrogates was a result of the vast majority of nutrients found in the water column originated from POTW loads.

Although insignificant, the negative and positive relationships between ammonia losses and nitrate production with increased WC_{dark} suggests water column nitrification, which was a prevalent water column metabolism in the LJR (Table 27). The positive correlations between sediment ammonia and phosphorus fluxes in relation to %VS and SOD is a result of OM decay. This is also supported by the inverse relationship between sediment nitrate removal, or denitrification, and sediment %VS. Denitrification at the sediment–water interface was the dominant nitrogen transformation measured in the LJR (Table 23).

5.5.5 Anoxic fluxes

Dissolved oxygen was removed from the SOD chambers through the addition of sodium sulphite to mimic anoxic conditions associated with an acute low DO event.

These events may occur during the die off of an upstream algal bloom or following a large urban storm event following an extended dry spell. By removing DO in the chamber, nitrification will stop, denitrification may increase, and polyphosphate accumulating organisms (PAOs) might release orthophosphate if rbCOD is available.

Fig. 65 provides a bar chart for sediment ammonia fluxes during aerobic (white bars) and anoxic (grey bars) conditions. Sediment ammonia fluxes increased during anoxia at all sites except the Cudahy Ln site, which had the highest ammonium fluxes measured in 2013. Anoxia resulted in a site average 15% increase in sediment ammonia fluxes in the LJR. When Cudahy Ln and the 1700 S sites are excluded, anoxia resulted in a 11% increase in ammonia fluxes. The 1700 S site had sediment %TS and %VS of 38% and 6% (Fig. 60, west bank) and a high CH_4 oxygen demand of 1.8 g-DO/m^2/d (see Chapter 5.6, west bank) in the west bank depositional zone where nutrient fluxes were measured. The benthal deposits present in depositional zones found in Reach 3, although less plentiful than downstream, are a source of ammonia to the LJR.

The removal of nitrate by the sediments increased at all sites during anoxia except the LNP NE and 700 S sites (Fig. 66). Anoxia resulted in a 3% increase in nitrate removal at the sediment–water interface and was associated with increased denitrification. The small increase in sediment denitrification during anoxia compared to background conditions is hypothesized to be a result of the sediments being anaerobic very close to the sediment–water interface during normal conditions. This would result in anoxic conditions influencing the sediment metabolism minimally since the sediments are already anaerobic.

Sediment phosphate fluxes decreased at all sites following anoxia (Fig. 67) except

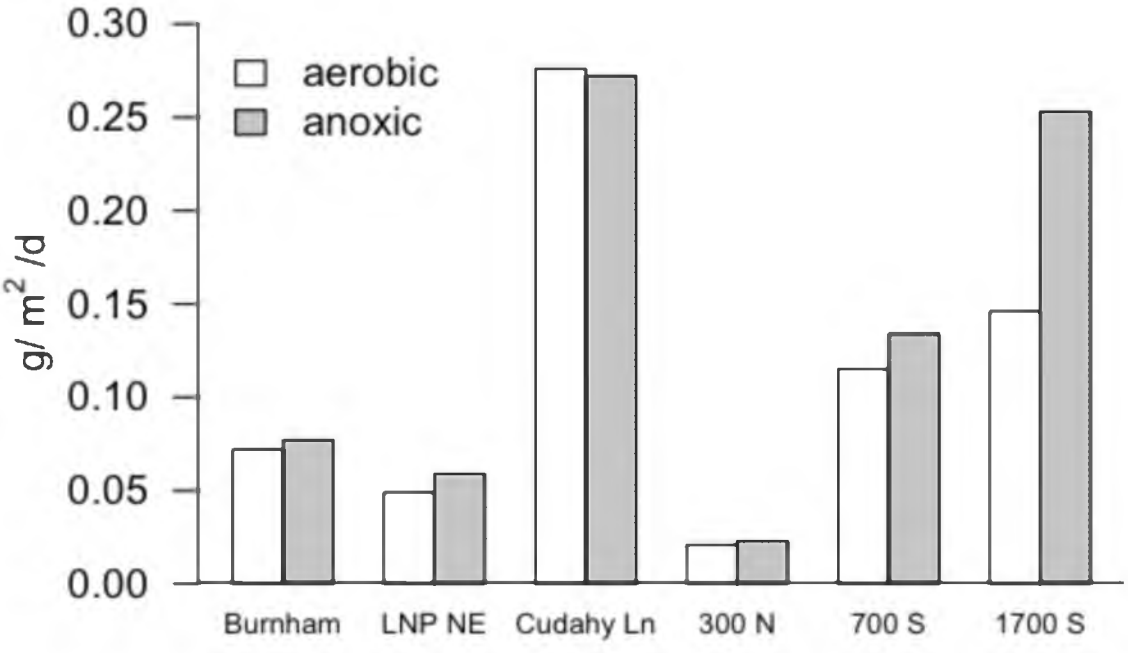

Fig. 65. Ammonia-N fluxes during anoxic conditions

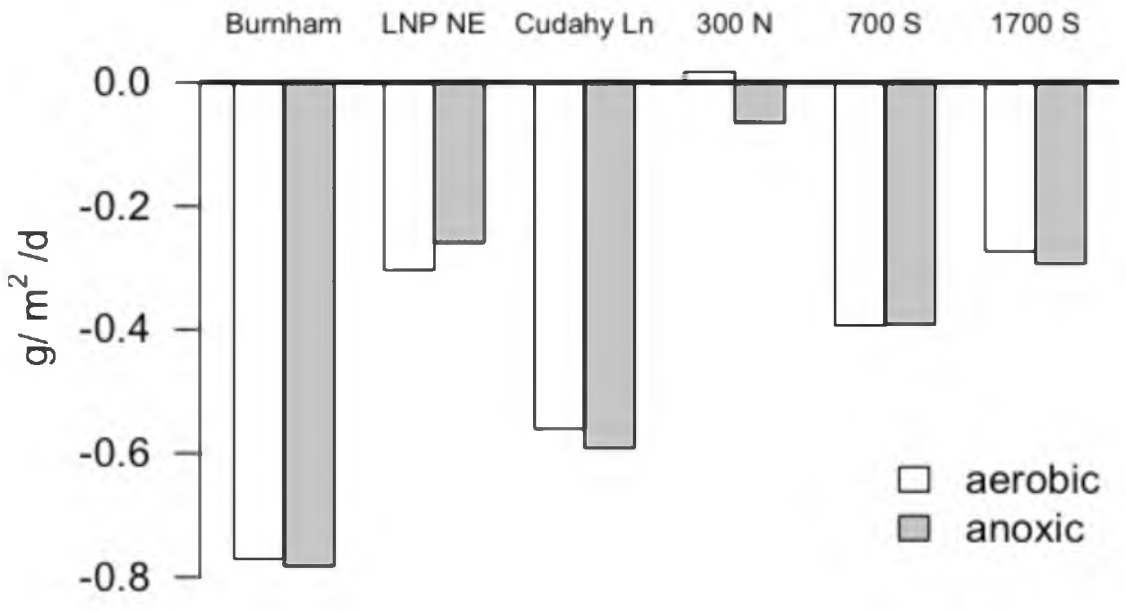

Fig. 66. Nitrate-N fluxes during anoxic conditions

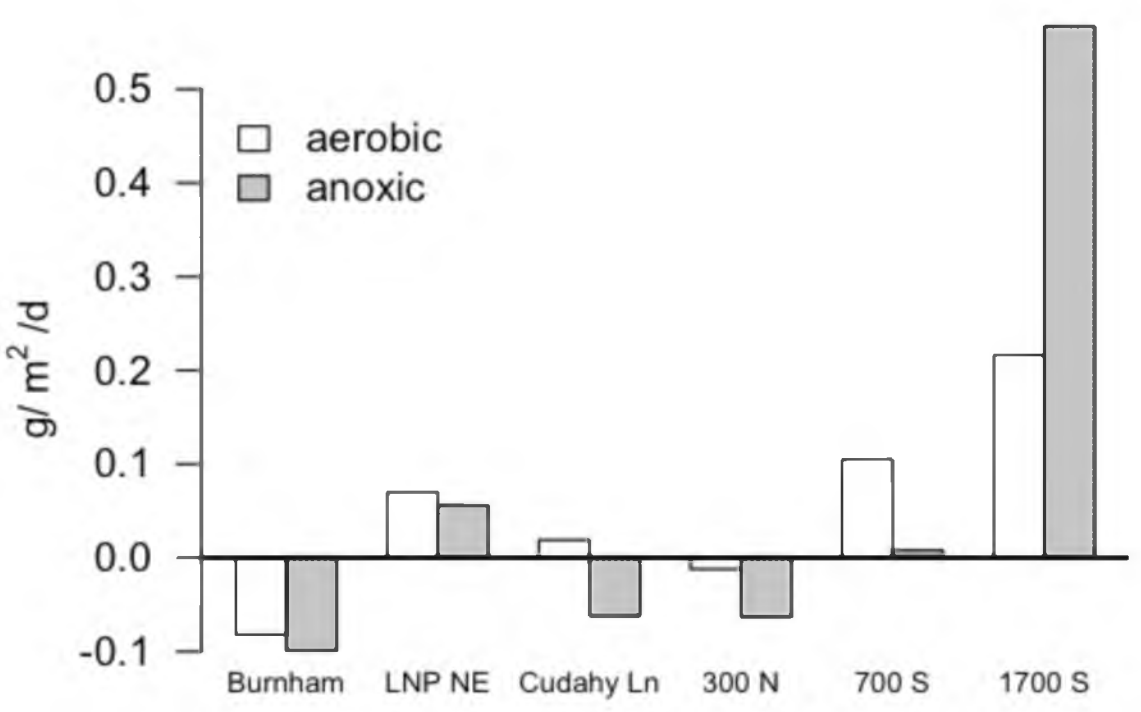

Fig. 67. Phosphate-P fluxes during anoxic conditions

for the 1700 S site. Although the other sites did not exhibit this large additional flux, the high phosphorus flux measured during aerobic conditions at the 1700 S suggest that benthal deposits found throughout the LJR are a source of dissolved phosphorus from the decay of sediment OM.

The onset of brief periods of anoxia in the Lower Jordan River will influence nutrient dynamics at the sediment–water interface slightly, but the general trend was that background fluxes were relatively uninfluenced by the 3-hour anoxic periods. This is most likely a result of the oxic-anoxic interface being very shallow in the sediment column (<2 cm).

5.5.6 pH lowering fluxes

The neutralizing of pH in the chambers while measuring nutrient fluxes was conducted to investigate the potential of increased nutrient loadings following changes in

water chemistry. Ammonia fluxes increased at all sites except the Burnham Dam site following pH lowering (Fig. 68). The increased ammonia fluxes are hypothesized to be a result of ion exchange between sorbed ammonium and the surface of organic and clay sediments. As pH decreases, additional hydronium ions, H_3O^+, are available to replace sediment sorbed ammonium cations (Mcnevin and Barford 2001).

The flux of orthophosphate from the sediments increased following reductions in pH at all sites except the 300 N site (Fig. 69). The calcareous inorganic sediments found in the LJR contain calcium bound P that could be liberated during decreases in ambient pH as part of the sediment buffering capacity. The average increase in DP fluxes from the sediments following the lowering of pH from 8 to 7 was 0.055 g-P/m^2/day (300 N excluded). This additional sediment phosphate load is greater than the suggested

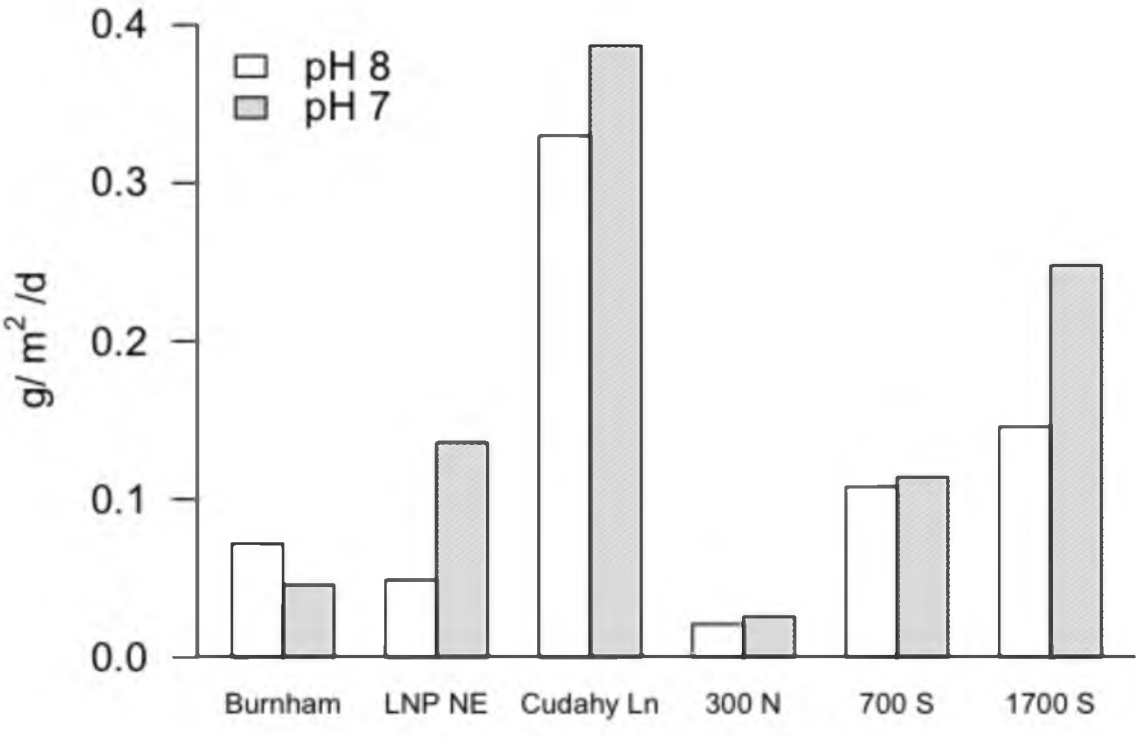

Fig. 68. Ammonia-N sediment flux following pH lowering

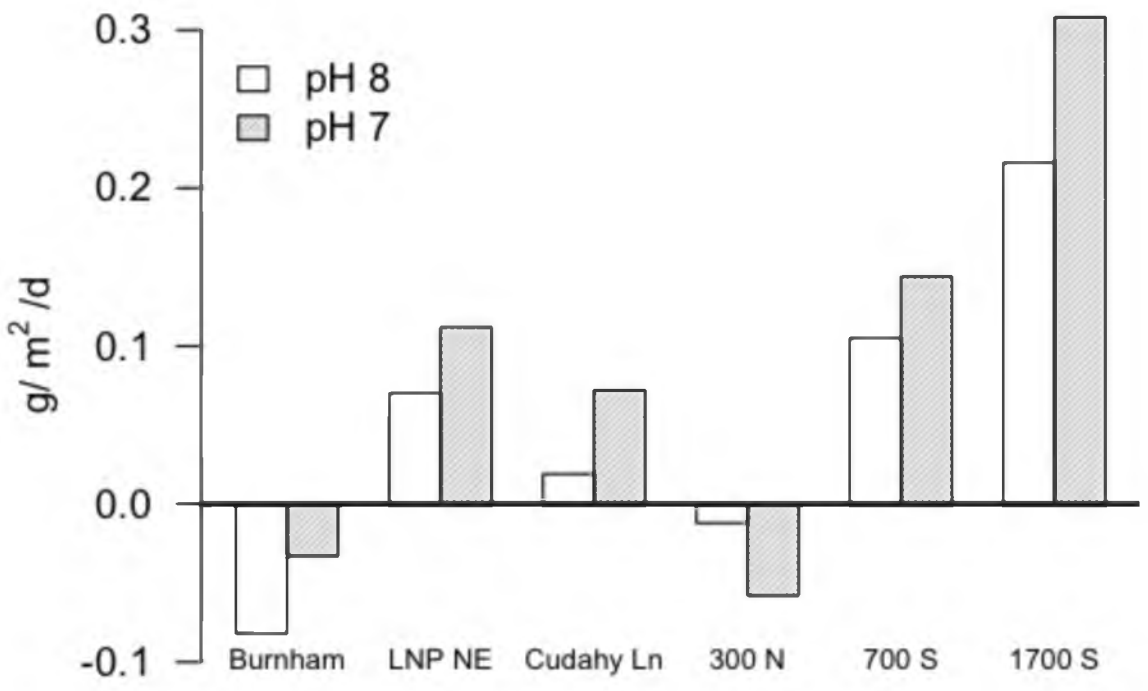

Fig. 69. Phosphate-P sediment flux following pH lowering

threshold concentration of 0.05 mg-P/L for a river draining to a lake (USEPA 1986), although with a LJR average ambient DP concentration of 0.37 mg-P/L (Table 22) the effects of sediment derived nutrient enrichment are minimal compared to the POTW nutrient discharge loads.

5.6 Methane Fluxes

5.6.1 River-wide sediment methane fluxes

The majority, up to 90%, of methane produced in the sediments is oxidized in the anoxic and aerobic zones of the uppermost sediment layers during diffusion (Wetzel 2001, pg. 642; Kuivila et al. 1988; Lidstrom and Somers 1984). Dissolved methane that is not oxidized in the sediments will be oxidized in the water column, further depleting ambient DO (Chapra 2008, pg. 458).

Fig. 70 provides the cumulative oxygen demand associated with methane production in the sediments ($CH_{4,OD}$) at three locations across the width of the river at depths of 0–2, 5, and 10 cm. Additional data can be found in Appendix H. The surface sediments were the most active in producing methane compared to deeper sediments. The east bank and thalweg at 1700 S produced no methane in the gravely sand substrate, but the benthal deposit near the west bank produced methane at fluxes similar to Reach 1. Surprisingly, the sediments at the LNP NE site produced very little methane across the

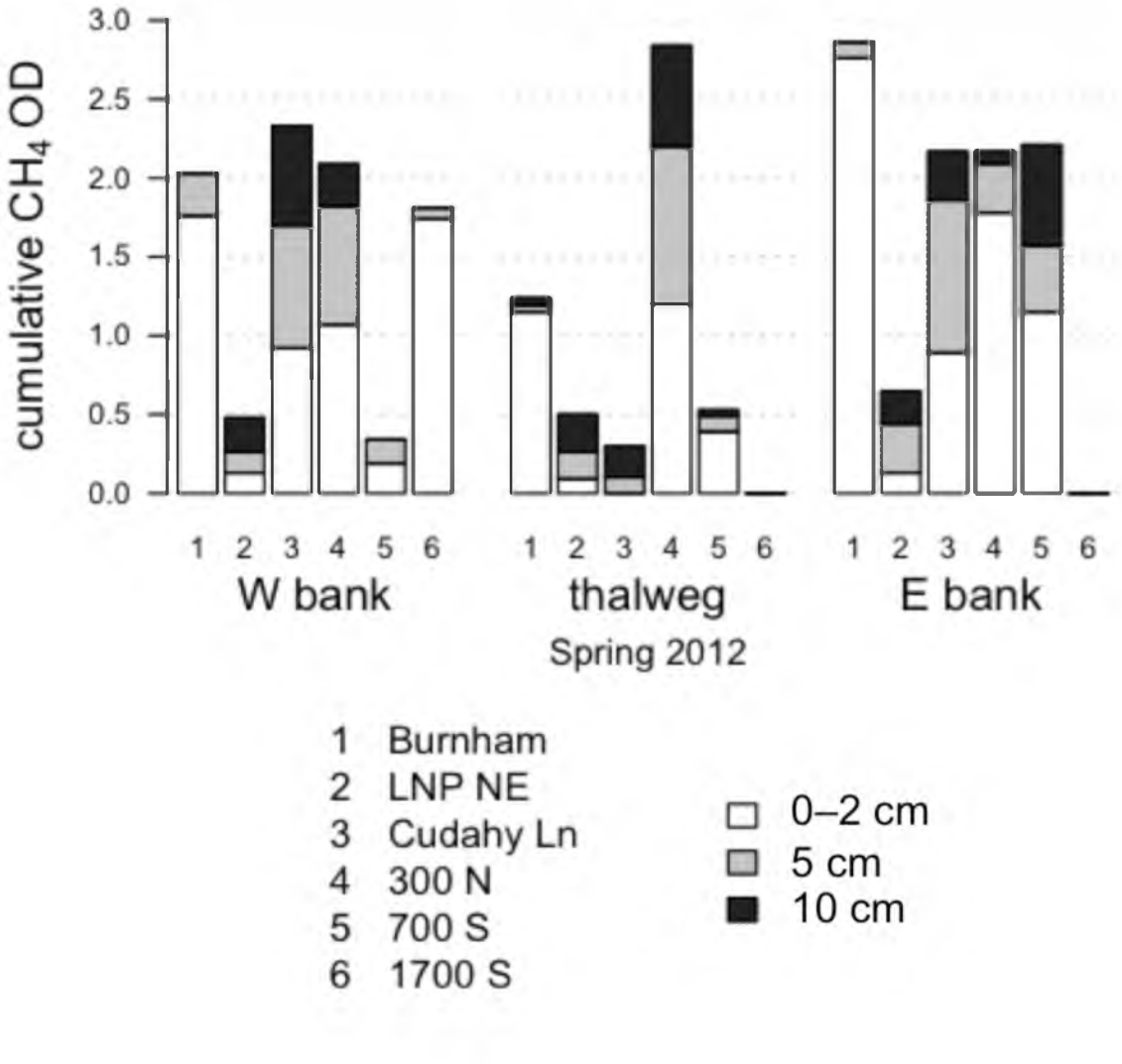

Fig. 70. Sediment column methane oxygen demand in the Lower Jordan River

width of the river and showed higher methane production rates at depths of 5 and 10 cm compared to the surface sediments. This was attributed to the influx and deposition of inorganic sediments from the 2011 high water event at this site.

Fig. 71 provides the river-wide average methane fluxes measured in 2012. The surface sediments were active in methane production throughout the LJR and were contributing to ambient oxygen deficits. The highest river-wide average surface sediment methane flux was measured at the Burnham Dam site in Reach 1 in the depositional zone located at the end of the Jordan River proper.

5.6.2 Swamp gas composition

Jordan River sediment biogas was composed of 60% methane by volume on average (Fig. 72). Prior researchers found methane contents ranging from 55–69% by

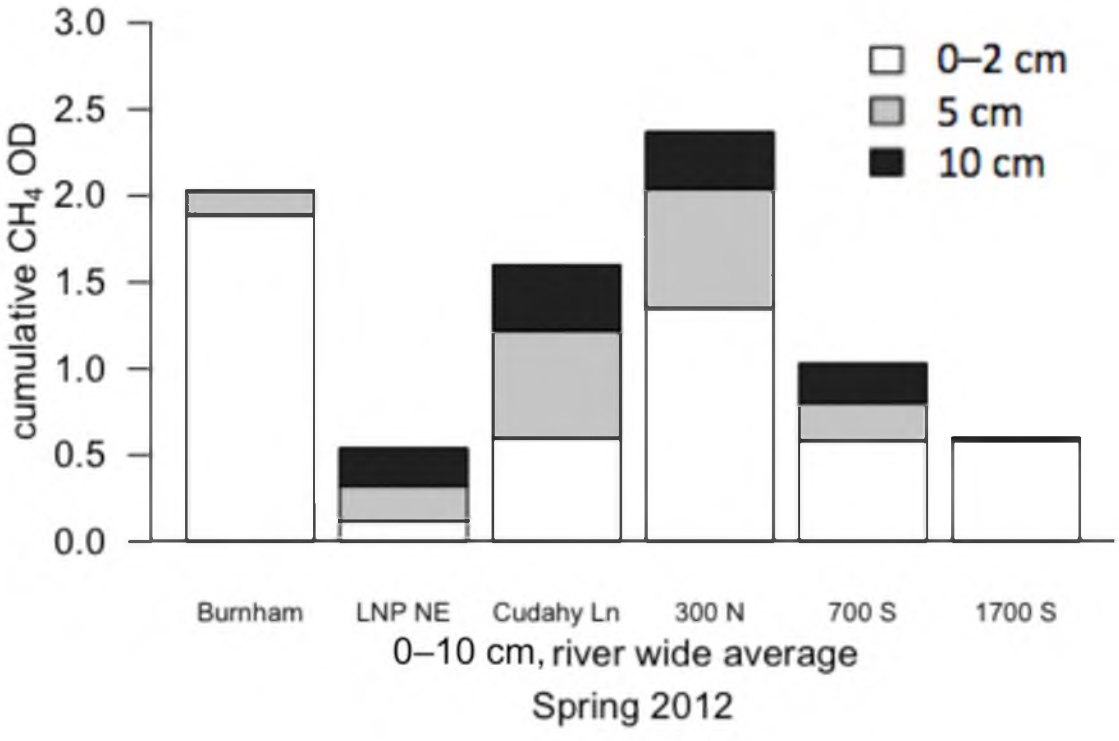

Fig. 71. River-wide average sediment column methane oxygen demand in the LJR

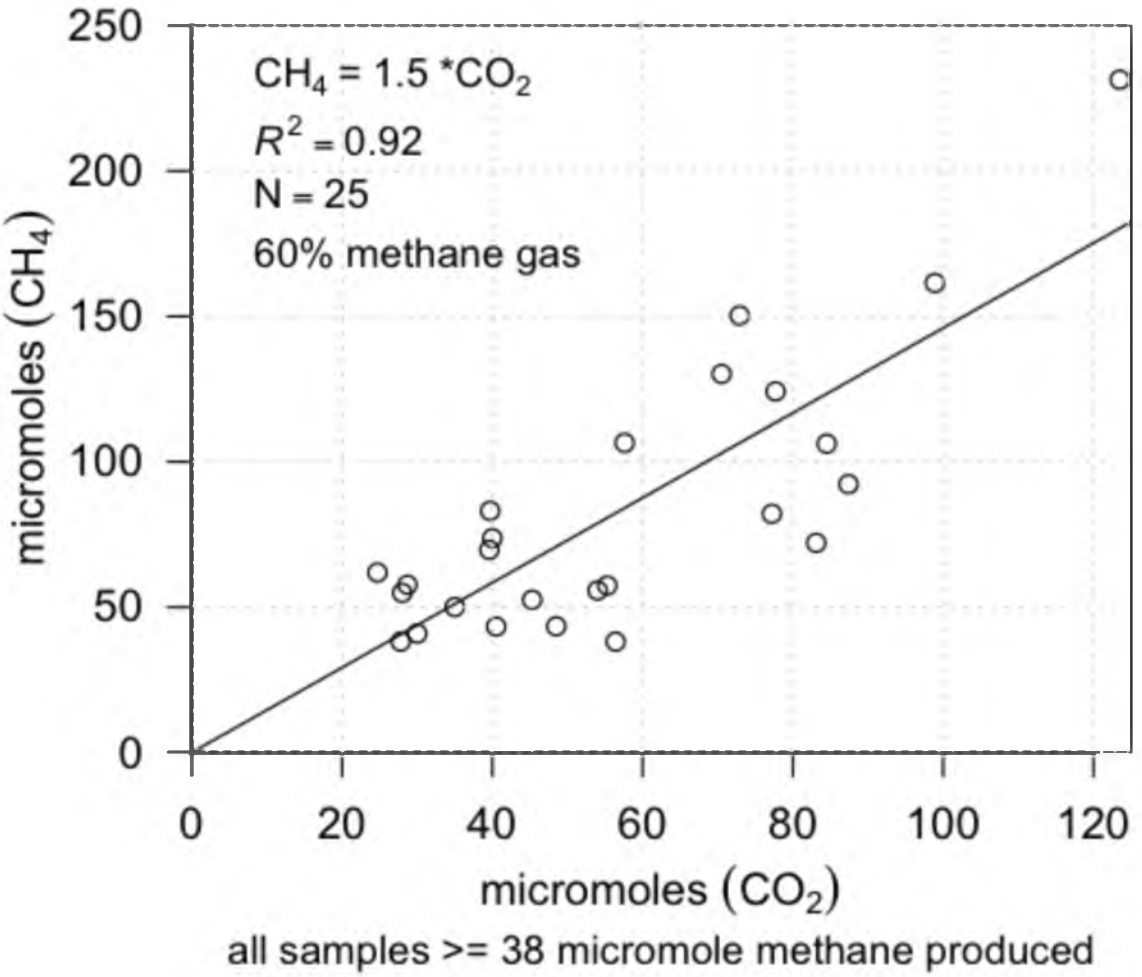

Fig. 72. Methane content of Lower Jordan River sediment gas

volume in the hypereutrophic Lake Postilampi, Finland (Huttunen et al. 2001). Typical methane concentrations found in biogas produced in a well-maintained POTW anaerobic digester is 60–70% methane (Appels et al. 2008; Deublein and Steinhauser 2008). The significance of this relationship is that for every mg of CH_4 gas oxidized at the sediment–water interface, a total of 1.67 mg of organic C was degraded in the sediments with 0.67 mg of CO_2 dissolving into the water column while contributing no additional ambient oxygen demand.

5.6.3 Sediment methane fluxes and %VS

Fig. 73 shows the relationship between the rate of sediment methane production and $\%VS_{bulk}$ at sediment depths of 0–2, 5, and 10 cm. Sediment methane fluxes were positively correlated with increased organic matter loadings (Kelly and Chynoweth 1981).

The surface sediments were the most active sediment layer in terms of methane production. The relationship between surface sediment %VS (0–2 cm) and the mass of methane produced per mass of wet sediment per day was

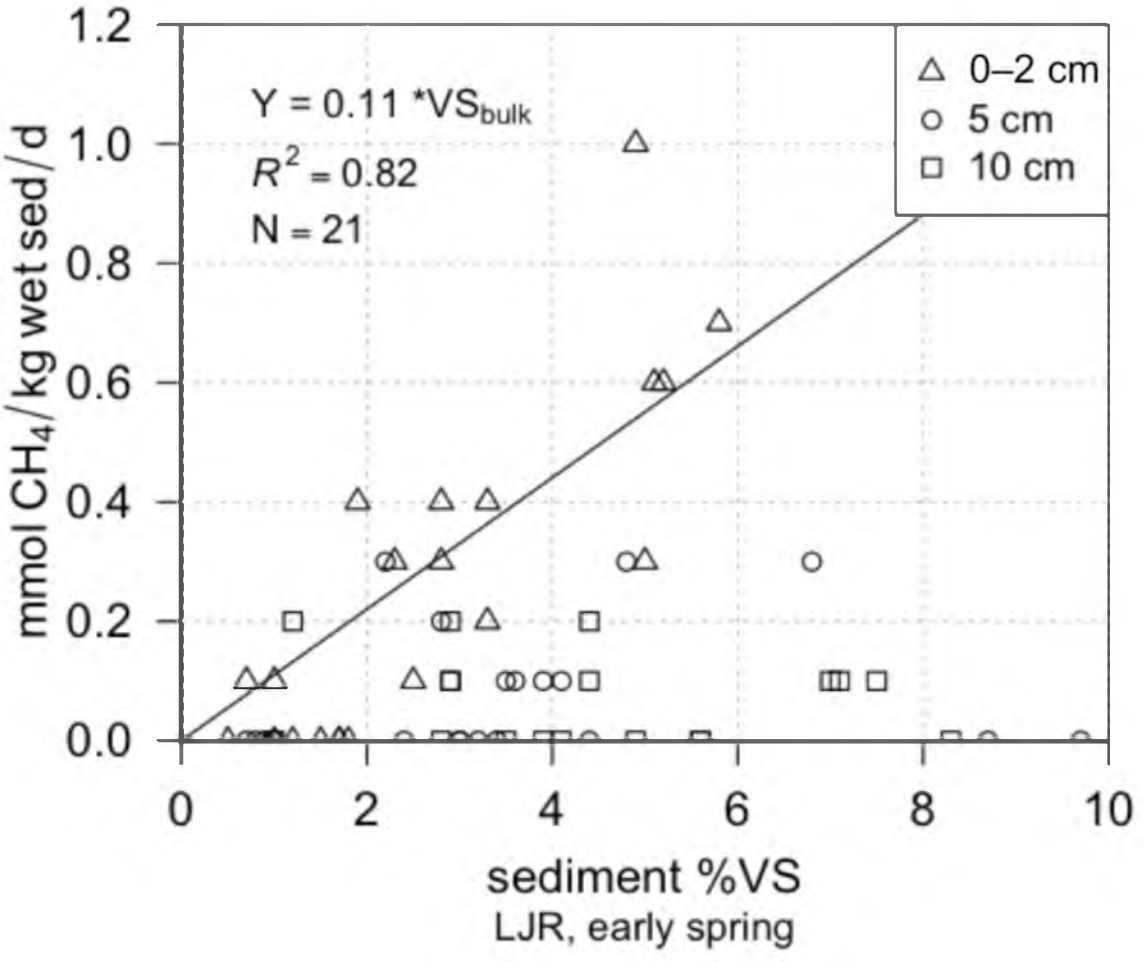

Fig. 73. Methane oxygen demand at different sediment depths

$$\frac{mmol\ CH_4}{kg\ wet\ sed * day} = 0.11 * \%VS \quad (23)$$

This relationship can be used to estimate the mass of methane produced in the surface sediments, but is not normalized to an aerial sediment flux. The sediments at depths of 5–20 cm (20 cm data not shown in Fig. 73) did produce methane in the LJR but at much slower rates, and the rates were decoupled from sediment OM content. Other studies observed that organic matter present in the top 20 cm of the sediment column served as substrate for methane generation, but methane production decreased with depth (Kelly and Chynoweth 1981). The surface sediments are the most recently deposited material and are more biologically active than deeper sediments that have already gone through a biological stabilization process (Fair et al. 1941).

After normalizing the Y-axis data points in Fig. 73 to an aerial estimate of methane oxygen demand, the relationship with 0–2 cm %VS becomes

$$CH_4OD = 0.32 * \%VS \quad (24)$$

$$CH_4OD = DO\ required\ to\ oxidize\ methane\ flux\ \left({}^{g\ DO}/_{m^2 * day}\right)$$

The above relationship can be used to estimate the surface sediment methane flux oxygen demand using sediment %VS as a surrogate in the LJR to help populate the Jordan River QUAL2kw model.

5.6.4 SOD and methane relationship

Methane oxidation associated with the top 0–2 cm of the sediments accounted for 56% of the measured SOD (Fig. 74). The remaining 44% of the SOD was associated with

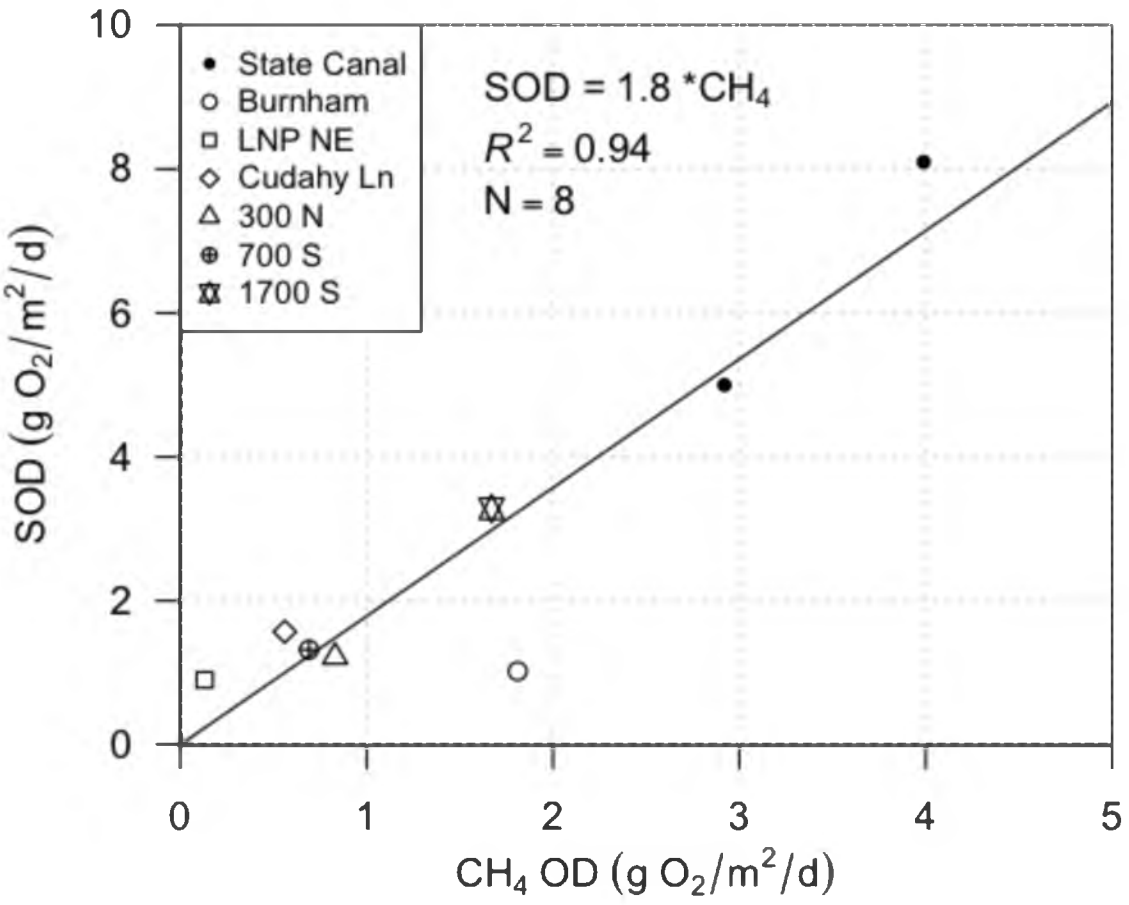

Fig. 74. Methane oxygen demand for different sediment depths

the faster aerobic metabolism at the sediment–water interface (Kristensen et al. 1995). The flux of other reduced chemicals, such as sulphide, will also exhibit an OD measured as SOD.

The sediments would require 2.5 to 4.8 years to cycle sediment OM under anaerobic conditions. This is much longer than the annual cycle (Fig. 64). The slower anaerobic sediment metabolism suggests that not all OM will be degraded in the sediments and recalcitrant OM will accumulate. This was observed in Fig. 73 where OM 5 cm and deeper did not undergo methanogenesis in a linear fashion.

5.6.5 Methanogenesis temperature dependency

Temperature dependencies were not observed for SOD, but were measured in the water column (Section 5.1.5 and 5.1.7). Table 30 provides Q_{10} values for methanogenesis rates in serum bottles collected during the winter months in State Canal, where the Q_{10} was roughly 2 at all eight tests. A Q_{10} of 2 implies that the metabolism will decrease by 50% if the temperature drops 10 °C and will double if the temperature increases by 10 °C.

A wide range in Q_{10} ratios ranging from 1.3 to 28 have been reported for methanogens. Additional factors such as quantity and quality of available substrates have been shown to heavily influence methanogenic activity at low temperatures (Kelly and Chynoweth 1981; Rath et al. 2002; van Hulzen et al. 1999). Temperature variations associated with SOD are assumed to be driven by the anaerobic sediment metabolism (Di Toro et al. 1990).

The general relationships between temperature and various metabolisms measured in the Jordan River during this study are provided on the following page.

Table 30. Q_{10} for methane production measured in State Canal

State Canal	Q_{10}
SOD_1	1.8
SOD_2	2.4
0–2 cm	1.9
0–2 cm	2
10 cm	1.8
0–2 cm	1.6
5 cm	1.9
10 cm	1.9
Mean	1.9

- WC_{dark} decreased with decreased ambient water temperature
- SOD was not influenced by decreased ambient water temperature
- sediment methane production measured in a laboratory setting consistently decreased by half when temperature decreased by 10 °C

This implies that other processes are occurring in the sediments of the Jordan River to maintain an annually consistent SOD flux. These may be attributed to

- Additional seasonal organic matter loadings occuring during autumn leaf shedding and during winter as urban stormwater runoff to provide additional substrate for sediment decomposition.
- Sediment methane production being always inhibited due to sediment diffusion limitations, leading to a constant annual flux of methane.

Both of these hypotheses are most likely occurring in the LJR.

5.6.6 Nutrient and methane fluxes

Sediment ammonia and phosphate fluxes were positively related to 0–2 cm methane fluxes ($p = 0.004$ and $p = 0.005$). Positive correlations between the amount of swamp gas and dissolved ammonia and phosphorus fluxes from the sediments were expected since all three of these parameters are associated with the anaerobic decay of OM.

Fig. 75 shows the relationship between nitrate consumption measured in the chambers and methane fluxes measured in serum bottles. The axes in this plot are presented as millimoles. Methane fluxes were a better predictor of sediment denitrification compared to ammonia and phosphorus fluxes. The dotted green line represents the theoretical stoichiometric relationship for denitrification utilizing methane.

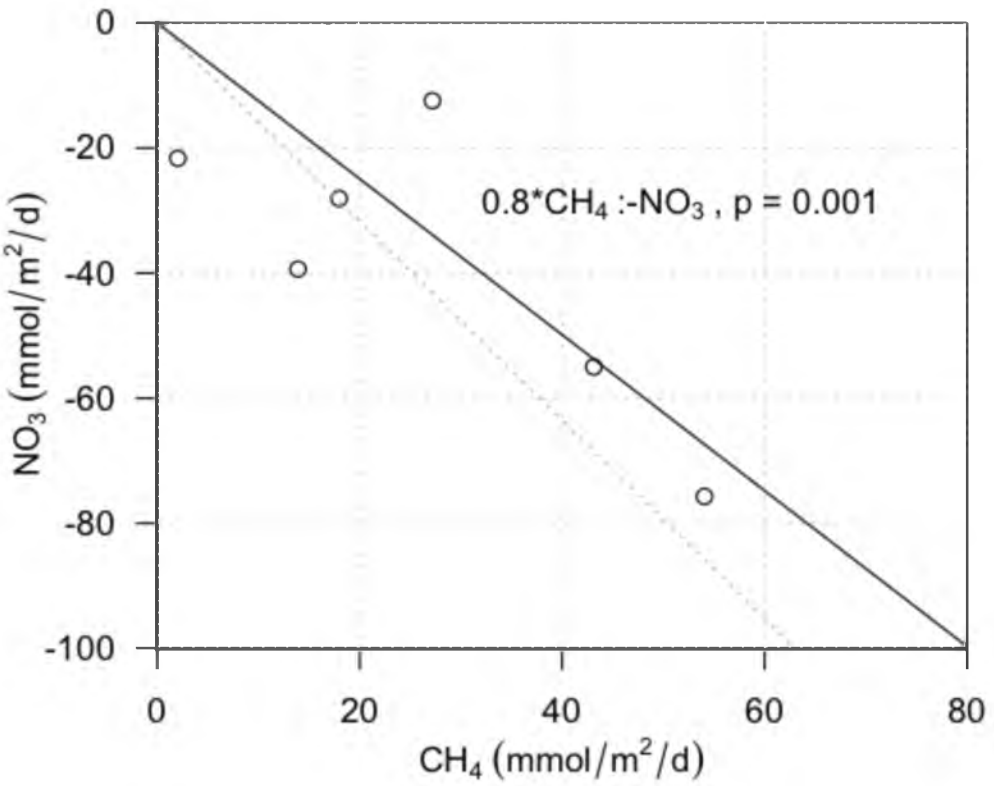

Fig. 75. 0–2 cm methane and nitrate molar fluxes

Fig. 75 predicts 0.8 moles of methane released from the sediments for every 1 mole of nitrate denitrified to dinitrogen gas. The ideal stoichiometric equation requires 0.63 moles of methane to reduce 1 mole of nitrate (Ahn et al. 2006).

$$5CH_4 + 8NO_3^- + 8H^+ \rightarrow 5CO_2 + 4N_2 + 14H_2O$$

Methane oxidized using nitrate as an electron acceptor will not be measured as an oxygen demand in the SOD chambers. The sediment methane fluxes calculated using lab techniques accounted for 50% of the SOD or 100% of the denitrification occurring at the sediment water interface. Other researchers calculated 42% of SOD being a result of methane oxidation (Gelda et al. 1995). In reality, methane is most likely being oxidized at the sediment–water interface utilizing both DO and nitrate as electron acceptors.

5.7 Jordan River DO and OM Mass Balances

5.7.1 Jordan River bathymetry

Jordan River cross sections were mapped at six sites and are provided in Fig. 76. The associated river-wide sediment sampling locations are represented by the black dots. The cross sections are presented as the river flows with the left and right representing the west and east banks, respectively. Bathymetry was obtained by measuring the depth of the Jordan River across the width at 2-feet intervals. Site bathymetry and calculated average flow velocities are provided in Table 31. The increase in calculated flow velocity in Reach 1 is a result of the cross-sectional area decreasing due to decreasing mean depths, a result of sedimentation behind Burnham Dam. The Lower Jordan River is managed for flood control in Salt Lake City and has very consistent mean daily flow rates throughout the year with the exception of storm events.

The river lengths and widths used to calculate standing stocks of OM in the Lower and Upper Jordan River are provided in Tables 32 and 33. These values were also used to calculate sediment derived nutrient loads to the LJR.

5.7.2 SOD chamber calculated OM decay rates

Estimates for OM degradation due to the seasonal average SOD and WC_{dark} using DO as a surrogate for decay are provided in Table 34. Assumptions used to convert an oxygen demand to the mass of oxidized dry OM are provided below Table 34. An estimated 355,896 kg/OM was oxidized in the LJR in the water column and at the sediment–water interface. SOD accounts for 54% of the ambient DO deficit in this scenario.

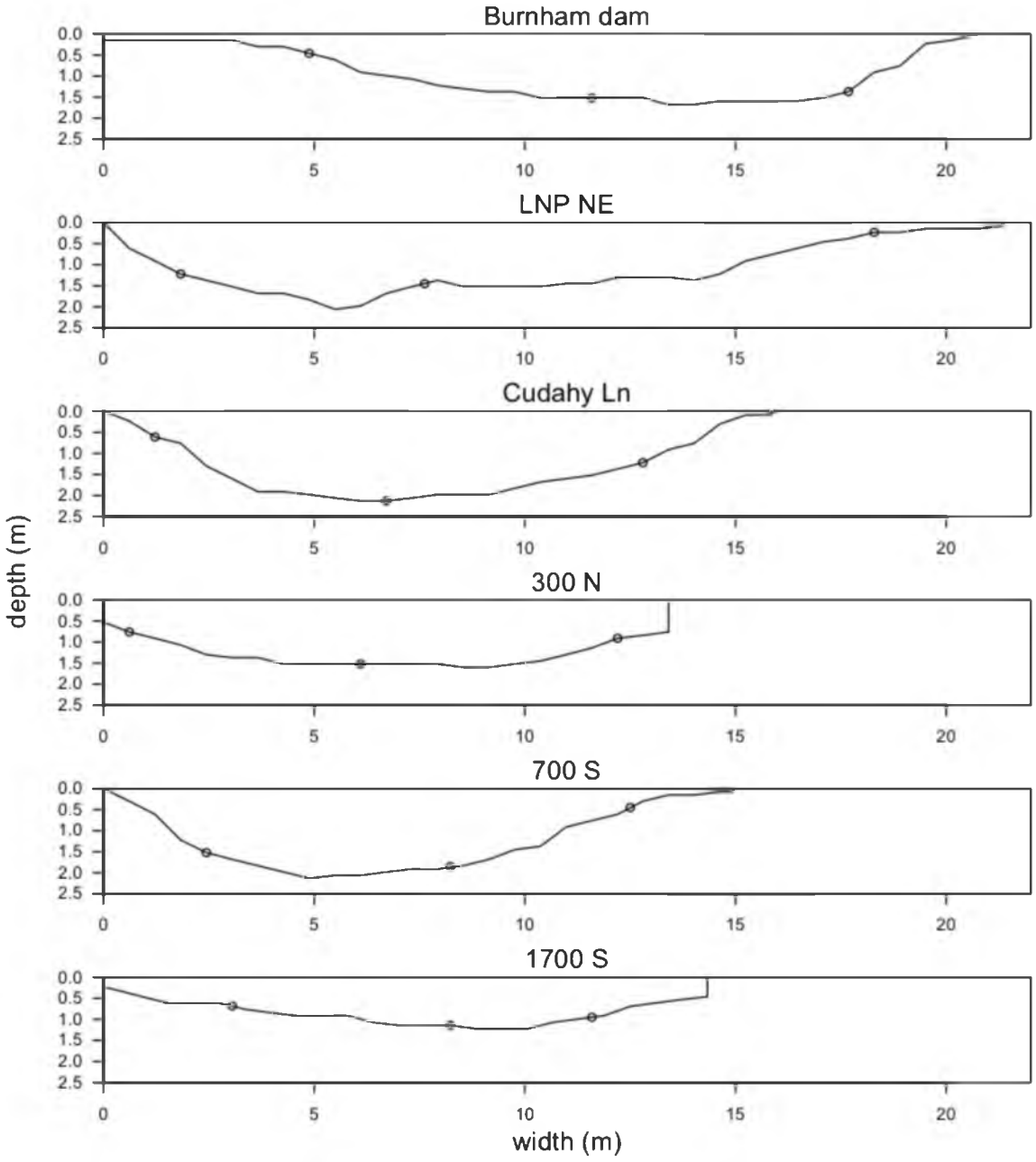

Fig. 76. Lower Jordan River cross sections and sediment sampling locations
Note: circles identify sediment sampling locations

Table 31. Site bathymetry and hydraulics

	mean depth (m)	width (m)	area (m^2)	flow* (cfs)	flow velocity (cm/sec)
Burnham Dam	1.0	21.0	18	235	37
LNP NE	1.2	21.0	20	240	34
Cudahy Ln	1.5	15.4	22	240	30
300 N	1.3	13.6	13	240	53
700 S	1.3	15.1	21	190	26
1700 S	0.9	14.5	19	165	24

*Mean annual daily flow = 250 cfs, 500 N (Salt Lake County gauge 960)
*Mean annual daily flow = 130 cfs, 1700 S (USGS gauge 10171000)

Table 32. Lower Jordan River hydraulic reach lengths, widths and depths

	length (m)	width (m)	% area of LJR	depth (m)
Reach 1	9000	20	46	1.5
Reach 2	7250	15	25	1.2
Reach 3	7250	15	29	1

Note: TMDL lengths (Table 1.1), measured widths
Note: Burnham to Burton dam section omitted from R1
Note: field measured depths

Table 33. Upper Jordan River hydraulic reach lengths and widths

	length (m)	width (m)	% area of UJR	depth (m)
Reach 4	14,150	19	25	0.8
Reach 5	2,750	17	5	0.8
Reach 6	18,000	15	32	0.5
Reach 7	6,750	11	12	0.3
Reach 8	15,450	38	27	1.2

Note: TMDL lengths (Table 1.1), Google Earth widths

Table 34. OM load estimates to and in the LJR

LJR annual SOD and BOD calculated OM decay loads (kg dry OM/year)				
	Reach 1	Reach 2	Reach 3	LJR
BOD_1	88,452	38,329	36,855	163,636
SOD	98,280	47,912	46,069	192,260
total	186,732	86,241	82,924	355,896

$BOD_1 = WC_{dark}$
used glucose equivalents to back calculate OM load
assumed BOD of 1.2 mg/L/d
assumed SOD = 2, 1.8, 1.5 for R1, R2, R3
$C_6H_{12}O_6 + 6O_2 = 6CO_2 + 6H_2O$
0.375 g-C/g DO
2 g-OM/g C
kg OM/year = (kg DO/day)*(12 kg C/32 kg DO)*(2 kg OM/kg C)*(364 d/yr)

5.7.3 NDM chamber OM production estimate

Using the seasonal average chamber NDM for the three sites in the UJR, a steady state annual OM load can be estimated using the following relationship:

$$\frac{kg\ dry\ OM}{yr} = NDM\left(\frac{g\ C}{2.67\ g\ O_2}\right)\left(\frac{g\ OM}{g\ C}\right)\left(\frac{365\ d}{yr}\right)\left(\frac{kg}{1000\ g}\right) * l * w \qquad (25)$$

$l = \ length\ of\ river\ (m)$
$w = \ average\ width\ of\ river\ (m)$

The instream production of OM based on the average UJR chamber derived NDM of 3 g-DO/m^2/d would produce roughly 540,000 kg dry OM/year (Table 35). This could account for 44% of the 1,221,491 kg OM/year estimated to enter the LJR at the Surplus Canal diversion (Utah DWQ 2013, Table 2.6, row A[1]).

The Surplus Canal diversion channels up to 90% of the annual stream flow from the LJR, but the majority of this water is diverted during spring runoff and base flow diversions are typically 50%. If 50% of the OM produced in the UJR entered the LJR

Table 35. UJR instream OM loads from primary production

kg OM/yr (chamber NDM)	
Reach 4	220,517
Reach 5	38,346
Reach 6	221,461
Reach 7	60,902
UJR total	541,225

during the 9 months of baseflow and the spring snowmelt is ignored, then 203,000 kg/yr of dry OM enters the LJR as macrophyte stocks, detached periphyton (metaphyton), and phytoplankton produced in the UJR. This would account for 17% of the OM load estimated to enter the LJR at the Surplus Canal diversion (Utah DWQ 2013, Table 3.9 upstream loads).

It should be noted that the Surplus Canal is an overflow weir and the LJR has an underflow dam design to direct additional flows associated with storm events and spring runoff down the Surplus Canal, not the LJR. The difference in dam design results in bedload CPOM entering the LJR, not the Surplus Canal. Therefore, if the remnants of yesterdays upstream primary production are transported downstream as bedload CPOM, not suspended sestonic matter, then the amount of OM entering the LJR will be higher than predicted with a 50% dilution based solely on streamflow diversions.

5.7.4 GW adjusted single-station OM production estimate

Upper Jordan River hydraulic reach based dry OM loads associated with primary production (PP) using the NDM estimated from the single-station diurnal DO model adjusted for GW having a DO concentration of 1 mg-DO/L are shown in Table 36. Instream contributions could account for 41% of the 1,221,491 kg OM/yr loading estimate to the UJR (Utah DWQ 2013, Table 2.6, row A[1]).

Table 36. UJR GW adjusted OM production load estimate

	kg OM/yr (single-station GW adj. NDM)	
	avg NDM (g DO/m^2/d)	kg dry OM/yr
Reach 4	3.5	256,380
Reach 5	2.2	28,471
Reach 6	1.8	135,393
Reach 7	3.8	77,399
UJR total		497,644

NDM*(g C/2.67 g O)*(2 g OM/g C)*(365 d/yr)*length*width*(kg/1000 g)

5.7.5 Sediment column OM standing stock (Spring 2012)

Table 37 provides aerial depth integrated river-wide standing stock OM estimates. This table is cumulative; therefore the 10 cm depth includes OM present in the sediments at 0–2 and 5 cm depths. The $OM_{aerial,sum}$ is the dry mass of OM present in the wet sediments at each depth per square meter. The $OM_{aer,stretch,sum}$ and $CPOM_{aer,stretch,sum}$ represent the amount of dry OM and CPOM found in the river stretches defined in Table 32.

The surface sediments had similar OM standing stocks during the Spring of 2012. The lowest 0–2 cm OM standing stocks were found in the sandy surface sediments of LNP NE and 700 S following the 2011 UJR high water event. The amount of OM present at 5 cm and 10 cm depths steadily increased with distance downstream from the Surplus Canal diversion. The mass of OM in the top 10 cm doubled between 700 S and LNP NE, consistent with observed ambient DO deficits.

Table 38 provides Reach based sediment OM estimates for the top 10 cm of the sediment column calculated using the values found in Table 32. These values can be used to describe the existing stockpiles of sediment OM in the LJR.

Table 37. Site and river stretch sediment OM standing stocks

	River-wide mean OM standing stock (depth cumulative)			
	depth (cm)	$OM_{aerial,sum}$	$OM_{aer,stretch,sum}$	$CPOM_{aer,stretch,sum}$
Burnham	0–2	71	3,953	133
	5	338	18,832	1,304
	10	576	32,118	1,857
LNP NE	0–2	42	1,902	216
	5	324	14,757	2,572
	10	580	26,474	5,580
Cudahy	0–2	66	5,016	1,256
	5	263	19,895	3,904
	10	470	35,535	6,568
300 N	0–2	61	5,245	2,182
	5	190	16,217	4,176
	10	314	26,776	5,963
700 S	0–2	43	2,179	885
	5	140	7,157	2,953
	10	271	13,815	4,587
1700 S	0–2	63	2,410	818

$OM_{aerial,sum}$ = g-OM/m^2/summed depth
$OM_{aer,stretch,sum}$ = Kg OM/river stretch/summed depth
$CPOM_{aer,stretch,sum}$ = Kg CPOM/river stretch/summed depth

Table 38. Reach based sediment OM standing stocks

$OM_{aerial,reach,summed}$ (kg dry OM, depth summed)				
depth	Reach 1	Reach 2	Reach 3	LJR OM
0-2	107,378	59,917	59,229	226,525
5	554,725	185,273	157,817	897,814
10	976,009	305,905	304,609	1,586,523

5.7.6 Riparian vegetation autumn leaf litter load estimate

Slow and fast leaf decay rates range from 0.5% to 1.5% of the mass per day (Cummins 1974; Sedell et al. 1974). This would require 1.25 years to degrade 90% of the mass of a slowly degrading leaf and 5 months for a rapidly degraded specie.

A crude estimate for fall leaf litter loads associated with riparian vegetation abutting the LJR is provided in Table 39. Based on aerial photography, the percent of the length of the LJR abutted by leaf shedding trees was visually estimated for all three hydraulic reaches. The trees are assumed to extend 3 meters over the river on both the east and west banks. The trees are assumed to drop a conservatively high 400 g-OM/m^2/yr during the fall leaf shedding and all leafs falling into the river settle to the sediments (Benfield 1997). For comparison, average annual riparian litterfall in the wet maritime climate of the Puget Sound, WA, was between 350–400 g-OM/m^2/yr (Roberts and Bibly 2009). In addition, it is assumed that 50% of the leaf litter that falls 3 meters onto land will laterally deposit in the river due to wind.

Table 39. Riparian leaf litter contribution to SOD estimate

	LJR Riparian vegetation leaf litter load estimate		
	% length	load (kg OM//yr)	SOD cycle (d)
Reach 1	10	3,240	12
Reach 2	35	8,190	62
Reach 3	30	8,100	64
total	24	19,530	37

% length = visual estimate of riparian vegetation
riparian vegetation estimated must drop leafs to be considered
load = fall leaf litter load, assume 400 g-OM/m^2/yr (Benfield 1997)
assume tree cover extends 3 m over river and all leafs enter river, both sides
assume 50% of leaf litter falling 3m into the riparian zone enters river
SOD cycle = days to oxidize leaf litter in sediments

Reach 1 is devoid of trees due to the alkaline soils associated with the flood plains of the Great Salt Lake, leading to a low percent length (% length) of the river abutted by riparian vegetation. If the leaf litter were evenly distributed over the sediments in each hydraulic reach and were completely oxidized at measured SOD fluxes, then the days required to oxidize riparian leaf litter in the sediments are provided in the last column of Table 39 as the "SOD cycle." These assumptions allow a comparison of riparian OM loads to the LJR and measured SOD decomposition rates.

Riparian vegetation litterfall would be degraded and oxidized to CO_2 in only 12 days in Reach 1. It takes an estimated 60 days for the sediments in Reaches 2 and 3 to cycle riparian leaf litter under these assumptions. When the full 19,530 kg dry OM is distributed evenly in the LJR, the sediments cycle the carbon in 37 days. 37 days is only 1/10 of a year, highlighting the reality of external and upstream OM loads degrading WQ in the urban LJR.

Low order pristine streams with a forest canopy have been shown to receive over 44% of the annual OM load as direct leaf litter (Fisher and Likens 1973). Although riparian leaf litter does add OM to the LJR, it is less than 2% of the estimated TMDL load to the LJR per the aforementioned assumptions.

The litterfall estimate accounts for 9% of the 0–2 cm sediment standing stock of OM measured during the Spring of 2012. Limiting riparian vegetation should not be viewed as a positive influence in urban WQ due to the meager OM load generated. The role of riparian habitat in providing shade and structure far outweigh the negative effects of the OM load associated with the urban riparian zone (Gregory et al. 1991).

5.7.7 OM loading and turnover estimate for the LJR

Fig. 77 shows the various types of OM observed in the LJR at different depths in the water column. In a lotic system, OM will settle, move downstream, break apart, and decay at different rates.

Table 40 provides a mass balance for OM in the LJR comparing data collected by the Utah DWQ and this research (Utah DWQ 2013). The rationale is that all OM that enters the LJR is either oxidized in the water column (WC_{dark}), remains suspended, and exits the LJR at Burnham Dam (VSS at Burnham), or settles to the bottom where it is either oxidized as SOD or accumulates as %VS. "BOD_1+SOD" was estimated in Section 5.7.2. "0–2 cm sediment VS" was the standing stock of sediment OM measured in the LJR during the Spring of 2012 and was estimated in Section 5.7.5. "NPDOC at Burnham" dam was calculated assuming 5 mg-C/L, a value typically measured in the LJR during this research (data not shown). "VSS at Burnham" dam is the mass of suspended dry OM that exits the LJR and was calculated assuming a volatile suspended solids (VSS) concentration of 8 mg VSS/L (Utah DWQ 2013, Fig. 3.2).

The "Utah DWQ" parameter is the TMDL estimated OM loads to the LJR (Utah DWQ 2013, Table 3.9). The "% unaccounted" is the percentage of the Utah DWQ estimate not accounted for in relation to the "measured total." The "forced total" parameter includes the OM found in the top 0–5 cm of the sediment column.

The parameters missing from this estimate include bedload CPOM, LWD, and the accumulation of sediment OM present in the backwaters of flow control structures. 49% of the "measured total" was associated with instream degradation processes (BOD_1+SOD), and 20% was associated with suspended VSS transported downstream

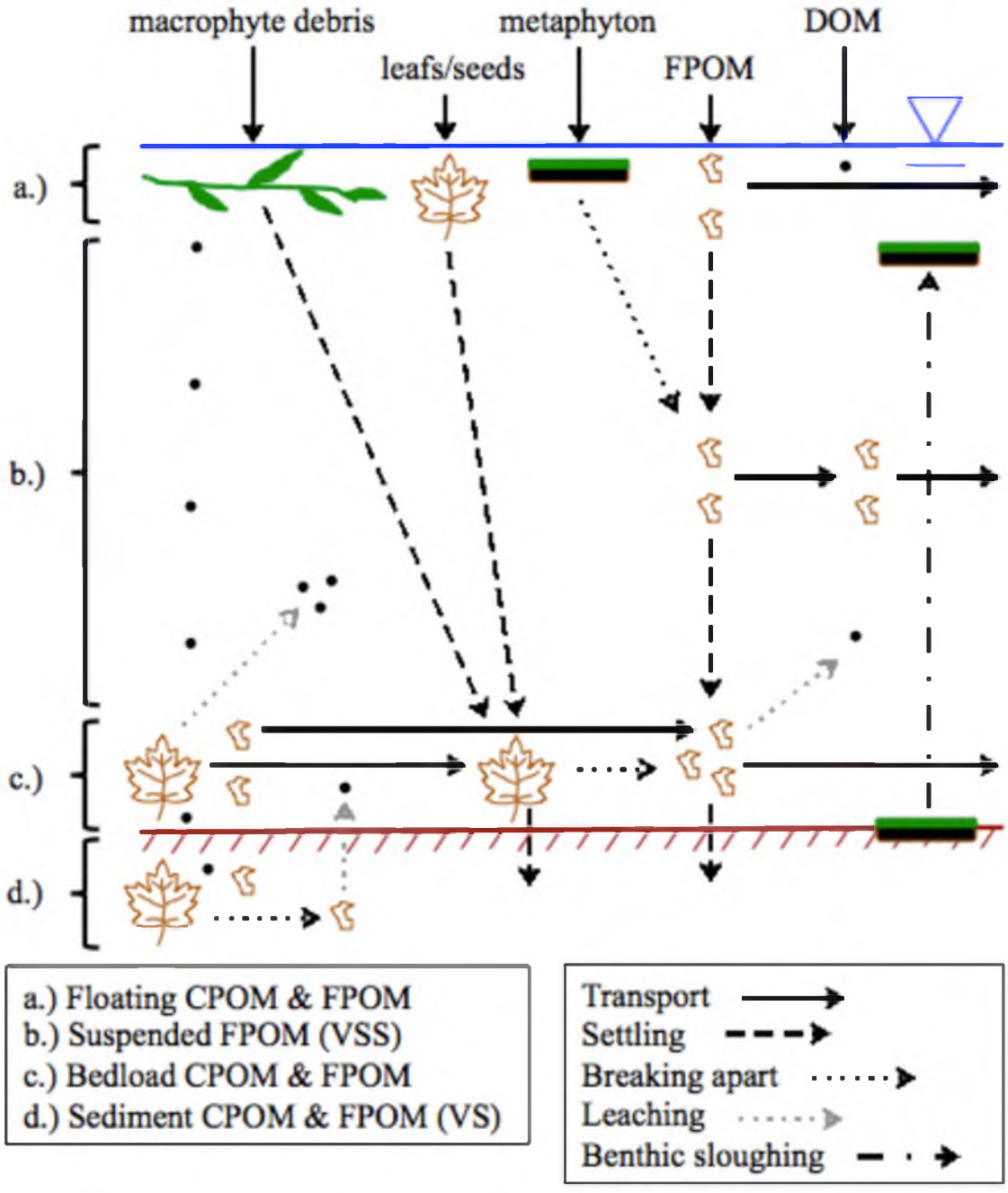

Fig. 77. OM loading schematic for mass balance

Table 40. OM load estimates to and within the LJR

LJR OM budget (kg dry OM/year)		Note:
BOD_1 + SOD	355,896	
0–2 cm sediment VS	226,525	a.
NPDOC at Burnham	176,601	b.
VSS at Burnham	141,281	c.
measured total	900,303	
Utah DWQ	2,225,523	d.
% unaccounted	60%	
Utah DWQ	1,004,031	e.
% unaccounted	10%	
forced total	1,394,992	f. and g.
% unaccounted	14%	

Notes:
a.) may be twice as high depending on time of year and other factors
b.) (5 g-C/m^3)(2 g-OM/g C)(200 cfs)(0.028 m^3/ft^3)(3153600 sec/yr)(kg/1000 g)
c.) (8 g VSS/m^3)(200 cfs)(0.028 m^3/ft^3)(3153600 sec/yr)(kg/1000 g)
d.) UJR and LJR loads
e.) LJR loads
f.) assumes top 5 cm of sediment contribute VS
g.) LJR load and 1/2 UJR load

into State Canal. The remaining 31% of the "measured total" was associated with surface sediment OM. 60% of the Upper and Lower Jordan River Utah DWQ OM load estimate is unaccounted for in relation to the "measured total." This large discrepancy may be attributed to the exclusion of OM associated with large woody debris (doubtful), bedload CPOM, and areas of extreme deposition. Another possibility is that the active sediment layer contributing to SOD and OM retention is deeper than 2 cm.

14% of the Utah DWQ organic load is missing when the UJR OM load is reduced by 50% and OM present in the top 0–5 cm are included in the standing stock of sediment OM. SOD would require 1.2 years to oxidize OM found in the top 0–2 cm of the

sediment column in this scenario, suggesting that OM is accumulating in the sediments, which is occurring, as shown by the presence of OM at depths greater than 5 cm (Fig. 60).

Fig. 78 provides a mass balance for the OM loading estimate. The red, green, and, black arrows represent loadings to the LJR, transport out of the system, and instream decay, respectively. Positive values mean OM is being added and negative values

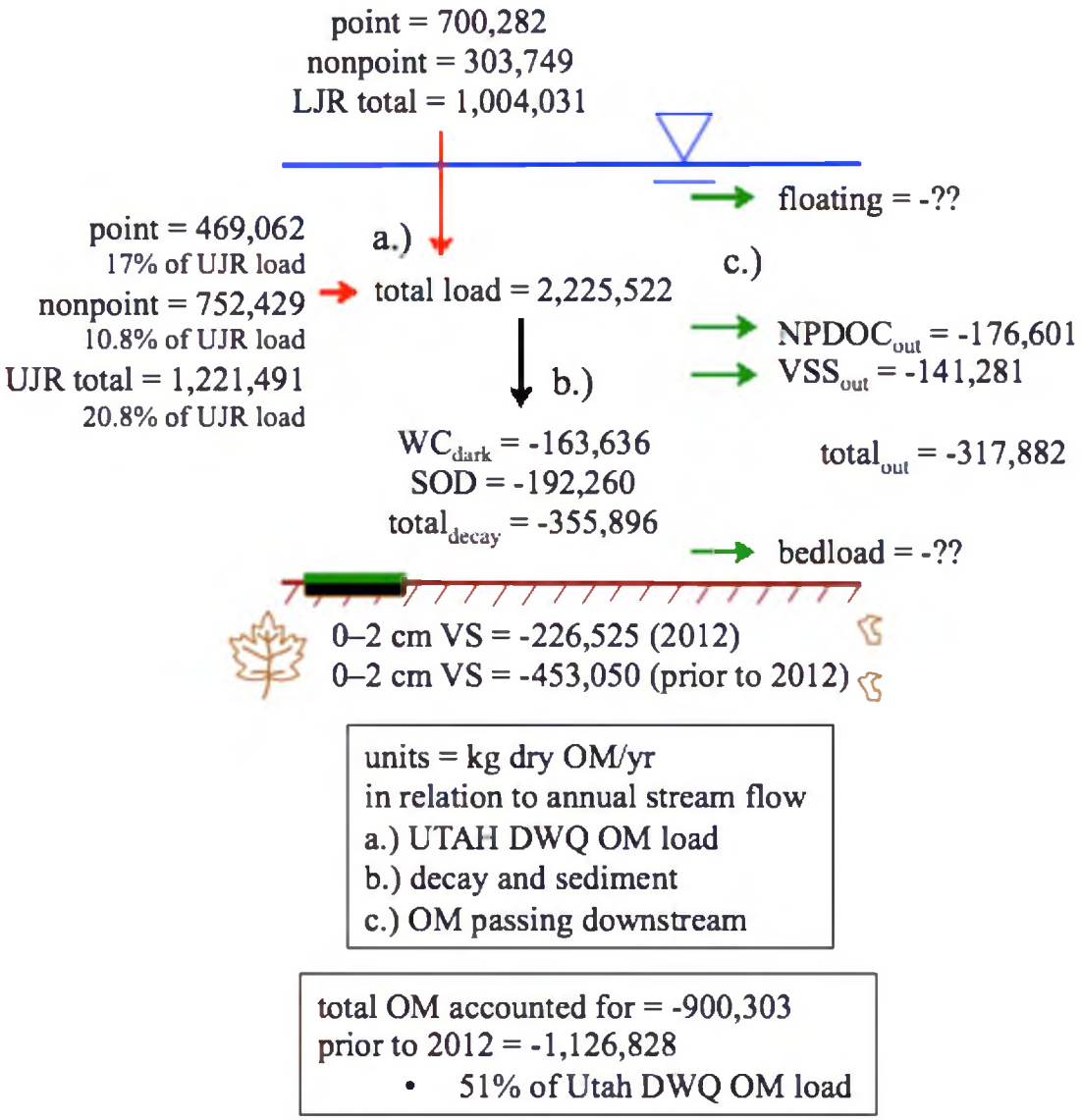

Figure 78. OM loading schematic for mass balance

represent OM losses.

The annual UJR chamber NDM OM production estimate was roughly 546,600 kg dry OM/year. This estimate would account for 57% of the Utah DWQ OM load in the UJR being a result of instream primary production with the benthos being the predominate source of primary production compared to phytoplankton. The annual UJR NDM OM estimated using the single-station diurnal DO model adjusted for GW resulted in a load of 286,400 kg dry OM/year, or 30% of the Utah DWQ UJR annual OM load. Although these estimates differ, the range of instream OM associated with photosynthesis ranges between 30–57% of the current estimated OM load to the UJR. Either way, the UJR River is a significant source of OM to the LJR as a result of eutrophication.

5.7.8 Sediment vs. POTW nutrient load comparison

Table 41 provides annual ammonium and orthophosphate loads to the Jordan River from POTW effluent calculated using average discharge concentrations and flow rates. Table 42 shows the percentage of the ambient dissolved nutrients in the LJR water column resulting from sediment OM decay compared to POTW discharges. The first column compares the LJR sediment load and the South Davis-S WWTP discharge in Reach 1. The sediments in the LJR are responsible of 36% and 43% of the ambient dissolved nutrients when the upstream WWTP discharges are ignored. The internal cycling of nutrients between the sediments and WC accounted for 28% and 21% of the total loads of the total N and P to the St. Johns River (Malecki et al. 2004).

The relatively low flow (3 MGD vs. 30+ MGD) of South Davis-S (SD-S) WWTP is the reason why the sediments are responsible for over 1/3 ambient dissolved nutrients in the LJR under this scenario. In reality, nutrients associated with POTW discharges are

Table 41. Nutrient loads associated with POTW discharges

WWTP nutrient loading (kg/year)			discharge (mg/L)		flow
	NH_4-N	PO_4-P	NH_4-N	PO_4-P	MGD
SD-S WWTP	21,840	6,552	5	1.5	3
CVWRF	128,419	228,301	1.8	3.2	49
SVWRF	83,866	135,117	1.8	2.9	32
Total	234,125	369,970			

Table 42. Sediment nutrient and POTW load comparison

% of sediment nutrient load vs. WWTP load			
	SD-S WWTP	SD-S + 1/2 CVWRF	all 3 POTWs
NH_4-N	36	12	5
PO_4-P	43	4	1

Note: % = sed. load/(sed. load + WWTP load)

already present in the WC at the start of the Lower Jordan River. To account for this, the second column includes South Davis-S and 50% of the effluent from CVWRF since the other 50% is assumed to be diverted down Surplus Canal during base flow conditions. In this scenario 12% and 4% of the ambient ammonium and phosphate were a result of OM decay in the sediments. The final column compares the sediments in the LJR to the annual nutrient loads associated with all three of the POTWs. In this scenario only 5% and 1% of the ambient nutrients were a result of sediment OM decay. The sediments are a source of the macronutrients N and P, but the contribution associated with POTW loads is much greater in the Jordan River.

CHAPTER 6

CONCLUSIONS

The key conclusions and linkages from the results of this research are provided in Fig. 79. The following descriptions summarize the five main research topics in terms of the relationship to the other topics and are presented in a clockwise fashion.

SOD in the Jordan River is a result of the oxidation of OM. Positive ammonium and orthophosphate sediment fluxes indicate OM decay, and the associated ammonia load will create a future NBOD demand in the water column during biological nitrification. Surficial sediment %VS was a reliable surrogate to estimate SOD in the silty sediments of the LJR, and 50% of the volatile matter was present as organic carbon. Roughly 1/3 of the surficial sediment OM found in Reaches 2 and 3 were present as CPOM, suggesting leaf litter associated with riparian vegetation and a terrestrial load associated with urban stormwater. Methane production in the surficial sediments could account for 50% of the observed SOD. The autotrophic NDM of the UJR may contribute up to 55% of the OM estimated by the Utah DWQ to enter the UJR (Utah DWQ 2013). This upstream OM load associated with eutrophication contributes to the DO deficits in the LJR.

Sediment ammonia and orthophosphate fluxes were positively related to sediment OM, while nitrate fluxes were inversely related to sediment OM due to denitrification. Dissolved ammonia and phosphorus fluxes were also positively related to methane fluxes. The strongest correlation between sediment methane and nutrient fluxes was

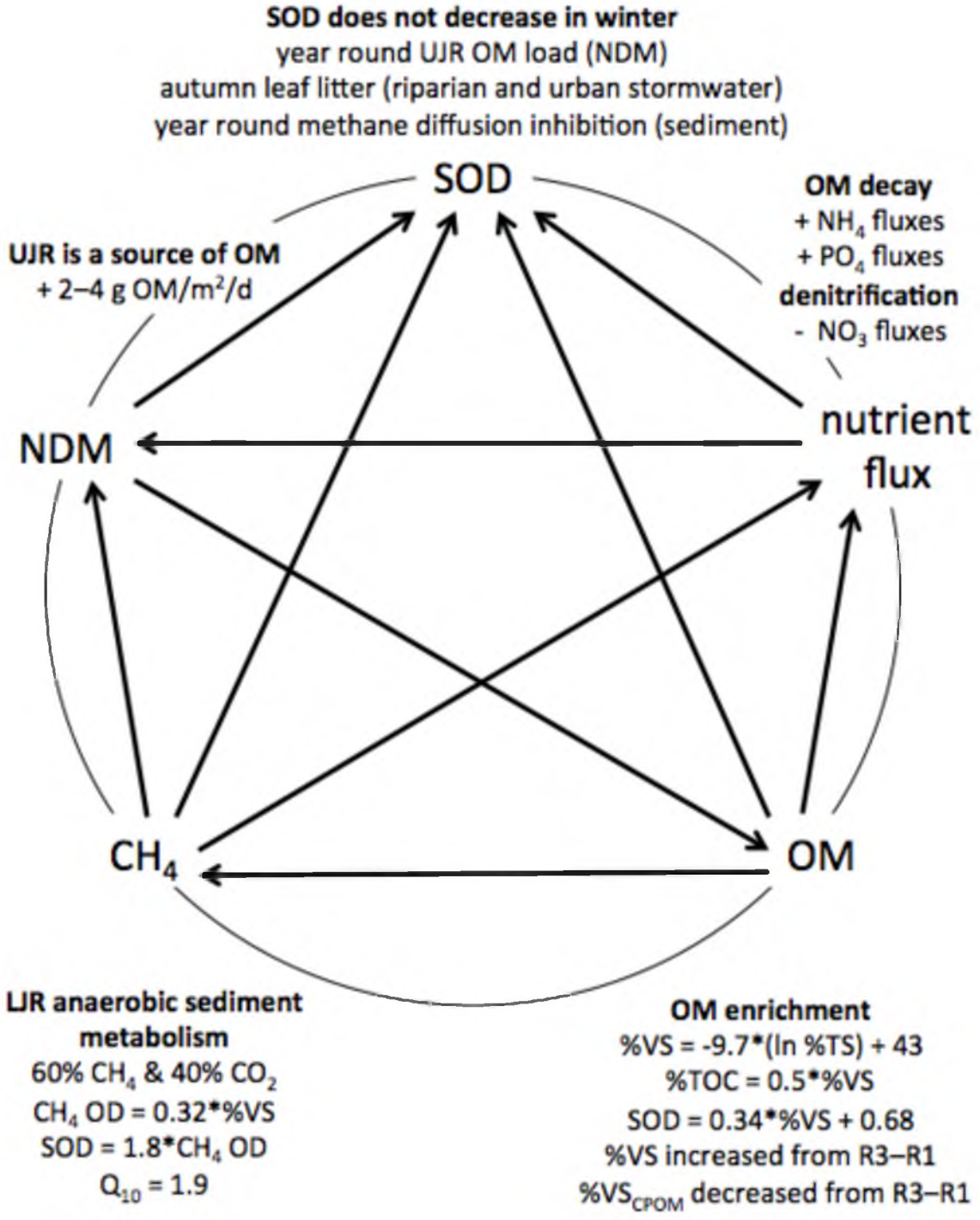

Fig. 79. Research linkages and key observations

denitrification, where denitrification fluxes were similar to the stoichiometric methane fluxes required to support the observed denitrification rates.

Sediment methane fluxes were positively related to sediment OM, and the swamp gas produced was roughly 60% methane and 40% carbon dioxide. Sediment methanogenesis was inversely related to ambient water temperature, unlike SOD and NDM.

In general, NDM was inversely related to positive ammonia, orthophosphate, and methane fluxes in the LJR. The UJR maintained a positive annual NDM, even upstream of WWTP discharges where ambient nutrient concentrations are the lowest in the river, yet high enough to support phototrophic growth. This implies that nonpoint sources, Utah Lake, and groundwater are providing ample nutrient loads to support eutrophication in the UJR.

Provided below are the objectives for this research and a list of observations and conclusions:

Objective 1: Measure seasonal SOD at locations representative of reach based sediment characteristics, downstream and upstream of wastewater and stormwater discharge points, and in other local surface waters.

- SOD fluxes increased with distance downstream in Reaches 3 to 1 (R_3 = -1.5, R_2 = -1.9, and R_3 = -2.3 g-DO/m^2/day).
- Reach 1 SOD fluxes suggest polluted sediments in regards to OM enrichment.
- The sediments were responsible for over 50% of the ambient DO deficit in the LJR during summer months during the majority of the sampling events

and over 75% of the DO deficit during more than half of the sampling events.

- SOD decreased for 1 year throughout the LJR following an influx of inorganic sediments associated with upstream erosion resulting from the unusually large snowpack in the Wasatch Mountains in the winter of 2010–2011.
- SOD fluxes did not decrease during the cold winter temperatures, but water column respiration (WC_{dark}) rates decreased.
- The upstream Utah Lake's water column was more active in terms of ambient lake dark metabolism compared to the sediments, implying that Utah Lake is a source of phytoplankton and sestonic OM to the downstream Jordan River.
- The downstream State Canal had the highest SOD fluxes measured (-6 to -8 g-DO/m^2/d), implying that the sediments downstream of the DO impaired LJR are increasingly enriched with OM along a gradient driven by topography

Objective 2: Evaluate the flux and fate of nutrients as they interact with the sediments and water column using SOD chambers during in situ conditions and after manipulating chamber DO and pH.

- During ambient dark conditions, the LJR sediments released ammonia and orthophosphate at average fluxes of 0.08 g-N/m^2/d and 0.05 g-P/m^2/d as a result of OM decay. The sediments removed nitrate at a flux of -0.2 g-N/m^2/d due to denitrification at the sediment–water interface.

- The WC produced nitrate at an average rate of 0.53 g-N/m^3/d during ambient conditions (WC nitrification).
- Anoxic conditions increased sediment ammonia and denitrification fluxes by roughly 10% and 3%, respectively. Phosphorus fluxes tended to decrease under anoxic conditions.
- Lowering pH from 8 to 7 units resulted in an additional PO_4-P sediment flux of 0.055 g-P/m^2/d.
- The sediments are a source of macronutrients in the LJR and will continue to be for some time due to OM decay.

Objective 3: Evaluate the contribution of primary production to DO dynamics and organic carbon fixation using transparent SOD chambers and diurnal ambient water quality data.

- The benthos were responsible for the majority of stream respiration and primary production (65% of light and dark metabolism).
- The UJR is a year round source of instream produced OM at a NDM flux between 2–4 g-DO/m^2/d (chamber measured).
- The single-station diurnal DO NDM model predicted autotrophic conditions in the UJR after adjusting for low DO groundwater intrusion (NDM = 1–4 g-DO/m^2/d in the UJR).
- 30–57% of the estimated Utah DWQ UJR OM load is a result of instream primary production (546,638 kg OM/year). A portion of this OM is a direct result of eutrophication.

Objective 4: Obtain sediment core samples at locations selected for SOD studies

and quantify the bulk sediments and fine/coarse particulate organic matters in terms of %TOC, %TS, and %VS to establish correlations between SOD and these parameters.

- %VS is a great surrogate for sediment OM in the LJR and 50% of the %VS is organic carbon (%TOC = 0.502 * %VS), whereas 37% of the %VS in the upstream Utah Lake is organic carbon.
- The surface sediments had a higher water content compared to the more compact subsurface sediments.
- 0–10 cm sediment column OM standing stocks increased from Reach 3 to 1.
- 0–10 cm sediment column $\%VS_{CPOM}$ decreased from Reach 3 to 1, suggesting CPOM may be from stormwater (FPOM sources are inconclusive since it may be degraded CPOM).
- Over 33% of the OM found in the surface sediments of Reaches 2 and 3 were CPOM.
- Surface sediment %VS is a practical surrogate for estimating SOD without chambers in the LJR (SOD = 0.34 * %VS + 0.68).

Objective 5: Evaluate methane fluxes from the sediments in the Lower Jordan River.

- Sediment gas composition was 60% CH_4 and 40% CO_2.
- The surface sediments (0–2 cm) produced the most methane compared to deeper sediment depths (5, 10, 15, and 20 cm).
- Methane production was positively related to surface sediment OM (CH_4 OD = 0.32 * $\%VS_{bulk}$).

- Sediment methanogenesis had a Q_{10} of 1.9.
- Methane fluxes from the top 0–2 cm of the sediment column could account for 56% of the observed SOD (SOD = 1.8 * CH_4 OD).
- Denitrification at the sediment–water interface was related to methane fluxes (1 mole of nitrate reduced for every 0.8 moles of methane).

APPENDIX A

SOD AND WC_{dark} DATA TABLES

Table 43. SOD measurements (a)

site	date	SOD_1	SOD_2	SOD_{avg}
State Canal	2/6/13	-5	-8.13	-6.57
Burnham	9/10/11	-1.32	-1.72	-1.52
Burnham	6/12/12	-1.02		-1.02
Burnham	6/14/13	-1.90	-4.80	-3.35
LNP NE	7/3/09	-4.17	-1.68	-2.93
LNP NE	10/10/09	-1.61	-1.71	-1.66
LNP NE	10/16/12	-1.77	-2.16	-1.97
LNP NE	1/9/10	-3.46	-2.6	-3.03
LNP NE	6/3/10	-2.67	-2.72	-2.70
LNP NE	7/16/10	-3.37		-3.37
LNP NE	8/24/10	-1.65		-1.65
LNP NE	12/25/10	-2.04	-2.88	-2.46
LNP NE	9/12/11	-1.63	-2.01	-1.82
LNP NE	4/3/12	-0.64	-1.15	-0.90
LNP NE	6/15/12	-1.78	-1.62	-1.70
LNP NE	6/15/13	-1.50		-1.50
LNP SW	7/3/09	-3.33	-2.5	-2.92
LNP Upper-N	8/25/09	-2.27	-2.11	-2.19
Cudahy Ln	10/10/09	-1.99	-2.38	-2.19
Cudahy Ln	1/16/10	-2.27	-2.8	-2.54
Cudahy Ln	6/3/10	-3.54	-3.04	-3.29
Cudahy Ln	6/13/12	-1.23	-1.92	-1.58
Cudahy Ln	6/13/13	-2.42	-4.17	-3.30
1700 N	9/14/11	-1.88	-2.24	-2.06
DWQ	6/29/09	-1.55	-1.84	-1.70
DWQ	1/17/10	-1.15	-1.15	-1.15
DWQ	6/7/10	-2.83	-3.53	-3.18
DWQ	7/15/10	-1.84		-1.84
DWQ	8/31/10	-4.15	-1.12	-2.64
DWQ	1/6/11	-1.14	-2.05	-1.60
DWQ	2/8/12	-0.78	-0.72	-0.75
DWQ	4/14/12	-0.73	-1.72	-1.23
300 N	6/12/13	-2.02	-2.65	-2.34
700 S	6/14/12	-1.1	-1.54	-1.32
700 S	6/10/13	-1.25	-1.78	-1.51

Note: g $DO/m^2/day$

Table 44. SOD measurements (b)

site	date	SOD_1	SOD_2	SOD_{avg}
900 S-N	6/26/09	-1.88	-0.69	-1.29
900 S-N	1/14/10	-2.11	-1.98	-2.05
900 S-N	6/8/10	-1.66		-1.66
900 S-S	6/26/09	-1.1	-1.96	-1.53
900 S-S	1/14/10	-1.02	-0.82	-0.92
900 S-S	6/8/10	-1.05	-0.79	-0.92
1300 S	9/13/11	-2.26		-2.26
1700 S-N	6/25/09	-1.05		-1.05
1700 S-N	6/26/09	-0.72	-0.49	-0.61
1700 S-N	7/8/09	-0.92	-0.75	-0.84
1700 S-N	1/10/10	-1.02	-1.88	-1.45
1700 S-N	5/24/10	-1.52	-2.12	-1.82
1700 S-N	9/15/11	-1.68	-1.8	-1.74
1700 S-N	4/16/12	-3.4	-3.16	-3.28
1700 S-N	6/10/13	-2.05	-3.28	-2.66
1700 S-S	7/14/10	-1		-1.00
1700 S-S	1/3/11	-0.63	-1.58	-1.11
2100 S	8/25/10	-1.09		-1.09
2100 S	1/7/11	-1.25	-2.14	-1.70
2300 S	7/7/09	-1.44	-1.08	-1.26
2300 S	1/17/10	-3.56	-3.66	-3.61
2600 S	6/2/10	-4.69		-4.69
2780 S-E	8/25/09	-1.85	-1.35	-1.60
2780 S-E	1/23/10	-5.07	-2.11	-3.59
2780 S-W	8/25/09	-2.42	-3.5	-2.96
2780 S-W	1/23/10	-2.5		-2.50
3600 S	8/26/09	-1.3	-0.64	-0.97
5400 S	7/16/09	-3.06	-1.67	-2.37
5400 S	1/12/10	-3.38	-2.66	-3.02
5400 S	7/19/10	-2.65		-2.65
5400 S	9/2/10	-0.11	-8.32	-4.22
5400 S	1/12/11	-2.16	-5.44	-3.80
7600 S	7/20/10	-6.69		-6.69
7600 S	9/1/10	-1.49	-0.66	-1.08
7600 S	1/15/11	-3.02	-5.37	-4.20
7800 S	7/16/09	-2.51	-0.2	-1.36
7800 S	1/12/10	-1.19		-1.19

Note: g $DO/m^2/day$

Table 45. SOD measurements (c)

site	date	SOD_1	SOD_2	SOD_{avg}
9000 S	7/16/09	-2.65		-2.65
9000 S	1/16/10	-0.99	-0.79	-0.89
9000 S	7/21/10	-0.82		-0.82
9000 S	9/3/10	-1.98	-0.85	-1.42
9000 S	1/20/11	-1.36		-1.36
SR-154	7/19/09	-2.44	-1.09	-1.77
14600 S	7/17/09	-1.67	-2.13	-1.90
US-73	7/17/09	-2.43	-1.94	-2.19
US-73	1/24/10	-0.49	-1.16	-0.83

Note: g $DO/m^2/day$

Table 46. SOD measurements (Utah Lake)

site	date	SOD_1	SOD_2	SOD_{avg}
Ut LK outlet	9/30/11	-1	-0.9	-0.95
Provo Bay	9/14/10		-5.21	-5.21
Geneva Steel	9/24/10	-2.09	-2.49	-2.29
Outside marina	8/2/12	-1.42	-1.19	-1.31
Goshen Bay	8/3/12	-1.42	-1.41	-1.42
Provo Bay entrance	8/3/12	-1.54	-1.12	-1.33
Goshen Bay entrance	8/4/12	-0.65	-1.06	-0.86
Pelican Point	8/4/12		-1.97	-1.97

Note: g $DO/m^2/day$

Table 47. WC_{dark} oxygen demand measurements

	WC_{dark} (g/m^3/day) or (mg/L/day)								
	Summer 2009	Jan. 2010	Jun. 2010	July 2010	Aug. 2010	Jan. 2011	Sept. 2011	June 2102	June 2103
Burnham							-0.58	-0.89	-0.49
LNP NE	-0.64	0	0	-0.96	-0.90	-0.92	-1.27	-0.78	-0.86
LNP SW	-0.11								
Cudahy	-0.57	0	-0.08					-0.73	-0.71
1700 N							-0.86		
300 N	0	0	0	-0.63	-1.31	0		0.00	-0.11
700 S								-1.70	-0.72
900 S-N	-0.87	0	-0.42						
900 S-S	-0.42	0	0						
1300 S							-0.30		
1700 S	-1.02	0	0	-0.92	-1.95	-0.96	-1.32	-0.89	-0.88
2100 S				-1.31	-2.62	-2.66			
2300 S	-0.30	0							
2600 S			-1.43						
2780 S-E	-0.87	0							
2780 S-W	0	0							
3600 S	-2.30								
5400 S	-3.88	-0.30		-1.57	-1.57	-0.70			
7600 S				-1.57	-0.22	-0.48			
7800 S	-2.60	0							
9000 S	-4.19	0		-1.35	-2.14	-0.09			
SR-154	-2.60								
US-73	-1.17	0							

APPENDIX B

DIURNAL DO PROFILES FOR SINGLE-STATION NDM

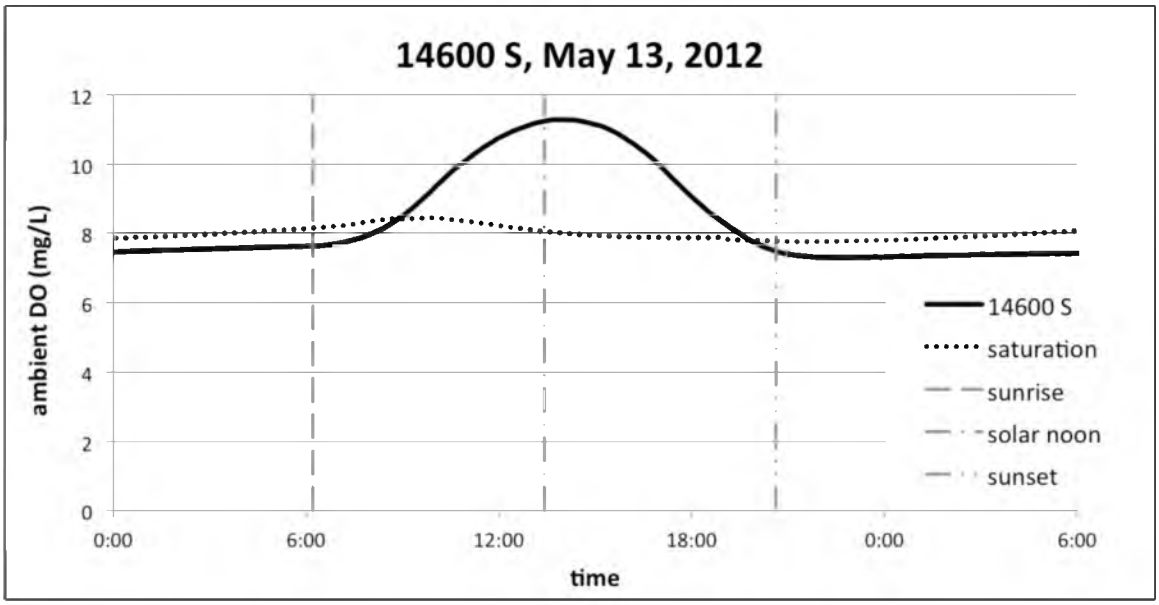

Fig. 80. 14600 S, 5-13-2012

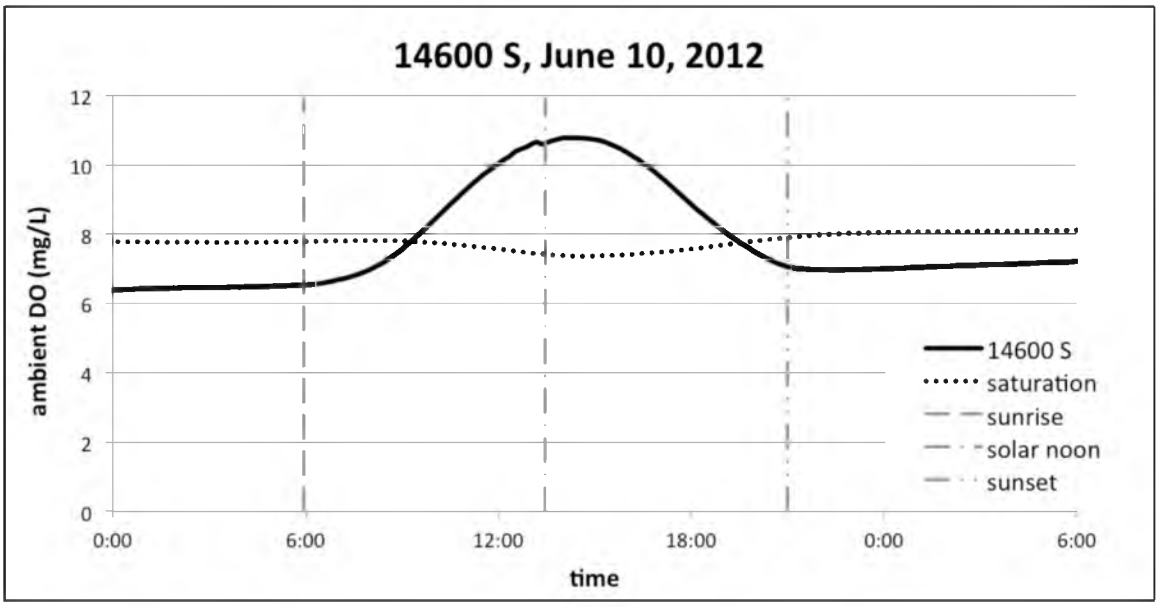

Fig. 81. 14600 S, 6-10-2012

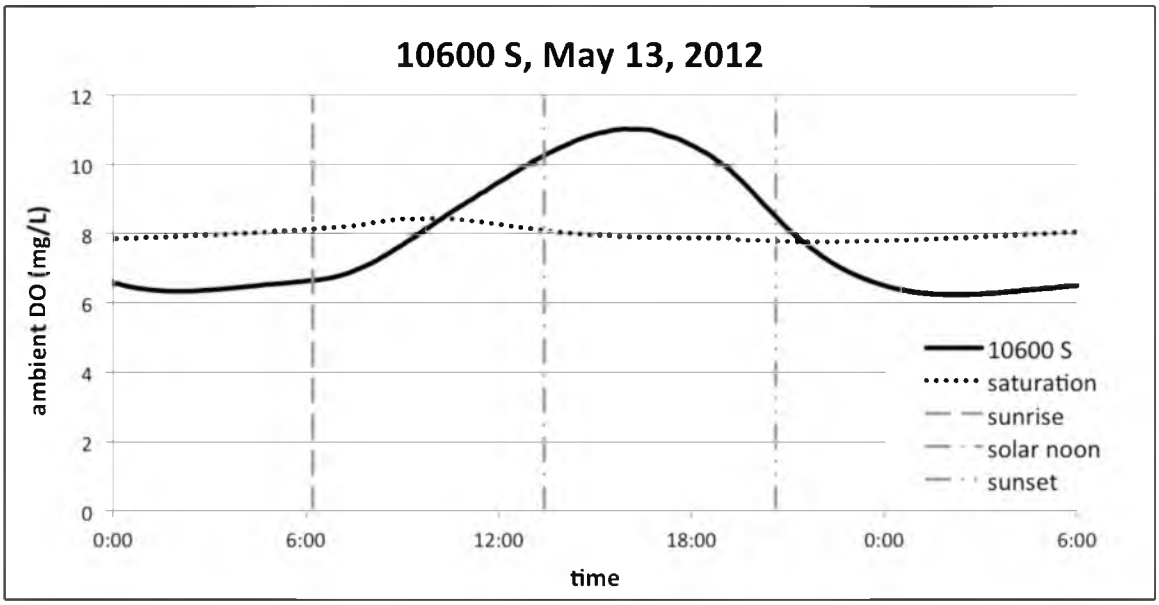

Fig. 82. 10600 S, 5-13-2012

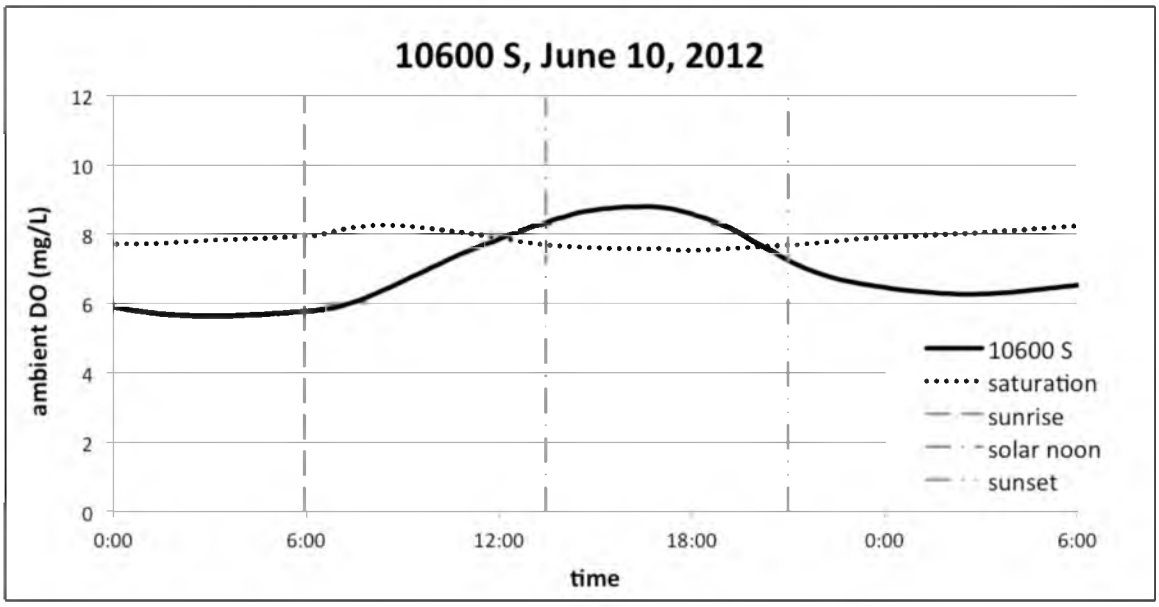

Fig. 83. 10600 S, 6-10-2012

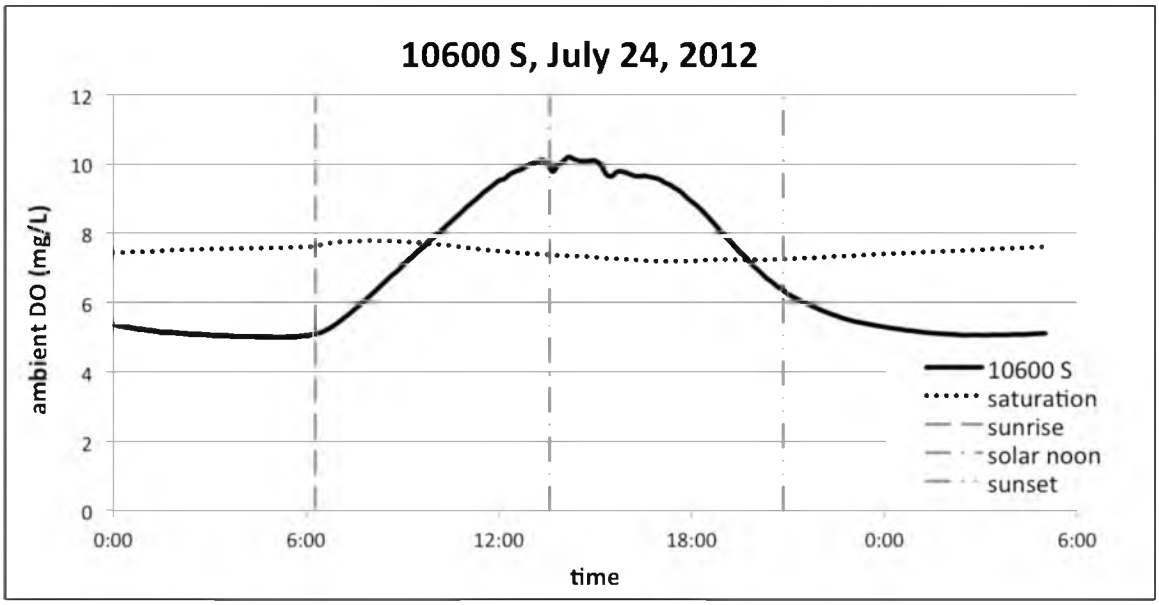

Fig. 84. 10600 S, 7-24-2012

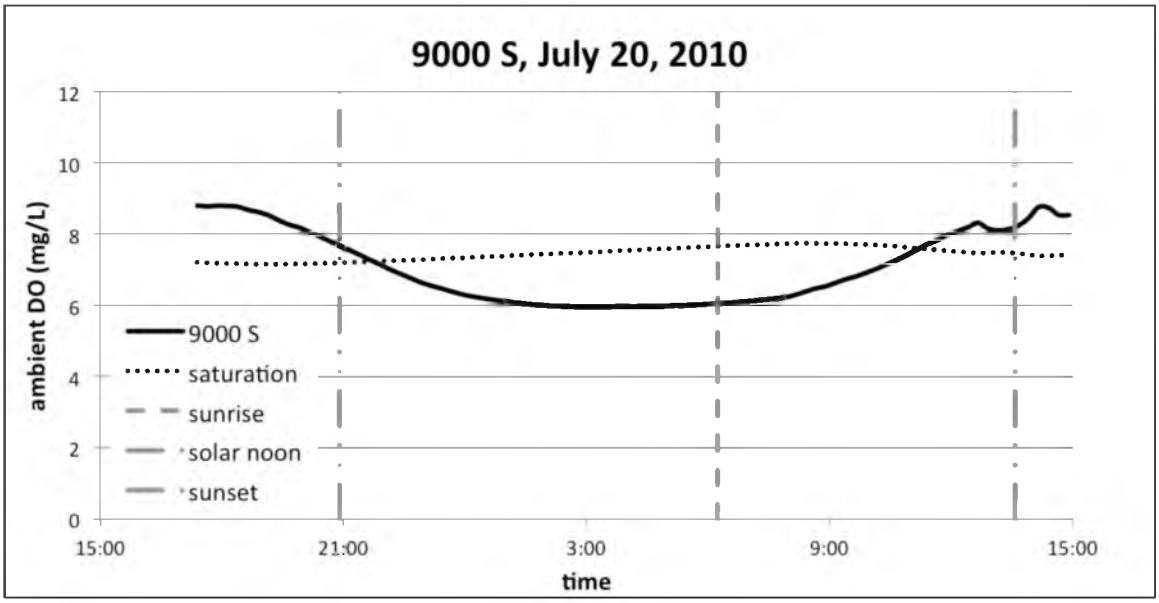

Fig. 85. 9000 S, 7-20-2010

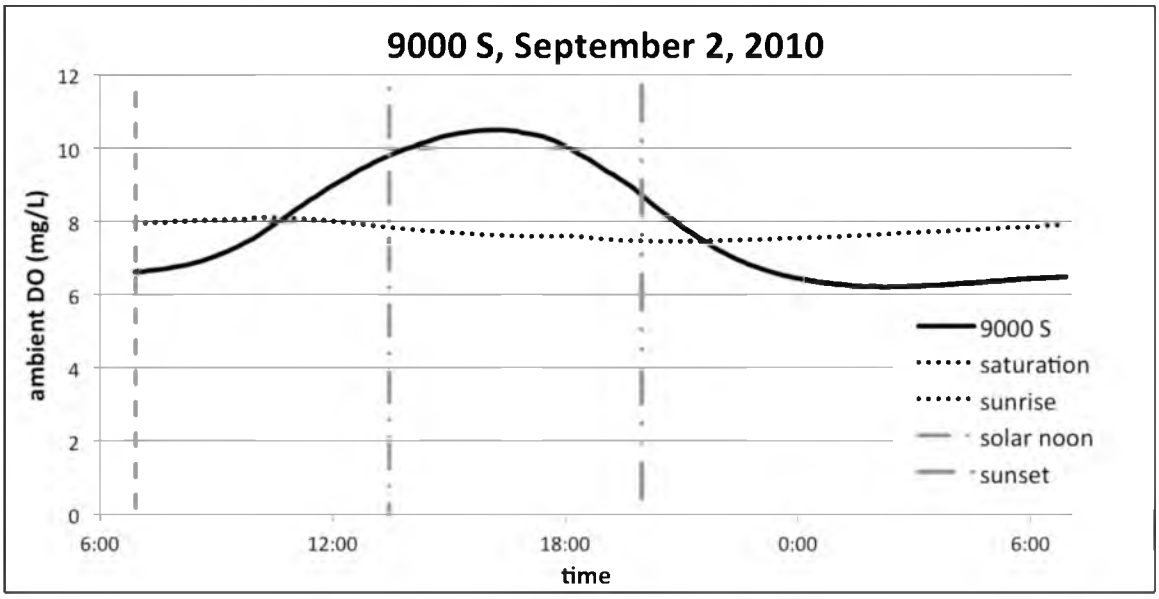

Fig. 86. 9000 S, 9-2-2010

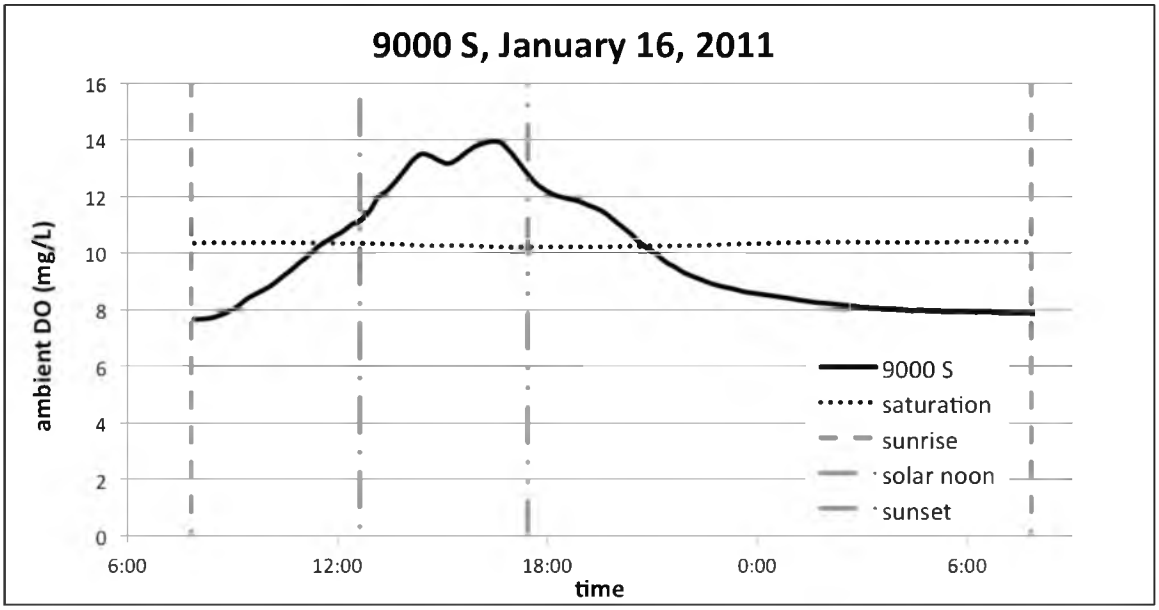

Fig. 87. 9000 S, 1-16-2011
Note: y-axis increased to 16 mg/L

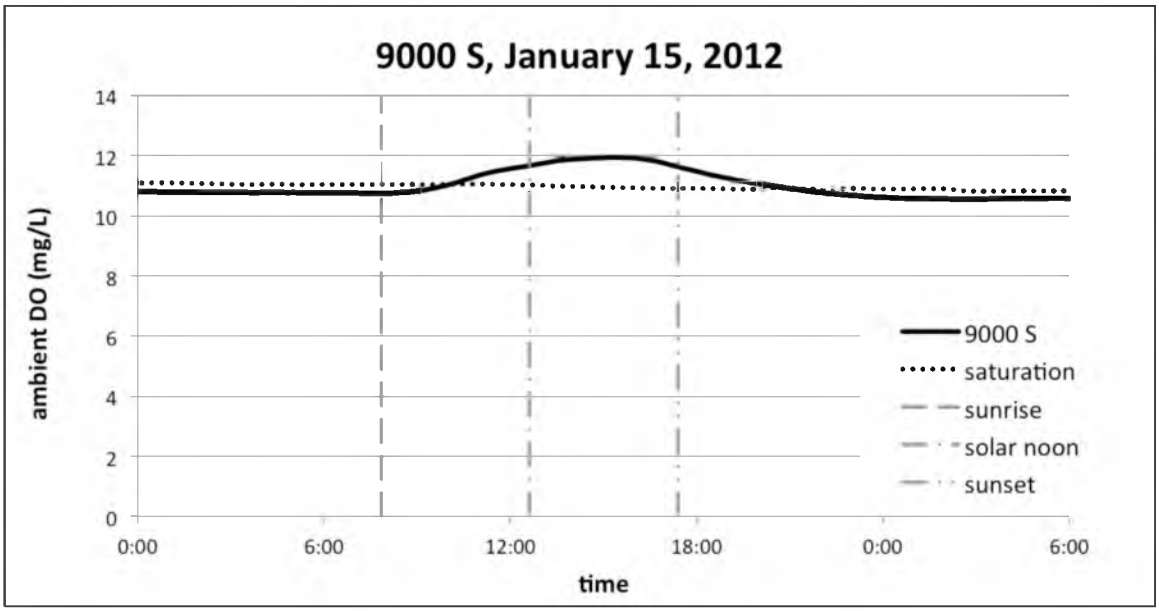

Fig. 88. 9000 S, 1-15-2012
Note: y-axis increased to 14 mg/L

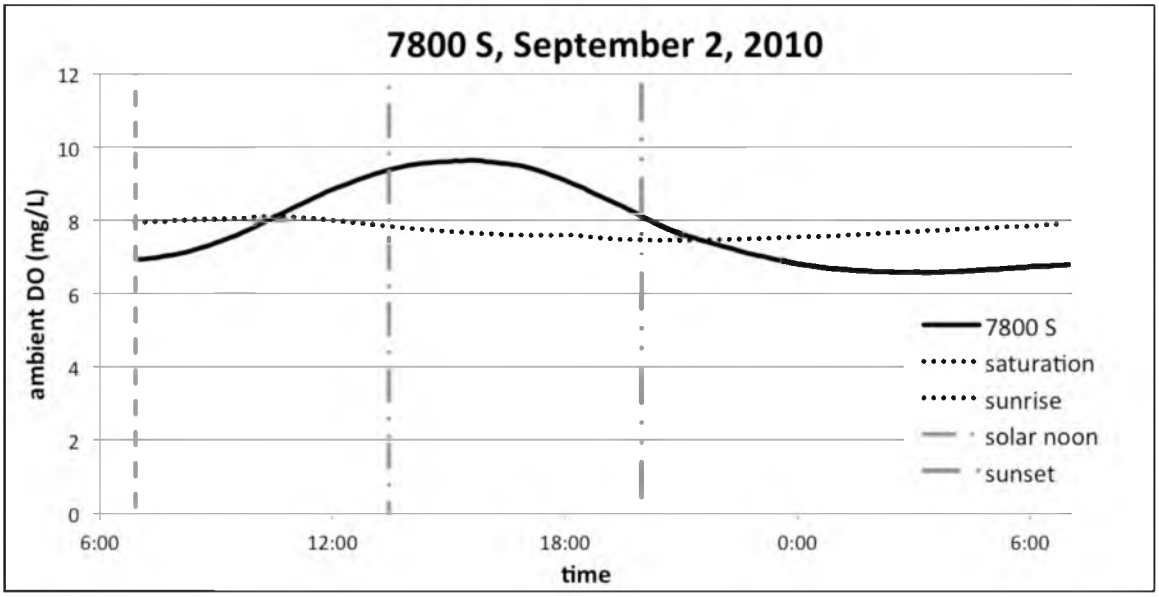

Fig. 89. 7800 S, 9-2-2010

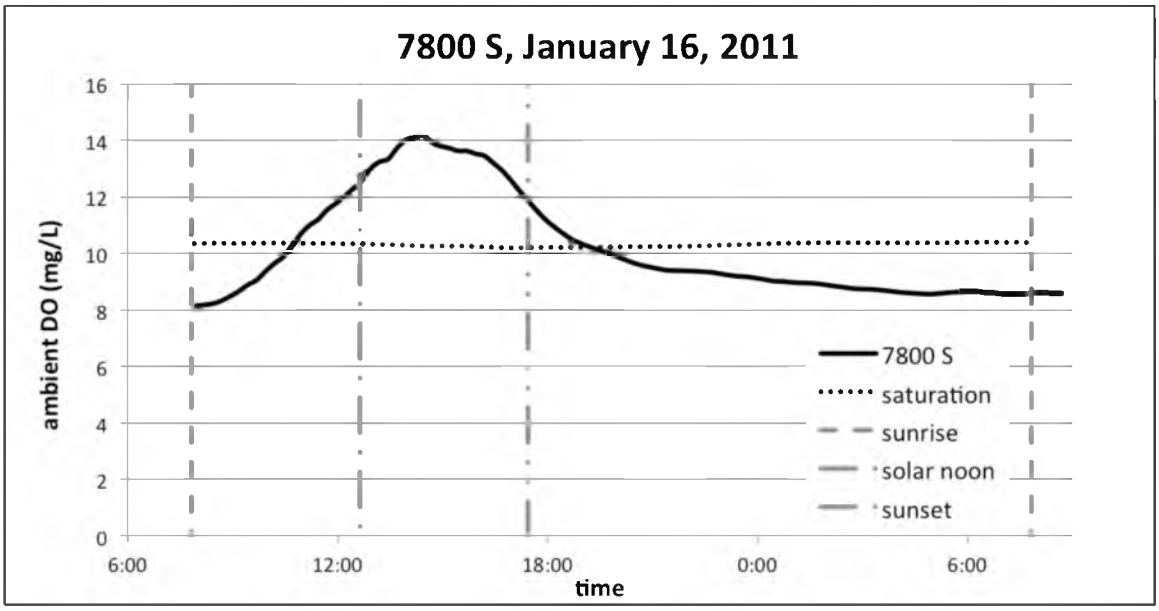

Fig. 90. 7800 S, 1-16-2011
Note: y-axis increased to 16 mg/L

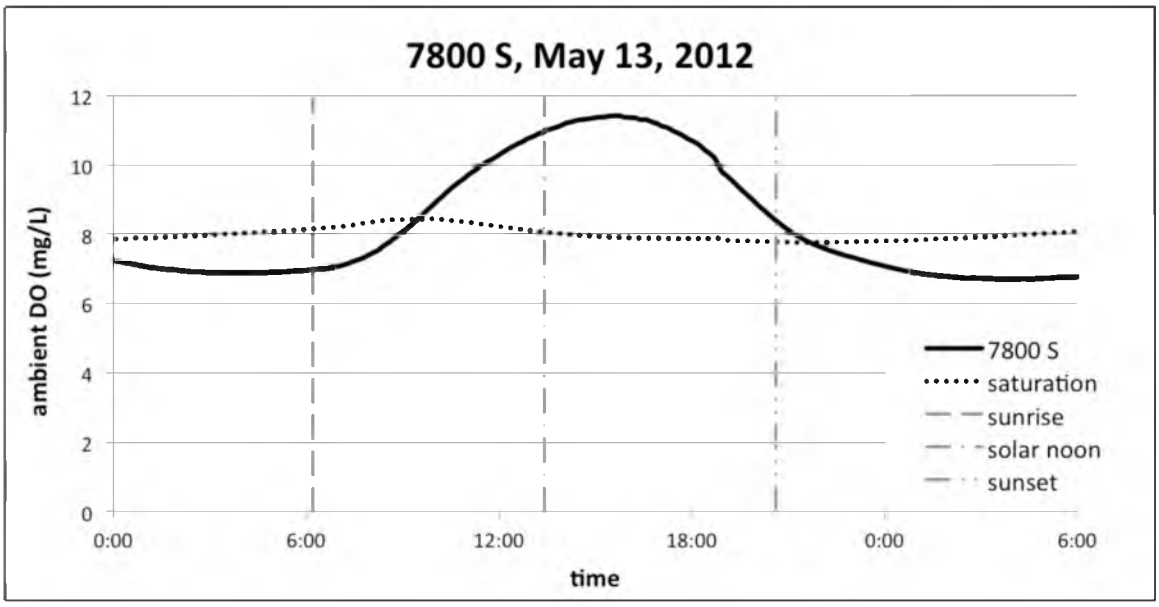

Fig. 91. 7800 S, 5-13-2012

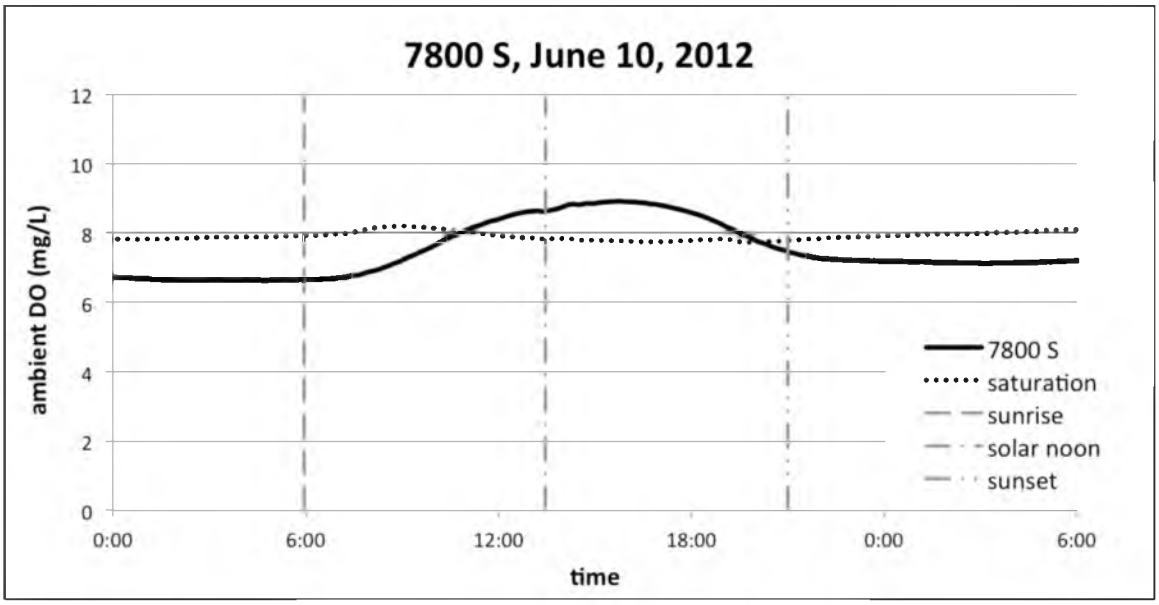

Fig. 92. 7800 S, 6-10-2012

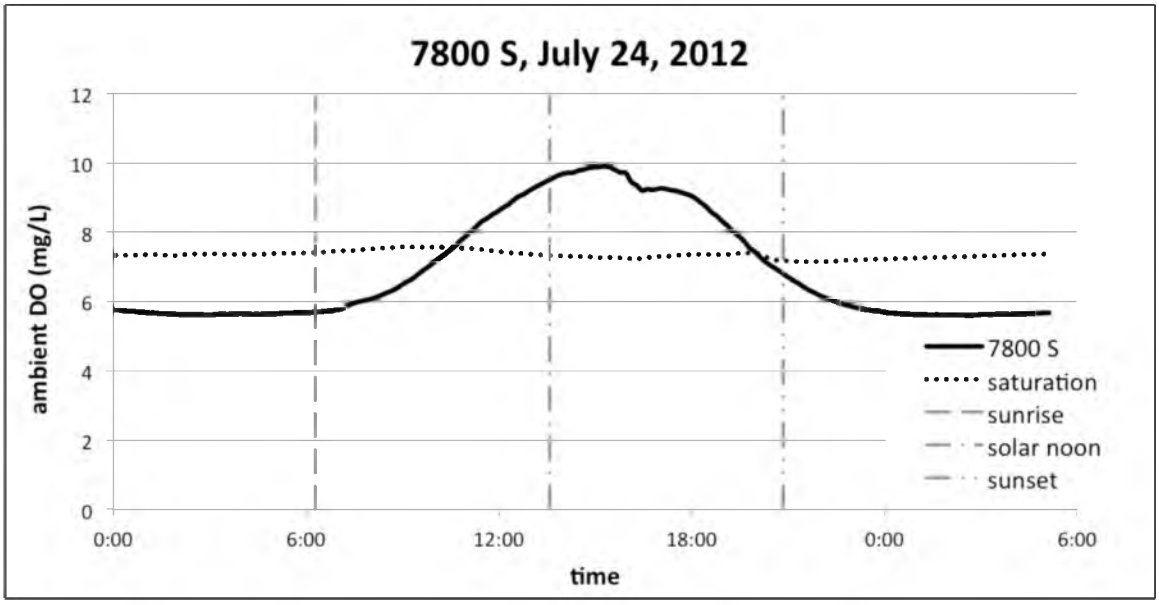

Fig. 93. 7800 S, 7-24-2012

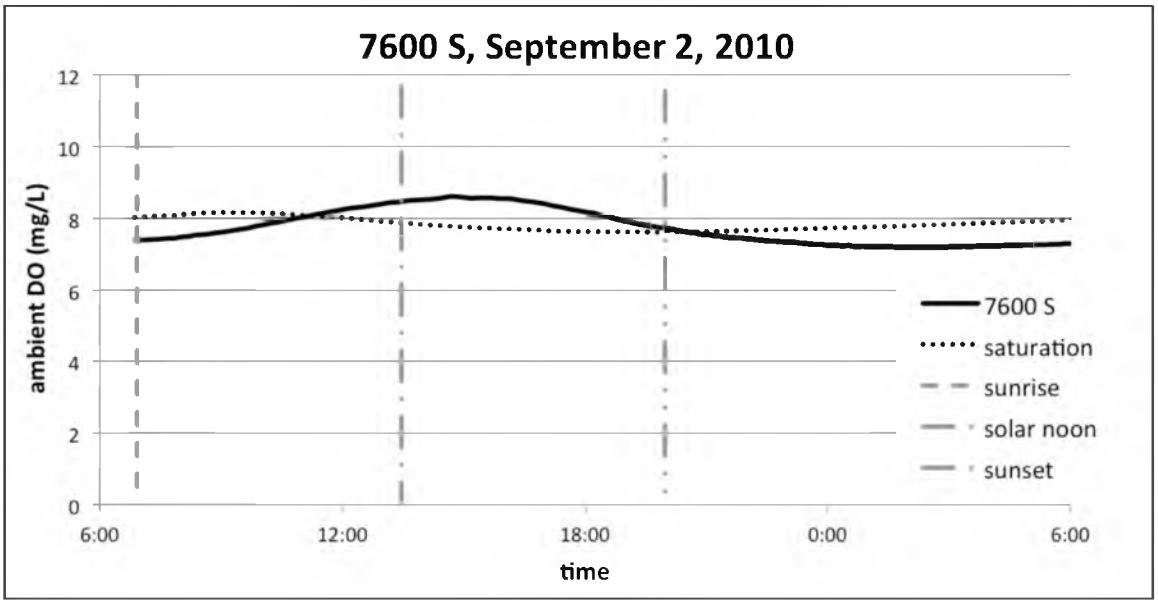

Fig. 94. 7600 S, 9-2-2010

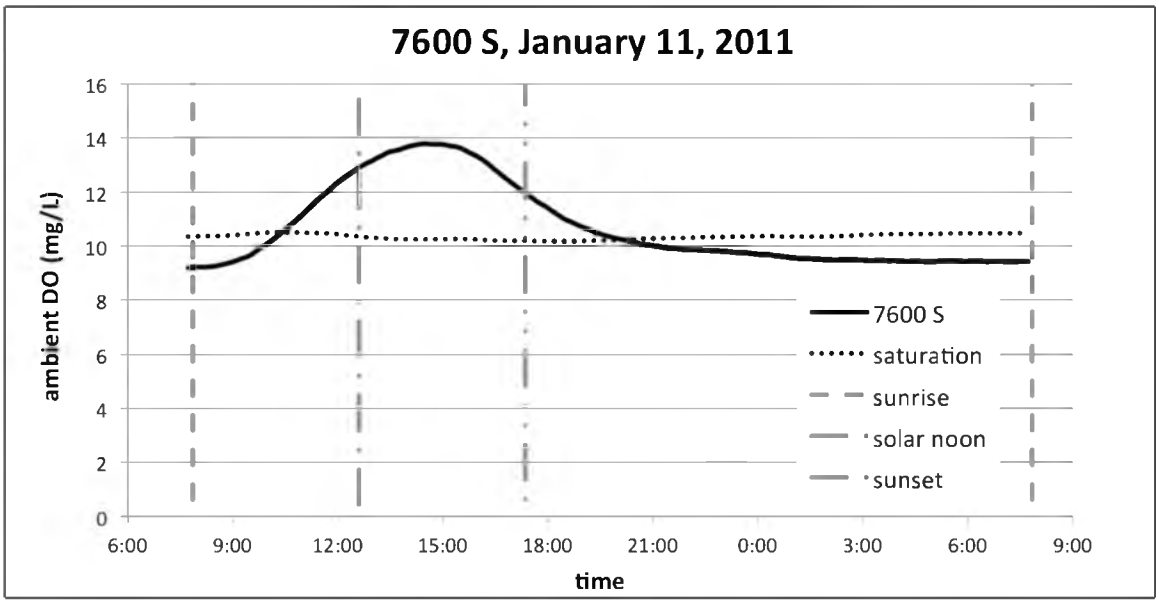

Fig. 95. 7600 S, 1-11-2011
Note: y-axis increased to 16 mg/L

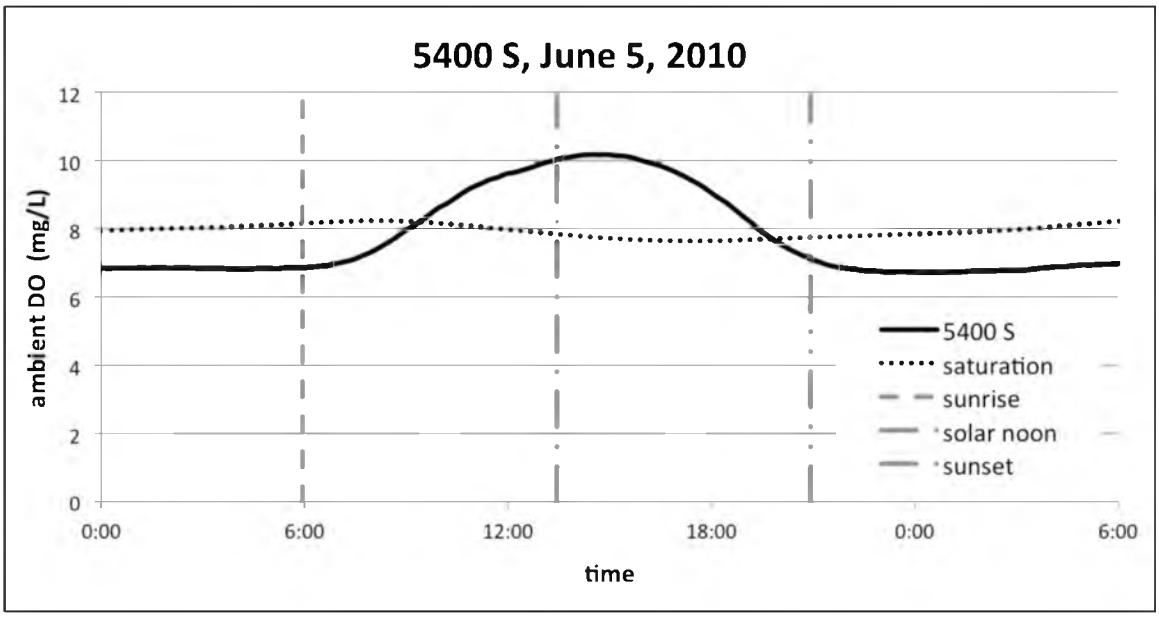

Fig. 96. 5400 S, 6-5-2010

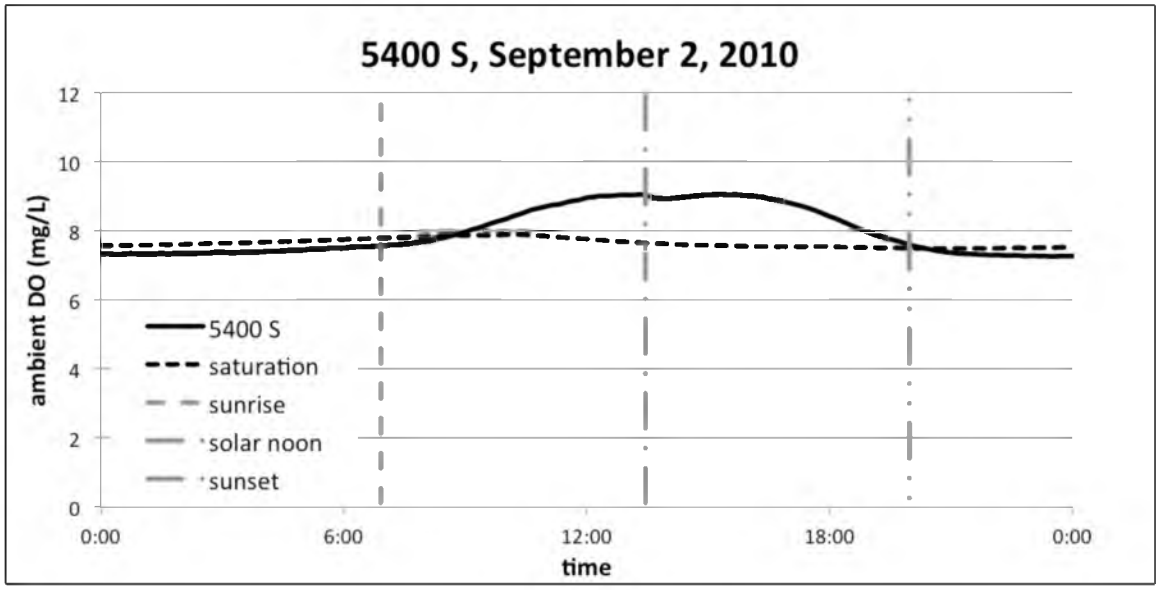

Fig. 97. 5400 S, 9-2-2010

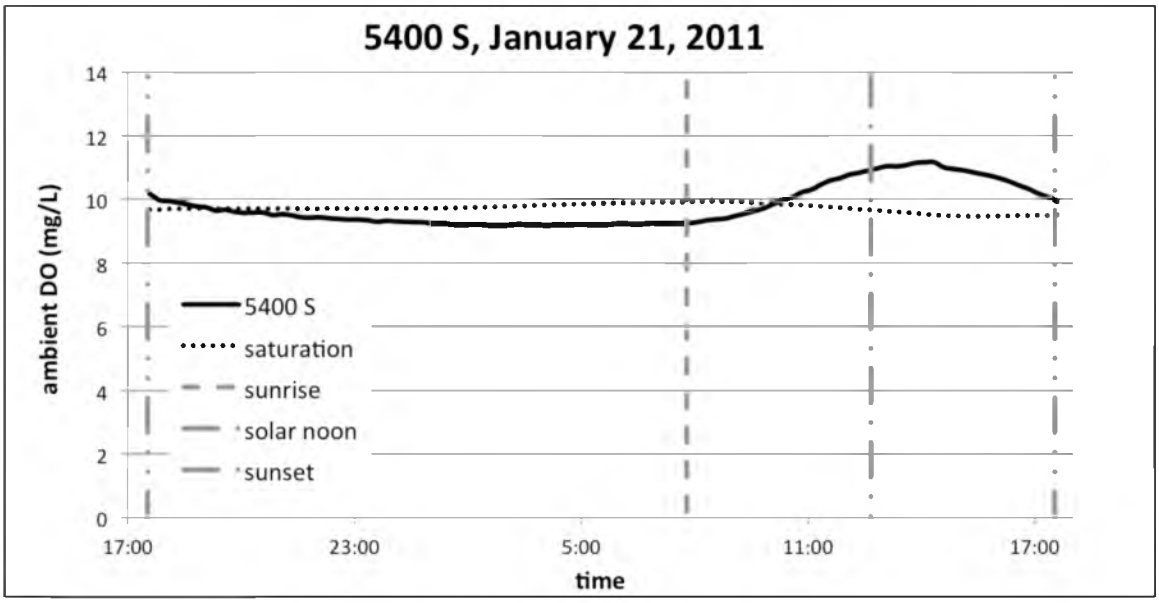

Fig. 98. 5400 S, 1-21-2011
Note: y-axis increased to 14 mg/L

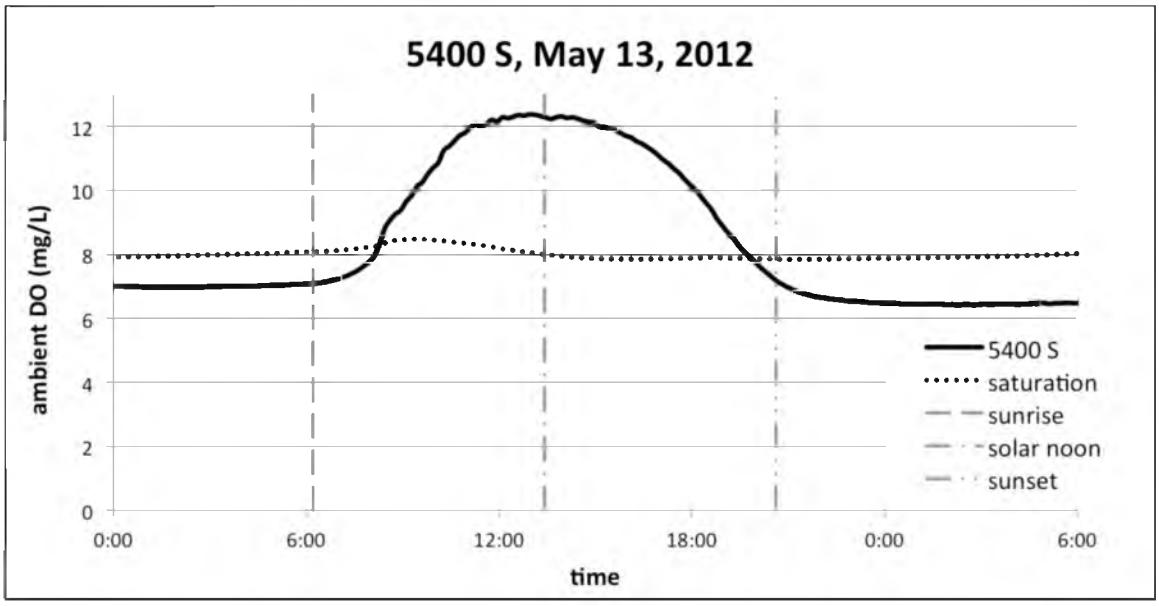

Fig. 99. 5400 S, 5-13-2012

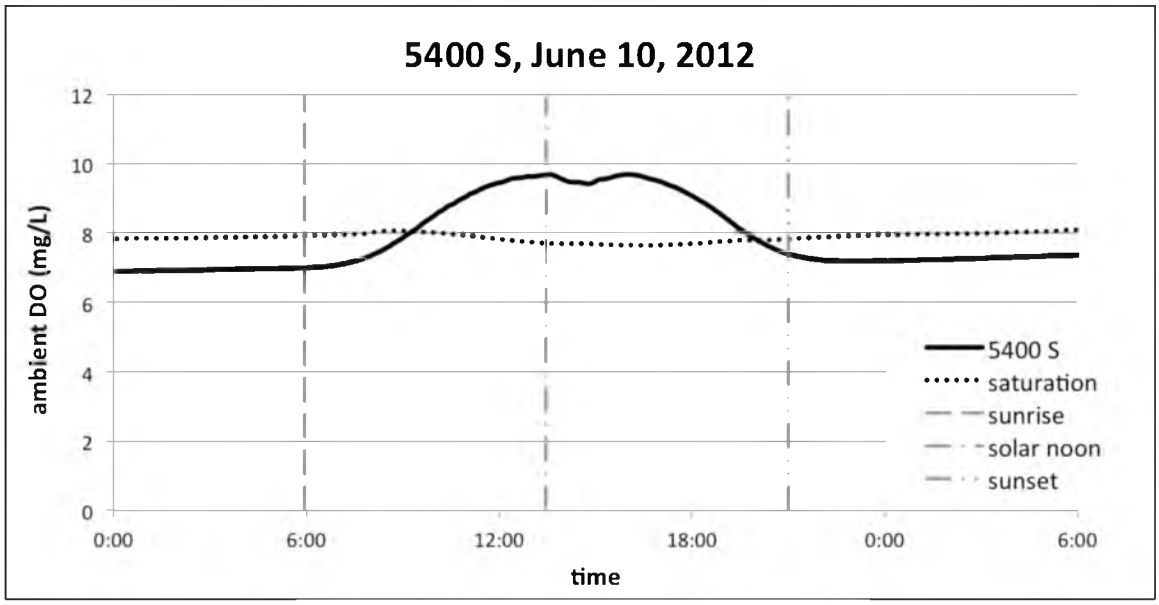

Fig. 100. 5400 S, 6-10-212

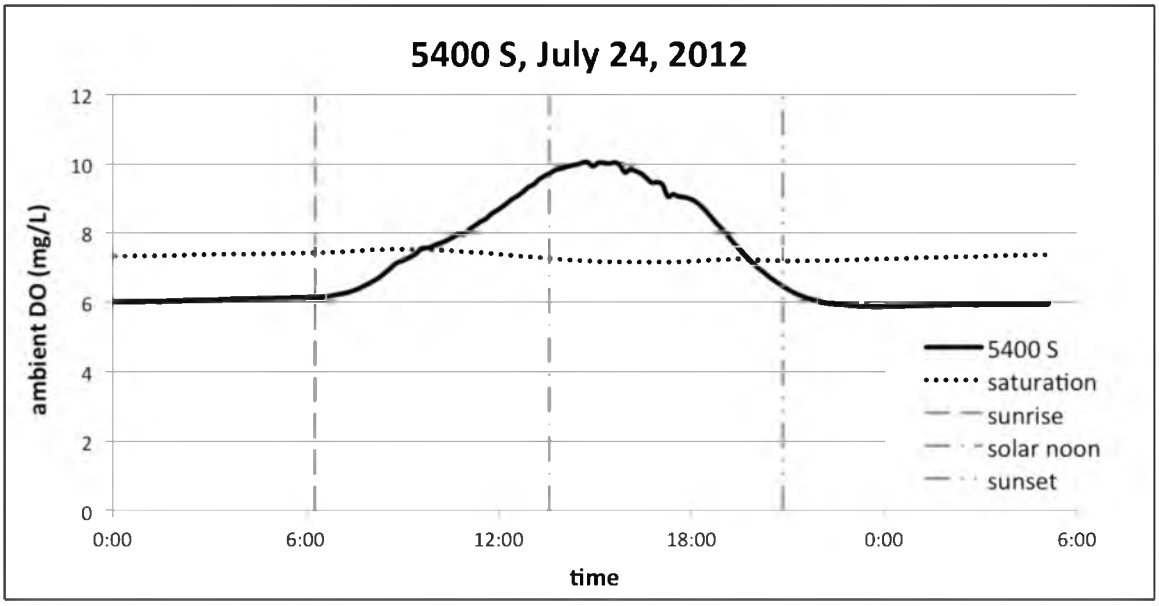

Fig. 101. 5400 S, 7-24-2012

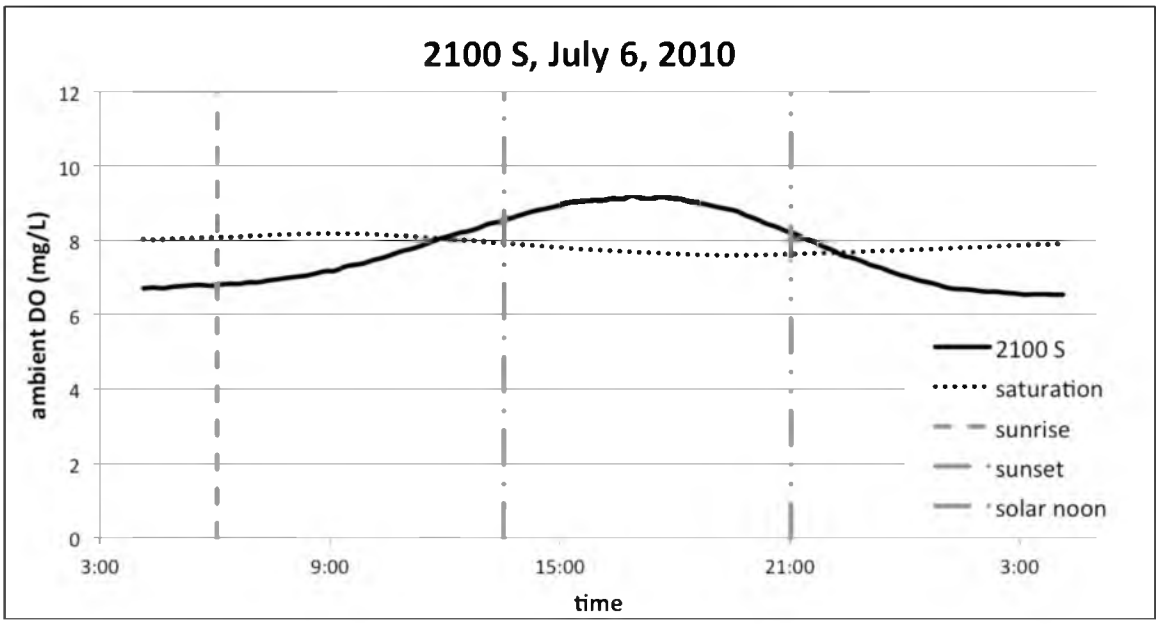

Fig. 102. 2100 S, 7-6-2010

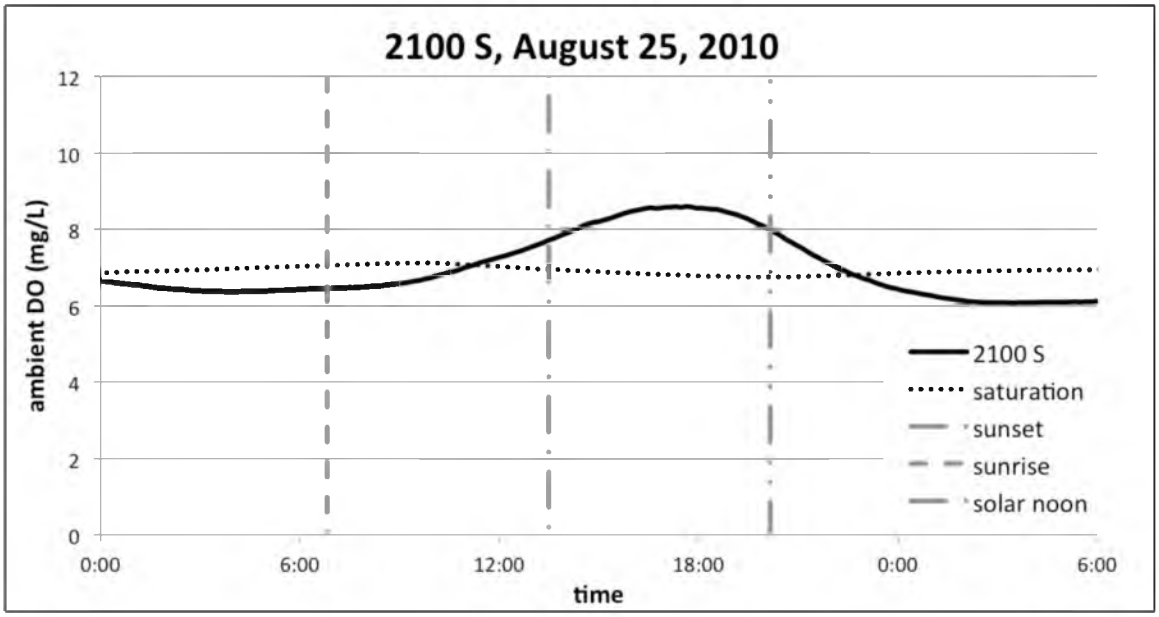

Fig. 103. 2100 S, 8-25-2010

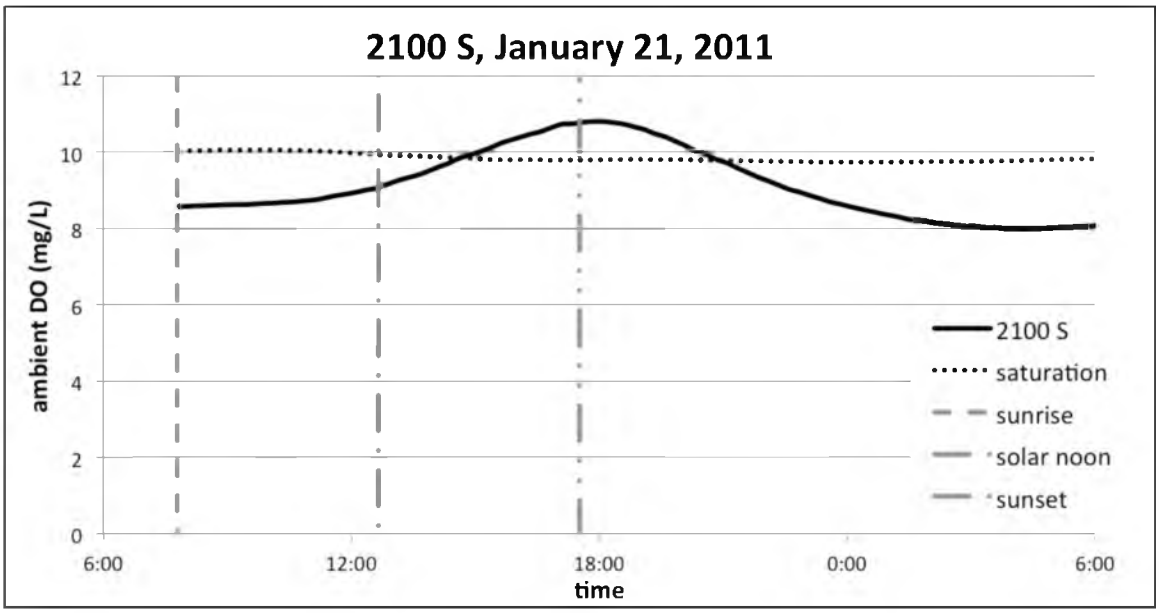

Fig. 104. 2100 S, 1-21-2011

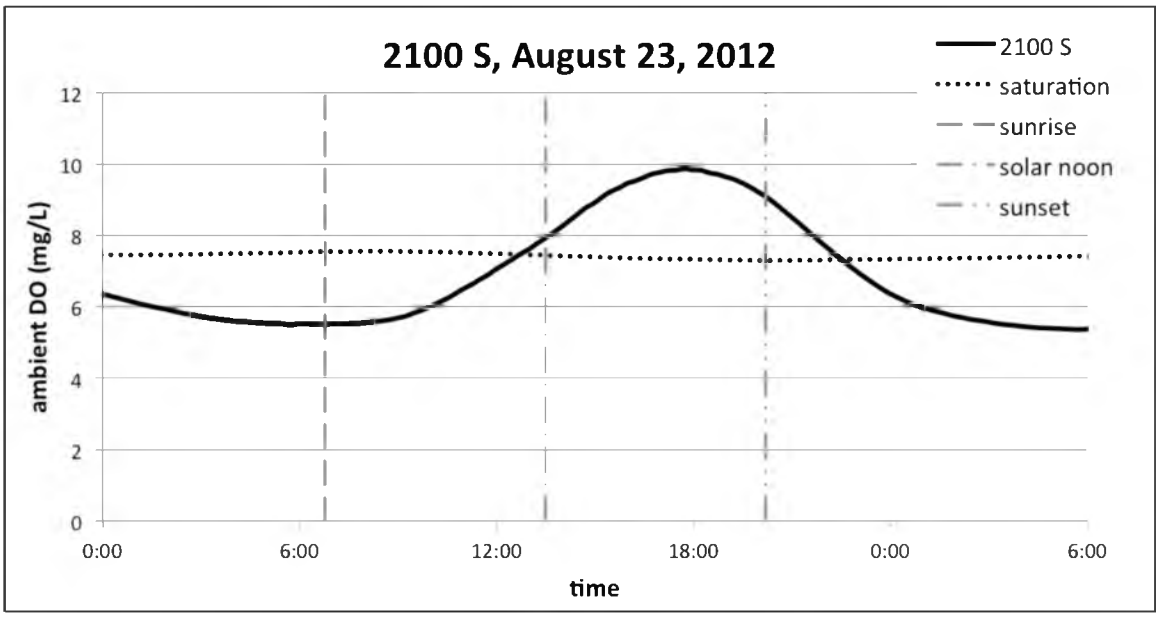

Fig. 105. 2100 S, 8-23-2012

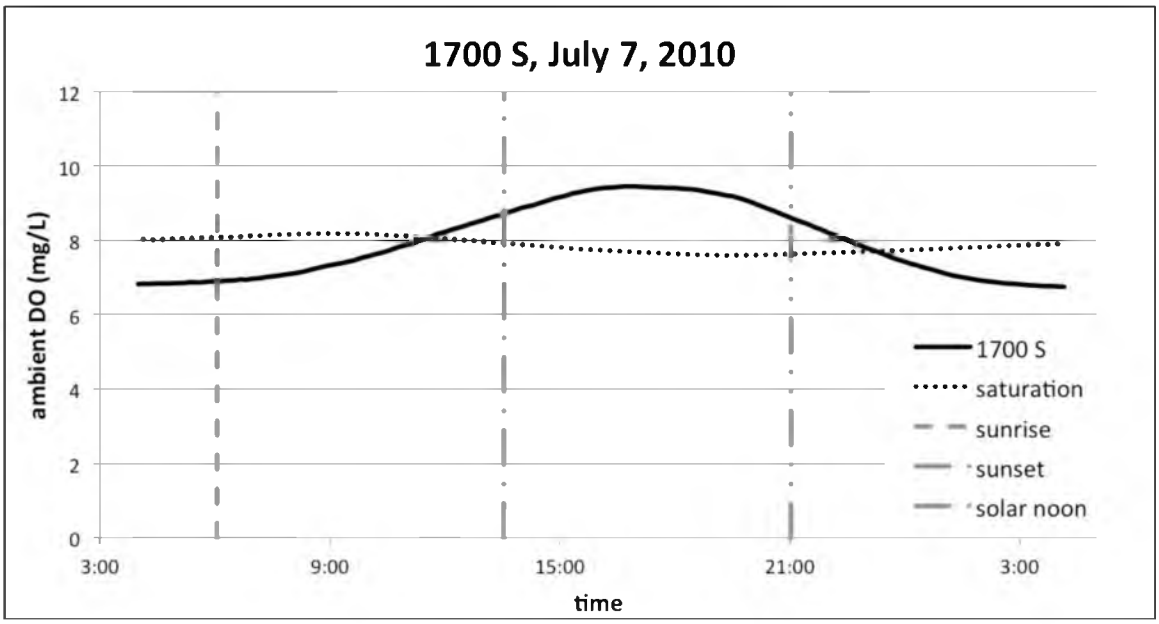

Fig. 106. 1700 S, 7-7-2010

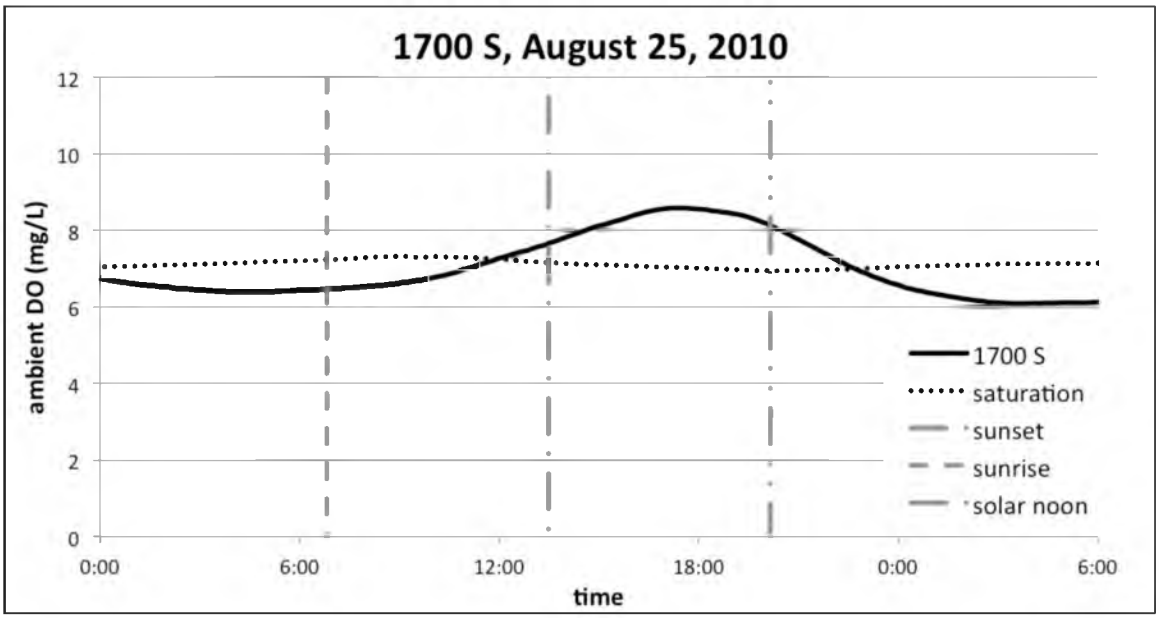

Fig. 107. 1700 S, 8-25-2010

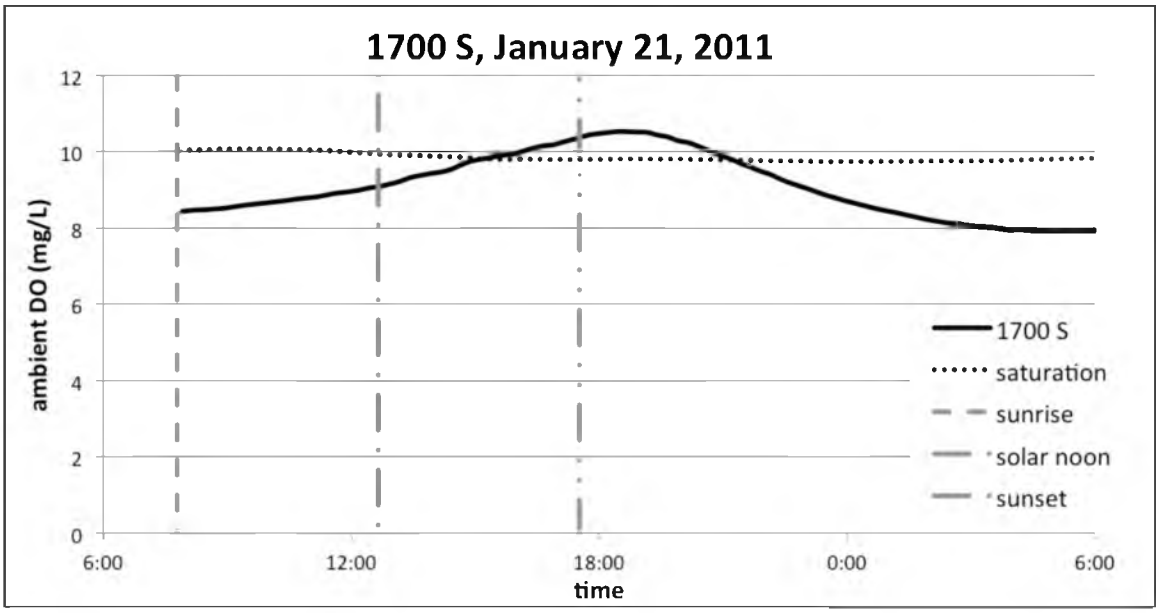

Fig. 108. 1700 S, 1-21-2011

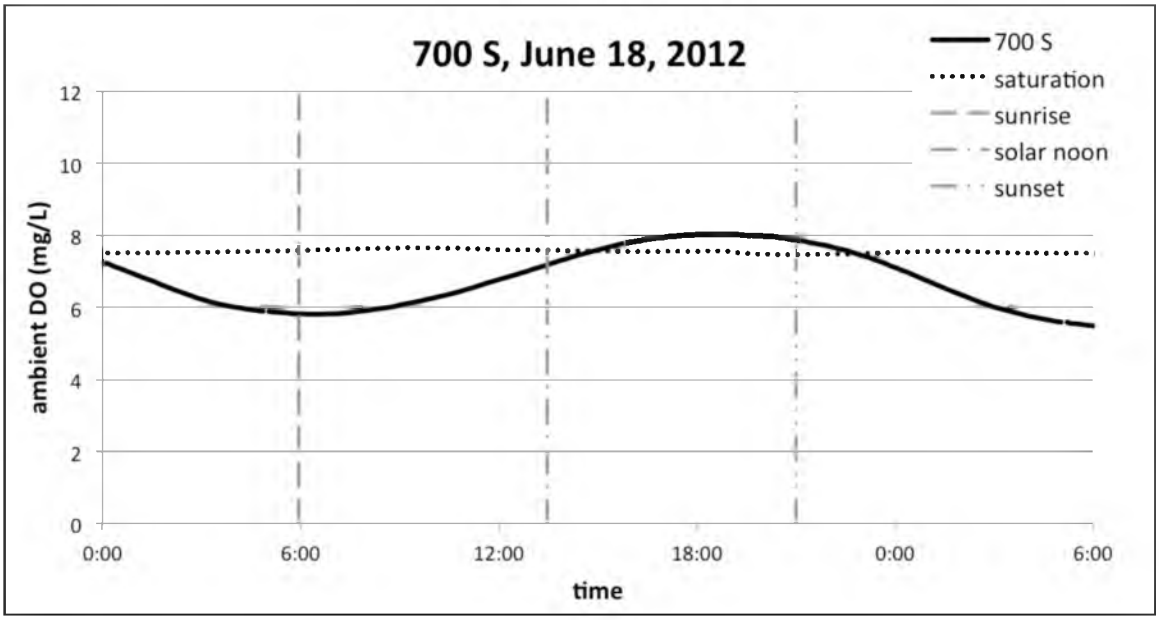

Fig. 109. 700 S, 6-18-2012

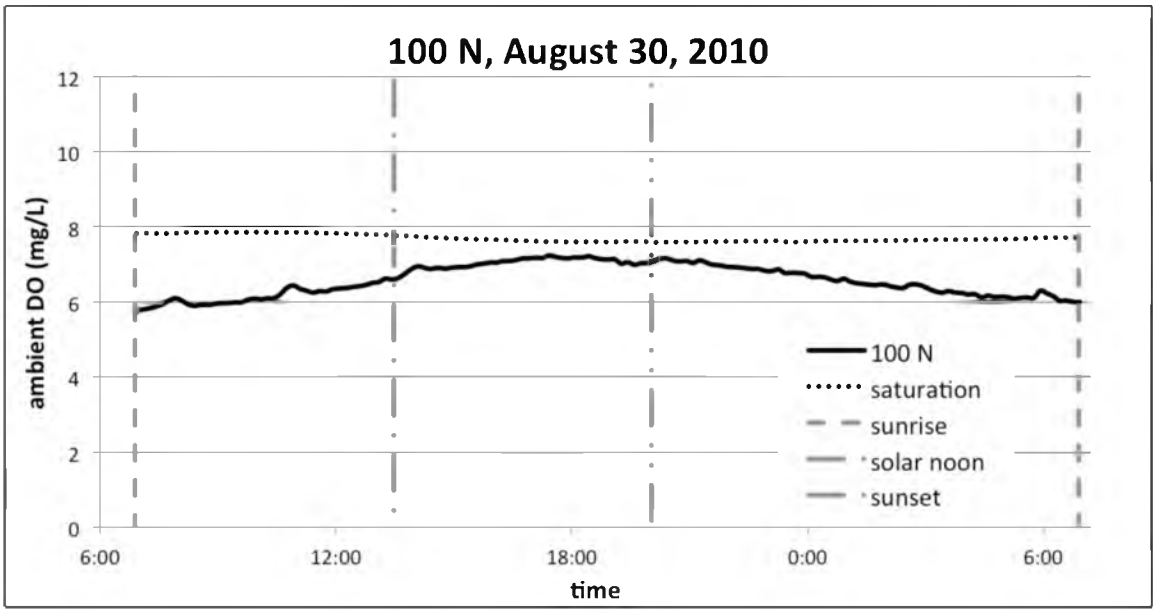

Fig. 110. 100 N, 8-30-2010

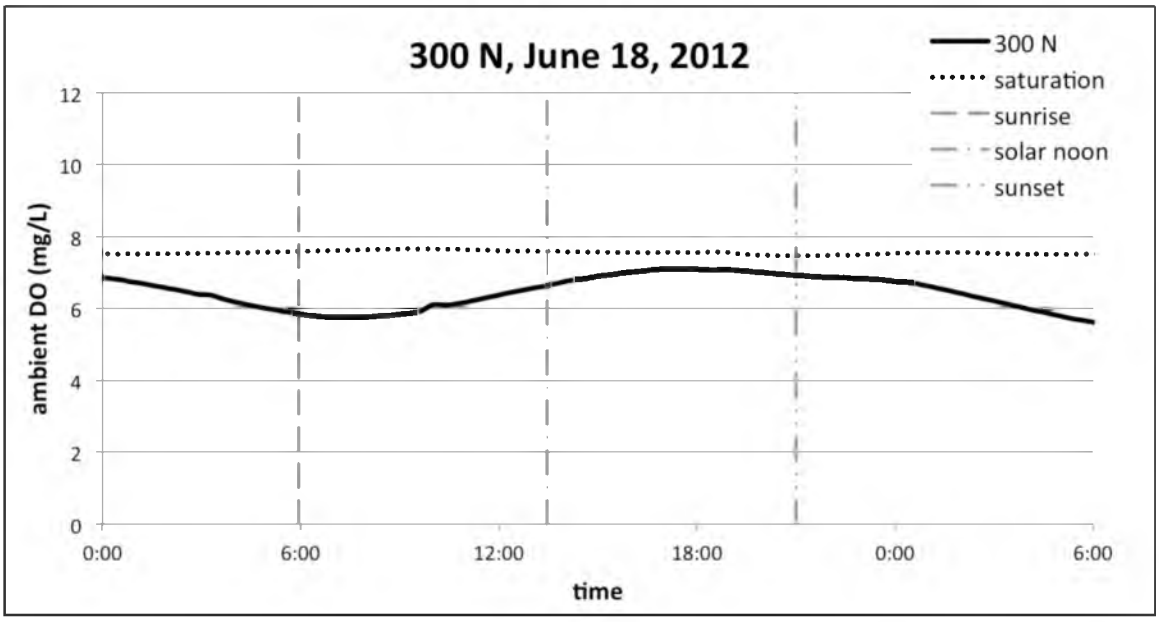

Fig. 111. 300 N, 6-18-2012

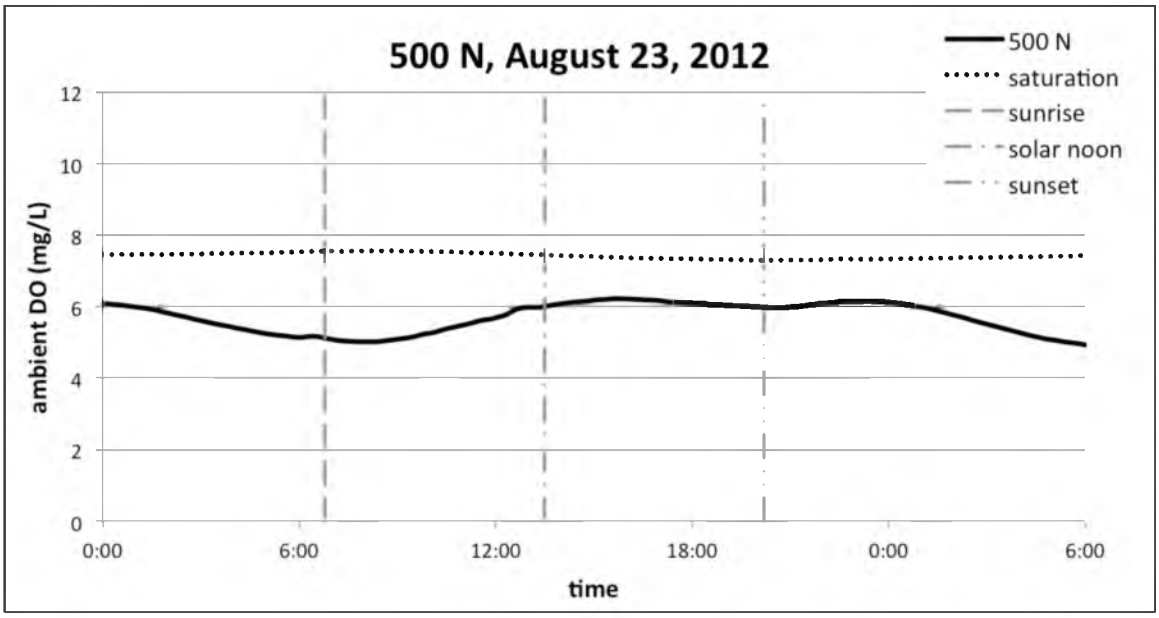

Fig. 112. 500 N, 8-23-2012

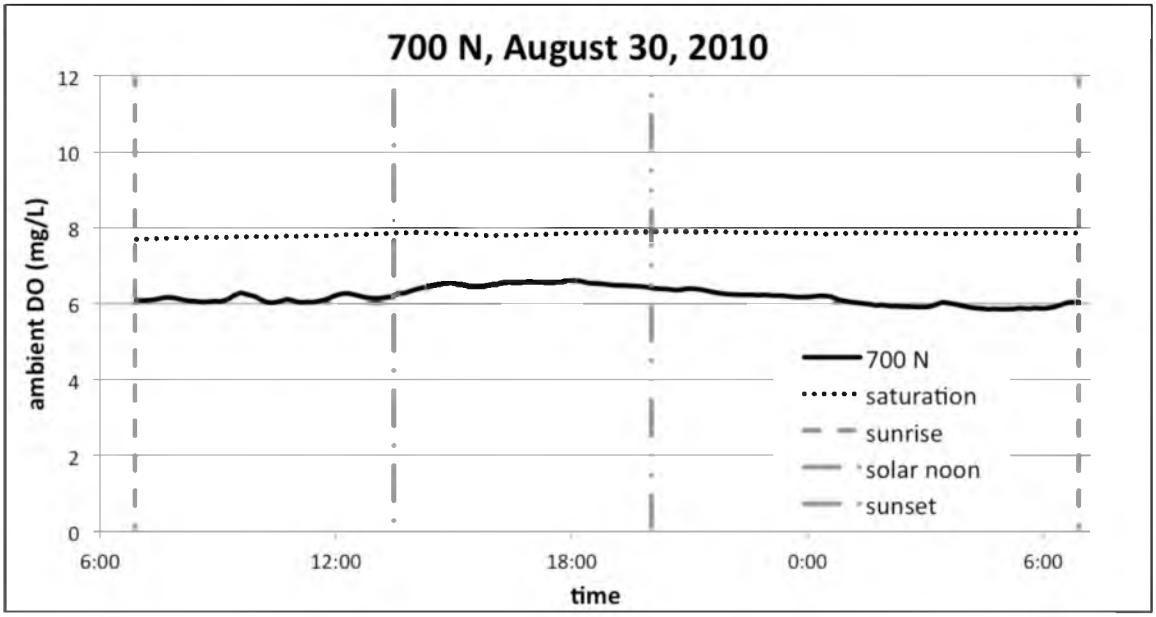

Fig. 113. 700 N, 8-30-2010

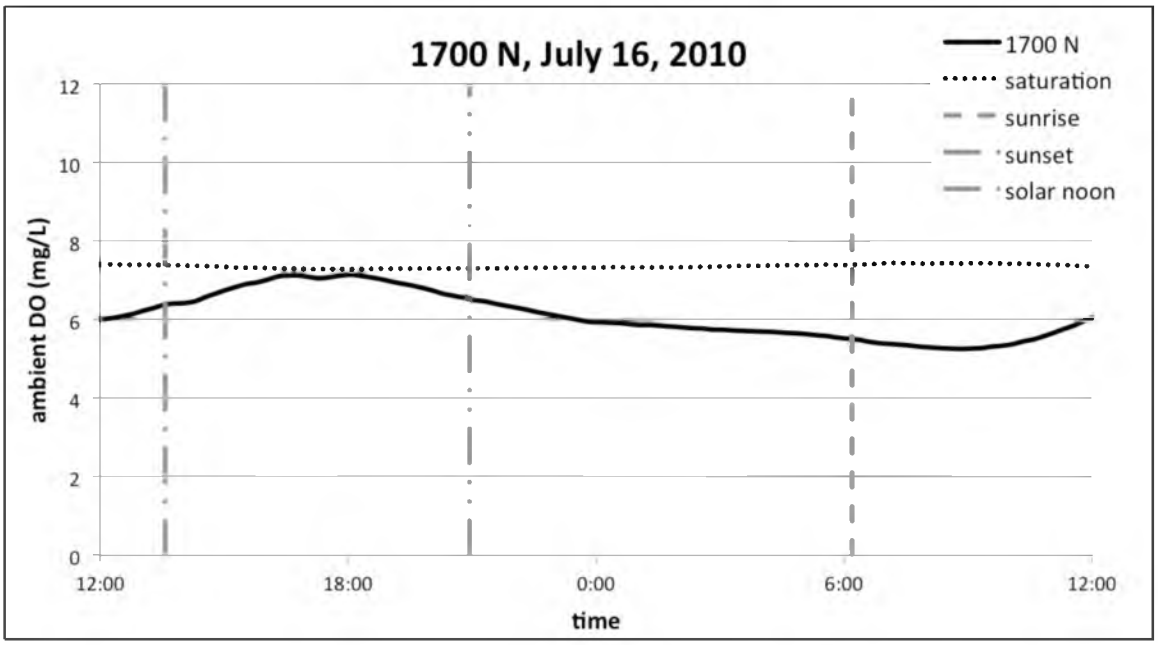

Fig. 114. 1700 N, 7-16-2010

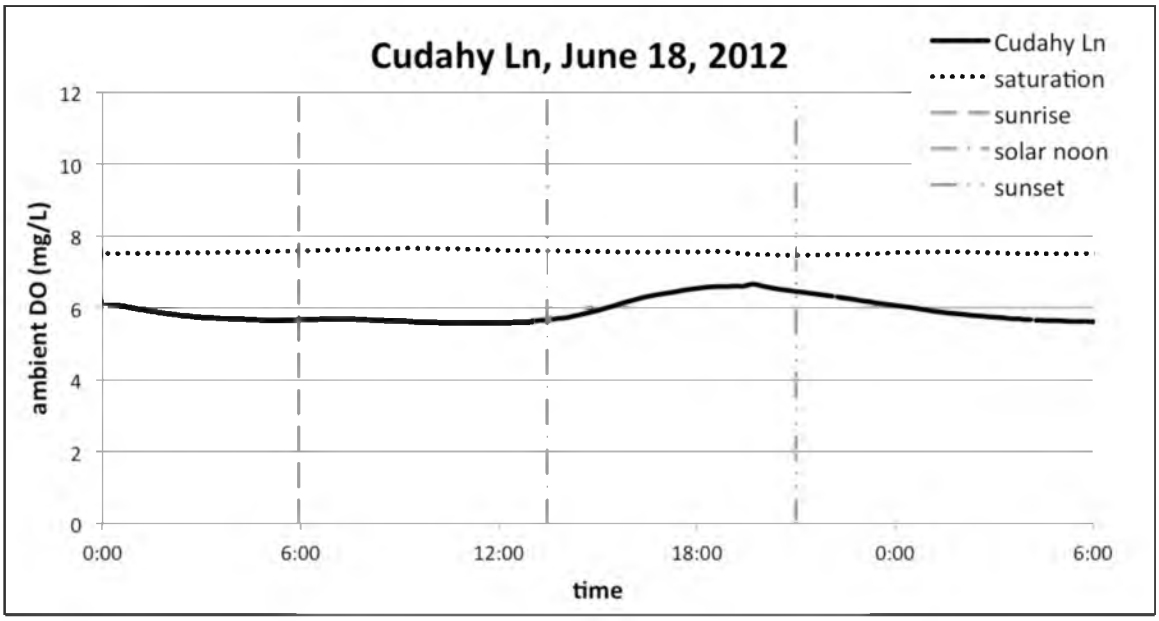

Fig. 115. Cudahy Lane, 6-18-2012

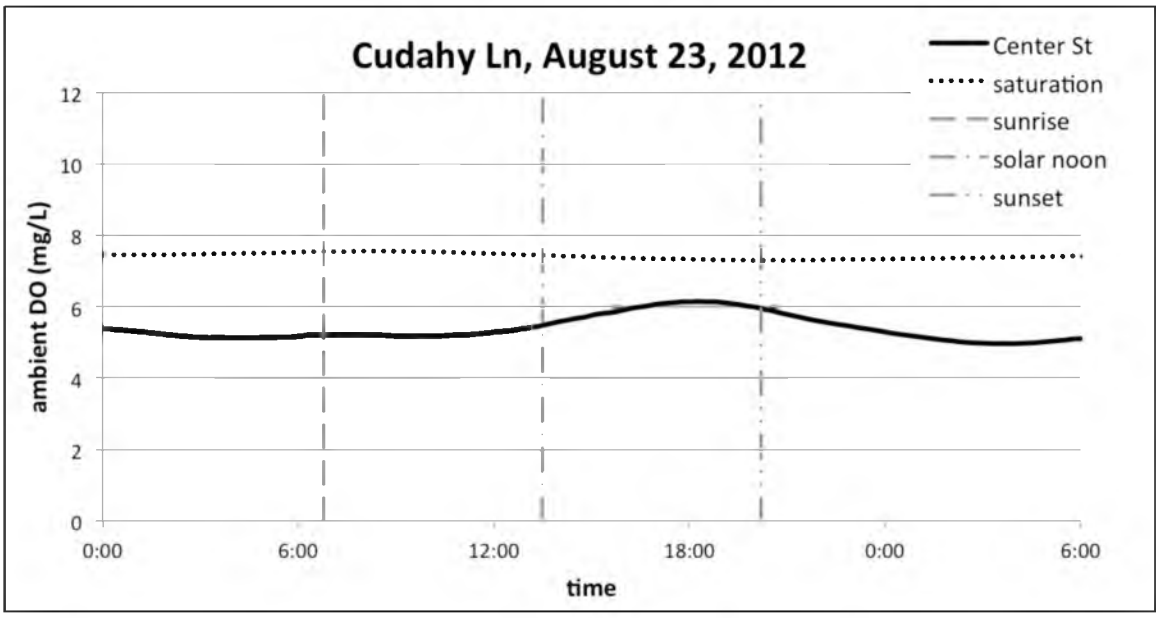

Fig. 116. Cudahy Lane, 8-23-2012

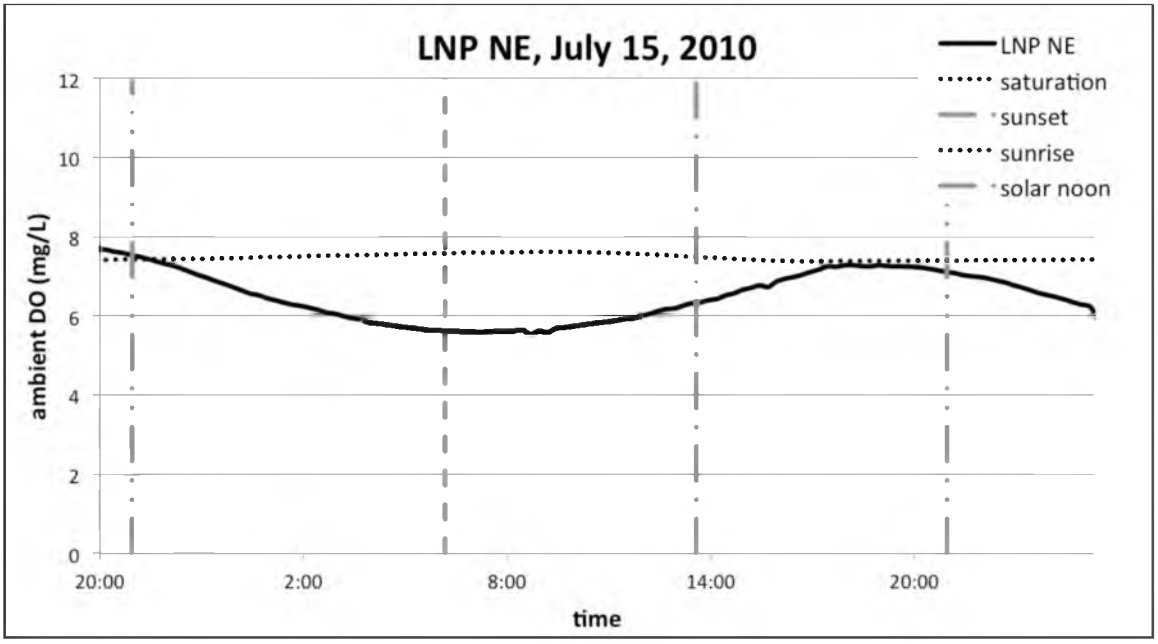

Fig. 117. LNP NE, 7-15-2010

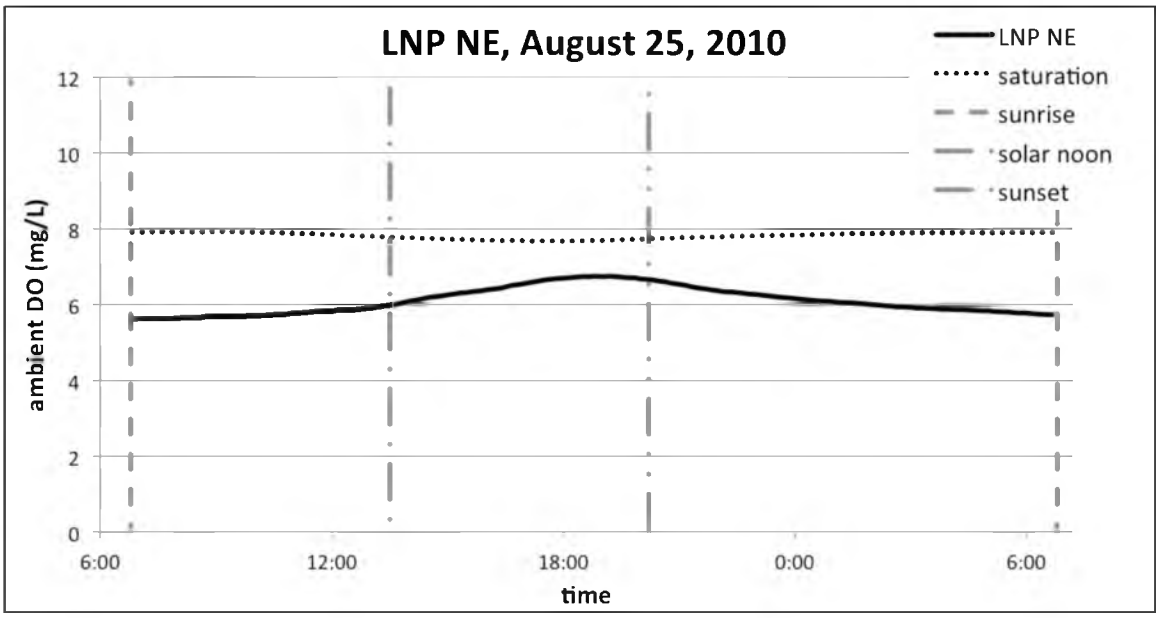

Fig. 118. LNP NE, 8-25-2010

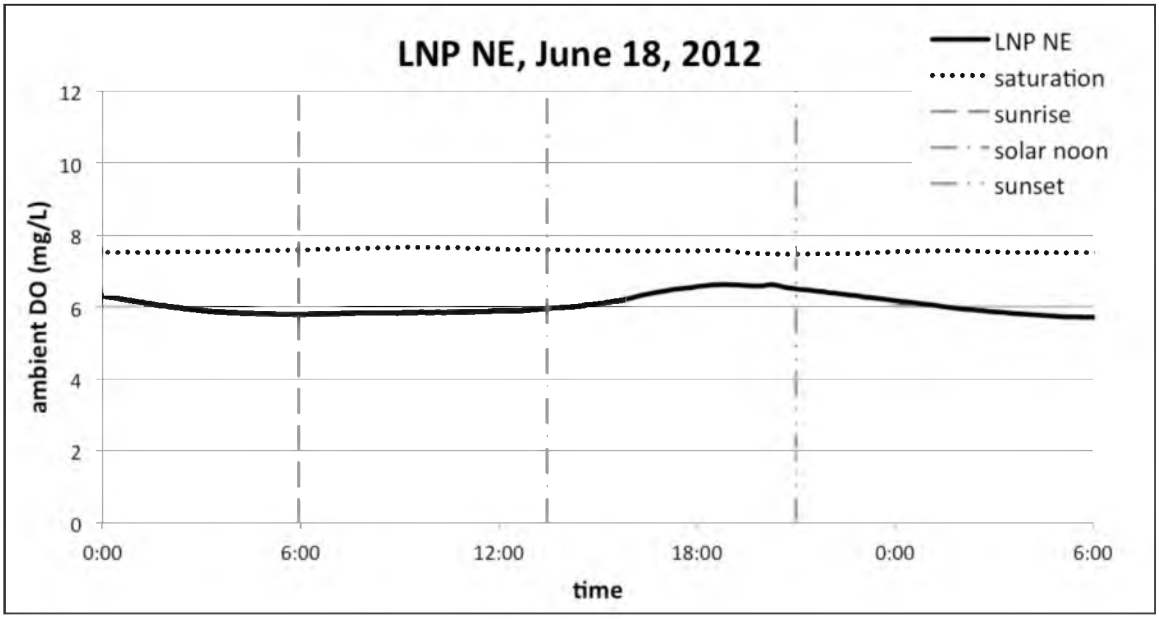

Fig. 119. LNP NE, 6-18-2012

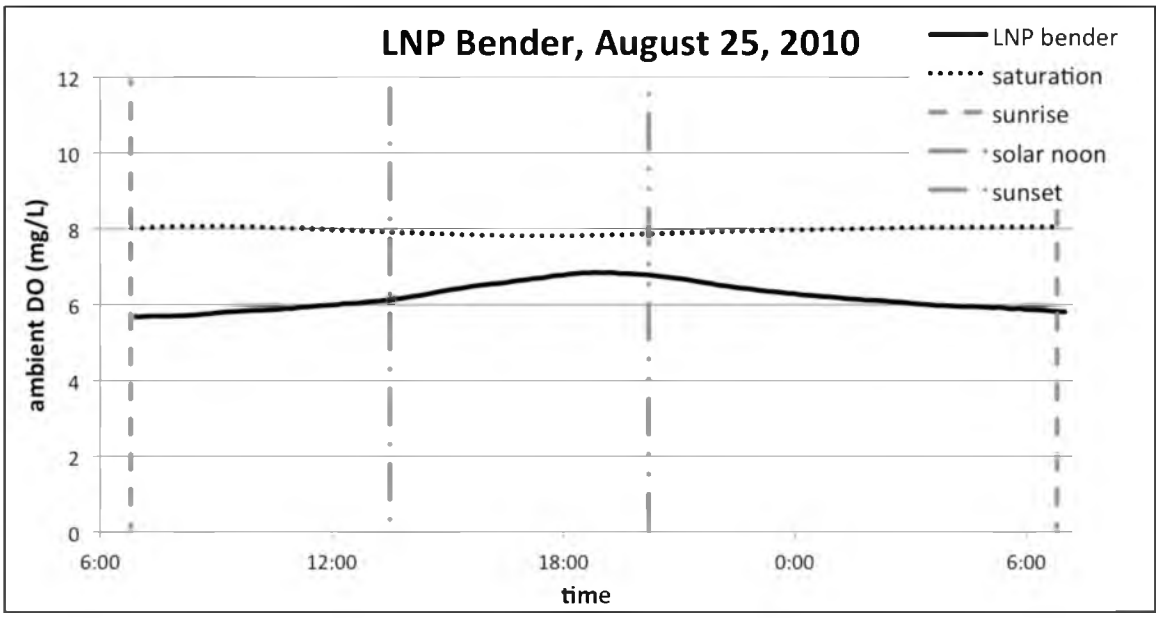

Fig. 120. LNP Bender, 8-25-2010

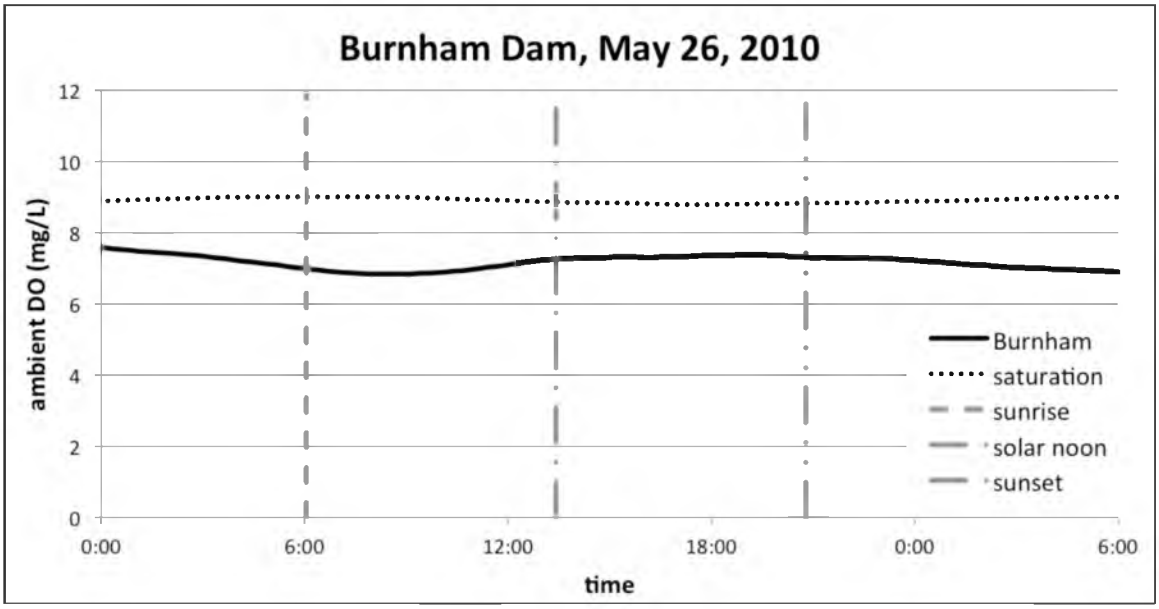

Fig. 121. Burnham Dam, 5-26-2010

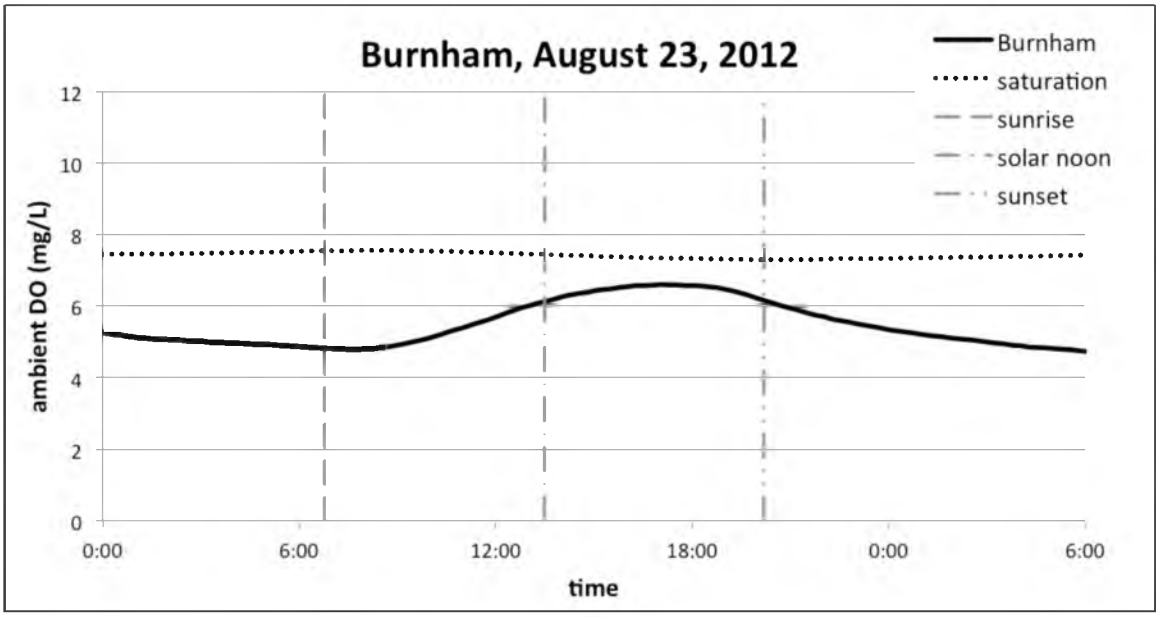

Fig. 122. Burnham Dam, 8-23-2012

APPENDIX C

SEDIMENT %TS AND %VS

Table 48. Sediment %TS and %VS (a)

site	reach	date	depth	%TS	%VS	note
LNP NE	1	5/20/10	0–2	46	4.5	
LNP NE	1	5/20/10	10	40	9.7	
LNP NE	1	5/20/10	20	56	4.4	
LNP NE	1	5/20/10	30	68	3.4	
Cudahy Ln	1	5/20/10	0–2	40	6.3	
Cudahy Ln	1	5/20/10	20	57	6.0	
Cudahy Ln	1	5/20/10	30	54	7.5	
1700 N	2	5/20/10	0–2	48	4.5	
1700 N	2	5/20/10	10	57	5.5	
1700 N	2	5/20/10	20	65	4.0	
1700 N	2	5/20/10	30	76	2.1	
300 N	2	5/20/10	0–2	53	3.3	
300 N	2	5/20/10	10	75	2.4	
300 N	2	5/20/10	20	55	8.4	
300 N	2	5/20/10	30	68	4.0	
900 S-N	3	5/24/10	0–2	62	2.6	
900 S-N	3	5/24/10	10	69	2.6	
900 S-N	3	5/24/10	20	69	2.1	
900 S-N	3	5/24/10	30	73	2.2	
900 S-S	3	5/20/10	0–2	72	1.2	
900 S-S	3	5/20/10	10	77	1.9	
900 S-S	3	5/20/10	20	76	0.7	
900 S-S	3	5/20/10	30	72	3.6	
1700 S	3	5/24/10	0–2	78	1.1	
1700 S	3	5/24/10	20	81	0.4	
1700 S	3	5/24/10	30	75	0.6	
1700 S-Pool	3	5/24/10	0–2	30	6.7	pool
1700 S-Pool	3	5/24/10	10	83	0.5	pool
1700 S-Pool	3	5/24/10	20	65	3.3	pool
Lehi		5/25/10	0–2	45	5.6	
Lehi		5/25/10	10	67	2.4	
Lehi		5/25/10	20	68	3.2	
Lehi		5/25/10	30	71	3.0	
LNP NE	1	6/3/10	0–2	47	5.6	
LNP NE	1	6/3/10	10	57	5.9	

Table 49. Sediment %TS and %VS (b)

site	reach	date	depth	%TS	%VS	note
LNP NE	1	6/3/10	20	66	3.9	
LNP NE	1	6/3/10	30	63	5.2	
LNP NE	1	6/3/10	40	71	3.0	
LNP NE	1	6/3/10	50	76	2.3	
Cudahy Ln	1	6/3/10	0–2	38	6.7	
Cudahy Ln	1	6/3/10	10	58	6.5	
Cudahy Ln	1	6/3/10	20	49	8.4	
Cudahy Ln	1	6/3/10	30	59	6.1	
Cudahy Ln	1	6/3/10	40	61	5.5	
Cudahy Ln	1	6/3/10	50	74	3.0	
900 S-N	3	6/8/10	0–2	52	5.0	
900 S-N	3	6/8/10	10	67	3.8	
900 S-N	3	6/8/10	20	70	2.4	
900 S-N	3	6/8/10	30	63	4.0	
900 S-N	3	6/8/10	40	62	4.4	
900 S-N	3	6/8/10	50	71	2.2	
900 S-N	3	6/8/10	60	67	3.9	
900 S-N	3	6/8/10	70	62	8.5	
900 S-N	3	6/8/10	0–2	64	5.7	
900 S-N	3	6/8/10	10	73	1.9	
900 S-N	3	6/8/10	20	72	2.0	
900 S-S	3	6/8/10	0–2	72	1.2	
900 S-S	3	6/8/10	10	78	1.0	
900 S-S	3	6/8/10	20	84	0.8	
900 S-S	3	6/8/10	30	68	3.9	
900 S-S	3	6/8/10	40	65	2.5	
900 S-S	3	6/8/10	50	70	4.7	
2100 S	3	6/11/10	0–2	72	0.9	
2100 S	3	6/11/10	6	78	0.4	
2100 S	3	6/11/10	12	74	0.6	
2100 S	3	6/11/10	18	73	0.8	
2100 S	3	6/11/10	24	74	1.0	
2100 S	3	6/11/10	30	73	1.7	
2100 S	3	6/11/10	40	73	2.0	
2100 S	3	6/11/10	50	76	1.5	
2100 S	3	6/11/10	60	78	1.3	
2100 S	3	6/11/10	0–2	90	0.8	
2100 S	3	6/11/10	5	89	0.4	
2100 S	3	6/11/10	10	93	0.4	

Table 50. Sediment %TS and %VS (c)

site	reach	date	depth	%TS	%VS	note
2100 S	3	6/11/10	20	89	0.4	
2100 S	3	6/11/10	30	82	0.8	
1900 S	3	7/13/10	0–2	69	1.6	
1900 S	3	7/13/10	5	76	1.1	
1900 S	3	7/13/10	10	83	0.6	
1900 S	3	7/13/10	20	69	2.6	
1900 S	3	7/13/10	27	83	0.8	
1300 S	3	7/14/10	0–2	47	10.2	
1300 S	3	7/14/10	5	53	11.2	
1300 S	3	7/14/10	10	72	4.1	
1300 S	3	7/14/10	20	60	7.0	
1300 S	3	7/14/10	30	64	10.2	
1700 S-S	3	7/15/10	0–2	71	1.7	
1700 S-S	3	7/15/10	5	81	0.7	
1700 S-S	3	7/15/10	10	84	1.0	
1700 S-S	3	7/15/10	20	83	0.4	
1700 S-S	3	7/15/10	30	76	1.0	
300 N	2	7/16/10	0–2	34	6.8	
300 N	2	7/16/10	5	55	5.2	
300 N	2	7/16/10	10	56	5.5	
300 N	2	7/16/10	20	65	3.5	
300 N	2	7/16/10	30	70	3.5	
300 N	2	7/16/10	45	79	2.4	
HC		8/9/10	0–2	67	1.5	
HC		8/9/10	5	67	3.0	
HC		8/9/10	10	41	9.4	
HC		8/9/10	20	76	1.9	
HC		8/9/10	30	78	1.1	
gas bubble		8/9/10	0–2	21	13.1	
gas bubble		8/9/10	5	29	11.7	
gas bubble		8/9/10	10	40	10.3	
gas bubble		8/9/10	20	29	17.5	
gas bubble		8/9/10	30	55	5.1	
1700 N	3	8/9/10	0–2	55	3.3	
1700 N	3	8/9/10	5	54	8.2	
1700 N	3	8/9/10	10	52	8.3	
1700 N	3	8/9/10	20	62	4.8	
1700 N	3	8/9/10	30	61	5.4	
above center St	2	8/9/10	0–2	37	7.2	

Table 51. Sediment %TS and %VS (d)

site	reach	date	depth	%TS	%VS	note
above center St	2	8/9/10	5	41	9.5	
above center St	2	8/9/10	10	47	7.8	
above center St	2	8/9/10	20	75	2.3	
above center St	2	8/9/10	30	67	4.6	
LNP NE	1	8/9/10	0–2	29	8.9	
LNP NE	1	8/9/10	5	37	9.0	
LNP NE	1	8/9/10	10	55	4.9	
LNP NE	1	8/9/10	30	53	7.4	
LNP NE	1	1/3/11	0–2	43	7.8	
LNP NE	1	1/3/11	5	41	9.7	
LNP NE	1	1/3/11	10	44	8.5	
LNP NE	1	1/3/11	20	52	7.1	
LNP NE	1	1/3/11	30	57	4.8	
LNP NE	1	1/3/11	40	60	4.5	
LNP NE	1	1/3/11	50	71	2.8	
LNP NE	1	1/3/11	0–2	45	6.9	tray 1
LNP NE	1	1/3/11	5	54	5.4	tray 1
LNP NE	1	1/3/11	0–2	43	7.7	tray 2
LNP NE	1	1/3/11	5	48	7.1	tray 2
300 N	2	1/6/11	0–2	31	10.5	
300 N	2	1/6/11	5	46	7.9	
300 N	2	1/6/11	10	65	4.4	
300 N	2	1/6/11	20	70	4.4	
300 N	2	1/6/11	30	74	2.3	
LNP NE	1	1/6/11	0–2	48	5.3	tray 1
LNP NE	1	1/6/11	5	58	5.4	tray 1
LNP NE	1	1/6/11	0–2	51	4.6	tray 2
LNP NE	1	1/6/11	5	56	5.6	tray 2
1700 S-S	3	1/7/11	0–2	77	1.0	
1700 S-S	3	1/7/11	5	77	1.1	
1700 S-S	3	1/7/11	10	79	1.1	
1700 S-S	3	1/7/11	20	85	0.5	
1700 S-S	3	1/7/11	30	86	0.5	
1700 S-S	3	1/7/11	0–2	44	4.3	tray 1
1700 S-S	3	1/7/11	5	75	0.9	tray 1
1700 S-S	3	1/7/11	0–2	57	2.5	tray 2
1700 S-S	3	1/7/11	5	79	0.9	tray 2
2100 S	3	1/7/11	0–2	90	0.5	
2100 S	3	1/7/11	5	91	0.2	

Table 52. Sediment %TS and %VS (e)

site	reach	date	depth	%TS	%VS	note
2100 S	3	1/7/11	10	91	0.1	
2100 S	3	1/7/11	20	86	0.4	
2100 S	3	1/7/11	30	89	0.8	
2100 S	3	1/7/11	0–2	83	1.0	tray 1
2100 S	3	1/7/11	5	86	0.6	tray 1
2100 S	3	1/7/11	0–2	86	0.5	tray 2
2100 S	3	1/7/11	5	86	0.7	tray 2
7600 S		1/15/11	0–2	86	0.7	
7600 S		1/15/11	5	88	0.4	
7600 S		1/15/11	10	89	0.4	
7600 S		1/15/11	20	92	0.4	
5400 S		1/12/11	0–2	87	0.6	
5400 S		1/12/11	5	92	0.4	
5400 S		1/12/11	10	92	0.4	
5400 S		1/12/11	20	93	0.3	
9000 S		1/20/11	0–2	84	0.6	
9000 S		1/20/11	5	88	0.4	
9000 S		1/20/11	10	93	0.3	
LNP NE		2/24/11	0–2	44	6.2	
LNP NE	1	2/24/11	5	53	5.9	
LNP NE	1	2/24/11	10	53	6.3	
LNP NE	1	2/24/11	20	54	6.8	
LNP NE	1	2/24/11	30	70	2.5	
LNP NE	1	2/24/11	40	63	4.6	
LNP NE	1	2/24/11	50	64	4.6	
LNP NE	1	2/24/11	60	73	2.2	
1700 N	2	2/24/11	0–2	41	6.0	
1700 N	2	2/24/11	5	52	6.2	
1700 N	2	2/24/11	10	51	7.7	
1700 N	2	2/24/11	20	66	3.8	
1700 N	2	2/24/11	30	68	3.0	
1700 N	2	2/24/11	40	66	3.8	
1700 N	2	2/24/11	50	72	2.4	
100 N	2	2/24/11	0–2	42	7.8	
100 N	2	2/24/11	5	56	7.0	
100 N	2	2/24/11	10	53	6.9	
100 N	2	2/24/11	20	74	1.4	
100 N	2	2/24/11	30	81	1.3	
100 N	2	2/24/11	40	74	2.2	

Table 53. Sediment %TS and %VS (f)

site	reach	date	depth	%TS	%VS	note
900 S-N	3	2/24/11	0–2	52	4.3	
900 S-N	3	2/24/11	5	53	6.7	
900 S-N	3	2/24/11	10	71	1.8	
900 S-N	3	2/24/11	20	69	2.5	
900 S-N	3	2/24/11	30	72	1.4	
HC		2/24/11	0–2	23	16.8	
HC		2/24/11	5	38	16.1	
HC		2/24/11	10	35	24.9	
HC		2/24/11	20	55	5.2	
HC		2/24/11	30	70	1.7	
HC		2/24/11	40	80	1.0	
HC		2/24/11	45	84	0.8	
LNP NE	1	4/14/11	0–2	60	2.3	
LNP NE	1	4/14/11	5	59	4.0	
LNP NE	1	4/14/11	10	43	9.1	
LNP NE	1	4/14/11	20	62	4.5	
LNP NE	1	4/14/11	30	70	3.7	
LNP NE	1	4/14/11	40	65	5.2	
100 N	2	4/14/11	0–2	48	6.4	
100 N	2	4/14/11	5	61	4.5	
100 N	2	4/14/11	10	73	3.2	
100 N	2	4/14/11	20	73	3.0	
100 N	2	4/14/11	30	72	3.3	
LNP NE	1	7/18/11	0–2	57	3.4	
LNP NE	1	7/18/11	5	72	1.2	
LNP NE	1	7/18/11	10	69	2.0	
LNP NE	1	7/18/11	15	49	8.5	
LNP NE	1	7/18/11	20	55	7.6	
LNP NE	1	7/18/11	30	65	4.9	
LNP NE	1	7/18/11	40	69	4.6	
LNP NE	1	7/18/11	50	67	4.6	
2500 S		7/23/11	0–2	69	1.4	
2500 S		7/23/11	5	72	2.0	
2500 S		7/23/11	10	69	3.4	
2500 S		7/23/11	15	71	2.5	
2500 S		7/23/11	20	65	4.3	
2500 S		7/23/11	30	61	5.8	
2500 S		7/23/11	40	51	7.8	
1300 S	3	7/25/11	0–2	36	12.1	

Table 54. Sediment %TS and %VS (g)

site	reach	date	depth	%TS	%VS	note
1300 S	3	7/25/11	10	58	6.1	
1300 S	3	7/25/11	15	67	4.5	
1300 S	3	7/25/11	20	62	6.4	
1300 S	3	7/25/11	25	54	10.2	
LNP NE	1	8/16/11	0–2	55	4.7	
LNP NE	1	8/16/11	5	61	4.4	
LNP NE	1	8/16/11	10	55	6.1	
LNP NE	1	8/16/11	15	60	4.7	
LNP NE	1	8/16/11	20	70	2.3	
LNP NE	1	8/16/11	30	70	1.9	
LNP NE	1	8/16/11	40	63	3.9	
LNP NE	1	8/16/11	50	73	2.7	
LNP NE	1	8/16/11	0–2	65	3.2	33' E
LNP NE	1	8/16/11	5	61	7.2	33' E
LNP NE	1	8/16/11	10	55	8.1	33' E
LNP NE	1	8/16/11	15	71	8.8	33' E
LNP NE	1	8/16/11	30	47	10.3	33' E
LNP NE	1	8/16/11	40	64	5.5	33' E
LNP NE	1	8/16/11	50	76	2.9	33' E
LNP NE	1	8/16/11	0–2	66	2.3	58' E
LNP NE	1	8/16/11	5	49	11.8	58' E
LNP NE	1	8/16/11	10	59	5.0	58' E
LNP NE	1	8/16/11	15	64	4.6	58' E
LNP NE	1	8/16/11	20	73	1.4	58' E
Burnham	1	9/12/11	0–2	57	4.0	
Burnham	1	9/12/11	5	58	4.6	
Burnham	1	9/12/11	10	60	5.0	
Burnham	1	9/12/11	15	58	6.2	
Burnham	1	9/12/11	20	62	5.3	
Burnham	1	9/12/11	30	66	3.4	
Burnham	1	9/12/11	40	72	3.0	
1300 S	3	9/13/11	0–2	71	1.4	
1300 S	3	9/13/11	5	43	15.1	
1300 S	3	9/13/11	10	43	17.6	
1300 S	3	9/13/11	20	55	10.1	
1300 S	3	9/13/11	25	63	5.4	
1700 N	2	9/14/11	0–2	41	6.5	
1700 N	2	9/14/11	5	54	5.8	
1700 N	2	9/14/11	10	57	5.4	

Table 55. Sediment %TS and %VS (h)

site	reach	date	depth	%TS	%VS	note
1700 N	2	9/14/11	15	72	2.2	
1700 N	2	9/14/11	20	58	6.8	
1700 N	2	9/14/11	30	59	6.7	
1700 N	2	9/14/11	40	63	4.9	
1700 S-N	3	9/14/11	0–2	45	4.9	
1700 S-N	3	9/14/11	5	64	4.1	
1700 S-N	3	9/14/11	10	69	3.0	
1700 S-N	3	9/14/11	15	72	2.6	
1700 S-N	3	9/14/11	20	68	3.5	
1700 S-N	3	9/14/11	25	85	0.5	
1300 S	3	1/10/12	0–2	56	2.2	
1300 S	3	1/10/12	5	76	2.0	
1300 S	3	1/10/12	10	75	2.2	
1300 S	3	1/10/12	15	74	2.0	
1300 S	3	1/10/12	20	74	2.6	
1300 S	3	1/10/12	30	46	15.8	
1700 N	2	1/18/12	0–2	76	0.6	
1700 N	2	1/18/12	5	82	0.6	
1700 N	2	1/18/12	10	83	0.5	
1700 N	2	1/18/12	15	37	13.0	
1700 N	2	1/18/12	20	49	8.0	
1700 N	2	1/18/12	30	37	16.0	
1700 N	2	1/18/12	40	33	18.1	
1700 N	2	1/18/12	0–2	73	0.7	29' W
1700 N	2	1/18/12	5	79	0.7	29' W
1700 N	2	1/18/12	10	76	1.4	29' W
1700 N	2	1/18/12	15	80	0.6	29' W
1700 N	2	1/18/12	20	83	0.6	29' W
1700 N	2	1/18/12	30	67	7.6	29' W
1700 N	2	1/18/12	40	80	1.2	29' W
1700 N	2	1/18/12	50	57	13.8	29' W
1700 N	2	1/18/12	0–2	71	0.9	43' W
1700 N	2	1/18/12	5	75	0.7	43' W
1700 N	2	1/18/12	10	77	0.6	43' W
1700 N	2	1/18/12	15	73	1.4	43' W
1700 N	2	1/18/12	20	74	1.1	43' W
1700 N	2	1/18/12	30	80	1.5	43' W
1700 N	2	1/18/12	40	79	0.9	43' W
1700 N	2	1/18/12	50	69	4.6	43' W

Table 56. Sediment %TS and %VS (i)

site	reach	date	depth	%TS	%VS	note
Rose Park	2	1/25/12	0–2	66	2.4	
Rose Park	2	1/25/12	5	72	2.5	
Rose Park	2	1/25/12	10	73	2.8	
Rose Park	2	1/25/12	15	73	2.1	
Rose Park	2	1/25/12	20	75	1.6	
Rose Park	2	1/25/12	0–2	66	1.3	15' W
Rose Park	2	1/25/12	5	75	1.0	15' W
Rose Park	2	1/25/12	10	73	1.3	15' W
Rose Park	2	1/25/12	15	77	0.7	15' W
Rose Park	2	1/25/12	20	75	1.1	15' W
Rose Park	2	1/25/12	40	65	5.2	15' W
Rose Park	2	1/25/12	50	70	3.1	15' W
Rose Park	2	1/25/12	60	75	2.4	15' W
Rose Park	2	1/25/12	70	70	4.4	15' W
Rose Park	2	1/25/12	0–2	79	0.8	28' W
Rose Park	2	1/25/12	5	79	0.7	28' W
Rose Park	2	1/25/12	10	76	1.0	28' W
Rose Park	2	1/25/12	15	78	1.9	28' W
Rose Park	2	1/25/12	20	76	2.6	28' W
Rose Park	2	1/25/12	30	76	1.0	28' W
Rose Park	2	1/25/12	40	81	0.5	28' W
Rose Park	2	1/25/12	0–2	75	1.3	40' W
Rose Park	2	1/25/12	5	81	1.0	40' W
Rose Park	2	1/25/12	10	77	2.7	40' W
Rose Park	2	1/25/12	15	77	1.0	40' W
Rose Park	2	1/25/12	20	61	8.4	40' W
Rose Park	2	1/25/12	30	68	3.3	40' W
Rose Park	2	1/25/12	40	66	6.1	40' W
Rose Park	2	1/25/12	50	64	3.0	40' W
300 N	2	2/8/12	0–2	64	2.5	
300 N	2	2/8/12	5	65	3.0	
300 N	2	2/8/12	10	69	3.5	
300 N	2	2/8/12	15	68	3.7	
300 N	2	2/8/12	20	78	1.7	
300 N	2	2/8/12	0–2	75	1.0	17' W
300 N	2	2/8/12	5	74	2.4	17' W
300 N	2	2/8/12	10	60	4.9	17' W
300 N	2	2/8/12	15	66	3.5	17' W
300 N	2	2/8/12	20	71	3.3	17' W

Table 57. Sediment %TS and %VS (j)

site	reach	date	depth	%TS	%VS	note
300 N	2	2/8/12	30	67	8.2	17' W
300 N	2	2/8/12	0–2	65	3.5	28' W
300 N	2	2/8/12	5	69	4.2	28' W
300 N	2	2/8/12	10	82	1.7	28' W
300 N	2	2/8/12	15	86	1.0	28' W
300 N	2	2/8/12	0–2	58	3.3	46' W
300 N	2	2/8/12	5	59	4.4	46' W
300 N	2	2/8/12	10	54	5.6	46' W
300 N	2	2/8/12	15	68	2.7	46' W
300 N	2	2/8/12	20	69	1.9	46' W
LNP NE	1	4/2/12	0–2	71	1.7	
LNP NE	1	4/2/12	5	76	3.6	
LNP NE	1	4/2/12	10	76	2.9	
LNP NE	1	4/2/12	15	82	1.6	
LNP NE	1	4/2/12	0–2	79	1.2	45' E
LNP NE	1	4/2/12	5	78	3.2	45' E
LNP NE	1	4/2/12	10	58	7.0	45' E
LNP NE	1	4/2/12	15	67	5.7	45' E
LNP NE	1	4/2/12	20	64	8.1	45' E
LNP NE	1	4/2/12	0–2	75	1.7	64' E
LNP NE	1	4/2/12	5	61	9.7	64' E
LNP NE	1	4/2/12	10	58	7.5	64' E
LNP NE	1	4/2/12	15	60	6.7	64' E
LNP NE	1	4/2/12	20	56	11.3	64' E
300 N	2	5/14/12	0–2	61	2.3	
300 N	2	5/14/12	5	66	2.8	
300 N	2	5/14/12	10	67	2.9	
300 N	2	5/14/12	15	70	2.9	
300 N	2	5/14/12	20	68	3.3	
300 N	2	5/14/12	0–2	74	1.2	18' W
300 N	2	5/14/12	5	79	1.2	18' W
300 N	2	5/14/12	10	74	1.6	18' W
300 N	2	5/14/12	15	69	3.0	18' W
300 N	2	5/14/12	20	72	2.4	18' W
300 N	2	5/14/12	0–2	64	2.8	28' W
300 N	2	5/14/12	5	77	2.2	28' W
300 N	2	5/14/12	10	82	1.2	28' W
300 N	2	5/14/12	15	73		28' W
300 N	2	5/14/12	20	81	1.2	28' W

Table 58. Sediment %TS and %VS (k)

site	reach	date	depth	%TS	%VS	note
300 N	2	5/14/12	0–2	50	5.2	46' W
300 N	2	5/14/12	5	59	4.1	46' W
300 N	2	5/14/12	10	65	3.9	46' W
300 N	2	5/14/12	15	76	3.6	46' W
300 N	2	5/14/12	20	82	0.5	46' W
1700 S-N	3	5/16/12	0–2	38	5.8	
1700 S-N	3	5/16/12	5	62	3.0	
1700 S-N	3	5/16/12	15	71	2.8	
1700 S-N	3	5/16/12	20	73	2.5	
1700 S-N	3	5/16/12	0–2	81	0.5	27' W
1700 S-N	3	5/16/12	5	84	0.9	27' W
1700 S-N	3	5/16/12	0–2	80	1.8	38' W
1700 S-N	3	5/16/12	5	82	1.0	38' W
1700 S-N	3	5/16/12	10	63	4.1	38' W
700 S	3	5/16/12	0–2	58	3.3	
700 S	3	5/16/12	5	65	3.5	
700 S	3	5/16/12	10	64	4.4	
700 S	3	5/16/12	15	60	7.0	
700 S	3	5/16/12	20	73	1.9	
700 S	3	5/16/12	0–2	77	1.0	22' E
700 S	3	5/16/12	5	88	0.7	22' E
700 S	3	5/16/12	10	73	1.0	22' E
700 S	3	5/16/12	15	70	3.1	22' E
700 S	3	5/16/12	20	73	2.1	22' E
700 S	3	5/16/12	0–2	80	0.7	30' E
700 S	3	5/16/12	5	85	0.8	30' E
Burnham	1	5/29/12	0–2	50	4.9	
Burnham	1	5/29/12	5	40	13.3	
Burnham	1	5/29/12	10	63	5.6	
Burnham	1	5/29/12	15	70	3.6	
Burnham	1	5/29/12	20	76	2.8	
Burnham	1	5/29/12	0–2	65	1.9	30' E
Burnham	1	5/29/12	5	44	8.7	30' E
Burnham	1	5/29/12	10	47	8.3	30' E
Burnham	1	5/29/12	15	56	5.5	30' E
Burnham	1	5/29/12	20	56	5.3	30' E
Burnham	1	5/29/12	0–2	47	5.1	52' E
Burnham	1	5/29/12	5	60	3.9	52' E
Burnham	1	5/29/12	10	52	6.1	52' E

Table 59. Sediment %TS and %VS (l)

site	reach	date	depth	%TS	%VS	note
Burnham	1	5/29/12	15	55	5.8	52' E
Burnham	1	5/29/12	20	60	5.2	52' E
Cudahy Ln	1	6/6/12	0–2	64	2.8	
Cudahy Ln	1	6/6/12	5	52	6.8	
Cudahy Ln	1	6/6/12	10	55	7.1	
Cudahy Ln	1	6/6/12	15	56	7.0	
Cudahy Ln	1	6/6/12	20	61	5.3	
Cudahy Ln	1	6/6/12	0–2	74	1.5	30'
Cudahy Ln	1	6/6/12	5	69	3.4	30'
Cudahy Ln	1	6/6/12	10	67	4.4	30'
Cudahy Ln	1	6/6/12	15	72	3.3	30'
Cudahy Ln	1	6/6/12	20	73	2.8	30'
Cudahy Ln	1	6/6/12	0–2	49	5.0	48'
Cudahy Ln	1	6/6/12	5	54	4.8	48'
Cudahy Ln	1	6/6/12	10	66	2.9	48'
Cudahy Ln	1	6/6/12	15	70	2.2	48'
Cudahy Ln	1	6/6/12	20	74	2.4	48'
HC		6/2/10	0–2	23	11.4	
HC		6/2/10	10	59	5.1	
HC		6/2/10	20	63	4.4	
HC		6/2/10	30	81	1.5	

Table 60. Hydraulic reach average sediment %TS

	%TS (2010–2013 samples)									
depth (cm)	0–2	5	10	15	20	30	40	50	# sites	# depths
Reach 1 avg.	51	54	56	60	63	62	65	72	35	163
Reach 2 avg.	58	66	67	69	70	68	69	66	29	157
Reach 3 avg.	63	70	72	75	73	72	71	76	35	170
Reach 4, BW	41	49	49	54	58	69	66		5	33
Reach 4, 5400 S	87	92	92	92	93				1	5
Reach 5, 7600 S	86	88	89	90	92				1	5
Reach 6, 9000 S	84	88	93						1	3
Reach 8, US-173	45	56	67	68	68	71			1	6

Note: data compiled from 542 samples

Table 61. Hydraulic reach average sediment %VS

	%VS (2010–2013 samples)							
depth (cm)	0–2	5	10	15	20	30	40	50
Reach 1 avg.	4.8	6.6	6.2	5.8	5.4	5.0	4.4	3.3
Reach 2 avg.	3.8	3.5	3.6	3.6	3.4	4.5	4.5	5.4
Reach 3 avg.	3.1	3.3	2.8	3.4	2.5	3.7	3.0	2.8
Reach 4, backwater	8.9	8.2	8.4	7.3	6.7	3.0	4.4	
Reach 4, 5400 S	0.6	0.4	0.4	0.4	0.3			
Reach 5, 7600 S	0.7	0.4	0.4	0.4	0.4			
Reach 6, 9000 S	0.6	0.4	0.3					
Reach 8, US-173	5.6	4.0	2.4	2.8	3.2	3.0		

Note: data compiled from 538 samples

APPENDIX D

SPRING 2012 RIVER-WIDE SEDIMENT CHARACTERIZATION

Table 62. River-wide sediment analysis (a)

Burnham Dam, 5/29/11						
depth	bank	$\%TS_{bulk}$	$\%VS_{bulk}$	$\%VS_{CPOM}$	$\%TOC_{bulk}$	TOC:VS
0–2	E	50	4.9	2.6	2.6	0.53
5	E	40	13.3	2.5		
10	E	63	5.6	1.4		
15	E	70	3.6	1.1		
20	E	76	2.8	0.8		
0–2	T	65	1.9	7.1	1.2	0.63
5	T	44	8.7	7.1		
10	T	47	8.3	3.7		
15	T	56	5.5	3.2	2.9	0.53
20	T	56	5.3	0.3		
0–2	W	47	5.1	0.4	2.8	0.55
5	W	60	3.9	14	2.1	0.54
10	W	52	6.1	7.4	3.7	0.61
15	W	55	5.8	4.5	3.8	0.66
20	W	60	5.2	6.3	3.4	0.65

Note: E = east bank, T = thalweg, and W = west bank

Table 63. River-wide sediment analysis (b)

700 S, 5/16/12						
depth	bank	$\%TS_{bulk}$	$\%VS_{bulk}$	$\%VS_{CPOM}$	$\%TOC_{bulk}$	TOC:VS
0–2	E	58	3.3	6.7	1.4	0.42
5	E	65	3.5	30.2	1.5	0.43
10	E	64	4.4	31.8	2.2	0.5
15	E	60	7	19	3.6	0.51
20	E	73	1.9	8.6	0.8	0.42
0–2	T	77	1	62.7		
5	T	88	0.7	55.8		
10	T	73	1	17.3		
15	T	70	3.1	24.5	2.1	0.68
20	T	73	2.1	13.6		
0–2	W	80	0.7	52.5		
5	W	85	0.8	38.6		

Table 64. River-wide sediment analysis (c)

LNP NE, 4/2/12						
depth	bank	$\%TS_{bulk}$	$\%VS_{bulk}$	$\%VS_{CPOM}$	$\%TOC_{bulk}$	TOC:VS
0–2	E	71	1.7	1		
5	E	76	3.6	18		
10	E	76	2.9	27		
15	E	82	1.6	10		
0–2	T	79	1.2	30		
5	T	78	3.2	26		
10	T	58	7	32		
15	T	67	5.7	12		
20	T	64	8.1	19		
0–2	W	75	1.7	3		
5	W	61	9.7	11		
10	W	58	7.5	18		
15	W	60	6.7	4		
20	W	57	11.3	39		

Table 65. River-wide sediment analysis (d)

LNP NE, 8/26/11						
depth	bank	$\%TS_{bulk}$	$\%VS_{bulk}$	$\%VS_{CPOM}$	$\%TOC_{bulk}$	TOC:VS
0–2	E		4.7		2.5	0.53
5	E		4.4		1.9	0.43
10	E		6.1		2.5	0.41
15	E		4.7		2.2	0.47
20	E		2.3		1	0.43
30	E		1.9		1	0.53
40	E		3.9		2	0.51
50	E		2.7		1.4	0.52
0–2	T		7.2		2.7	0.38
10	T		8.1		3.5	0.43
30	T		10.3		4.3	0.42
40	T		5.5		1.6	0.29
10	W		5		2.7	0.54
20	W		1.4		0.4	0.29

Table 66. River-wide sediment analysis (e)

Cudahy Ln, 6/6/12						
depth	bank	$\%TS_{bulk}$	$\%VS_{bulk}$	$\%VS_{CPOM}$	$\%TOC_{bulk}$	TOC:VS
0–2	E	64	2.8	0	1.2	0.43
5	E	52	6.8	1.7	3.5	0.51
10	E	55	7.1	1.7	3.9	0.55
15	E	56	7	2.5	3.8	0.54
20	E	61	5.3	0.7	2.8	0.53
0–2	T	74	1.5	70		
5	T	69	3.4	47.6		
10	T	67	4.4	39.7	2.4	0.55
15	T	72	3.3	27.9		
20	T	73	2.8	40.3		
0–2	W	49	5	5.1	2.3	0.46
5	W	54	4.8	4.1	2.4	0.5
10	W	66	2.9	9.7	1.4	0.48
15	W	70	2.2	4.7	0.8	0.36
20	W	75	2.4	7.1		

Table 67. River-wide sediment analysis (f)

1700 S, 5/16/12						
depth	bank	$\%TS_{bulk}$	$\%VS_{bulk}$	$\%VS_{CPOM}$	$\%TOC_{bulk}$	TOC:VS
0–2	E	80	1.8	37.6		
10	E	63	4.1	6.8	2	0.49
0–2	T	81	0.5	51.9		
0–2	W	38	5.8	12.4	2.4	0.53
5	W	62	3	17.4		
15	W	71	2.8	30.6		
20	W	73	2.5	4		

Table 68. River-wide sediment analysis (g)

		300 N, 5/24/12				
depth	bank	$\%TS_{bulk}$	$\%VS_{bulk}$	$\%VS_{CPOM}$	$\%TOC_{bulk}$	TOC:VS
0–2	W	61	2.3	0	0.9	0.39
5	W	66	2.8	0.9	1.2	0.43
10	W	67	2.9	1.2	1.5	0.52
15	W	70	2.9	36.5		
20	W	69	3.3	18.7		
0–2	T	74	1.2	92.4		
5	T	79	1.2	28.8		
10	T	74	1.6	18.6	0.8	0.5
15	T	69	3	45.1	2	0.67
20	T	72	2.4	15.1		
0–2	T	64	2.8	54.8	1.4	0.5
5	T	77	2.2	27.6		
10	T	82	1.2	32.9		
20	T	81	1.2	16.9		
0–2	E	50	5.2	19.2		
5	E	59	4.1	15.4	2.3	0.56
10	E	65	3.9	15	2.5	0.64
15	E	76	3.6	6.5		
20	E	82	0.5	30.1		

APPENDIX E

JORDAN RIVER SEDIMENT PORE WATER AND C:N RATIOS

Table 69. Lower Jordan River pore water

site info.	depth (cm)	%TS	%VS	pore water concentrations (mg/L) NPDOC	NH_4-N	PO_4-P
Burnham	0–2	28	10.1	46.8	3.5	5.3
5/24/13	5	33	10.6	50.8	25.1	5.8
	10	52	7.7	79.4	37.5	8.7
LNP NE	0–2	57	3.1		5.6	3.6
5/24/13	5	69	2.7	55.4	55.6	5.1
	10	57	5.9	109.0	124.9	2.6
	15	59		101.5	170.4	3.2
	20	53	7.7	96.6	174.0	3.1
Cudahy Ln	0–2	34	7.8	62.7	2.3	4.9
5/24/13	5	43	7.3	76.1	47.7	5.6
	10	56	4.7	73.1	107.3	3.3
	15	54	6.9	87.1		6.1
	20	61	6.2	125.4	151.1	5.6
300 N	0–2	66	3.3	83.9	8.6	3.7
5/24/13	5	69		85.8	15.7	4.0
	10	59	6.2	63.8	17.3	4.9
	15	85		66.6	10.9	4.0
700 S	0–2	59	3.7	38.5	12.8	7.2
5/24/13	5	66	4.9	54.6	44.7	4.6
	10	67	4.8	91.1	65.5	6.0
	15	72	3.1	70.8	91.9	5.1
	20	71	2.6	63.4	81.0	4.5
1700 S-N	0–2	59	1.8	30.0	7.0	8.6
5/24/13	5	65	2.2	46.2	11.0	8.5
	10	69	2.7	76.4	14.0	6.8
	15	77	1.5	127.0	17.0	8.3
	20	77	1.0	58.9	10.7	6.4

Notes: dilluted all samples with 200 mL Milli-Q water

$[(H_2O \text{ mass})(x) + (200)(0)] / (200 + H_2O \text{ mass}) = y$

x = pore water nutrient concentration

y = dilluted measurement

NO_2-N non detect

NO_3-N below detection limits

Table 70. Upper Jordan River sediment pore water (a)

site	location (ft)	depth (cm)	NH_4-N (mg/L)	NO_3-N (mg/L)	PO_4-P (mg/L)	NPDOC (mg/L)	DO (mg/L)	pH
5400 S		ambient	0.28	2.83	0.81	4.3	8.9	8.8
5400 S	15	30	0.06	0.82	0.09	3.9	2.2	7.6
5400 S	15	60	0.03	0.21	0.05	3.2	2.23	7.5
5400 S	15	90	0.09	2.81	0.04	2.2	2.6	7.4
5400 S	29	30	0.16	0.58	0.1	4.4	3.2	7.7
5400 S	29	60	0.08	0.24	0.05	4.4	3	7.3
5400 S	29	90	0.03	0.22	0.05	2.9	2.3	7.5
5400 S	48	30	0.01	3.21	0.05	5.6	3	7.4
5400 S	48	60	0.06	4.13	0.04	2.7	2.5	7.3
5400 S	48	90	0.04	4.06	0.05	2.9	2.3	7.2
5400 S	eddy	30	0.05	3.73	0.06	1.8	2.8	7.9
5400 S	eddy	60	0.09	3.94	0.14	5.3	2.5	7.7
5400 S	eddy	90	0.01	3.47	0.14	6.6	4.3	7.6
7600 S		ambient	0.57	1.07	0.08	5.6		
7600 S	15	30	0.14	0.28	0.05	2.9		
7600 S	15	60	0.07	0.29	0.04	3.8		
7600 S	15	90	0.26	0.31	0.03	3.7		
7600 S	15	30	0.14	0.33		3.3		
7600 S	15	60	0.05	0.31	0.04	3.6		
7600 S	15	90	0.23	0.11	0.04	3.1		
7600 S	eddy	30	0.12	0.1	0.05	2.7		
7600 S	eddy	60	0.07	0.11	0.03	3.6		
7600 S	eddy	90	0.08	0.87	0.04	3.4		

Note: 5400 S sampled on 7-22-2012
7600 S sampled on 7-27-2012

Table 71. Upper Jordan River sediment pore water (b)

site	location (ft)	depth (cm)	NH_4-N (mg/L)	NO_3-N (mg/L)	PO_4-P (mg/L)	NPDOC (mg/L)	DO (mg/L)	pH
9000 S		ambient	0.06	1.1	0.08	5.6	8.3	8.2
9000 S	17	30	0.05	0.73	0.04	4.3	1.7	7.5
9000 S	17	60	0.06	0.9	0.03	6	1.8	7.3
9000 S	17	90	0.09	0.88	0.03	8.4	1.8	7.3
9000 S	27	30	0.02	0.62	0.04	1.8	2.3	7.3
9000 S	27	60	0.05	0.77	0.03	2.3	1.8	7.3
9000 S	27	90	0.04	0.8	0.03	2.3	1.7	7.3
9000 S	45	30	0.03	0.6	0.04	1.9	1.9	7.3
9000 S	45	60	0.04	0.64	0.04	2.1	1.8	7.3
9000 S	45	90	0.03	0.72	0.03	1.8	1.9	7.3
9000 S	15	30	0.07	1.04	0.05	4	2.5	7.6
9000 S	15	60	0.05	1.03	0.03	2.5	1.8	7.6
9000 S	15	90	0.05	1.11	0.03	2.1	2.2	7.6
10600 S		ambient	0.03	1.1	0.14	4.3	8.2	8.7
10600 S	9	30	0.01	1.32	0.05	1.3	3.3	8.1
10600 S	9	60	0.02	1.09	0.04	1.5	3.5	7.9
10600 S	9	90	0.02	1.53	0.03	2.8	3	7.8
10600 S	22	30	0.01	1.43	0.04	1.6	2.8	7.7
10600 S	22	60	0.01	1.52	0.03	1.5	2.4	7.7
10600 S	22	90	0.02	1.48	0.04	1.7	3.2	7.6
10600 S	38	30	0.04	0.65	0.06	3.1	3.5	7.6
10600 S	38	60	0.01	0.91	0.06	2.6	3.2	7.5
10600 S	38	90	0.01	1.53	0.04	1.5	3.3	7.5

Note: 9000 S sampled on 7-18-2012
10600 S sampled on 7-23-2012

Table 72. Upper Jordan River sediment pore water (c)

site	location (ft)	depth (cm)	NH_4-N (mg/L)	NO_3-N (mg/L)	PO_4-P (mg/L)	NPDOC (mg/L)	DO (mg/L)	pH
10600 S	stream	30	0.06	0.15	0.05	5.7	3.1	8
10600 S	stream	60	0.09	0.06	0.09	4.3	3.4	7.7
10600 S	stream	90	0.02	0.31	0.06	3	3.8	7.5
14600 S		ambient	0.06	0.75	0.05	3.7	7.6	8.4
14600 S	15	30	0.03	2.07	0.06	1.6	6.2	8
14600 S	15	60	0.02	2.13	0.06	1.5	6.5	7.8
14600 S	15	90	0.02	2.22	0.06	1.4	6.8	7.8
14600 S	20	30	0.02	1.91	0.05	1.4	7	7.8
14600 S	20	60	0	2.2	0.04	0.8	6.9	7.7
14600 S	20	90	0.01	1.99	0.05	1	6.8	7.6

Note: 10600 S sampled on 7-23-2012
14600 S sampled on 7-24-2012

Table 73. Sediment C:N molar ratios and stable isotope data

site	$^{13}C/^{12}C_{PDB}$	$^{15}N/^{14}N_{AIR}$	organic C (%)	organic N (%)	C:N ratio
Burnham	-26.7	8.8	3.9	0.32	11.9
LNP NE	-25.8	6.9	1.8	0.14	13.4
Cudahy Ln.	-23.9	9	5.4	0.46	11.7
Redwood Rd.	-25.5	8.4	3.8	0.35	10.9
300 N	-26.1	8.1	4.9	0.41	12.1
700 S	-22.5	-	0.4	0.03	11.7
1300 S	-20.7	-	3.1	0.11	28.3
1300 S	-25.8	7.7	1.9	0.13	14
1700 S	-25.3	-	1.3	0.1	12.3
2300 S	-20.5	8.3	1	0.09	11.6
900 S	-20.5	-	0.7	0.05	14.9
(stormwater pond)	-22.8	-	0.9	0.05	19
Mill Cr.	-24.2	6.1	1.9	0.18	10.6
(below CVWRF)	-23.5	5.6	1.7	0.15	11.3
Mill Cr.	-25.8	3.6	3.1	0.18	16.7
(above CVWRF)	-26	3.6	3.2	0.2	15.8
algal mat	-18.8	9.6	28.3	2.7	10.5
(900 S pond)	-18.9	9.3	28.9	2.72	10.6
gutter leaves	-27.3	1.8	45.4	0.62	73.2
(U of U)	-27.5	1.6	45.9	0.61	74.6

APPENDIX F

JORDAN RIVER AND UTAH LAKE SEDIMENT MINERALOGY

Table 74. Lower Jordan River sediment mineralogy (a)

site	% carbonates	% clays	% feldspars	% silica oxides	% other
LNP NE	21	17	21	42	0
Cudahy Ln	18	18	26	39	0
1700 N	20	14	22	45	0
300 N	11	11	29	41	8
900 S-N	14	10	22	54	0
900 S-S	4	10	28	39	19
1700 S	7	7	33	51	2
2300 S	19	12	23	46	0
US-173	40	21	15	24	0
Lower Jordan River avg	13	12	26	44	4
*Utah Lake outlet	63	9	10	13	5
**Utah Lake avg	50	8	15	19	6

* Utah Lake sample taken 2 miles east of Saratoga Springs

** Utah Lake avg consists of 12 samples

Table 75. Lower Jordan River sediment mineralogy (b)

Sediment mineral composition by % mass (top 0–2 cm)									
	LNP NE	Cudahy Ln	1700 N	300 N	900 S-N	900 S-S	1700 S	2300 S	US 173
calcite	13.2	11.5	12.2	9.6	8.8	3.8	2.4	12.2	34.1
aragonite	2.4	2.6	2.8	0.9	2.6	0.3	2.4	2.9	2
dolomite	4.9	3.9	4.6	0.4	2.2	0.2	2.3	4.2	3.8
smectite	0.3	0.2	0.2	0.5	0.1	0.1		0.1	0.3
illite	11.7	11.3	9.8	4.1	6.3	3.8	4.2	8.3	12.4
kaolinite	3.7	4.7	3.1	3.8	2.3	3.7	0.8	2.7	5
chlorite	1.3	1.5	1.1	2.6	0.8	2.3	2.3	0.8	2.9
quartz	40.4	37.5	43.7	41	53.3	38.5	47.4	45.5	23.4
amphibole	1.2	1.2	1		1		3.3	0.9	0.9
plagioclase	10.1	12.2	10.5	3.8	9.7	2.6	17.2	9.4	7.8
K-feldspar	10.9	13.4	11.1	25.3	12.4	25.3	15.4	13.1	7.5
magnetite							2.1		
pyrite	0.1			0.2					
zeolite				8.1		19.3			

Table 76. Utah Lake sediment mineralogy

site #	site	% carbonate	% clay	% feldspar	% silica oxide	% other
1	Provo Bay	58	8	14	16	4
1	Provo Bay (3–6 cm)	67	10	10	9	5
2	Entrance to Provo Bay	13	5	24	52	6
4	S.W. Goshen Bay	48	8	15	23	6
5	Goshen Bay	56	11	13	15	4
6	Geneva Steel	41	7	14	34	4
7	Geneva Steel	51	8	16	19	6
8	2 miles E. Saratoga Springs	63	9	10	13	5
10	1 mile E. f Pelican	36	4	17	38	5
11	Midlake	62	11	11	10	6
11	Midlake	69	10	9	7	5
11	Midlake (2–4 cm)	65	9	11	9	6

APPENDIX G

SEDIMENT NUTRIENT FLUXES AND WATER COLUMN RATES

Table 77. Nutrient dynamics (a)

		WC_{dark} ($g/m^3/day$)			SOD_{avg} ($g/m^2/day$)		
site	date	NH_4-N	NO_3-N	PO_4-P	NH_4-N	NO_3-N	PO_4-P
State Can.	2/6/13	-0.14	0.82	-0.02	2.46	-1.06	0.92
Burnham	6/12/12	0.12	0.88	1	0	-0.62	-0.07
Burnham	6/14/13	0.17	0.82	0.23	0.07	-0.98	-0.08
LNP NE	6/3/10	0.07	0.07	0.07	-0.14	-0.01	0.04
LNP NE	4/3/12	0.23	0.29	-0.09	-0.05	-0.1	0.03
LNP NE	6/15/12	0.3	0.86	0.1	0.02	-0.02	0.06
LNP NE	6/15/13	-0.02	-0.07	-0.02	0.05	-0.3	0.07
Cudahy Ln	6/3/10	-0.07	0	0	-0.12	-0.01	0.17
Cudahy Ln	6/13/12	-0.53	2.41	0.16	0.17	-0.28	0.02
Cudahy Ln	6/13/13	0.03	0.27	0.03	0.33	-0.6	0.02
300 N	6/7/10	-0.14	0.24	-0.31	0.12	0.01	0.15
300 N	4/14/12	-0.31	0.58	-0.1	0.06	-0.11	0.02
300 N	6/12/13	-0.02	0.21	0.14	0.02	0.02	-0.01
700 S	6/14/12	0.16	2.36	0.4	0.04	-0.15	0.01
700 S	6/10/13	0.03	0.82		0.11	-0.39	
900 S-N	6/8/10	0	-0.31	0.07	-0.01	-0.13	0.01
900 S-S	6/8/10	0.07	0.14	-0.24	-0.08	-0.03	0.09
1700 S-N	5/24/10	-0.07	0	-0.07	0.06	-0.07	0.15
1700 S-N	4/16/12	0.04	-0.58	-0.14	0.14	-0.17	-0.02
1700 S-N	6/10/13	0.05	-0.67	0.07	0.15	-0.2	0.22

Table 78. Nutrient dynamics (b)

		SOD_1 ($g/m^2/day$)			SOD_2 ($g/m^2/day$)		
site	date	NH_4-N	NO_3-N	PO_4-P	NH_4-N	NO_3-N	PO_4-P
State Can.	2/6/13	2.44	-0.67	-0.24	2.49	-1.45	2.09
Burnham	6/12/12	-0.02	-0.66	-0.09	0.01	-0.57	-0.05
Burnham	6/14/13	0.03	-0.56	-0.11	0.12	-1.4	-0.06
LNP NE	6/3/10	-0.09	-0.02	0.04	-0.18	0	0.04
LNP NE	4/3/12	-0.06	-0.05	0.02	-0.04	-0.14	0.05
LNP NE	6/15/12	-0.02	-0.12	0.05	0.07	0.09	0.07
LNP NE	6/15/13				0.05	-0.3	0.07
Cudahy Ln	6/3/10	-0.11	0	0.27	-0.12	-0.02	0.07
Cudahy Ln	6/13/12	0.19	-0.2	0.07	0.14	-0.36	-0.04
Cudahy Ln	6/13/13	0.28	-0.54	-0.05	0.38	-0.65	0.09
300 N	6/7/10	0.09	0.03	0.12	0.15	-0.01	0.17
300 N	4/14/12	0.08	-0.11	0.02	0.03	-0.11	0.02
300 N	6/12/13	0.03	-0.04	-0.01	0.02	0.07	-0.02
700 S	6/14/12	0.03	-0.3	0.01	0.06	0.01	0.02
700 S	6/10/13	0.08	-0.4		0.14	-0.39	
900 S-N	6/8/10	0	-0.19	-0.04	-0.02	-0.06	0.05
900 S-S	6/8/10	-0.11	-0.02	0.08	-0.04	-0.04	0.1
1700 S-N	5/24/10	0.05	-0.09	0.24	0.07	-0.05	0.05
1700 S-N	4/16/12	0.14	-0.2	0	0.14	-0.13	-0.03
1700 S-N	6/10/13	0.07	-0.08	0.07	0.22	-0.33	0.36

Table 79. Nutrient dynamics (c)

		WC_{dark} ($g/m^3/day$)			SOD_{avg} ($g/m^2/day$)		
site	date	NH_4-N	NO_3-N	PO_4-P	NH_4-N	NO_3-N	PO_4-P
2600 S	6/2/10	0.07	-0.07	0.07	-0.72	0.05	0.42
5400 S	1/12/11	0.2	1.44	-0.04	-0.05	-0.54	-0.03
5400 S*	1/12/11				-0.03	-0.34	-0.08
7600 S	1/15/11	-0.03	-0.5	-0.38	-0.01	-0.34	0.14
7600 S*	1/15/11				-0.01	0.17	0.07
9000 S	1/20/11	-0.01	-0.13	-0.37	-0.08	-0.03	0.07
9000 S*	1/20/11				0.02	-0.07	0.09

Note: * identifies TOD chamber

Table 80. Nutrient dynamics (d)

		SOD_1 ($g/m^2/day$)			SOD_2 ($g/m^2/day$)		
site	date	NH_4-N	NO_3-N	PO_4-P	NH_4-N	NO_3-N	PO_4-P
2600 S	6/2/10	-0.5	0.03	0.37	-0.94	0.06	0.46
5400 S	1/12/11	-0.03	-0.45	-0.04	-0.06	-0.62	-0.01
5400 S*	1/12/11	-0.01	-0.45	-0.06	-0.05	-0.24	-0.11
7600 S	1/15/11	0.04	-0.21	0.17	-0.05	-0.47	0.12
7600 S*	1/15/11	0.02	0.14	0.08	-0.03	0.2	0.06
9000 S	1/20/11	-0.13	-0.03	0.08	-0.03	-0.03	0.06
9000 S*	1/20/11	-0.01	0	0.1	0.06	-0.14	0.07

Note: * identifies TOD chamber

APPENDIX H

SEDIMENT METHANE PRODUCTION

Table 81. Lower Jordan River sediment methane production (a)

site	depth (cm)	location	%VS	CH_4 (mmol/kg wet sed./day)	CO_2	$CH_{4,OD}$ (g DO/m^2/d)
Burnham	0–2	8' E	4.9	0.635	0.611	3.55
Burnham	5	8' E	13.3	0.042	0.206	0.21
Burnham	10	8' E	5.6	0	0.122	0
Burnham	0–2	30' E	1.9	0.213	0.837	1.34
Burnham	5	30' E	8.7	0	0.162	0
Burnham	10	30' E	8.3	0.048	0.125	0.26
Burnham	0–2	52' E	5.1	0.431	0.509	2.36
Burnham	5	52' E	3.9	0.116	0.286	0.71
LNP NE	0–2	18' W	1.7	0.038	0.147	0.25
LNP NE	5	18' W	3.6	0.089	0.172	0.61
LNP NE	10	18' W	2.9	0.06	0.248	0.41
LNP NE	15	18' W	1.6	0.049	0.146	0.35
LNP NE	20	18' W	1.4	0.052	0.189	0.37
LNP NE	0–2	45' W	1.2	0.026	0.113	0.18
LNP NE	5	45' W	3.2	0.049	0.19	0.34
LNP NE	10	45' W	7	0.078	0.318	0.47
LNP NE	15	45' W	5.7	0.083	0.27	0.53
LNP NE	20	45' W	8.1	0.098	0.689	0.61
LNP NE	0–2	64' W	1.7	0.038	0.109	0.26
LNP NE	5	64' W	9.7	0.041	0.12	0.25
LNP NE	10	64' W	7.5	0.071	0.176	0.43
LNP NE	15	64' W	6.7	0.075	2.606	0.46
LNP NE	20	64' W	11.3	0.116	0.235	0.69

Note: Burnham dam sampled on 5-29-2012
LNP NE sampled on 4-2-2012

Table 82. Lower Jordan River sediment methane production (b)

site	depth (cm)	location	%VS	CH_4 (mmol/kg wet sed./day)	CO_2	$CH_{4,OD}$ (g DO/m^2/d)
Cudahy	0–2	8' E	2.8	0.178	0.377	1.11
Cudahy	5	8' E	6.8	0.387	0.266	2.21
Cudahy	10	8' E	7.1	0.131	0.396	0.77
Cudahy	0–2	30' E	1.5	0	0.114	0
Cudahy	5	30' E	3.4	0.042	0.077	0.28
Cudahy	10	30' E	4.4	0.09	0.126	0.58
Cudahy	0–2	48' E	5	0.182	0.192	1.01
Cudahy	5	48' E	4.8	0.273	0.481	1.57
Cudahy	10	48' E	2.9	0.426	1.127	2.71
300 N	0–2	8' W	2.3	0.269	0.25	1.64
300 N	5	8' W	2.8	0.268	0.284	1.71
300 N	10	8' W	2.9	0.207	0.351	1.32
300 N	0–2	28' W	2.8	0.531	0.46	3.34
300 N	5	28' W	2.2	0.332	0.395	2.28
300 N	10	28' W	1.2	0.082	0.134	0.58
300 N	0–2	46' W	5.2	0.305	0.328	1.7
300 N	5	46' W	4.1	0.065	0.124	0.39
300 N	10	46' W	3.9	0.039	0.067	0.25

Note: Cudahy Ln sampled on 6-6-2012
300 N sampled on 5-14-2012

Table 83. Lower Jordan River sediment methane production (c)

site	depth (cm)	location	%VS	CH_4 (mmol/kg wet sed./day)	CO_2	$CH_{4,OD}$ (g DO/m^2/d)
700 S	0–2	8' E	3.3	0.226	0.291	1.36
700 S	5	8' E	3.5	0.093	0.337	0.59
700 S	10	8' E	4.4	0.207	0.462	1.3
700 S	0–2	18' E	1	0.039	0.113	0.27
700 S	5	18' E	0.7	0	0.073	0
700 S	10	18' E	1	0	0.075	0
700 S	0–2	32' E	0.7	0.026	0.12	0.18
700 S	5	32' E	0.8	0	0.089	0
1700 S-N	0–2	10' W	5.8	0.654	0.47	3.29
1700 S-N	5	10' W	3	0.047	0.106	0.29
1700 S-N	10	10' W	2.8	0	0.085	0
1700 S-N	0–2	27' W	0.5	0	0.034	0
1700 S-N	5	27' W	0.9	0	0.028	0
1700 S-N	0–2	38' W	1.8	0	0.025	0
1700 S-N	5	38' W	1	0	0.041	0
1700 S-N	10	38' W	4.1	0	0.079	0

Note: 700 S sampled on 6-6-2012
1700 S- N sampled on 5-16-2012

REFERENCES

Ahn, Y. H. (2006). "Sustainable nitrogen elimination biotechnologies: A review." *Process Biochem.*, 41(8), 1709–1721.

Allan, J. D. (1995). *Stream ecology*, Chapman & Hall, New York.

Amon, R. M., and Benner, R. (1996). "Bacterial utilization of different size classes of dissolved organic matter." *Limnol. Oceanogr.*, 41(1), 41–51.

APHA, AWWA, WEF. (2005). *Standard Methods for the Examination of Water and Wastewater*, (A. D. Eaton, L. S. Clesceri, E. W. Rice, and A. E. Greenberg, Eds.), Americal Public Health Association, Washington, DC.

Appels, L., Baeyens, J., Degrève, J., and Dewil, R. (2008). "Principles and potential of the anaerobic digestion of waste-activated sludge." *Prog. Energ. Combust.*, 34(6), 755–781.

Baines, S. B., and Pace, M. L. (1991). "The production of dissolved organic matter by phytoplankton and its importance to bacteria: Patterns across marine and freshwater systems." *Limnol. Oceanogr.*, 36(6), 1078–1090.

Baity, H. G. (1938). "Some factors affecting the aerobic decomposition of sewage sludge deposits." *Sewage Work J.*, 10(3), 539–568.

Ball, D. F. (1964). "Loss-On-Ignition as an estimate of organic matter and organic carbon in non-calcareous soils." *J. Soil Sci.*, 15(1), 84–92.

Banks, R. B., and Herrera, F. F. (1977). "Effect of Wind and Rain on Surface Reaeration." *J. Environ. Eng.*, 103(3), 489–504.

Barcelona, M. J. (1983). "Sediment oxygen demand fractionation, kinetics and reduced chemical substances." *Water Res.*, 17(9), 1081–1093.

Bastviken, D., Cole, J., Pace, M., and Tranvik, L. (2004). "Methane emissions from lakes: Dependence of lake characteristics, two regional assessments, and a global estimate." *Global Biogeochem. Cy.*, 18(4), 1–12.

Beaudoin, A. (2003). "A comparison of two methods for estimating the organic content of sediments." *J. Paleolimnol.*, 29(3), 387–390.

Beck, M. B. (1987). "Water quality modeling: A review of the analysis of uncertainty." *Water Resour. Res.*, 23(8), 1393–1442.

Benfield, E. F. (1997). "Comparison of litterfall input to streams." *J. N. Am. Benthol. Soc.*, 16(1), 104–108.

Bernhardt, E. S., and Palmer, M. A. (2007). "Restoring streams in an urbanizing world." *Freshw. Biol.*, 52(4), 738–751.

Berthelson, C. R., Cathcart, T. P., and Pote, J. W. (1996). "In situ measurement of sediment oxygen demand in catfish ponds." *Aquac. Eng.*, 15(4), 261–271.

Bertrand-Krajewski, J.-L., Chebbo, G., and Saget, A. (1998). "Distribution of pollutant mass vs volume in stormwater discharges and the first flush phenomenon." *Water Res.*, 32(8), 2341–2356.

Biggs, B. J., and Close, M. E. (1989). "Periphyton biomass dynamics in gravel bed rivers: The relative effects of flows and nutrients." *Freshw. Biol.*, 22(2), 209–231.

Booth, D. B. (1990). "Stream-channel incision following drainage-basin urbanization." *J. Am. Water Resour. As.*, 26(3), 407–417.

Bott, T. L., Brock, J. T., Baattrup-Pedersen, A., Chambers, P. A., Dodds, W. K., Himbeault, K. T., Lawrence, J. R., Planas, D., Snyder, E., and Wolfaardt, G. M. (1997). "An evaluation of techniques for measuring periphyton metabolism in chambers." *Can. J. Fish. Aquat. Sci.*, 54(3), 715–725.

Bott, T. L., Brock, J. T., Cushing, C. E., Gregory, S. V., King, D., and Petersen, R. C. (1978). "A comparison of methods for measuring primary productivity and community respiration in streams." *Hydrobiologia*, 60(1), 3–12.

Bott, T. L., Brock, J. T., Dunn, C. S., Naiman, R. J., Ovink, R. W., and Petersen, R. C. (1985). "Benthic community metabolism in four temperate stream systems: An inter-biome comparison and evaluation of the river continuum concept." *Hydrobiologia*, 123(1), 3–45.

Bouck, G. R., Nebeker, A. V., and Stevens, D. G. (1976). *Mortality, saltwater adaptation and reproduction of fish during gas supersaturation.* US Environmental Protection Agency, Office of Research and Development, Environmental Research Laboratory, Duluth, MN, 1-64.

Boughton, W. C., and Neller, R. J. (1981). "Modifications to stream channels in the Brisbane Metropolitan Area, Australia." *Environ. Conserv.*, 8(4), 299–305.

Boulton, A. J., Findlay, S., Marmonier, P., Stanley, E. H., and Valett, H. M. (1998). "The functional significance of the hyporheic zone in streams and rivers." *Annu. Rev. Ecol.*

Syst., 29, 59–81.

Boyd, J. (2000). "New face of the Clean Water Act: A critical review of the EPA's new TMDL rules." *Duke Environ. Law Policy Forum*, 11(39), 39–87.

Boynton, W. R., and Kemp, W. M. (1985). "Nutrient regeneration and oxygen consumption by sediments along an estuarine salinity gradient." *Mar. Ecol.-Prog. Ser.*, 23(1), 45–55.

Bratbak, G., and Dundas, I. (1984). "Bacterial dry matter content and biomass estimations." *Appl. Environ. Microb.*, 48(4), 755–757.

Bridge, J. W. (2005). *High resolution in-situ monitoring of hyporheic zone biogeochemistry*. Environment Agency, Almondsbury, UK, 1–51.

Brunke, M., and Gonser, T. (1997). "The ecological significance of exchange processes between rivers and groundwater." *Freshw. Biol.*, 37(1), 1–33.

Butcher, R. W. (1947). "Studies in the ecology of rivers: VII. The algae of organically enriched waters." *J. Ecol.*, 35, 186–191.

Butts, T. A. (1974). *Measurements of sediment oxygen demand characteristics of the Upper Illinois Waterway*. Illinois State Water Survey, Urbana, IL, 1–36.

Butts, T. A., and Evans, R. L. (1978). *Sediment oxygen demand studies of selected northeastern Illinois streams*. Illinois State Water Survey, Urbana, IL.

Cabrita, M. T., and Brotas, V. (2000). "Seasonal variation in denitrification and dissolved nitrogen fluxes in intertidal sediments of the Tagus estuary, Portugal." *Mar. Ecol. Prog. Ser.*, 202, 51–65.

Caldwell, J. M., and Doyle, M. C. (1995). *Sediment oxygen demand in the Lower Willamette River, Oregon, 1994*. US Department of the Interior, US Geological Survey, Portland, OR, 1–19.

Callender, E., and Hammond, D. E. (1982). "Nutrient exchange across the sediment-water interface in the Potomac River estuary." *Estuar. Coast. Shelf Sci.*, 15(4), 395–413.

Carlson, R. E. (1977). "A trophic state index for lakes." *Limnol. Oceanogr.*, 22(2), 361–369.

Casas, J. J. (1996). "Environmental patchiness and processing of maple leaf litter in a backwater of a mountain stream: Riffle area vs. debris dams." *Arch. Hydrobiol.*, 136(4), 489–508.

Casey, R. J. (1990). *Sediment oxygen demand during the winter in the Athabasca River and the Wapiti-Smoky River system, 1990*. Alberta Environment, Standards and Approvals Division and Environmental Assessment Division, Edmonton, AB, 1–59.

Casper, P., Maberly, S. C., Hall, G. H., and Finlay, B. J. (2000). "Fluxes of methane and carbon dioxide from a small productive lake to the atmosphere." *Biogeochemistry*, 49(1), 1–19.

Cavinder, T. (2002). *Reaeration rate determination with a diffusion dome*. United States Environmental Protection Agency, Athens, GA, 1–11.

Cerco, C. F. (1989). "Estimating estuarine reaeration rates." *J. Environ. Eng. (New York)*, 115(5), 1066–1070.

Chapman, A. D., and Schelske, C. L. (1997). "Recent appearance of Cylindrospermopsis (cyanobacteria) in five hypereutrophic Florida lakes." *J. Phycol.*, 33(2), 191–195.

Chapra, S. C. (2008). *Surface water-quality modeling*. Waveland Press, Long Grove, IL, 1-844.

Chapra, S. C., and Di Toro, D. M. (1991). "Delta method for estimating primary production, respiration, and reaeration in streams." *J. Environ. Eng. (New York)*, 117(5), 640–655.

Chiaro, P. S., and Burke, D. A. (1980). "Sediment oxygen demand and nutrient release." *J. Environ. Eng. (New York)*, 106(1), 177–195.

Christensen, J. P., Smethie, W. M., Jr, and Devol, A. H. (1987). "Benthic nutrient regeneration and denitrification on the Washington continental shelf." *Deep Sea Res. A*, 34(5), 1027–1047.

Churchill, M. A., Elmore, H. L., and Buckingham, R. A. (1962). "The prediction of stream reaeration rates." *Int. J. Air Water Pollut.*, 6, 467–504.

Cleveland, C. C., and Liptzin, D. (2007). "C:N:P stoichiometry in soil: Is there a 'Redfield ratio' for the microbial biomass?." *Biogeochemistry*, 85(3), 235–252.

Copeland, B. J., and Duffer, W. R. (1964). "Use of a clear plastic dome to measure gaseous diffusion rates in natural waters." *Limnol. Oceanogr.*, 9(4), 494–499.

Covar, A. P. (1976). "Selecting the proper reaeration coefficient for use in water quality models." United States Environmental Protection Agency, Cincinnati, OH, 340–343.

Cowan, J. L. W., and Boynton, W. R. (1996). "Sediment-water oxygen and nutrient exchanges along the longitudinal axis of Chesapeake Bay: Seasonal patterns, controlling factors and ecological significance." *Estuaries*, 19(3), 562–580.

Cox, B. (2003). "A review of dissolved oxygen modelling techniques for lowland rivers." *Sci. Total Environ.*, 314, 303–334.

Cummins, K. W. (1974). "Structure and function of stream ecosystems." *BioScience*, 24(11), 631–641.

Cushing, C. E., Minshall, G. W., and Newbold, J. D. (1993). "Transport dynamics of fine particulate organic matter in two Idaho streams." *Limnol. Oceanogr.*, 38(6), 1101–1115.

Dauer, D. M., Rodi, A. J., and Ranasinghe, J. A. (1992). "Effects of low dissolved oxygen events on the macrobenthos of the lower Chesapeake Bay." *Estuaries*, 15(3), 384–391.

Dean, W. E., Jr. (1974). "Determination of carbonate and organic matter in calcareous sediments and sedimentary rocks by loss on ignition: Comparison with other methods." *J. Sediment, Res. A Sediment Petrol Process*, 44(1), 242–248.

Deletic, A. (1998). "The first flush load of urban surface runoff." *Water Res.*, 32(8), 2462–2470.

DeSimone, L. A., and Howes, B. L. (1996). "Denitrification and nitrogen transport in a coastal aquifer receiving wastewater discharge." *Environ. Sci. Technol.*, 30(4), 1152–1162.

Deublein, D., and Steinhauser, A. (2008). *Biogas from Waste and Renewable Resources*. John Wiley & Sons, Weinheim, Germany, 1-433.

Di Toro, D. M., Paquin, P. R., Subburamu, K., and Gruber, D. A. (1990). "Sediment oxygen demand model: methane and ammonia oxidation." *J. Environ. Eng. (New York)*, 116(5), 945–986.

Diaz, R. J., and Rosenberg, R. (2008). "Spreading dead zones and consequences for marine ecosystems." *Science*, 321(5891), 926–929.

Dillon, P. J., and Rigler, F. H. (1974). "The phosphorus-chlorophyll relationship in lakes." *Limnol. Oceanogr.*, 19(5), 767–773.

Dodds, W. K. (2006). "Nutrients and the 'dead zone': The link between nutrient ratios and dissolved oxygen in the northern Gulf of Mexico." *Front. Ecol. Environ.*, 4(4), 211–217.

Dodds, W. K. (2007). "Trophic state, eutrophication and nutrient criteria in streams." *Trends Ecol. Evol.*, 22(12), 669–676.

Dodds, W. K., Jones, J. R., and Welch, E. B. (1998). "Suggested classification of stream

trophic state: Distributions of temperate stream types by chlorophyll, total nitrogen, and phosphorus." *Water Res.*, 32(5), 1455–1462.

Doyle, M. C., and Lynch, D. D. (2005). *Sediment Oxygen Demand in Lake Ewauna and the Klamath River, Oregon, June 2003*. US Department of the Interior, US Geological Survey, Reston, VA, 1–24.

Dubrovsky, N. M., Burow, K. R., Clark, G. M., Gronberg, J. M., Hamilton, P. A., Hitt, K. J., Mueller, D. K., Munn, M. D., Nolan, B. T., Puckett, L. J., Rupert, M. G., Short, T. M., Spahr, N. E., Sprague, L. A., and Wilber, W. G. (2010). *The quality of our nation's water*. US Department of the Interior, US Geological Survey, Reston, VA, 1-174.

Edmondson, W. T., and Lehman, J. T. (1981). "The effect of changes in the nutrient income on the condition of Lake Washington." *Limnol. Oceanogr.*, 26(1), 1–29.

Edwards, R. W., and Rolley, H. (1965). "Oxygen consumption of river muds." *Journal of Ecology*, 53(1), 1–19.

Ellis, B. K., Stanford, J. A., and Ward, J. V. (1998). "Microbial assemblages and production in alluvial aquifers of the Flathead River, Montana, USA." *J. North. Am. Benthol. Soc.*, 17(4), 382–402.

Ellis, J. B. (1977). "The characterization of particulate solids and quality of water discharged from an urban catchment." *IAHS-AISH P.*, (123), 283–291.

Ensign, S. H., and Doyle, M. W. (2006). "Nutrient spiraling in streams and river networks." *J. Goephys. Res. Biogeosci.*, 111(G04009), 1–13.

Fair, G. M., Moore, E. W., and Thomas, H. A., Jr. (1941). "The natural purification of river muds and pollutional sediments." *Sewage Work. J.*, 13(2), 270–307.

Fillos, J., and Swanson, W. R. (1975). "The release rate of nutrients from river and lake sediments." *J. Water Pollut. Control Fed.*, 47(5), 1032–1042.

Fischer, H., Wanner, S. C., and Pusch, M. (2002). "Bacterial abundance and production in river sediments as related to the biochemical composition of particulate organic matter (POM)." *Biogeochemistry*, 61(1), 37–55.

Fisher, M. M., Reddy, K. R., and James, R. T. (2005). "Internal nutrient loads from sediments in a shallow, subtropical lake." *Lake and Reserv. Manag.*, 21(3), 338–349.

Fisher, S. G., and Likens, G. E. (1973). "Energy flow in Bear Brook, New Hampshire: An integrative approach to stream ecosystem metabolism." *Ecol. Monogr.*, 43(4), 421–439.

Fisher, T. R., Carlson, P. R., and Barber, R. T. (1982). "Sediment nutrient regeneration in three North Carolina estuaries." *Estuar. Coast. Shelf Sci.*, 14(1), 101–116.

Forja, J. M., and Gómez-Parra, A. (1998). "Measuring nutrient fluxes across the sediment-water interface using benthic chambers." *Mar. Ecol. Prog. Ser.*, 164, 95–105.

Gardiner, R. D., Auer, M. T., and Canale, R. P. (1984). "Sediment Oxygen Demand in Green Bay (Lake Michigan)." *Proc., Environmental Engineering.* ASCE, Los Angeles, CA, 514–519.

Gelda, R. K., Auer, M. T., and Effler, S. W. (1995). "Determination of sediment oxygen demand by direct measurement and by inference from reduced species accumulation." *Mar. Freshw. Res.*, 46(1), 81–88.

Gessner, M. O., Chauvet, E., and Dobson, M. (1999). "A perspective on leaf litter breakdown in streams." *Oikos*, 85(2), 377–384.

Giles, H., Pilditch, C. A., and Bell, D. G. (2006). "Sedimentation from mussel (Perna canaliculus) culture in the Firth of Thames, New Zealand: Impacts on sediment oxygen and nutrient fluxes." *Aquaculture*, 261(1), 125–140.

Gleick, P. H. (1993). *Water in Crisis.* Pacific Institute for Studies in Development, Environment, and Security, Stockholm Environment Institute. Oxford University Press, Inc., New York, NY, 11–24.

Glew, J. (1988). "A portable extruding device for close interval sectioning of unconsolidated core samples." *J. Paleolimnol.*, 1(3), 235–239.

Glew, J. R., Smol, J. P., and Last, W. M. (2001). *Tracking environmental change using lake sediments. Volume 1: Basin analysis, coring, and chronological techniques.* Kluwer Academic Publishers, Dordrecht, The Netherlands, 73–105.

Goonetilleke, A., Thomas, E., Ginn, S., and Gilbert, D. (2005). "Understanding the role of land use in urban stormwater quality management." *J. Environ. Manage.*, 74(1), 31–42.

Grace, M. R., and Imberger, S. J. (2006). *Stream metabolism: Performing & interpreting measurements. Water Studies Centre Monash University, Murray Darling Basin Commission and New South Wales Department of Environment and Climate Change*, Water Studies Centre Monash University, Murray Darling Basin Commission and New South Wales Department of Environment and Climate Change 204.

Gregory, S. V., Swanson, F. J., McKee, W. A., and Cummins, K. W. (1991). "An ecosystem perspective of riparian zones." *BioScience*, 41(8), 540–551.

Groffman, P. M., and Crawford, M. K. (2003). "Denitrification potential in urban riparian zones." *J. Environ. Qual.*, 32(3), 1144–1149.

Gromaire-Mertz, M. C., Garnaud, S., Gonzalez, A., and Chebbo, G. (1999). "Characterisation of urban runoff pollution in Paris." *Water Sci. Technol.*, 39(2), 1–8.

Hall, R. O., and Tank, J. L. (2005). "Correcting whole-stream estimates of metabolism for groundwater input." *Limnol. Oceanogr. Methods*, 3, 222–229.

Hatt, B. E., Fletcher, T. D., Walsh, C. J., and Taylor, S. L. (2004). "The influence of urban density and drainage infrastructure on the concentrations and loads of pollutants in small streams." *Environ. Manage.*, 34(1), 112–124.

Hauer, F. R., and Lamberti, G. A. (2007). *Methods in stream ecology*. Academic Press, Burlington, MA.

Heaney, J. P., and Huber, W. C. (1984). "Nationwide assessment of urban runoff impact on recieving water quality." *J. Am. Water Resour. As.*, 20(1), 35–42.

Heckathorn, H. A., and Gibs, J. (2010). *Sediment Oxygen Demand in the Saddle River and Salem River Watersheds, New Jersey, July–August 2008*. U.S. Department of the Interior, U.S. Geological Survey, Reston, VA.

Heiri, O., Lotter, A. F., and Lemcke, G. (2001). "Loss on ignition as a method for estimating organic and carbonate content in sediments: Reproducibility and comparability of results." *J. Paleolimnol.*, 25(1), 101–110.

Henriksen, K., Rasmussen, M. B., and Jensen, A. (1983). "Effect of bioturbation on microbial nitrogen transformations in the sediment and fluxes of ammonium and nitrate to the overlaying water." *Ecological Bulletins*, 35, 193–205.

Higashino, M., Gantzer, C. J., and Stefan, H. G. (2004). "Unsteady diffusional mass transfer at the sediment/water interface: Theory and significance for SOD measurement." *Water Res.*, 38(1), 1–12.

Hilton, J., and Irons, G. P. (1998). *Determining the causes of "apparent eutrophication" effects*. Environment Agency R&D technical report, 21.

Hilton, J., O'Hare, M., Bowes, M. J., and Jones, J. I. (2006). "How green is my river? A new paradigm of eutrophication in rivers." *Sci. Total Environ.*, 365(1), 66–83.

Hogsett, M., and Goel, R. (2013). "Dissolved oxygen dynamics at the sediment–water column interface in an urbanized stream." *Environ. Eng. Sci.*, 30(10), 594–605.

Huttunen, J. T., Lappalainen, K. M., Saarijärvi, E., Väisänen, T., and Martikainen, P. J. (2001). "A novel sediment gas sampler and a subsurface gas collector used for

measurement of the ebullition of methane and carbon dioxide from a eutrophied lake." *Sci. Total Environ.*, 266(1), 153–158.

Huttunen, J. T., Vaisanen, T. S., Hellsten, S. K., and Martikainen, P. J. (2006). "Methane fluxes at the sediment-water interface in some boreal lakes and reservoirs." *Boreal Environ. Res.*, 11(1), 27–34.

Imberger, S. J., Thompson, R. M., and Grace, M. R. (2011). "Urban catchment hydrology overwhelms reach scale effects of riparian vegetation on organic matter dynamics." *Freshw. Biol.*, 56(7), 1370–1389.

Imberger, S. J., Walsh, C. J., and Grace, M. R. (2008). "More microbial activity, not abrasive flow or shredder abundance, accelerates breakdown of labile leaf litter in urban streams." *J. North Am. Benthol. Soc.*, 17(3), 549–561.

Jenkins, J. (2005). *The humanure handbook*. Joseph Jenkins, Inc., Grove City, PA.

Kaplan, L. A., and Bott, T. L. (1982). "Diel fluctuations of DOC generated by algae in a piedmont stream." *Limnol. Oceanogr.*, 27(6), 1091–1100.

Kelly, C. A., and Chynoweth, D. P. (1981). "The contributions of temperature and of the input of organic matter in controlling rates of sediment methanogenesis." *Limnol. Oceanogr.*, 26(5), 891–897.

Kelso, B., Smith, R. V., Laughlin, R. J., and Lennox, S. D. (1997). "Dissimilatory nitrate reduction in anaerobic sediments leading to river nitrite accumulation." *J. Appl. Environ. Mircobial.*, 63(12), 4679–4685.

Konen, M. E., Jacobs, P. M., Burras, C. L., Talaga, B. J., and Mason, J. A. (2002). "Equations for predicting soil organic carbon using loss-on-ignition for North Central U.S. soils." *Soil Sci. Soc. Am. J.*, 66(6), 1878–1881.

Kristensen, E., Ahmed, S. I., and Devol, A. H. (1995). "Aerobic and anaerobic decomposition of organic matter in marine sediment: Which is fastest?" *Limnol. Oceanogr.*, 40(8), 1430–1437.

Kuivila, K. M., Murray, J. W., Devol, A. H., Lidstrom, M. E., and Reimers, C. E. (1988). "Methane cycling in the sediments of Lake Washington." *Limnol. Oceanogr.*, 33(4), 571–581.

Larned, S. T. (2003). "Effects of the invasive, nonindigenous seagrass Zostera japonica on nutrient fluxes between the water column and benthos in a NE Pacific estuary." *Mar. Ecol. Prog. Ser.*, 254, 69–80.

Larsen, D. P., Schults, D. W., and Malueg, K. W. (1981). "Summer internal phosphorus supplies in Shagawa Lake, Minnesota." *Limnol. Oceanogr.*, 26(4), 740–753.

Lee, G. F., Rast, W., and Jones, R. A. (1978). "Water Report: Eutrophication of water bodies: Insights for an age old problem." *Environ. Sci. Technol.*, 12(8), 900–908.

Leipe, T., Tauber, F., Vallius, H., Virtasalo, J., Uscinowicz, S., Kowalski, N., Hille, S., Lindgren, S., and Myllyvirta, T. (2010). "Particulate organic carbon (POC) in surface sediments of the Baltic Sea." *Geo-Marine Letters*, 31(3), 175–188.

Leu, H.-G., Ouyang, C. F., and Pai, T.-Y. (1997). "Effects of flow velocity and depth on the rates of reaeration and BOD removal in a shallow open channel." *Water Sci. Technol.*, 35(8), 57–67.

Lewis, W. M., and Morris, D. P. (1986). "Toxity of nitrite to fish: A review." *Trans. Am. Fish. Soc.*, 115(2), 183–195.

Lidstrom, M. E., and Somers, L. (1984). "Seasonal study of methane oxidation in Lake Washington." *J. Appl. Environ. Microbiol.*, 47(6), 1255–1260.

Litke, D. W. (1999). *Review of phosphorus control measures in the United States and their effects on water quality*. US Geological Survey, Denver, CO, 43.

Ludsin, S. A., Kershner, M. W., Blocksom, K. A., Knight, R. L., and Stein, R. A. (2001). "Life after death in Lake Erie: Nutrient controls drive fish species richness, rehabilitation." *Ecol. Appl.*, 11(3), 731–746.

Lytle, D. A., and Poff, N. L. (2004). "Adaptation to natural flow regimes." *Trends Ecol. Evol.*, 19(2), 94–100.

Machelor Bailey, E. K., Stankelis, R. M., Smail, P. W., Greene, S., Rohland, W. R., and Boynton, W. R. (2003). *Dissolved oxygen and nutrient flux estimation from sediments in the Anacostia River*. University of Maryland Center for Environmental Science, Solomons, MD, 1–97.

Mackenthun, A. A., and Stefan, H. G. (1998). "Effect of flow velocity on sediment oxygen demand: Experiments." *J. Environ. Eng. (New York)*, 124(3), 222–230.

Mackereth, F. J. H. (1966). "Some chemical observations on post-glacial lake sediments." *Philos. Trans. R. Soc. Lond., B., Biol. Sci.*, 250(765), 165–213.

Madenjian, C. P. (1990). "Patterns of oxygen production and consumption in intensively managed marine shrimp ponds." *Aquac. Res.*, 21(4), 407–417.

Makepeace, D. K., Smith, D. W., and Stanley, S. J. (1995). "Urban stormwater quality: Summary of contaminant data." *Crit. Rev. Environ. Sci. Technol.*, 25(2), 93–139.

Malcolm, I. A., Soulsby, C., Youngson, A. F., Hannah, D. M., McLaren, I. S., and Thorne, A. (2004). "Hydrological influences on hyporheic water quality:

Implications for salmon egg survival." *Hydrol. Process.*, 18(9), 1543–1560.

Malecki, L. M., White, J. R., and Reddy, K. R. (2004). "Nitrogen and phosphorus flux rates from sediment in the lower St. Johns River estuary." *J. Environ. Qual.*, 33(4), 1545–1555.

Marsden, M. W. (1989). "Lake restoration by reducing external phosphorus loading: The influence of sediment phosphorus release." *Freshw. Biol.*, 21(2), 139–162.

Matlock, M. D., Kasprzak, K. R., and Osborn, G. S. (2003). "Sediment oxygen demand in the Arroyo Colorado River." *J. Am. Water Resour. As.*, 39(2), 267–275.

McDonnell, A. J., and Hall, S. D. (1969). "Effect of environmental factors on benthal oxygen uptake." *J. Water Pollut. Control Fed.*, 41(8), 353–363.

McDowell, W. H., and Fisher, S. G. (1976). "Autumnal processing of dissolved organic matter in a small woodland stream ecosystem." *Ecology*, 57(3), 561–569.

McGroddy, M. E., Daufresne, T., and Hedin, L. O. (2004). "Scaling of C: N: P stoichiometry in forests worldwide: Implications of terrestrial Redfield-type ratios." *Ecology*, 85(9), 2390–2401.

McNevin, D., and Barfprd, J. (2001). "Inter-relationship between adsorption and pH in peat biofilters in the context of a cation-exchange mechanism." *Water Res.*, 35(3), 736–744.

Meentemeyer, V., Box, E. O., and Thompson, R. (1982). "World patterns and amounts of terrestrial plant litter production." *BioScience*, 32(3), 125–128.

Melillo, J. M., Naiman, R. J., Aber, J. D., and Eshleman, K. N. (1983). "The influence of substrate quality and stream size on wood decomposition dynamics." *Oecologia*, 58(3), 281–285.

Meyer, J. L., Paul, M. J., and Taulbee, W. K. (2005). "Stream ecosystem function in urbanizing landscapes." *J. North. Am. Benthol. Soc.*, 24(3), 602–612.

Miller, W., and Boulton, A. J. (2005). "Managing and rehabilitating ecosystem processes in regional urban streams in Australia." *Hydrobiologia*, 552(1), 121–133.

Minshall, G. W. (1978). "Autotrophy in stream ecosystems." *BioScience*, 28(12), 767–771.

Minshall, G. W., Petersen, R. C., Bott, T. L., Cushing, C. E., Cummins, K. W., Vannote, R. L., and Sedell, J. R. (1992). "Stream ecosystem dynamics of the Salmon River, Idaho: An 8th-order system." *J. North Am. Benthol. Soc.*, 11(2), 111–137.

Mueller, D. K., and Helsel, D. R. (1996). *Nutrients in the nations waters–Too much of a good thing?* US Geological Survey, Denver, CO, 1–31.

Murphy, P. J., and Hicks, D. B. (1986). *In-situ method for measuring sediment oxygen demand.* (K. J. Hatcher, Ed.), Sediment Oxygen Demand: Processes, Modeling and Measurement, Athens, GA, 307–323.

Naiman, R. J., and Bilby, R. E. (1998). *River Ecology and Management.* Springer Verlag, New York, NY.

Nakamura, Y., and Stefan, H. G. (1994). "Effect of flow velocity on sediment oxygen demand: Theory." *J. Environ. Eng. (New York)*, 120(5), 996–1016.

Newbold, J. D., Elwood, J. W., O'Neill, R. V., and Winkle, W. V. (1981). "Measuring nutrient spiralling in streams." *Can. J. Fish. Aquat. Sci.*, 38(7), 860–863.

Newbold, J. D., Mulholland, P. J., Elwood, J. W., and O'Neill, R. V. (1982). "Organic carbon spiralling in stream ecosystems." *Oikos*, 38(3), 266–272.

O'Connor, D. J., and Dobbins, W. E. (1956). "The mechanism of reaeration in natural streams." *T. Am. Soc. Civ. Eng.*, 123(1), 641–666.

Odum, H. T. (1956). "Primary production in flowing waters." *Limnol. Oceanogr.*, 1(2), 102–117.

Olsen, L. M., Ozturk, M., and Sakshaug, E. (2006). "Photosynthesis-induced phosphate precipitation in seawater: Ecological implications for phytoplankton." *Mar. Ecol. Prog. Ser.*, 319, 103–110.

Owens, M., Edwards, R. W., and Gibbs, J. W. (1964). "Some reaeration studies in streams." *Air Water Pollut.*, 8, 469-486.

Paerl, H. W., Pinckney, J. L., Fear, J. M., and Peierls, B. L. (1998). "Ecosystem responses to internal and watershed organic matter loading: Consequences for hypoxia in the eutrophying Neuse River Estuary, North Carolina, USA." *Mar. Ecol. Prog. Ser.*, 166, 17–25.

Parr, L. B., and Mason, C. F. (2003). "Long-term trends in water quality and their impact on macroinvertebrate assemblages in eutrophic lowland rivers." *Water Res.*, 37(12), 2969–2979.

Parr, L. B., and Mason, C. F. (2004). "Causes of low oxygen in a lowland, regulated eutrophic river in Eastern England." *Sci. Total Environ.*, 321(1), 273–286.

Pascoal, C., and Cassio, F. (2004). "Contribution of fungi and bacteria to leaf litter decomposition in a polluted river." *J. Appl. Environ. Microbiol.*, 70(9), 5266–5273.

Pauer, J. J., and Auer, M. T. (2000). "Nitrification in the water column and sediment of a hypereutrophic lake and adjoining river system." *Water Res.*, 34(4), 1247–1254.

Paul, M. J., and Meyer, J. L. (2001). "Streams in the urban landscape." *Annu. Rev. Ecol. Syst.*, 333–365.

Pelletier, G. J., Chapra, S. C., and Tao, H. (2006). "QUAL2Kw – A framework for modeling water quality in streams and rivers using a genetic algorithm for calibration." *Environ. Model. Softw.*, 21(3), 419–425.

Pimentel, D., Zuniga, R., and Morrison, D. (2005). "Update on the environmental and economic costs associated with alien-invasive species in the United States." *Ecol. Econ.*, 52(3), 273–288.

Pusch, M., Fiebig, D., Brettar, I., Eisenmann, H., Ellis, B. K., Kaplan, L. A., Lock, M. A., Naegeli, M. W., and Traunspurger, W. (1998). "The role of micro-organisms in the ecological connectivity of running waters." *Freshw. Biol.*, 40(3), 453–495.

Rath, A. K., Ramakrishnan, B., and Sethunathan, N. (2002). "Temperature dependence of methane production in tropical rice soils." *Geomicrobiol. J.*, 19(6), 581–592.

Reay, W. G., Gallagher, D. L., and Simmons, G. M. (1995). "Sediment-water column oxygen and nutrient fluxes in nearshore environments of the lower Delmarva Peninsula, USA." *Mar. Ecol. Prog. Ser.*, 118, 215–215.

Redfield, A. C. (1934). "On the proportions of organic derivations in sea water and their relation the the composition of plankton." James Johnstone Memorial Volume, Liverpool, UK, 176–192.

Refsgaard, J. C., van der Sluijs, J. P., Højberg, A. L., and Vanrolleghem, P. A. (2007). "Uncertainty in the environmental modelling process – A framework and guidance." *Environ. Model. Softw.*, 22(11), 1543–1556.

Reid, M., Thoms, M., Rowan, J. S., Duck, R. W., and Werritty, A. (2006). "Linking pattern and process: the effects of hydraulic conditions on cobble biofilm metabolism in an Australian upland stream." *IAHS-AISH P*, 322–330.

Renfro, W. C. (1963). "Gas-bubble mortality of fishes in Galveston Bay, Texas." *Trans. Am. Fish. Soc.*, 92(3), 320–322.

Ro, K. S., and Hunt, P. G. (2006). "New Unified Equation for Wind-Driven Surficial Oxygen Transfer into Stationary Water Bodies." *Biol. Eng. Trans.*, 49(5), 1615–1622.

Roberts, M. L., and Bilby, R. E. (2009). "Urbanization alters litterfall rates and nutrient inputs to small Puget Lowland streams." *J. North Am. Benthol. Soc.*, 28(4), 941–954.

Rolley, H., and Owens, M. (1967). "Oxygen consumption rates and some chemical properties of river muds." *Water Res.*, 1(11), 759–766.

Rudolfs, W. (1932). "Relation between biochemical oxygen demand and volatile solids of the sludge deposits in the Connecticut River." *Sewage Work. J.*, 4(2), 315–321.

Rutherford, J. C., Wilcock, R. J., and Hickey, C. W. (1991). "Deoxygenation in a mobile-bed river–I. Field studies." *Water Res.*, 25(12), 1487–1497.

Ryder, D. S., and Miller, W. (2005). "Setting goals and measuring success: Linking patterns and processes in stream restoration." *Hydrobiologia*, 552(1), 147–158.

Sedell, J. R., Triska, F. J., Hall, J. D., Anderson, N. H., and Lyford, J. H. (1974). "Sources and fates of organic inputs in coniferous forest streams." *Integrated research in the coniferous forest biome. Seattle: Bulletin of the Coniferous Forest Biome Ecosystem Analysis Studies, University of Washington.* 57–69.

Segers, R. (1998). "Methane production and methane consumption: a review of processes underlying wetland methane fluxes." *Biogeochemistry*, 41(1), 23–51.

Spencer, R. G. M., Pellerin, B. A., Bergamaschi, B. A., Downing, B. D., Kraus, T. E. C., Smart, D. R., Dahlgren, R. A., and Hernes, P. J. (2007). "Diurnal variability in riverine dissolved organic matter composition determined by in situ optical measurement in the San Joaquin River (California, USA)." *Hydrol. Process.*, 21(23), 3181–3189.

Stackelberg, von, N. O., and Neilson, B. T. (2012). "A collaborative approach to calibration of a riverine water quality model." *J. Water Res. Pl.-ASCE*, 140(3), 393–405.

Stanley, D. W., and Hobbie, J. E. (1981). "Nitrogen recycling in a North Carolina coastal river." *Limnol. Oceanogr.*, 26(1), 30–42.

Streeter, H. W., and Phelps, E. B. (1958). *A study of the pollution and natural purification of the Ohio River*. United States Public Health Service, Washington, DC, 1–80.

Stringfellow, W., Herr, J., Litton, G., Brunell, M., Borglin, S., Hanlon, J., Chen, C., Graham, J., Burks, R., Dahlgren, R., Kendall, C., Brown, R., and Quinn, N. (2009). "Investigation of river eutrophication as part of a low dissolved oxygen total maximum daily load implementation." *Water Sci. Technol.*, 59(1), 9.

Stumm, W., and Morgan, J. J. (1996). *Aquatic Chemistry*. John Wiley & Sons, New York, NY.

Sweeney, B. W., Bott, T. L., Jackson, J. K., Kaplan, L. A., Newbold, J. D., Standley, L.

J., Hession, W. C., and Horwitz, R. J. (2004). "Riparian deforestation, stream narrowing, and loss of stream ecosystem services." *Proc. Natl. Acad. Sci. U.S.A.*, 101(39), 14132–14137.

Tchobanoglous, G., Burton, F. L., and Stensel, H. D. (2003). *Wastewater Engineering*. McGraw Hill, New York.

Tenore, K. R. (1972). "Macrobenthos of the Pamlico river estuary, North Carolina." *Ecol. Monogr.*, 42(1), 51–69.

Thomas, N. A. (1970). *Sediment oxygen demand investigations of the Willamette River*. Water Pollution Control Administration, National Field Investigations Center, Memorandum Report, Portland, OR.

Todd, M. J., Vellidis, G., Lowrance, R. R., and Pringle, C. M. (2009). "High sediment oxygen demand within an instream swamp in Southern Georgia: Implications for low dissolved oxygen levels in coastal blackwater streams." *J. Am. Water Resour. Assoc.*, 45(6), 1493–1507.

Tsivoglou, J. B., Cohen, S. D., Shearer, S. D., and Godsil, P. J. (1968). "Tracer measurement of stream reaeration. II. Field studies." *Water Environ. Res.*, 40(2), 285–305.

Uchrin, C. G., and Ahlert, W. K. (1985). "In situ sediment oxygen demand determinations in the Passaic River (NJ) during the late summer/early fall 1983." *Water Res.*, 19(9), 1141–1144.

USEPA. (1978). *Rates, constants, and kinetics formulations in surface water quality modeling*. United States Environmental Protection Agency, Athens, GA.

USEPA. (1985). *Rates, constants, and kinetics formulations in surface water quality modeling*. United States Environmental Protection Agency, Athens, GA, 1-471.

USEPA. (1986). *Quality criteria for water*. United States Environmental Protection Agency, Washington, DC, 1–477.

USEPA. (1993). *Nitrogen control*. United States Environmental Protection Agency, Washington, DC, 1–326.

USEPA. (2001). "METHOD 1684 Total, Fixed, and Volatile Solids in Water, Solids, and Biosolids." United States Environmental Protection Agency, Washington, DC, 1-16.

USEPA. (2006). *Wadeable Streams Assessment: A Collaborative Survey of the Nation's Streams*. United States Environmental Protection Agency, Washington, DC, 1–113.

USEPA. (2008). *State Adoption of Numeric Nutrient Standards (1998–2008)*. United

States Environmental Protection Agency, Washington, DC, 1–96.

USEPA. (2010a). *Methane and nitrous oxide emissions from natural sources*. United States Environmental Protection Agency, Washington, DC, 1–194.

USEPA. (2010b). *National Lakes Assessment*. United States Environmental Protection Agency, Office of Water and Office of Research and Development, Washington, DC, 1–118.

Utah DWQ. (2007). *Utah Lake TMDL: Pollutant Loading Assessment & Designated Beneficial Use Impairment Assessment*. Prepared by PSOMAS and SWCA, Salt Lake City, UT, 1–88.

Utah DWQ. (2013). *Jordan River Total Maximum Daily Load Water Quality Study - Phase 1*, Prepared by Cirrus Ecological Solutions, LC, Logan, UT and Stantec Consulting Inc., Salt Lake City, UT, 170.

Utley, B. C., Vellidis, G., Lowrance, R., and Smith, M. C. (2008). "Factors affecting sediment oxygen demand dynamics in blackwater streams of Georgia's coastal plain." *J. Am. Water Resour. Assoc.*, 44(3), 742–753.

Van Hulzen, J. B., Segers, R., Van Bodegom, P. M., and Leffelaar, P. A. (1999). "Temperature effects on soil methane production: an explanation for observed variability." *Soil Biol. Biochem.*, 31(14), 1919–1929.

Vannote, R. L., Minshall, G. W., Cummins, K. W., Sedell, J. R., and Cushing, C. E. (1980). "The river continuum concept." *Can. J. Fish. Aquat. Sci.*, 37(1), 130–137.

Vollenweider, R. A. (1971). *Scientific fundamentals of the eutrophication of lakes and flowing waters, with particular reference to nitrogen and phosphorus as factors in eutrophication*. Organisation for Economic Co-operation and Development, Paris.

Vollenweider, R. A. (1976). "Advances in defining critical loading levels for phosphorus in lake eutrophication." *Mem. Ist. Ital. Idrobiol.*, 33, 53–83.

Walker, R. R., and Snodgrass, W. J. (1986). "Model for Sediment Oxygen Demand in Lakes." *J. Environ. Eng. (New York)*, 112(1), 25–43.

Wallace, J. B., Whiles, M. R., Eggert, S., Cuffney, T. F., Lugthart, G. J., and Chung, K. (1995). "Long-term dynamics of coarse particulate organic matter in three Appalachian Mountain streams." *J. North Am. Benthol. Soc.*, 14(2), 217–232.

Walsh, C. J., Roy, A. H., Feminella, J. W., Cottingham, P. D., Groffman, P. M., and Morgan, R. P., II. (2005). "The urban stream syndrome: Current knowledge and the search for a cure." *J. North Am. Benthol. Soc.*, 24(3), 706–723.

Wang, W. (1981). "Kinetics of sediment oxygen demand." *Water Res.*, Elsevier, 15(4), 475–482.

Webster, J. R., and Benfield, E. F. (1986). "Vascular plant breakdown in freshwater ecosystems." *Annu. Rev. Ecol. Syst.*, 17, 567–594.

Webster, J. R., Wallace, J. B., and Benfield, E. F. (1995). *River and Stream Ecosystems of the World*. (C. E. Cushing, K. W. Cummins, and G. W. Minshall, Eds.), Los Angeles, CA, 117–187.

Welch, H. E. (1968). "Relationships between assimiliation efficiencies and growth efficiencies for aquatic consumers." *Ecology*, 49(4), 755–759.

Wetzel, R. G. (2001). *Limnology: Lake and river ecosystems*. Elsevier, San Diego, CA.

Wetzel, R. G., and Likens, G. E. (2000). *Limnological analysis*. Springer, New York, NY.

Wright, K. K., Baxter, C. V., and Li, J. L. (2005). "Restricted hyporheic exchange in an alluvial river system: implications for theory and management." *J. North Am. Benthol. Soc.*, 24(3), 447–460.

Young, R. G., Matthaei, C. D., and Townsend, C. R. (2008). "Organic matter breakdown and ecosystem metabolism: functional indicators for assessing river ecosystem health." *J. North Am. Benthol. Soc.*, 27(3), 605–625.

Ziadat, A. H., and Berdanier, B. W. (2004). "Stream depth significance during in-situ sediment oxygen demand measurements in shallow streams." *J. Am. Water Resour. Assoc.*, 40(3), 631–638.